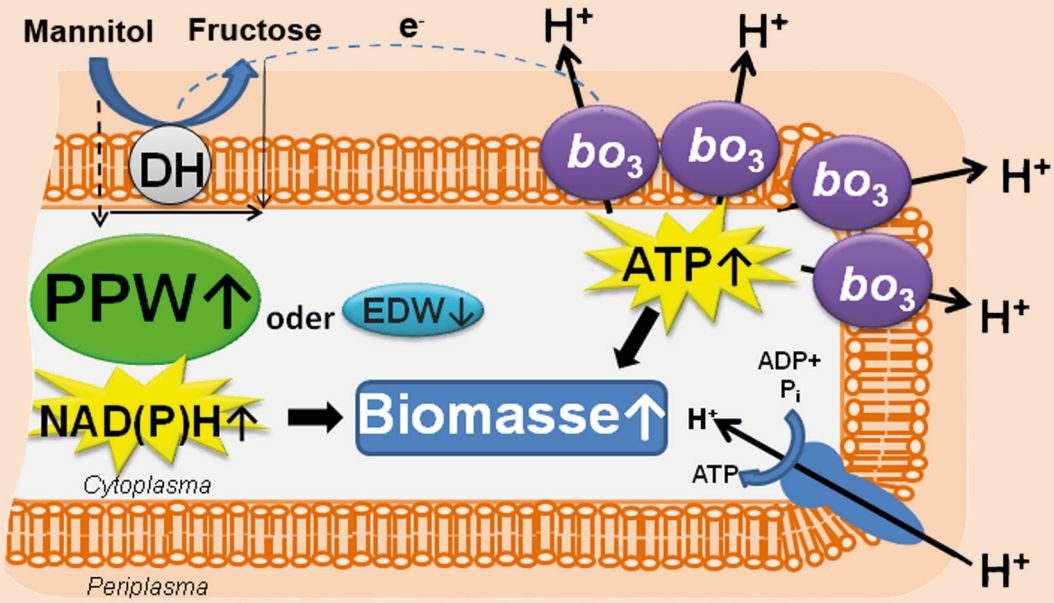

Gluconobacter oxydans strain development: Studies on central carbon metabolism and respiration

Janine Richhardt

Member of the Helmholtz Association

JÜLICH
FORSCHUNGSZENTRUM

Schriften des Forschungszentrums Jülich
Reihe Gesundheit / Health Band / Volume 63

Forschungszentrum Jülich GmbH
Institute of Bio- and Geosciences (IBG)
Biotechnology (IBG-1)

Gluconobacter oxydans strain development: Studies on central carbon metabolism and respiration

Janine Richhardt

Schriften des Forschungszentrums Jülich
Reihe Gesundheit / Health

Band / Volume 63

ISSN 1866-1785

ISBN 978-3-89336-851-8

Bibliographic information published by the Deutsche Nationalbibliothek.
The Deutsche Nationalbibliothek lists this publication in the Deutsche Nationalbibliografie; detailed bibliographic data are available in the Internet at http://dnb.d-nb.de.

Publisher and Distributor:	Forschungszentrum Jülich GmbH Zentralbibliothek 52425 Jülich Phone +49 (0) 24 61 61-53 68 · Fax +49 (0) 24 61 61-61 03 e-mail: zb-publikation@fz-juelich.de Internet: http://www.fz-juelich.de/zb
Cover Design:	Grafische Medien, Forschungszentrum Jülich GmbH
Printer:	Grafische Medien, Forschungszentrum Jülich GmbH
Copyright:	Forschungszentrum Jülich 2013

Schriften des Forschungszentrums Jülich
Reihe Gesundheit / Health Band / Volume 63

D 61 (Diss., Düsseldorf, Univ., 2012)

ISSN 1866-1785
ISBN 978-3-89336-851-8

The complete volume is freely available on the Internet on the Jülicher Open Access Server (JUWEL) at http://www.fz-juelich.de/zb/juwel

The thesis in hand has been performed at the
Institute of Bio- and Geosciences 1: Biotechnology, Forschungszentrum Jülich GmbH,
from October 2009 until November 2012 under the supervision of Prof. Dr. Michael Bott.

Printed with the permission
of the Faculty of Mathematics and Natural Sciences
of the Heinrich-Heine-University Düsseldorf

Examiner: Prof. Dr. Michael Bott
Institute of Bio- and Geosciences 1: Biotechnology
Forschungszentrum Jülich GmbH

Coexaminer: Prof. Dr. Joachim Ernst
Department Biologie
Molekulare Mykologie
Heinrich-Heine-University Düsseldorf

Date of oral examination: 13.12.2012

Results described in this this dissertation have been published in the following original publications:

Hanke T, **Richhardt J**, Polen T, Sahm H, Bringer S, Bott M (2012) Influence of oxygen limitation, absence of the cytochrome bc_1 complex and low pH on global gene expression in *Gluconobacter oxydans* 621H using DNA microarray technology. Journal of Biotechnology 157:359– 372

Richhardt J, Bringer S, Bott M (2012) Mutational Analysis of the Pentose Phosphate and Entner-Doudoroff Pathway in *Gluconobacter oxydans* Reveals Improved Growth of an Δ*edd* Δ*eda* Mutant on Mannitol. Applied and Environmental Microbiology (2012) Applied and Environmental Microbiology 78: 6975 - 6986

Richhardt J, Bringer S, Bott M (2013) Role of the pentose phosphate pathway and the Entner-Doudoroff pathway in glucose metabolism of *Gluconobacter oxydans* 621H Δ*upp*. Appl Microbiol Biotechnol DOI 10.1007/s00253-013-4707-2

Richhardt J*, Luchterhand, B*, Bringer S, Büchs J, Bott M (2013) Characterization of cytochrome *bd*- and cytochrome bo_3-terminal oxidase deletion mutants of *G. oxydans* reveals bo_3 oxidase as the rate-limiting factor of the respiratory chain To be submitted to the Journal of Bacteriology

* both authors contributed equally to this work

Results of further projects not discussed in this thesis:

Ostermann S, **Richhardt J**, Bringer S, Bott M, Oldiges M (2013) Use of ^{13}C glucose for focused pathway discrimination in *G. oxydans* 621H. Manuscript in preparation

Table of contents

Abbreviations

2-KGA	2-ketogluconate
5-KGA	5-ketogluconate
ATP	Adenosine-5'-triphosphate
DH	Dehydrogenase
DO	Dissolved oxygen
EDP	Entner-Doudoroff pathway
EMP	Embden-Meyerhoff-Parnas pathway
et al.	et alii
NADH	Nicotinamide adenine dinucleotide
NADPH	Nicotinamide adenine dinucleotide phosphate
OD_{600}	Optical density at 600 nm
PPP	Pentose phosphate pathway
TCA cycle	Tricarboxylic acid cycle
UQ	Ubiquinone

Further abbreviations not included in this section are according to international standards, as for example listed in the author guidelines of the FEBS Journal.

1. Abstract

Even though *Gluconobacter oxydans* has been used since a long time in industrial processes, knowledge on the metabolism and physiology of this organism, which is characterized by superb oxidation capabilities on the one hand and a very low cell yield on the other hand, is quite limited. To promote a rational design of new producer strains, central carbon metabolism and respiration of *G. oxydans* was investigated in this work by construction and characterization of defined deletion mutants.

The role of the two functional sugar degradation pathways, the pentose phosphate pathway (PPP) and the Entner-Doudoroff pathway (EDP), was studied with mutants lacking the genes for 6-phosphogluconate dehydratase and 2-keto-3-deoxy-6-phosphogluconate aldolase (Δ*edd-eda*) or the gene for 6-phosphogluconate dehydrogenase (Δ*gnd*). During growth with mannitol, inactivation of the EDP (Δ*edd-eda* mutant), but also overexpression of 6-phosphogluconate dehydrogenase (*gnd*), resulted in a 24% increase in final optical density (OD_{600}) compared to the reference strain and in a 43% increase of the cell yield in the first growth phase. This positive effect was not observed with glucose as carbon source. Inactivation of the PPP (Δ*gnd* mutant), but also overexpression of the *edd-eda* genes, caused strong growth reduction and the complete absence of a second growth phase. Secondary mutations in the *zwf* gene arose in the Δ*gnd* mutant causing inactivation of glucose 6-phosphate dehydrogenase. With mannitol as the carbon source the resulting strains lacked both, a functional PPP and a functional EDP, and probably survived by using the yeast extract present in the medium. These results indicate that the PPP is the major and energetically more efficient route for sugar metabolism in *G. oxydans*.

The role of the two terminal oxidases, cytochrome bo_3 and cytochrome *bd*, for growth and biomass formation was elucidated by mutants lacking either the *cyoBACD* genes or the *cydAB* genes. Whereas the Δ*cydAB* deletion did not influence the growth characteristics, the Δ*cyoBACD* deletion resulted in growth inhibition, presumably caused by a 56% decrease of the H^+/O ratio. Overexpression of the *cyoBACD* genes resulted in a significant increase of the final OD_{600} by 20% and an increase of the cell yield by 11%. These results indicate that cytochrome bo_3 is the major and energetically more efficient terminal oxidase in *G. oxydans*.

The results described above show that biomass formation by *G. oxydans* can be improved by deletion of the EDP, by an increased carbon flux over the PPP, and by an increased electron flux over cytochrome bo_3 oxidase. A combination of these approaches might be used to reduce the costs for *G. oxydans* biomass formation.

1. Zusammenfassung

Obwohl *Gluconobacter oxydans* schon sehr lange in industriellen Prozessen eingesetzt wird, ist wenig bezüglich des Metabolismus und der Physiologie dieses Bakteriums bekannt, das einerseits durch eine stark ausgeprägte Oxidationsfähigkeit und andererseits durch eine geringe Zellausbeute gekennzeichnet ist. Um neue oder verbesserte Produktionsstämme mittels *metabolic engineering* konstruieren zu können, wurde der zentrale Kohlenstoffwechsel und die Atmungskette von *G. oxydans* durch Konstruktion und Charakterisierung ausgewählter Deletionsmutanten untersucht.

Die Rolle der beiden funktionalen Zuckerabbauwege, des Pentosephosphat-Wegs (PPW) und des Entner-Doudoroff-Wegs (EDW), wurde mittels Deletionsmutanten, denen entweder das Gen für die 6-Phosphogluconatdehydratase und die 2-Keto-3-deoxy-6-phosphogluconat-Aldolase (Δ*edd-eda*), oder das Gen für die 6-Phosphogluconat-dehydrogenase (Δ*gnd*) fehlt, untersucht. Bei Wachstum mit Manntiol als Kohlenstoffquelle führte sowohl die Inaktivierung des EDW als auch die Überexpression des 6-Phosphogluconatdehydrogenase Gens (*gnd*) zu einer um 24% erhöhten finalen optischen Dichte (OD_{600}) im Vergleich zum Referenzstamm und zu einer um 43% gesteigerten Zellausbeute in der ersten Wachstumsphase. Dieser positive Effekt konnte mit Glucose als Kohlenstoffquelle nicht beobachtet werden. Die Inaktivierung des PPW (Δ*gnd*-Mutante) sowie die Überexpression der *edd-eda*-Gene führte zu einer starken Inhibierung des Wachstums und der kompletten Abwesenheit der zweiten Wachstumsphase. In der Δ*gnd* Mutante traten Sekundärmutationen im *zwf*-Gen auf, was eine Inaktivierung der Glucose-6-Phosphatdehydrogenase zur Folge hatte. Den daraus resultierenden Stämmen fehlte mit Mannitol als Kohlenstoffquelle sowohl ein funktionaler PPW als auch ein funktionaler EDW und sie überlebten vermutlich durch den im Medium enthaltenen Hefeextrakt. Diese Ergebnisse zeigen, dass der PPW der Hauptstoffwechselweg und der energetisch effizientere Weg für den Zuckermetabolismus in *G. oxydans* ist.

Die Rolle der beiden terminalen Oxidasen, Cytochrom bo_3 und Cytochrom *bd*, bezüglich Wachstum und Biomassebildung wurde mit Mutanten untersucht, bei denen entweder die *cyoBACD*- oder die *cydAB*-Gene deletiert wurden. Während die Δ*cydAB*-Deletion keinen Einfluss auf die Wachstumseigenschaften aufzeigte, resultierte die Δ*cyoBACD*-Deletion in einer Wachstumsinhibierung, die vermutlich auf ein um 56% verringertes H^+/O-Verhältnis zurückzuführen ist. Überexpression der *cyoBACD*-Gene resultierte in einer signifikanten Erhöhung der End-OD_{600} um 20% und einer gesteigerten Zellausbeute um 11%. Diese

Ergebnisse deuten an, dass die Cytochrom bo_3-Oxidase die Haupt- und energetisch effizientere terminale Oxidase in *G. oxydans* ist.

Die oben beschriebenen Ergebnisse zeigen, dass die Biomassebildung in *G. oxydans* durch Deletion des EDW, einen erhöhten Fluss durch den PPW und einem erhöhten Elektronenfluss durch die Cytochrom bo_3-Oxidase erhöht werden kann. Eine Kombination dieser Ansätze könnte verwendet werden um die Kosten für Biomassebildung von *G. oxydans* zu reduzieren.

.

2. Introduction

2.1. The genus *Gluconobacter*

Acetic acid bacteria are Gram-negative obligately aerobic rod-shaped α-proteobacteria belonging to the family *Acetobacteriaceae* (Kersters et al. 2006). The family can be divided into ten genera; among these are *Acetobacter*, *Gluconobacter*, *Gluconacetobacter*, *Asaia, Kozakia* and *Acidomonas* (Yamada and Yukphan 2008). In 1935 the genus *Gluconobacter* was proposed for the first time for strains that could rapidly oxidize glucose to gluconic acid, but were unable to oxidize acetate (Asai 1935; Yamada and Yukphan 2008). Up to now, this feature is still used for the classification of acetic acid bacteria into two physiological groups. While members of the genera *Acetobacter*, *Acidomonas*, *Asaia*, *Gluconacetobacter* and *Kozakia* can oxidize acetate and lactate via the tricarboxylic acid (TCA) cycle and the glyoxylate shunt to CO_2, members of the genus *Gluconobacter* cannot oxidize acetate, due to a missing glyoxylate shunt and an incomplete TCA cycle (Leisinger 1965; Greenfield and Claus 1972; De Ley et al. 1984; Chinnawirotpisan et al. 2003; Prust et al. 2005).

The genus *Gluconobacter* forms a phylogenetic cluster consisting of five species: *G. oxydans*, *G. frateurii*, *G. cerinus*, *G. albidus* and *G. thailandicus* (Yamada et al. 1999; Euzeby 2005). They naturally occur in sugar-rich habitats like fruits and flowers, but are also found in alcoholic beverages and soft drinks (Gupta et al. 2001; Battey et al. 2002). In contrast to the genera *Acetobacter* and *Gluconacetobacter*, which are peritrichously flagellated, members of the genus *Gluconobacter* possess polar flagella (De Ley et al. 1984). Cells of *G. oxydans* are oval and rod-shaped and have a size of 0.9 x 1.55 to 2.63 µm, depending on the growth phase (Heefner and Claus 1976). In liquid culture they are found as single cells or as pairs and rarely as short chains (Fig. 1) (Gupta et al. 2001). *Gluconobacter* strains are usually cultivated in sugar rich media, e.g. in up to 30% (w/v) glucose, supplemented with yeast extract or casitone (Raspor and Goranovič 2008). Favored carbon sources for growth are sugars and sugar-alcohols like glucose, fructose, mannitol, or sorbitol (Olijve and Kok 1979a). The optimal growth temperature of *G. oxydans* lies between 25°C and 30°C. The preferred pH range is between pH 5.5 and pH 6, however *G. oxydans* can also grow in complex medium at a pH of 2.5 (Olijve and Kok 1979b; Gupta et al. 2001).

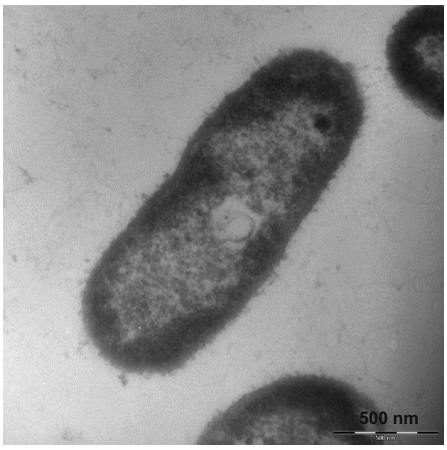

Fig. 1: Electron-microscopical picture of *G. oxydans*.
The picture was kindly provided by Sebastian Kokoschka, working group M. Hoppert, Department of General Microbiology, Institute of Microbiology and Genetics, University of Göttingen.

In 2005, the genome sequence of *G. oxydans* 621H was published, which led to new insights into its metabolic capabilities (Prust et al. 2005). The circular chromosome has a size of 2.7 Mbp with a G+C content of 60.8%. In addition, five plasmids were identified (pGOX1-5), ranging in size between 2.7 kb and 163.1 kb, resulting in an overall DNA size of 2.9 Mbp. In total, 2664 open reading frames (ORF) were identified. Functional assignments were made for 1877 of these ORFs. The proteins derived from 446 ORFs showed similarity to hypothetical proteins of other bacteria. 341 ORFs were found to be unique for *Gluconobacter* when the genome sequence was published. The genome sequence revealed a number of interesting facts concerning the metabolism and the respiratory chain of *G. oxydans*. It confirmed that the TCA cycle is incomplete as genes for succinate dehydrogenase and succinyl CoA synthetase were absent (Greenfield and Claus 1972; Prust et al. 2005). Furthermore, the gene encoding 6-phosphofructokinase was absent, preventing sugar catabolism via the Embden-Meyerhof pathway (EMP). Therefore, the Entner-Doudoroff pathway (EDP) and the pentose phosphate pathway (PPP) are the only pathways for intracellular sugar metabolism (Hauge et al. 1955; Kersters and De Ley 1968b; a; Prust et al. 2005). Concerning the respiratory chain, genes encoding two terminal oxidases, cytochrome bo_3 oxidase and cytochrome *bd* oxidase, were identified. These oxidases had already been biochemically characterized (Matsushita et al. 1987; Matsushita et al. 1989; Prust et al. 2005). Interestingly, like *A. aceti* and *A. pasteurianus*, *G. oxydans* possesses genes encoding a cytochrome bc_1 complex and a soluble cytochrome *c*, but lacks the genes

characteristic for cytochrome *c* oxidase, e.g. for the Cu_A-center containing subunit II (Prust et al. 2005; Azuma et al. 2009). The function of the cytochrome bc_1 complex in *A. aceti*, *A. pasteurianus* and *G. oxydans* is yet unresolved.

2.1.1 Biotechnological importance of *G. oxydans*

Due to its many membrane-bound dehydrogenases, *G. oxydans* has the ability to rapidly oxidize sugars and sugar alcohols regio- and stereoselectively in the periplasm. The conversion takes place nearly quantitatively. Therefore, *Gluconobacter* strains have been used for a long time in biotechnological processes requiring regio- and stereoselective oxidations that would be impossible by classical organic chemistry or give only poor yields (Gupta et al. 2001; Deppenmeier et al. 2002). Since the catalytic centers of the membrane-bound dehydrogenases are oriented to the periplasm, substrate uptake into the cell is not necessary and the products can directly enter the culture supernatant via the porins of the outer membrane. Important biotechnological applications of *G. oxydans* are the oxidation of D-sorbitol to L-sorbose in the Reichstein-Grüssner synthesis of vitamin C, the oxidation of glycerol to the tanning agent dihydroxyacetone, or the oxidation of D-aminosorbitol to L-aminosorbose, a key intermediate in the synthesis of the antidiabetic drug miglitol (Claret et al. 1992; Schedel 2000; Bremus et al. 2006; Raspor and Goranovič 2008; Hancock 2009). Furthermore, *G. oxydans* whole cells, as well as the enzymes like glucose dehydrogenase, have been used as biosensors for the analysis of various compounds like alcohols and sugars (Svitel et al. 2006). As the *G. oxydans* genome contains 77 ORFs encoding putative dehydrogenases/oxidoreductases with unknown functions, it can be assumed that the application of *G. oxydans* in the synthesis of chiral alcohols, aldehydes, ketones and carboxylic acids will extend in the next years (Prust et al. 2005).

2.2. Carbon metabolism

Aerobically growing microorganisms usually oxidize their energy sources into CO_2 and water. During this process, they generate energy and precursors for biosynthesis. Incomplete oxidation of substrates occurs only under special circumstances, e.g. excess of carbon substrates or the presence of inhibitory compounds (Deppenmeier et al. 2002). In contrast, acetic acid bacteria like *G. oxydans* are famous for their rapid and incomplete oxidation of sugars and sugar-alcohols. *G. oxydans* possesses a great number of membrane-bound dehydrogenases that oxidize sugars and sugar alcohols in the periplasm, leading to near-

quantitative accumulation of the oxidation products into the medium (Deppenmeier et al. 2002). Only a small percentage of the carbon source is taken up by the cells for the formation of biomass, resulting in very low growth yields (Olijve and Kok 1979a).

In the cytoplasm, sugar metabolism occurs only via the EDP or the PPP, as the EMP is non-functional (part 2.1). This is a shared feature in many obligate aerobic organisms. It is assumed that this is due to the limited contribuition of the phosphofructokinase to energy generation compared to energy generated through oxidative phosphorylation under aerobic conditions (Baart et al. 2010). Pfk catalyzes the irreversible phosphorylation of fructose 6-phosphate (F6P) to fructose 1,6-bisphosphate (FBP) using ATP, whereas via the PPP NAD(P)H is formed that can be used for energy generation via the respiratory chain. Even though the presence of the EDP in *G. oxydans* was known since the 1960ies, it has not been studied until the genome sequence was published (Kersters and De Ley 1968b; Prust et al. 2005). The PPP on the other hand is well studied and has been shown to take part in intracellular sugar metabolism (Hauge et al. 1955; Olijve and Kok 1979a).

Growth of *G. oxydans* can often be divided into two phases: Phase I is characterized by a rapid oxidation of the carbon source in the periplasm by the membrane-bound dehydrogenases. This phase correlates with a high demand for oxygen, a low CO_2 formation, and good growth. In phase II, the oxidized carbon source is slowly taken up by the cells. This phase correlates with poor growth, an increased formation of CO_2 as well as of acetate as a product, whereas the demand for oxygen is reduced (Hanke 2010; Krajewski et al. 2010; Schweikert 2011). Due to the fact that only a minor part of the energy and carbon source is taken up by the cells, the growth yields obtained are very low. Strain *G. oxydans* IFO3293 reaches a cell yield of 0.09 $g_{cdw}/ g_{glucose}$, whereas *E. coli* reaches a value of 0.49 $g_{cdw}/g_{glucose}$ and *Bacillus subtilis* of 0.32 $g_{cdw}/g_{glucose}$ (Dauner et al. 2002; Soini et al. 2008; Krajewski et al. 2010). One hypothesis explaining the poor growth yield of *G. oxydans* is based on its natural habitats. As the organism lives in sugar-rich habitats, the energy and carbon source is probably seldom a limiting factor for growth. Thus, by rapid oxidation of the energy and carbon source in the periplasm, which in many cases causes an acidification of the surrounding media, growth of competitors might be inhibited, giving *G. oxydans* an advantage. It seems as if *G. oxydans* has adapted perfectly to its environmental conditions, but, of course, other explanations for the growth characteristics might be possible as well.

2.2.1 Mannitol metabolism

Mannitol is known as a carbon source on which *G. oxydans* reaches high cell densities. Therefore, it is taken as an ideal substrate for growth characterization (Gossele et al. 1981). In contrast to a strong pH decrease during glucose catabolism, the pH drops only slightly

during mannitol oxidation, which can be advantageous for experimental studies. A scheme of the mannitol metabolism of *G. oxydans* is presented in Fig. 2.

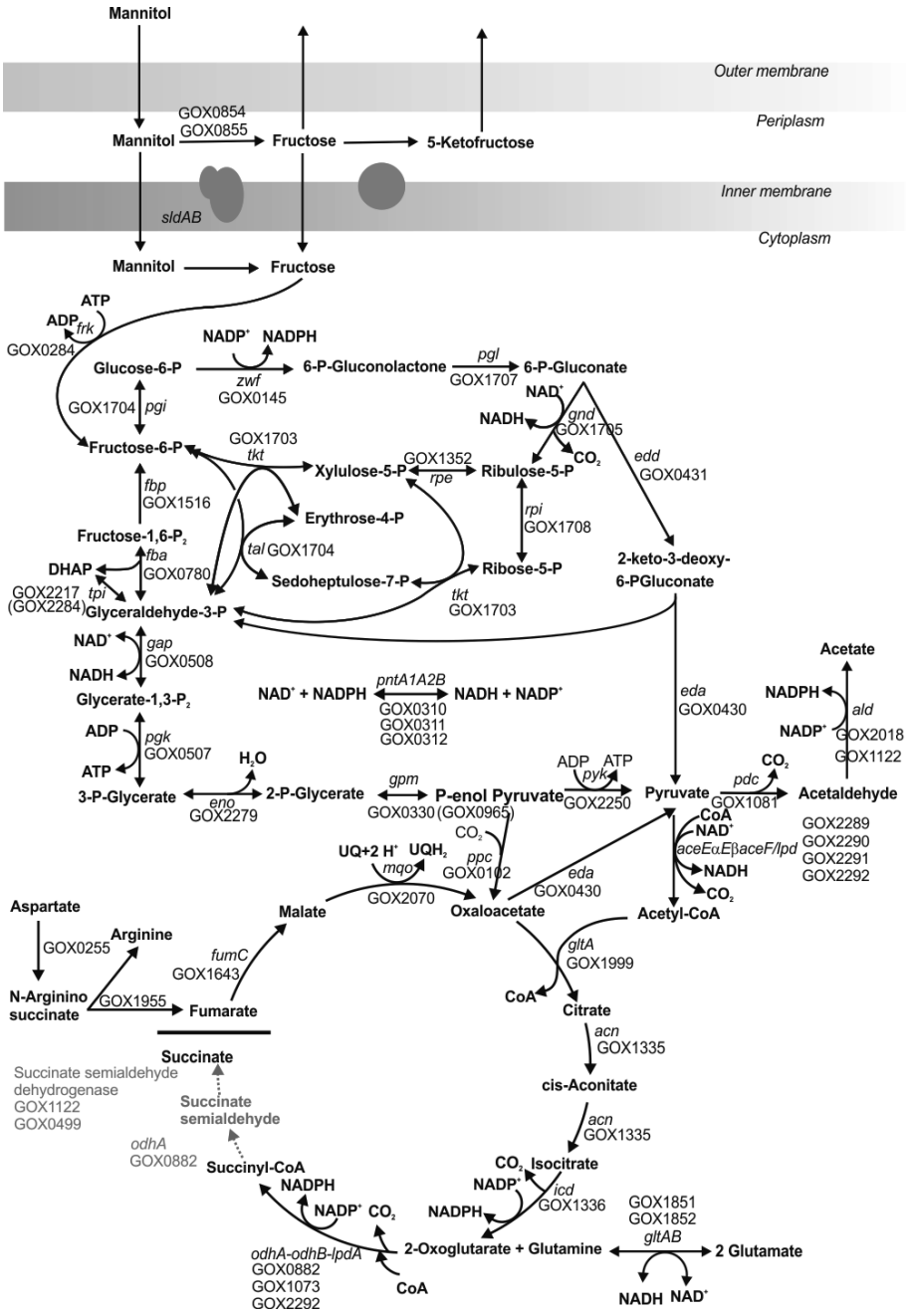

Fig. 2: Scheme of the central carbon metabolism of *G. oxydans* with the substrate mannitol.

In the first growth phase, which is accompanied by fast growth, mannitol is almost completely oxidized in the periplasm to fructose by the membrane-bound major polyol dehydrogenase SldAB (GOX0854, GOX0855). Only a very small amount of mannitol is taken up by the cells via a putative mannitol/sorbitol ABC transporter (GOX2182-2185), which involves a periplasmic binding protein (Prust et al. 2005). In the cytoplasm mannitol is directly oxidized to fructose, most probably by an enzyme different from sorbitol dehydrogenase (GOX1432) (Parmentier et al. 2005). The onset of growth phase II is when mannitol is nearly completely consumed and is associated with a reduced growth rate in comparison to phase I. Fructose can be further oxidized by a yet uncharacterized dehydrogenase to 5-ketofructose. Part of the fructose is taken up by the cells by an unknown transporter. In the cytoplasm, fructose is phosphorylated by fructokinase (GOX0284, *frk*) to fructose 6-phosphate. The phosphoglucose isomerase (GOX1704, *pgi*) converts fructose 6-phosphate into glucose 6-phosphate, which is then catablized by the PPP or the EDP. Acetate, which accumulates in the medium during cultivation, is formed from pyruvate via acetaldehyde in reactions catalyzed by pyruvate decarboxylase (GOX1081) and acetaldehyde dehydrogenases (GOX1122 and 2018) (Krajewski et al. 2010; Peters et al. 2012). Due to the absence of phosphotransacetylase and acetate kinase, acetate cannot be formed from acetyl-CoA in *G. oxydans*.

Changes associated with the transition from growth phase I to growth phase II on the transcriptomic and at the protein level have recently been studied (Schweikert 2011). DNA microarray analysis revealed that genes of the PPP are expressed at a higher level with fructose instead of mannitol as carbon source. This is in agreement with an increased formation of CO_2 in the second growth phase. Enzyme assays demonstrated an increased activity of the PPP enzymes in phase II. In contrast, genes of the EDP were stronger expressed in growth phase I than in growth phase II. However, since in glucose-grown cells carbon flux through the EDP was found to be lower than flux through the PPP also in phase I, the PPP is probably more active than the EDP in both phases (Hanke et al., in preparation).

2.2.2 Glucose metabolism

Although growth of *G. oxydans* with glucose as carbon source has already been studied in the past with respect to growth characteristics, little is known about the participation of the EDP and the PPP during glucose/gluconate oxidation until now (Olijve and Kok 1979a; Olijve and Kok 1979b). A scheme of the central carbon metabolism with glucose as carbon source is presented Fig. 3.

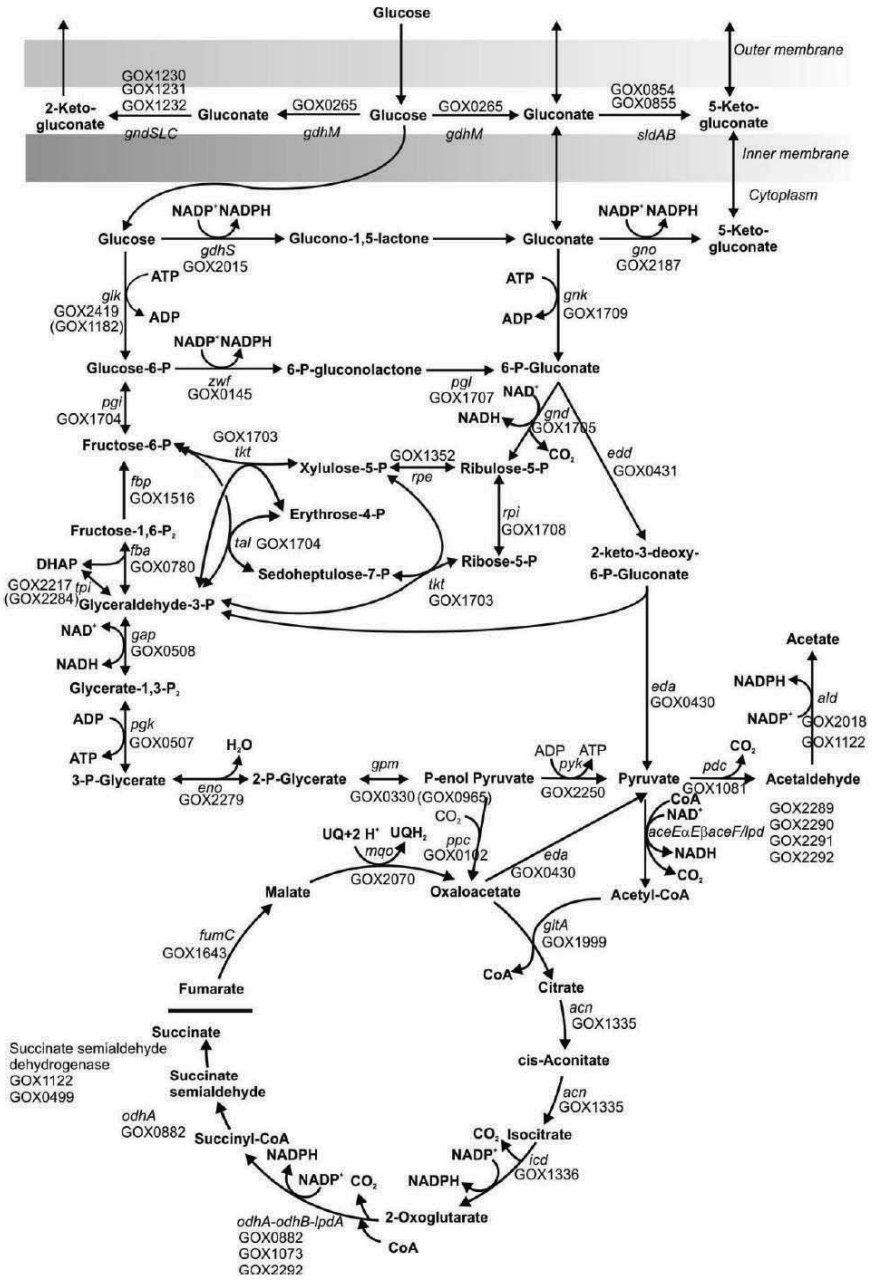

Fig. 3: Scheme of the central carbon metabolism of *G. oxydans* with the substrate glucose.

In phase I, glucose is rapidly oxidized in the periplasm to gluconate by the membrane-bound glucose dehydrogenase (GOX0265, *gdhM*). This phase is accompanied by reasonably good growth, a high demand for oxygen, and a low formation of CO_2, as only small amounts of the carbon source are taken up by the cells by a yet unknown transport system. *G. oxydans* possesses the components EI (GOX0812), HPr (GOX0813), EIIA (GOX0814) and HPr kinase (GOX0816) of the phospho*enol*pyruvate-dependent phosphotransferase system (PTS), however it lacks EII^B and EII^C components (Prust et al. 2005). Therefore, a transport function of the PTS is unlikely and the physiological role of the remaining components not yet clear. In the cytoplasm, glucose is further converted via glucose dehydrogenase (GOX2015, *gdhS*) or glucose kinase (GOX1182, *glkA* and GOX2419, *glkB*). The onset of phase II is when the primary substrate glucose has been almost totally converted to gluconate. This phase is hallmarked by reduced biomass formation, an increased formation of CO_2, a reduced demand for oxygen, and an alkalinization of the medium due to the uptake of gluconic acid. Gluconate is either converted into 2-ketogluconate (2-KGA) or 5-ketogluconate (5-KGA) in the periplasm or it is taken up by a permease (GOX2188). The intracellular gluconate can be converted into 5-KGA by a gluconate-5-dehydrogenase (*gno*, GOX2187) or phosphorylated by gluconate kinase (*gnk*, GOX1709). Glucose 6-phosphate and 6-phosphogluconate are catabolized in the cytoplasm through either of the two pathways, PPP or EDP.

In a recent study, DNA microrarray analysis, enzyme activity measurements and ^{13}C metabolic flux analysis (^{13}C-MFA) were used to characterize the two growth phases with glucose as carbon source (Hanke 2010). DNA microarray analysis was used to compare the mRNA levels of cells in the first and second growth phase. As described for growth on mannitol versus growth on fructose, the genes encoding the PPP showed an elevated mRNA level in the second growth phase. This is in agreement with an increased formation of CO_2 and a higher activity of the enzymes of the PPP. ^{13}C-MFA was performed to determine the fluxes throught the PPP and the EDP. In the first growth phase, 90% of the glucose was oxidized in the periplasm to gluconate, and part of the gluconate further to 2-KGA. Only 10% of glucose was taken up by the cells, where it was mainly oxidized to gluconate and further to 5-KGA. A minor part of glucose and gluconate was phosphorylated and then metabolized predominantly via the PPP. In phase II, gluconate was taken up by the cells or further oxidized in the periplasm to 2-KGA. The majority of gluconate in the cytoplasm was metabolized via the PPP. Thus, in phase I and II the cytoplasmic sugar catabolism proceeded predominantly via the PPP and the EDP played only a minor role, particularly in phase II (Hanke et al., in preparation).

2.2.3 PPP vs. EDP in the light of energetic efficiency

Due to the absence of phosphofructokinase in *G. oxydans*, the EMP is disrupted and intracellular sugar metabolism occurs via the EDP or the PPP, with 6-phosphogluconate as the common substrate. The two pathways differ in energetic efficiency and formation of reduction equivalents. Conversion of 1 mol glucose 6-phosphate solely via the EDP yields 2 mol acetate or acetyl-CoA + 2 mol CO_2 + 4 mol NAD(P)H + 2 mol ATP. In the absence of phosphofructokinase, the PPP operates cyclic, as fructose 6-phosphate formed by transaldolase or transketolase is converted to glucose 6-phosphate, which enters the oxidative PPP again. This has recently been shown for an *Escherichia coli* Δ*pfkA* mutant (Siedler et al. 2011). Therefore, conversion of 1 mol glucose 6-phosphate via the PPP in the absence of phosphofructokinase yields 1 mol acetate or acetyl-CoA + 4 mol CO_2 + 8 mol NAD(P)H + 2 mol ATP (Kruger and von Schaewen 2003). Thus, the partially cyclic PPP yields twice as much NAD(P)H than the EDP. The two dehydrogenases of the oxidative PPP were shown to have dual coenzyme specificities, but based on the kinetic properties it was proposed that *in vivo* glucose 6-phosphate dehydrogenase utilizes $NADP^+$ and 6-phosphogluconate dehydrogenase NAD^+ as cofactor (Tonouchi et al. 2003; Rauch et al. 2010). The acetaldehyde dehydrogenases (GOX1122 and GOX2018) of *G. oxydans* are NADP-dependent (Schweiger et al. 2007; Krajewski et al. 2010). *G. oxydans* possesses a PntA1A2B transhydrogenase (GOX0310-0312) that can theoretically convert NADPH to NADH. NADH is then reoxidized by the respiratory chain via NADH dehydrogenase and used for the generation of proton-motive force and ATP by oxidative phosphorylation (Jackson et al. 2002; Rauch et al. 2010). Hence, as the sole use of the PPP would lead to the formation of increased amounts of NAD(P)H, it can be expected that the cells would gain a growth advantage due to the higher ability to generate proton motive force.

2.3. Respiratory chain

Aerobic bacterial respiratory chains can be terminated either by a cytochrome *c* oxidase or by a quinol oxidase (Anraku 1988). Cytochrome *c* oxidase is found in oxidase-positive bacteria like *Pseudomonas* or *Azotobacter*, whereas quinol oxidase is found in oxidase-negative bacteria like *E. coli* and *G. oxydans*. Furthermore, in some bacterial respiratory chains both types of terminal oxidases are present (Lauraeus et al. 1991; Ludwig 1992). The respiratory chains of *E. coli* and *G. oxydans* contain the ubiquinol oxidases cytochrome bo_3 and cytochrome *bd* as terminal oxidases. Whereas cytochrome bo_3 oxidase is an active proton pump (Puustinen et al. 1989; Chepuri et al. 1990), cytochrome *bd* oxidase is not, but

can also contribute to the generation of an electrochemical proton gradient (Miller and Gennis 1985; Borisov et al. 2011). *E. coli* and *G. oxydans* differ with respect to the presence of a proton-pumping NADH dehydrogenase. In the following section, the respiratory chain composition of *G. oxydans* will be presented in more detail. Furthermore, there will be a comparison of energy conservation by the *E. coli* respiratory chain versus that by the *G. oxydans* respiratory chain.

2.3.1 The respiratory chain of *G. oxydans*

G. oxydans possesses a branched respiratory chain consisting of two terminal ubiquinol oxidases, cytochrome bo_3 oxidase and cytochrome *bd* oxidase (Ameyama et al. 1987) (Fig. 4). The former is encoded by the *cyoBACD* genes (GOX1911-1914), the latter by the *cydAB* genes (GOX0278 and GOX0279). The genome sequence also revealed genes for a cytochrome bc_1 complex (GOX0565-0567) and a soluble cytochrome *c* (GOX0258). However, genes encoding a cytochrome *c* oxidase are absent (Prust et al. 2005). Thus, the function of the cytochrome bc_1 complex in *G. oxydans* is not known yet. Electrons are directly transferred from the membrane-bound dehydrogenases to the ubiquinol pool (UQ_{10}), from where they are channeled to the terminal oxidases. Furthermore, the organism contains a type II non-proton pumping single subunit NADH dehydrogenase, whereas the genes encoding a proton-pumping NADH:ubiquinone oxidoreductase are absent.

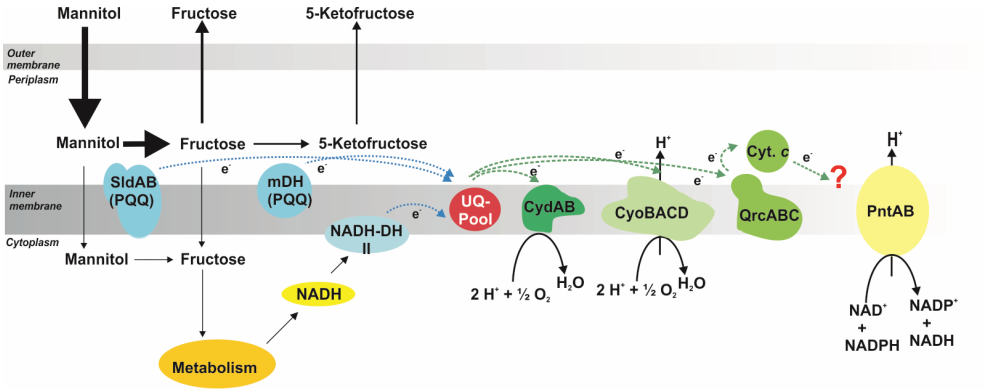

Fig. 4: Scheme of the respiratory chain of *G. oxydans* during mannitol oxidation. SldAB, major polyol dehydrogenase; CydAB, cytochrome *bd* oxidase; CyoBACD, cytochrome bo_3 oxidase; QrcABC, cytochrome bc_1 complex, PntAB, transhydrogenase. The proton pumping activity of the transhydrogenase is only assumed and not yet proven in *G. oxydans*.

Cytochrome bo_3 was first analyzed in the 1970s by Daniel using a membrane fraction of *A. suboxydans* (later renamed to *G. oxydans*) (Daniel 1970). He stated, that *A. suboxydans* possesess an *o*-type cytochrome as terminal oxidase. In 1987, the terminal oxidase was purified and characterized (Matsushita et al. 1987). It consists of four non-identical subunits and contains heme *b*, heme *o* and a copper atom as prosthetic group, similar to the *E. coli* cytochrome bo_3 oxidase (Fig. 5) (Chepuri et al. 1990; Schultz and Chan 1998). The ubiqinol oxidase was inhibited by cyanide or quinone analogues (Matsushita et al. 1987). After genome sequencing, genes GOX1911-1914 were assigned as *cyoBACD*, encoding cytochrome bo_3 oxidase (Prust et al. 2005).

Cyochrome *bd* oxidase of *G. oxydans* is described as cyanide-insensitive terminal oxidase and was shown to be expressed at higher levels at pH 4 compared to pH 6 (Matsushita et al. 1989). Genes GOX0278 and GOX0279 were annotated as *cydA* and *cydB*, encoding cytochrome *bd* oxidase. Sequence analysis revealed that these genes have a higher similarity to *cyoA* and *cyoB* from *Pseudomonas aeruginosa* and *Zymomonas mobilis* than to *cydA* and *cydB* from *E. coli* or *Campylobacter jejuni*. Therefore, a renaming of the operon in CioAB was proposed (Mogi et al. 2009). First biochemical and spectroscopic properties of cytochrome *bd* oxidase indicated the presence of heme b_{558}, heme b_{595} and heme *d* (Fig. 5) (Mogi et al. 2009). Cytochrome *bd* oxidases are thought to play a role in bacteria under microaerobic conditions as it has been demonstrated e.g. for *E. coli* (Georgiou et al. 1988; D'Mello et al. 1996; Mogi et al. 2009). In *G. oxydans* cytochrome *bd* oxidase is supposed to function as a bypass oxidase, that takes part in the reoxidation of the ubiquinol generated by the rapid periplasmic oxidation of sugar/alcohols (Matsushita et al. 2004). Furthermore it is supposed to play a role at low pH values (Matsushita et al. 1989; Hanke et al. 2012).

As described above, the terminal oxidases take part in the formation of a proton gradient across the membrane. Furthermore, *G. oxydans* possesses a proton-translocating nicotinamide adenine dinucleotide transhydrogenase (GOX0310-GOX0312, *pntA1A2B*) (Deppenmeier and Ehrenreich 2009). In many bacteria and animal mitochondria, transhydrogenases are able to couple the reversible hydride transfer between NADPH + H^+ and NAD^+ with the translocation of protons across the membrane (Cotton et al. 2001; Bizouarn et al. 2002; Pedersen et al. 2008).

$$\mathbf{H^+_{out} + NADH + NADP^+ \leftrightarrow H^+_{in} + NAD^+ + NADPH}$$

As *G. oxydans*, in comparison to other organisms, produces NADPH not only via the PPP but also via incomplete oxidation reactions in the cytoplasm, it is assumed that *G. oxydans* does not face the problem to generate NADPH for anabolic processes, but to regenerate NADP.

The genome sequence gave the hint, that the regeneration of NADP may occur via transhydrogenase and in addition may translocate protons across the membrane, thereby participating in the formation of a membrane potential (Prust 2004). The resulting NADH might then be reoxidized by the membrane-bound type II NADH dehydrogenase. This might be an additional way to build up proton-motive force and to synthesize ATP via ATP synthase.

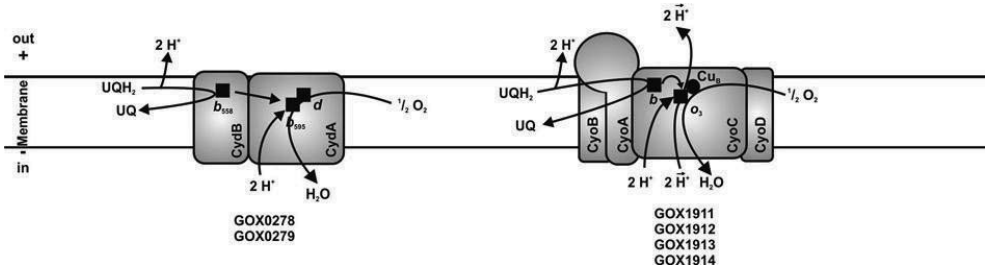

Fig. 5: Schematic representation of subunit composition, cofactors, topology, electron flow and involvement in the generation of a proton-motive force for the terminal oxidases of the *G. oxydans* respiratory chain. Heme groups are indicated by black squares, copper ions by black circles; UQ, ubiquinone; $\overrightarrow{H^+}$, vectorial proton transfer.

2.3.2 Energy generation via the respiratory chain

G. oxydans possesses 32 membrane-bound dehydrogenases, 11 with known and 21 with unknown substrate specificity (Deppenmeier et al. 2002). These dehydrogenases directly transfer electrons to the ubiquinone pool, whereas in other organisms like *E. coli* the electrons stem from the cytoplasmic space. Electron transfer from ubiquinol to oxygen is catalyzed by two terminal oxidases, cytochrome *bd* and cytochrome bo_3. The ability of proton translocation across the membrane via the terminal oxidases is important for the efficiency of cellular growth.

By reconstitution of the purified cytochrome bo_3 oxidase of *G. suboxydans* it was shown that the enzyme generates a proton electrochemical gradient (inside of the vesicle negative and alkaline) of -140 mV during ubiquinol oxidation (Matsushita et al. 1987). For *E. coli* the value was determined to be -145 mV (Kita et al. 1982). Thus, the cytochrome bo_3 oxidase of *G. oxydans*, as the one of *E. coli*, presumably function as an active proton pump (Matsushita et al. 1987; Puustinen et al. 1989; Puustinen et al. 1991). The cytochrome *bd* oxidase of *G. oxydans* on the other hand is not an active proton pump, nevertheless, the catalyzed reaction is also assumed to be able to build up proton motive force. In *E. coli,* the protons

from quinone oxidation are released in the periplasmic space, whereas the protons used for the generation of water are taken from the cytoplasmic space, (Miller and Gennis 1985). Hence, the reaction is coupled to charge separation across the membrane and the formation of proton-motive force and the H^+/O ratio is assumed to be 2. The H^+/O ratio of cytochrome bo_3 oxidase is assumed to be four. It is composed of charge separation across the membrane as described above plus active proton pumping. This is in good agreement with values reported for *E. coli* that are in a range of 3.4-4.0 (Lawford and Haddock 1973). They measured the change in the pH after the addition of defined amounts of air-saturated KCl solution to an *E. coli* cell culture. The cells were grown with different carbon sources and different substrates were added prior to the oxygen pulse, but these alterations did not have a significant effect on the H^+/O ratio. Nevertheless, the ratio might even be higher depending on the combination and composition of the respiratory chain as either H^+-pumping NDH-I or the non-pumping NDH-II reduces ubiquinone and the resulting ubiquinole is than reoxidized by either cytochrome bo_3 (translocating 4 H^+/O) or cytochrome *bd* (translocating 2 H^+/O) (Minohara et al. 2002). As an example, plasmid based expression of *cyoABCDE* in an *E. coli* strain lacking both, cytochrome *bd* and cytochrome bo_3 oxidase, leads to an improved H^+/O ratio of 5.2 compared to the wild type strain having an H^+/O ratio of 4.8, whereas the Δ*cyoBACD* deletion mutant only has a H^+/O ratio of 3.81 (Minohara et al. 2002).

In contrast to *G. oxydans*, *E. coli* possesses two NADH-ubiquinone reductases, NDH-I, a multi-subunit proton-pumping complex enzyme (Brandt et al. 2003), and the single-subunit NDH-II, which lacks an energy coupling site (Calhoun et al. 1993). Since the electrogenic NDH-I is preferentially synthesized during anaerobic growth in the presence of alternate electron acceptors, during aerobic growth the nonelectrogenic NDH-II is the dominant NADH:Q oxidoreductase (Tran and Unden 1998). The genome of *G. oxydans* only encodes the gene for NDH-II (Prust et al. 2005) and therefore, NADH oxidation does not add to the H+/O ratio in both organisms under aerobic conditions.

2.4. Aims of this work

Despite the usefulness of the acetic acid bacterium *G. oxydans* and its promising potential in industrial biotechnology, current knowledge on its metabolism and the respiratory chain is quite limited. This situation hampers the rational design of production strains and the optimization of existing biotechnological processes using this organism. The publication of the genome sequence in 2005 was followed by a rapid development of molecular techniques for the characterization of *G. oxydans* (Kallnik et al. 2010; Meyer et al. 2012). The lack of an

effective method for the generation of deletion mutants was overcome by the development of the *upp*-method, as the formerly used *sacB* deletion method was time consuming and not always successfull (Katzen et al. 1999; Hanke et al. 2012; Peters et al. 2012).

In this work, the importance of EDP and the PPP for intracellular sugar metabolism should be investigated by construction and analysis of two deletion mutants. One should lack the gene for 6-phosphogluconate dehydrogenase (GOX1705, *gnd*), thus inactivating the PPP. In the other, the genes encoding 6-phosphogluconate dehydratase and KDPG aldolase should be deleted (GOX0431 and GOX0430; *edd* and *eda*), thus inactivating the EDP. The resulting strains should be characterized with respect to growth on different carbon sources, enzyme activities, changes in global gene expression as well as by-product formation.

A key feature of G. oxydans is its capability for rapid oxidation of substrates in the periplasm by several membrane-bound dehydrogenases and two terminal oxidases. A second aim of this work was to determine the importance of the two terminal oxidases, the cytochrome bo_3 oxidase and the cytochrome *bd* oxidase. For this purpose, deletion mutants should be constructed lacking either the *cyoBACD* genes or the *cydAB* genes and characterized with respect to growth, H^+/O ratios, and cytochrome content. The genome sequence had revealed the presence of genes for a cytochrome bc_1 complex, whereas genes encoding cytochrome *c* oxidase were absent. Thus, the function of the bc_1 complex is unclear. Growth characterization of a strain lacking the genes for the cytochrome bc_1 complex revealed inhibited growth at pH 4 with mannitol as carbon source (Hanke 2010). In this work, this phenomenon should be analyzed using DNA microarray technology in order to get hints on the function of the cytochrome bc_1 complex.

3. Results

In the first part of this thesis the importance of the PPP and the EDP in intracellular carbon metabolism of *G. oxydans* was studied. The publication “Mutational analysis of the pentose phosphate and Entner-Doudoroff pathway in *Gluconobacter oxydans* reveals improved growth of an Δ*edd* Δ*eda* mutant on mannitol” (Applied and Environmental Microbiology, vol. 78, pp. 6975-6986) describes the construction and characterization of two deletion mutants lacking either the gene for 6-phosphogluconate dehydrogenase (PPP disrupted) or the genes for 6-phosphogluconate dehydratase or KDPG aldolase (EDP disrupted). The work showed that neither of the two pathways is essential for growth on mannitol, but whereas absence of the PPP caused growth inhibition, absence of the EDP improved growth on mannitol.

The manuscript “Role of the pentose phosphate pathway and the Entner-Doudoroff pathway in glucose metabolism of *Gluconobacter oxydans* 621H” (submitted) shows that neither of the two pathways is essential for growth with glucose. Absence of the EDP led to a reduced formation of acetate in the second growth phase, indicating that the EDP is a major route for acetate formation in *G. oxydans.* Furthermore, sensitivity of *G. oxydans* cells to pH values above 6 was demonstrated in this study.

In the second part of this thesis, selected components of the respiratory chain of *G. oxydans* were studied. The publication “Influence of oxygen limitation, absence of the cytochrome bc_1 complex and low pH on global gene expression in *Gluconobacter oxydans* 621H using DNA microarray technology” (Journal of Biotechnology, vol. 157, pp. 359–372) shows a transcriptome comparison of a cytochrome bc_1 deletion mutant versus the reference strain. The transcriptome pattern obtained was similar to the one observed in a comparison of cells grown under oxygen limitation versus oxygen excess, indicating a function of the cytochrome bc_1 complex in respiration. Unfortunately, hints on the electron end acceptor of the bc_1 complex or its specific function were not obtained by this approach.

In the manuscript “Properties of *Gluconobacter oxydans* mutants lacking either cytochrome bo_3 oxidase or cytochrome *bd* oxidase” (to be submitted), the deletion mutants Δ*cyoBACD* and Δ*cydAB* were characterized with respect to growth, product formation, H^+/O-ratios and cytochrome spectra. The results indicated that the cytochrome bo_3 oxidase is the main terminal oxidase and is actively taking part in the formation of an electrochemical proton gradient across the membrane. The results gave rise to the question whether the formation of H_2O from oxygen might occur on the periplasmic rather than on the cytoplasmic side of the cell membrane.

3.1. Improved growth of *G. oxydans* Δ*edd* Δ*eda* on mannitol

Own contribution to this publication: about 70 %. I performed all experimental work described in the publication and wrote a draft of the manuscript. I am first author of the publication.

Published in: Applied and Environmental Microbiology, Vol. 78, pp. 6975-6986

Impact factor: 3.829

AEM
Journals.ASM.org

Mutational Analysis of the Pentose Phosphate and Entner-Doudoroff Pathways in *Gluconobacter oxydans* Reveals Improved Growth of a Δ*edd* Δ*eda* Mutant on Mannitol

Janine Richhardt, Stephanie Bringer, and Michael Bott
Institut für Bio- und Geowissenschaften, IBG-1: Biotechnologie, Forschungszentrum Jülich, Jülich, Germany

The obligatory aerobic acetic acid bacterium *Gluconobacter oxydans* 621H oxidizes sugars and sugar alcohols primarily in the periplasm, and only a small fraction is metabolized in the cytoplasm. The latter can occur either via the Entner-Doudoroff pathway (EDP) or via the pentose phosphate pathway (PPP). The Embden-Meyerhof pathway is nonfunctional, and a cyclic operation of the tricarboxylic acid cycle is prevented by the absence of succinate dehydrogenase. In this work, the cytoplasmic catabolism of fructose formed by oxidation of mannitol was analyzed with a Δ*gnd* mutant lacking the oxidative PPP and a Δ*edd* Δ*eda* mutant devoid of the EDP. The growth characteristics of the two mutants under controlled conditions with mannitol as the carbon source and enzyme activities showed that the PPP is the main route for cytoplasmic fructose catabolism, whereas the EDP is dispensable and even unfavorable. The Δ*edd* Δ*eda* mutant (lacking 6-phosphogluconate dehydratase and 2-keto-3-deoxy-6-phosphogluconate aldolase) formed 24% more cell mass than the reference strain. In contrast, deletion of *gnd* (6-phosphogluconate dehydrogenase) severely inhibited growth and caused a strong selection pressure for secondary mutations inactivating glucose-6-phosphate dehydrogenase, thus preventing fructose catabolism via the EDP also. These Δ*gnd zwf mutants (with a mutation in the *zwf* gene causing inactivation of the glucose-6-phosphate dehydrogenase) were almost totally disabled in fructose catabolism but still produced about 14% of the carbon dioxide of the reference strain, possibly by catabolizing substrates from the yeast extract. Overexpression of *gnd* in the reference strain improved biomass formation in a similar manner as deletion of *edd* and *eda*, further confirming the importance of the PPP for cytoplasmic fructose catabolism.**

Gluconobacter oxydans is a Gram-negative, strictly aerobic, rod-shaped alphaproteobacterium belonging to the family of acetic acid bacteria (10). It has been used for a long time in industrial biotechnology, mainly in the production of vitamin C and 6-amino-L-sorbose, a key intermediate for the synthesis of the anti-diabetic drug miglitol (20). *G. oxydans* 621H, whose genome sequence has been determined (19), possesses two spatially separated modes of sugar catabolism. One occurs in the periplasm, where membrane-bound dehydrogenases catalyze the oxidation of sugars and sugar alcohols and feed the electrons into the respiratory chain. The second mode is located in the cytoplasm, where sugars can be catabolized either via the pentose phosphate pathway (PPP) or via the Entner-Doudoroff pathway (EDP) (see Fig. 1). Due to the absence of a gene encoding 6-phosphofructokinase, the Embden-Meyerhof-Parnas pathway (EMP) is nonfunctional (19). Likewise, the tricarboxylic acid (TCA) cycle is incomplete because the genes for succinate dehydrogenase and also succinyl-coenzyme A (CoA) synthetase are lacking (19).

In this work, we addressed the question of the importance of the PPP and the EDP for cytoplasmic sugar catabolism in *G. oxydans*. To this end, mutants defective in either pathway were constructed and analyzed with respect to their growth on mannitol, DNA microarray analyses, and enzyme activities. The results indicate that the PPP is essential for fructose catabolism, whereas the EDP is dispensable.

MATERIALS AND METHODS

Materials. Chemicals were obtained from Sigma-Aldrich (Taufkirchen, Germany), Qiagen (Hilden, Germany), Merck (Darmstadt, Germany), and Roche Diagnostics (Mannheim, Germany).

Bacterial strains, plasmids, media, and growth conditions. The bacterial strains and plasmids used in this study are listed in Table 1. The *Escherichia coli* strains were cultivated in lysogeny broth (LB) medium or on LB agar plates at 37°C (2, 3) When required, kanamycin was added to a final concentration of 50 μg ml^{-1}. *Gluconobacter oxydans* ATCC 621H Δ*upp* (ATCC 621H is identical to DSM2343), which lacks the *upp* gene for uracil phosphoribosyltransferase, was obtained from Armin Ehrenreich (Technical University of Munich, Germany). The strain was cultivated on mannitol medium containing 220 mM (4% [wt/vol]) mannitol, 5 g $liter^{-1}$ yeast extract, 2.5 g $liter^{-1}$ $MgSO_4 \cdot 7H_2O$, 1 g $liter^{-1}$ $(NH_4)_2SO_4$, 1 g $liter^{-1}$ KH_2PO_4, and 10 μM thymidine. The initial pH value of the medium was 6.0. *G. oxydans* possesses a natural resistance toward cefoxitin; as a precaution to prevent bacterial contamination, cefoxitin was added to the medium at a concentration of 50 μg ml^{-1}. When required, kanamycin (50 μg ml^{-1}) was added. Precultures were grown in baffled shaking flasks at 30°C and 140 rpm. For determination of growth parameters, DNA microarray analyses, and enzyme activity measurements, the cells were cultivated in 250 ml of the same medium in a bioreactor system (DASGIP, Jülich, Germany) composed of four 400-ml vessels, each equipped with electrodes for measuring the dissolved oxygen concentration (DO) and the pH. The system allows us to constantly control these two parameters. The carbon dioxide concentration in the exhaust gas was measured continuously by an infrared spectrometer. The pH was kept at pH 6.0 by

Received 17 April 2012 **Accepted** 18 July 2012
Published ahead of print 27 July 2012
Address correspondence to Stephanie Bringer, st.bringer-meyer@fz-juelich.de, or Michael Bott, m.bott@fz-juelich.de.
Supplemental material for this article may be found at http://aem.asm.org/.

doi:10.1128/AEM.01166-12

TABLE 1 Bacterial strains, plasmids, and oligonucleotides used in this work

Bacterial strain, plasmid, or oligonucleotide	Description or primer sequence (5′→3′ sequence)[a]	Reference, source, or added restriction site
Strains		
E. coli DH5αF′	*endA1 hsdR17* (r_K^- m_K^+) *supE44 thi-1 recA1 gyrA96 relA1* Δ(*lacIZYA–argF*)*U169 deoR* F′ [ϕ80d*lacZ*Δ(*lacZ*)M15]	6
E. coli S17-1	Δ*recA endA1 hsdR17 supE44 thi-1 tra*$^+$	24
G. oxydans Δ*upp*	*G. oxydans* 621H derivative with a deletion of GOX0327 coding for uracil phosphoribosyltransferase	A. Ehrenreich (TU Munich)
G. oxydans Δ*upp* Δ*edd* Δ*eda*	*G. oxydans* Δ*upp* derivative with a deletion of the *edd* (GOX0431) and *eda* (GOX0430) genes coding for 6-phosphogluconate dehydratase and 2-keto-3-desoxy-6-phosphogluconate aldolase	This work
G. oxydans Δ*upp* Δ*gnd*	*G. oxydans* Δ*upp* derivative with a deletion of the *gnd* gene (GOX1705) coding for 6-phosphogluconate dehydrogenase	This work
G. oxydans Δ*upp* Δ*gnd zwf*$^+$	*G. oxydans* Δ*upp* Δ*gnd* derivative with a mutation in *zwf* (GOX0145), causing inactivation of the encoded glucose-6-phosphate dehydrogenase	This work
Plasmids		
pAJ63a	Kan^r; pK18mobGII derivative; *lacZ mob oriV*, GOX0327 and GOX0328	A. Ehrenreich (TU Munich); 9
pAJ-*edd-eda*	Kan^r; pAJ63a derivative used for marker-free deletion of the *edd* and *eda* genes; contains an overlap extension PCR product covering the 20-bp upstream region of *edd* and the 36-bp downstream region of *eda*	This work
pAJ-*gnd*	Kan^r; pAJ63a derivative used for marker-free deletion of the *gnd* gene; contains an overlap extension PCR product covering 20-bp upstream region and the 67-bp downstream region of *gnd*	This work
pBBR1p384	Kan^r; pBBR1MCS-2 derivative containing the 5′ untranslated region of *gox0384*	U. Deppenmeier (University of Bonn); 11
pBBR1p384-*edd-eda*	Kan^r; pBBR1p384 derivative expressing *edd* and *eda*	This work
pBBR1p384-*gnd*	Kan^r; pBBR1p384 derivative expressing *gnd*	This work
Oligonucleotides		
edd-eda_forw_FlA	AACTGCTCCCAGTGTGAGTG	
edd-eda_rev_FlA	CGTGAAGAGTGCCGCCATCTGGAAATACTCGCTACTCGGCTGATGCCTGC	
edd-eda_forw_FlB	GAGTATTTCCAGATGGCGGCACTCTTCACGGTCTGATCTTCGAAGCGTTT	
edd-eda_rev_FlB	ATAAGGCCAGAGCGAGAGTC	
edd-eda_mut_forw	GGCGTTCATGATGTCCTG	
edd-eda_mut_rev	CCCAGAAGGCAGAGAATG	
edd-eda_forw	TATCCCGAGCAGATCAAG	
edd-eda_rev	ACATCGCGCAGGATATCG	
gnd_forw_FlA	GGATGGTCCGCTGTCCTTC	
gnd_rev_FlA	CTTTTCGACGTGTCCCATGACTTATGCTCCTGCCAGTGCTTTGTGGATCG	
gnd_forw_FlB	GGAGCATAAGTCATGGGACACGTCGAAAAGAAATGAGCCTGCGTCCCGCA	
gnd_rev_FlB	TGCACCATCCAGTAGGAC	
gnd_mut_forw	ACTGACTTCGGCCTATGC	
gnd_mut_rev	GCCCTGCTCGTGCTGCACGAAG	
gnd_forw	GGCGGACATGGCAAAGCTTC	
gnd_rev	CCAGACTTCCGCGATGTCAC	
zwf_forw	CGCTGCACGAACACAGCATC	
zwf_rev	ACCAGCTCAGCTTGCTGAAC	
Compl_edd-eda_forw_EcoRI	CCGGAAGAATTCCGAGTAGCGAGTATTTCCAG	EcoRI
Compl_edd-eda_rev_XhoI	TCGAGTCTCGAGGCAACATTCTGACGGCATCC	XhoI
Compl_gnd_forw_EcoRI	CCGGAAGAATTCCACTGGCAGGAGCATAAGTC	EcoRI
Compl_gnd_rev_XhoI	GGTTCACTCGAGGGCTGGCTGGTCATTGATGG	XhoI

[a] Underlined sequences denote complementary regions for overlap extension-PCR.

automatic titration of 2 M NaOH. The oxygen availability was kept constant at 15% DO by mixing air, O_2, and N_2. Calibration was performed by gassing with air (100% DO) and N_2 (0% DO). The agitation speed was kept constant at 900 rpm. Control and recording of all data was carried out by the Fedbatch Pro software program (DASGIP, Jülich, Germany).

Cultivation of the bacteria for complementation of deletion mutants was performed in 500-ml baffled shaking flasks containing 100 ml mannitol medium. Incubation was at 140 rpm and 30°C in an Infors shaker (Basel, Switzerland).

Cloning and DNA techniques. The standard methods of DNA manipulation as described by Sambrook and Russell (22) were used. For PCRs, genomic DNA isolated from *G. oxydans* 621H Δ*upp* mutant strain was used as the template. Competent cells of *E. coli* were prepared with $CaCl_2$ and transformed by the method of Hanahan et al. (6). DNA sequencing was performed by Agowa (Berlin, Germany) and Eurofins

MWG Operon (Ebersberg, Germany). Oligonucleotides were synthesized by Biolegio (Nijmegen, Netherlands) and are listed in Table 1.

Construction of strains carrying in-frame deletion mutations. Strains carrying in-frame deletion mutations of the *edd* (GOX0431) and *eda* (GOX0430) genes and of *gnd* (GOX1705) were constructed via a two-step homologous recombination protocol developed by the research group of Armin Ehrenreich (B. Peters, A. Junker, K. Brauer, D. Kostner, M. Mientus, W. Liebl, and A. Ehrenreich, submitted for publication). The *G. oxydans* Δ*upp* mutant strain lacks the GOX0327 gene that codes for uracil phosphoribosyltransferase (UPRTase). UPRTase is a key enzyme for the usage of uracil, as it converts uracil to UMP, an intermediate of pyrimidine biosynthesis. The toxic pyrimidine analogue 5-fluorouracil (5-FU) can also be converted by UPRTase to 5-fluoro-UMP. This can be further converted to 5-fluoro-dUMP, a strong inhibitor of thymidylate synthase, which is essential for DNA synthesis and repair. The strain lacking the *upp* gene possesses resistance against 5-FU. When the first homologous recombination event has taken place and the plasmid, which contains the *upp* gene (GOX0327), together with GOX0328, is integrated into the chromosome, the strain becomes 5-FU sensitive again. The GOX0328 gene was cloned together with GOX0327, since it presumably contains the promoter sequence of the *upp* gene (Armin Ehrenreich, personal communication). For the second homologous recombination event, 5-FU can be used for counterselection, as only cells that have excised the plasmid are able to grow.

The procedure will be described for *gnd*; deletion of *edd* and *eda* was performed analogously. Five-hundred-base-pair sections of the up- and downstream regions of *gnd* were amplified using the primer pairs gnd-_forw_FlA/gnd_rev_FlA (forw stands for forward, and rev stands for reverse) and gnd_forw_FlB/gnd_rev_FlB using Phusion DNA polymerase (Fisher Scientific, Schwerte, Germany). The two PCR fragments were fused by overlap extension PCR using the oligonucleotide pair gnd_forw_FlA/gnd_rev_FlB using Platinum Pfx DNA polymerase (Invitrogen, Darmstadt, Germany). The resulting 1-kb product was cloned into the SmaI-restricted plasmid pAJ63a, which is nonreplicative in *G. oxydans*.

The pAJ-*gnd* plasmid was used in performing an allelic exchange by homologous recombination into the chromosome of the *G. oxydans* 621H Δ*upp* mutant strain. *E. coli* S17-1 was transformed with pAJ-*gnd* and used as a donor strain for conjugational DNA transfer of the plasmids into *G. oxydans*. For mating, *E. coli* was cultivated in 100 ml LB medium with kanamycin and *G. oxydans* was cultivated in 100 ml complex medium with cefoxitin. The cells were cultivated to an optical density at 600 nm (OD_{600}) of 0.6 to 0.8; 50 ml of each culture was harvested by centrifugation and washed twice with mannitol medium. Cells from both cultures were resuspended in 0.5 ml mannitol medium, mixed thoroughly, dropped on mannitol medium agar, and incubated overnight at 30°C. The cells were washed from the plate with 1 ml mannitol medium. One hundred microliters of the undiluted suspension and 100 μl of the 10-fold-diluted suspension were plated onto mannitol medium agar containing kanamycin and cefoxitin, which selects for *G. oxydans* cells harboring the plasmid. The remaining undiluted suspension was centrifuged, and the pellet was resuspended in 100 μl mannitol medium and also plated on agar plates described above. The plates were incubated for 2 to 4 days at 30°C until colonies formed. Colonies were screened by PCR for chromosomal integration of pAJ-*gnd* via a single homologous crossover event using the oligonucleotides gnd_mut_forw (mut stands for mutant) and gnd_mut_rev. Positive clones were inoculated overnight in 20 ml mannitol medium containing cefoxitin and kanamycin and used as a preculture for the enforcement of excision. An aliquot (2 ml) of the overnight culture was harvested, washed twice with recombination medium (2.5 g $liter^{-1}$ yeast extract, 1 g $liter^{-1}$ $MgSO_4 \cdot 7H_2O$) and resuspended in 500 μl recombination medium. A 2.5-ml portion of recombination medium was inoculated with the washed cells and incubated for 6 to 8 h at 30°C. Afterwards, the cells were diluted (up to 10^{-3}) and spread on mannitol medium plates containing cefoxitin and 60 μg ml^{-1} 5′-fluorouracil. The plates were incubated for about 3 days at 30°C. Fluorouracil-resistant colonies were screened by PCR for the chromosomal deletion of *gnd* using the oligonucleotide pair gnd_mut_forw/gnd_mut_rev. Of three (*edd eda*) and eight (*gnd*) positive clones, the up- and downstream regions of the deleted gene(s) were sequenced, and the corresponding strains were named *G. oxydans* Δ*upp* Δ*gnd* clones 1 to 8 and *G. oxydans* Δ*upp* Δ*edd* Δ*eda* clones 1 to 3. The *zwf* gene of the eight *G. oxydans* Δ*upp* Δ*gnd* strains was sequenced using the oligonucleotides zwf_forw and zwf_rev.

Plasmid-based expression of the *edd* and *eda* genes and of the *gnd* gene. For complementation of the deletion mutants, the broad-host-range plasmid pBBR1p384 was used. The procedure will be described for *gnd*, but expression of *edd* and *eda* was performed analogously. The *gnd* gene with its native ribosome binding site was amplified using Phusion DNA polymerase (Fisher Scientific, Schwerte, Germany) with the primers Compl_gnd_forw_EcoRI (Compl stands for complementation) and Compl_gnd_rev_XhoI. The PCR product was digested with EcoRI and XhoI and cloned into the EcoRI/XhoI-restricted plasmid pBBR1p384. The resulting plasmid, pBBR1p384-*gnd*, was transformed into *E. coli* S17-1 and used for conjugational DNA transfer of the plasmid into *G. oxydans*. Mating was performed as described above under "Construction of strains carrying in-frame deletion mutations" except that the cells were diluted up to 10^{-3} before they were spread on mannitol agar plates containing cefoxitin and kanamycin. For growth experiments of the strains expressing the genes, a 20-ml preculture (mannitol medium) was used for the inoculation of 100 ml mannitol medium in a 500-ml baffled shaking flask to an OD_{600} of 0.3. The cultures were incubated at 30°C and 140 rpm in an Infors shaker (Basel, Switzerland). At selected time points, samples were taken for measurement of optical density.

RNA preparation, cDNA labeling, and DNA microarray analysis. The protocol for RNA preparation and cDNA labeling as well as the *G. oxydans* DNA microarrays were described recently by Hanke et al. (7). For the transcriptome comparisons of Δ*upp* Δ*gnd* *zwf** cells (with a mutation in the *zwf* gene causing inactivation of the glucose-6-phosphate dehydrogenase) versus Δ*upp* cells and of Δ*upp* Δ*edd* Δ*eda* cells versus Δ*upp* cells, hybridization was carried out for 16 to 18 h at 42°C using a MAUI hybridization system (BioMicro Systems, Salt Lake City, UT). For the transcriptome comparison of Δ*upp* Δ*gnd* cells versus Δ*upp* cells, hybridization was done in a water bath for 16 to 18 h at 42°C. Each transcriptome comparison was repeated independently at least three times in biological replicates. To filter for differentially expressed genes, the following criteria had to be fulfilled: (i) flags of ≥0 (GenePix Pro 6.0), (ii) signal/noise ratio of ≥5 for Cy5 (F635Median/B635Median, GenePix Pro 6.0) or Cy3 (F532Median/B532Median, GenePix Pro 6.0), (iii) mRNA ratio of ≥2.0 (lower ones allowed in the case of operons) or ≤0.5 (higher ones allowed in the case of operons), (iv) in a paired Student *t* test, relative RNA levels had to be significantly different from the values for all spots ($P < 0.05$).

Determination of substrates and products by HPLC analysis. One-milliliter samples from culture were centrifuged for 5 min at 13,000 × *g*, and the supernatant was filtered through a 0.2-μm filter (Millipore, MA) prior to high-performance liquid chromatography (HPLC) analysis. Mannitol, fructose, and 5-ketofructose were quantified with a Rezex RCM-Monosaccharide 300- by 7.8-mm column (Phenomenex, Aschaffenburg, Germany) at 60°C using H_2O as the eluent at a flow rate of 0.6 ml min^{-1}. Substances were detected by a refractive index detector. The retention times for 5-ketofructose, fructose, and mannitol were 13.47, 15.13, and 19.84 min, respectively. Calibration curves were made using a series of standards ranging from 1 to 10 g $liter^{-1}$ mannitol or fructose and from 1 to 5 g $liter^{-1}$ 5-ketofructose. Acetate concentrations were measured with an organic acid resin 300- by 8-mm column (CS-Chromatographie Service, Langerwehe, Germany) at 40°C using 0.1 M H_2SO_4 as the eluent at a flow rate of 0.5 ml min^{-1}. Acetate was detected with an UV detector at 215 nm, and the retention time was 20.3 min. A calibration curve was made using acetate standards from 1 to 10 mM.

Enzyme assays. For *in vitro* determinations of enzyme activities, culture samples (10 ml) were taken after 12 h of cultivation (Δ*upp* and Δ*upp*

Δ*edd* Δ*eda* cells) or at an OD_{600} of 1.5 (Δ*upp*, Δ*upp* Δ*gnd*, and Δ*upp* Δ*gnd zwf** cells), and centrifuged at 10,414 × *g* for 3 min. The cells were resuspended in 800 μl of 50 mM Tris-HCl (pH 7.5) and disrupted at 4°C by bead beating (three times for 15 s each time) with 0.1-mm-diameter glass beads using a Silamat S5 (Ivoclar Vivadent GmbH, Germany). The crude extracts were centrifuged at 16,000 × *g* (4°C, 30 min) to remove intact cells and cell debris, and the supernatants were used as cell extracts. Glucose-6-phosphate dehydrogenase and 6-phosphogluconate dehydrogenase activities were measured photometrically at 340 nm and 30°C using three different dilutions of the cell extract according to standard methods (16). Protein concentrations were determined by the method of Bradford (4) using bovine serum albumin as the standard.

Determination of cell weight (dry weight). At three different time points during the growth of *G. oxydans* Δ*upp* and *G. oxydans* Δ*upp* Δ*edd* Δ*eda* mutant strains on mannitol in a bioreactor system with four vessels, the optical densities at 600 nm were determined, and 10-ml culture from each bioreactor was harvested by centrifugation for 5 min at 4°C and 10,397 × *g*. The supernatants were discarded, and the cells were washed with 5 ml H_2O and harvested again by centrifugation (5 min at 4°C and 10,397 × *g*). The supernatants were discarded, and the cells were resuspended in 1 ml H_2O and transferred into aluminum trays of known weight. The cells were dried for 24 h at 110°C, and then the trays were weighed again. A linear correlation between cell weight (dry weight) and OD_{600} was obtained, and an OD_{600} of 1 corresponded to 0.32 g of cells (dry weight) per liter.

Microarray data accession number. The data discussed in this publication have been deposited in NCBI's Gene Expression Omnibus and are accessible through GEO Series accession number GSE38933 (http://www.ncbi.nlm.nih.gov/geo/query/acc.cgi?acc=GSE38933).

RESULTS

Mannitol catabolism in *G. oxydans*. In this work, we addressed the question of the importance of the PPP and the EDP in cytoplasmic sugar catabolism by *G. oxydans*. For our studies, we used mannitol, which is one of the preferred carbon sources of this species. A scheme of the central carbon metabolism of *G. oxydans*, including the reactions involved in mannitol catabolism is shown in Fig. 1. In Fig. 2 and Tables 2 and 3, growth in mannitol medium, substrate consumption, product formation, and carbon balances are shown for the reference strain, namely, the *G. oxydans* Δ*upp* strain, and the deletion mutants described below. In the first growth phase (growth phase I), which is associated with fast growth, the major part of mannitol is rapidly oxidized in the periplasm to fructose by the major polyol dehydrogenase SldAB (GOX0854 and GOX0855). In the second growth phase, which starts when mannitol is almost completely converted and is associated with slower growth, part of the fructose is further oxidized to 5-ketofructose by a yet uncharacterized enzyme. A minor part of mannitol is taken up via a putative mannitol/sorbitol ABC transporter (GOX2182 to GOX2185), which involves a periplasmic binding protein (GOX2185) (19). Fructose can also be taken up, but the responsible transporter is not known yet. In the cytoplasm, mannitol is directly oxidized to fructose, most probably by an enzyme different from sorbitol dehydrogenase (GOX1432) (18). Fructose is phosphorylated by fructokinase (GOX0284, *frk*) to fructose-6-phosphate, which is converted by phosphoglucose isomerase (GOX1704, *pgi*) to glucose-6-phosphate, the precursor of both the PPP and the EDP. As mentioned before, 6-phosphofructokinase is absent in *G. oxydans* 621H. Acetate, which accumulates in the medium during cultivation (Fig. 2), is synthesized from pyruvate via acetaldehyde in reactions catalyzed by pyruvate decarboxylase (GOX1081) and an NADP-dependent acetaldehyde dehydrogenase (GOX2018) (Fig. 1) (12).

Characterization of *G. oxydans* Δ*upp* Δ*gnd* and Δ*upp* Δ*gnd zwf cells lacking 6-phosphogluconate dehydrogenase or also lacking glucose-6-phosphate dehydrogenase.** In order to test the role of the oxidative part of the PPP in fructose catabolism, the *gnd* gene encoding 6-phosphogluconate dehydrogenase was deleted as described in Materials and Methods. Thirty-four kanamycin-sensitive and 5-FU-resistant clones were analyzed by PCR, and eight clones were found to have the desired *gnd* deletion (named Δ*upp* Δ*gnd* clones 1 to 8). In the first set of experiments, the enzymatic activities of glucose-6-phosphate dehydrogenase (G6P-DH) and 6-phosphogluconate dehydrogenase (6PG-DH) were tested in cell extracts of the eight mutant clones harvested in the mid-exponential growth phase. The reference strain, the *G. oxydans* Δ*upp* strain, showed a G6P-DH activity of 0.53 ± 0.020 μmol min^{-1} mg of $protein^{-1}$ and a 6PG-DH activity of 0.07 ± 0.005 μmol min^{-1} mg of $protein^{-1}$ (Table 4). As expected, no 6PG-DH activity (≤0.001 μmol min^{-1} mg of $protein^{-1}$) was measured in the eight Δ*upp* Δ*gnd* clones, confirming that *gnd* is the only gene coding for this activity. Surprisingly, however, five of the clones (clones 1 to 5) also had no G6P-DH activity (≤0.004 μmol min^{-1} mg of $protein^{-1}$), and three clones (clones 6 to 8) exhibited reduced activity (0.32, 0.15, and 0.33 μmol min^{-1} mg of $protein^{-1}$). Therefore, the *zwf* gene (GOX0145) of the eight clones was amplified and sequenced. In the reference strain, codons 158 to 161 consist of a GCC ACC GCC ACC sequence. In clones 1 to 5, lacking detectable G6P-DH activity, a duplication of the sequence GCC ACC at this position was found, resulting in a 3-fold repeat of this two-codon unit and an addition of two amino acids (aa) (Ala-Thr), prolonging the annotated protein, including the N-terminal methionine from 489 aa to 491 aa. This mutation was the only one found in the *zwf* genes of Δ*gnd* clones 1 and 2 and resulted in a complete inactivation of G6P-DH. Clones 3 to 5 contained in addition 1-bp insertions in different codons, always resulting in a frameshift causing a shortened protein of 259 aa. In clones 6 to 8 showing a reduced G6P-DH activity, no mutation in the *zwf* coding region or the *zwf* promoter region was identified. The results described above suggest that there is a strong selection pressure in the Δ*gnd* mutant for secondary mutations in the *zwf* gene. Unfortunately, we are not aware of energy sources for *G. oxydans* whose metabolism does not involve G6P-DH and which therefore would allow us to delete *gnd* without selection pressure for secondary *zwf* mutations. Therefore, despite this drawback, one Δ*gnd* mutant with an intact *zwf* gene (clone 8) and one Δ*gnd* mutant with a defective *zwf* gene (clone 2) were chosen for the following studies.

The two mutant strains, the Δ*upp* Δ*gnd* and Δ*upp* Δ*gnd zwf** mutant strains, showed 30% and 42% reduced growth rates and 62% and 56% reduced final OD_{600} values (Fig. 2A and B and Table 2). In particular, no biphasic growth was observed. Both mutants completely consumed mannitol, but not as rapidly as the reference strain, due to the slower growth. The reference strain (Δ*upp* strain) required about 8 h for complete mannitol consumption, the Δ*upp* Δ*gnd* strain required about 9 h, and the Δ*upp* Δ*gnd zwf** strain required about 12 h (Fig. 2D and E). Compared to the Δ*upp* strain, fructose uptake was strongly reduced in the Δ*upp* Δ*gnd* strain (88% less than the reference strain) and even stronger in the Δ*upp* Δ*gnd zwf** strain (94% less), which correlates with the absence of a second growth phase. Ketofructose was still formed,

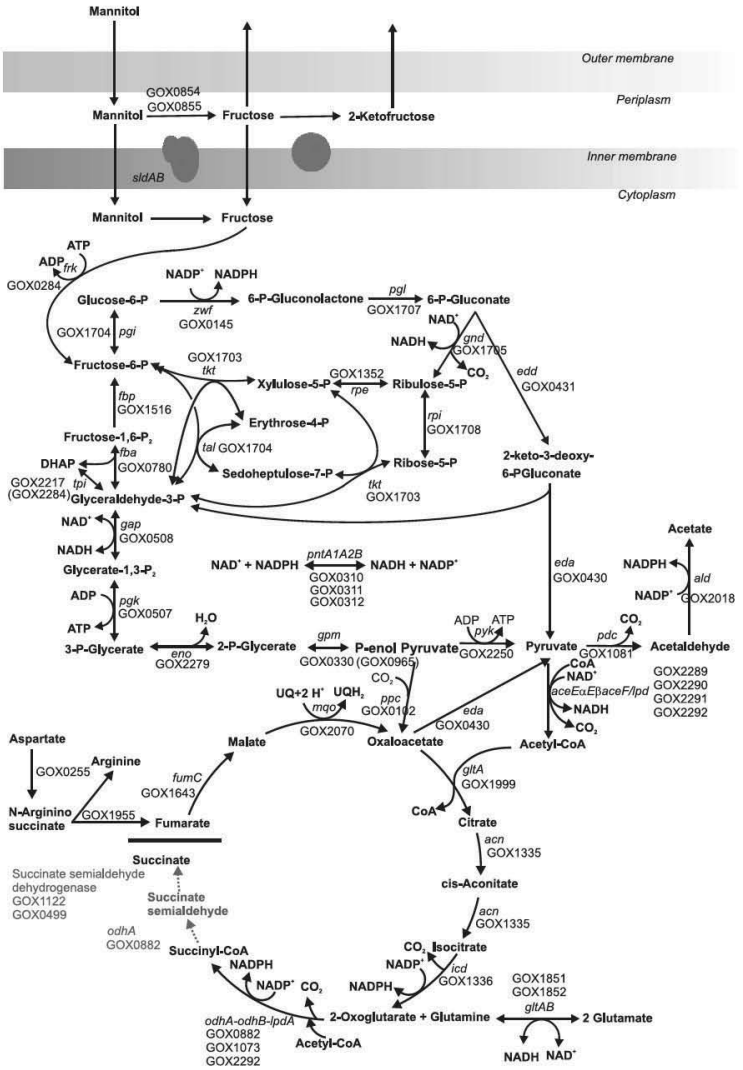

FIG 1 Scheme of the central carbon metabolism of *G. oxydans* with the substrate mannitol. Glucose-6-P, glucose-6-phosphate; Fructose-1,6-P_2, fructose-1,6-bisphosphate; DHAP, dihydroxyacetone phosphate; UQ, ubiquinone; P-enol Pyruvate, phosphoenolpyruvate. Enzymes and genes in gray type could possibly fulfill the depicted functions.

but only 65% (Δ*upp* Δ*gnd*) and 32% (Δ*upp* Δ*gnd zwf**) of the value obtained by the reference strain (Δ*upp*).

The final acetate concentrations formed by the Δ*upp* Δ*gnd* mutants and the Δ*upp* Δ*gnd zwf** mutants were reduced by 25% and 72%, respectively, compared to the reference strain (Fig. 2D and E). Even more drastic were the consequences with respect to carbon dioxide (Fig. 3A and B and Tables 2 and 3). The amount of CO_2 formed was decreased by 84% (Δ*upp* Δ*gnd* mutant) and by 86% (Δ*upp* Δ*gnd*

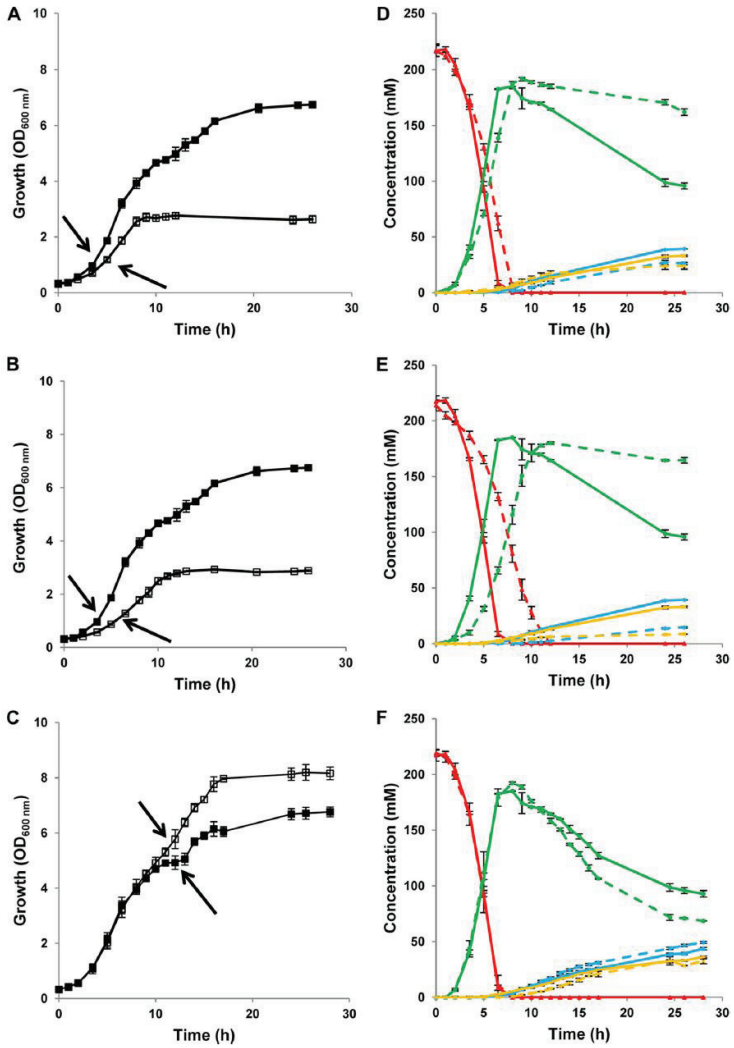

FIG 2 (A to C) Growth of *G. oxydans* deletion strains (open symbols) and the reference strain (*G. oxydans* Δ*upp* strain) (filled symbols). *G. oxydans* Δ*upp* Δ*gnd* (A), Δ*upp* Δ*gnd zwf** (B), and Δ*upp* Δ*edd* Δ*eda* (C) deletion strains were used. (D to F) Substrate consumption and product formation of *G. oxydans* deletion strains (dashed lines) and the reference strain (*G. oxydans* Δ*upp* strain) (solid lines). Δ*upp* Δ*gnd* (D), Δ*upp* Δ*gnd zwf** (E), and Δ*upp* Δ*edd* Δ*eda* (F) strains were used. The cells were cultivated in mannitol medium at 15% dissolved oxygen at pH 6. Mean values ± standard deviations (error bars) for 3 independent cultures are shown. Mannitol (red), fructose (green), 5-ketofructose (blue), and acetate (yellow) are shown. The black arrows indicate the time points of cell harvest for enzyme activity measurements and DNA microarray analysis.

TABLE 2 Growth parameters and percentage of carbon dioxide production due to acetate formation of four *G. oxydans* strains[a]

Growth phase	Parameter[b]	Value[c] of the parameter for *G. oxydans* 621H strain with the following genotype:			
		Δ*upp*	Δ*upp* Δ*gnd*	Δ*upp* Δ*gnd zwf**	Δ*upp* Δ*edd* Δ*eda*
1st	Growth rate (h^{-1})	0.43 ± 0.02	0.30 ± 0.00	0.25 ± 0.02	0.44 ± 0.02
	OD_{600}	3.92 ± 0.18	2.55 ± 0.14	2.78 ± 0.06	4.05 ± 0.27
	Mannitol consumed	216 ± 5	219 ± 4	210 ± 2	218 ± 3
	Fructose formed	182 ± 5	192 ± 1	180 ± 1	192 ± 2
	5-Ketofructose formed	3 ± 0	2 ± 0	2.4 ± 0.1	4.4 ± 1.3
	Difference (mannitol − fructose − ketofructose)[d]	31 ± 5	24 ± 3	28 ± 3	22 ± 2
	$Y_{x/s}$ (g g^{-1} of sugar consumed)[e]	0.21 ± 0.02	0.17 ± 0.01	0.17 ± 0.01	0.30 ± 0.01
2nd	OD_{600}	2.72 ± 0.24	−0.01 ± 0.02	0.11 ± 0.05	4.18 ± 0.08
	Fructose consumed	87 ± 1	30 ± 2	16 ± 3	122 ± 2
	5-Ketofructose formed	37 ± 1	24 ± 1	12 ± 1	42 ± 1
	Difference (fructose − ketofructose)[d]	50 ± 0	6 ± 2	3 ± 4	80 ± 1
	$Y_{x/s}$ (g g^{-1} of sugar consumed)	0.10 ± 0.01	NSG	NSG	0.09 ± 0.00
1st and 2nd	OD_{600}	6.64 ± 0.20	2.54 ± 0.13	2.89 ± 0.03	8.23 ± 0.21
	Mannitol consumed	216 ± 5	219 ± 4	210 ± 2	218 ± 3
	Fructose formed	95 ± 5	162 ± 3	165 ± 3	70 ± 2
	5-Ketofructose formed	40 ± 1	26 ± 1	15 ± 0.8	47 ± 0
	Difference (mannitol − fructose consumed)[d]	84 ± 5	33 ± 3	33 ± 1	106 ± 3
	Acetate formed	32 ± 1	24 ± 3	9 ± 0	28 ± 1
	CO_2 formed	263 ± 12	43 ± 4	37 ± 1	359 ± 5
	Ratio of acetate to CO_2 formed (%)	12	55	23	8

[a] Cells were cultivated in mannitol medium at 15% dissolved oxygen and pH 6 in a bioreactor. For the first growth phase (phase I), the parameters were calculated after 8 h (Δ*upp*), 9 h (Δ*upp* Δ*gnd*), 12 h (Δ*upp* Δ*gnd zwf**), and 8 h (Δ*upp* Δ*edd* Δ*eda*). For the second growth phase (phase II), the parameters were calculated after 26 h of growth.
[b] Substrate and product concentrations are given in millimolar.
[c] The mean values ± standard deviations for three biological replicates are shown. NSG, no significant growth.
[d] The value indicates the amount of sugar (alcohol) taken up into the cytoplasm.
[e] $Y_{x/s}$, cell yield, in grams cell dry weight per gram of sugar consumed.

*zwf** mutant). Whereas the Δ*upp* Δ*gnd* mutant can metabolize fructose via the ED pathway, the Δ*upp* Δ*gnd zwf** mutant presumably no longer has any possibility to catabolize fructose-6-phosphate or glucose-6-phosphate. Therefore, acetate and CO_2 formed by the latter strain are probably derived from the catabolism of amino acids or other components of the yeast extract present in the medium. As a consequence, the ratio of acetate to carbon dioxide of the Δ*upp* Δ*gnd zwf** mutant was only 42% of that of the Δ*upp* Δ*gnd* mutant (Table 2). The cell yields of the Δ*upp* Δ*gnd* and Δ*upp* Δ*gnd zwf** mutants in growth phase I were decreased by 19% (Table 2). As shown in Table 3, the carbon balances of the mutants and the reference strain amounted to more than 90%.

Characterization of *G. oxydans* Δ*upp* Δ*edd* Δ*eda* cells lacking the Entner-Doudoroff pathway. In order to test the role of the ED pathway in fructose catabolism, the *edd* and *eda* genes encoding the key enzymes of the EDP, 6-phosphogluconate dehydratase and 2-keto-3-deoxy-6-phosphogluconate aldolase, were deleted as described in Materials and Methods. Twelve kanamycin-sensitive and 5-FU-resistant clones were analyzed by PCR, and three clones were found to have the desired *gnd* deletion (named Δ*upp* Δ*edd* Δ*eda* clones 1 to 3), one of which (clone 1) was used for further studies. The Δ*upp* Δ*edd* Δ*eda* strain lacks the EDP and leaves the PPP as the sole route for cytoplasmic sugar catabolism. The mutant was characterized with respect to growth and enzyme activities and compared to the reference strain, the *G. oxydans* Δ*upp* strain.

In contrast to the reference strain, which clearly showed biphasic growth on mannitol, the two phases were much less pro-

TABLE 3 Carbon balances of four *G. oxydans* strains[a]

Carbon balance parameter	Value of the indicated parameter for *G. oxydans* 621H strain with the following genotype:							
	Δ*upp*		Δ*upp* Δ*gnd*		Δ*upp* Δ*gnd zwf**		Δ*upp* Δ*edd* Δ*eda*	
	mmol C[b]	%	mmol C	%	mmol C	%	mmol C	%
Mannitol consumed	1,296 ± 29	100	1,298 ± 9	100	1,261 ± 14	100	1,307 ± 18	100
Biomass formed	80 ± 12	6	34 ± 2	3	39 ± 0	3	110 ± 3	8
Metabolites formed	875 ± 27	68	1,178 ± 8	91	1,093 ± 19	87	755 ± 10	59
CO_2 formed	263 ± 12	20	43 ± 4	3	37 ± 1	3	359 ± 5	27
% carbon found in products		94		97		93		94

[a] Cells were cultivated in mannitol medium at 15% dissolved oxygen and pH 6 in a bioreactor. All parameters were calculated after 26 h of growth.
[b] The mean values ± standard deviations for three biological replicates are shown.

TABLE 4 Specific activities of glucose-6-phosphate dehydrogenase and 6-phosphogluconate dehydrogenase in cell extracts of four *G. oxydans* strains[a]

Enzyme and sample time[b]	Enzyme activity[c] (μmol min^{-1} mg of protein^{-1}) in *G. oxydans* strain with the following genotype:			
	Δ*upp*	Δ*upp* Δ*gnd*	Δ*upp* Δ*gnd zwf**	Δ*upp* Δ*edd* Δ*eda*
G6P-DH				
12 h	0.40 ± 0.002	ND	ND	0.45 ± 0.003
OD_{600} of 1.5	0.53 ± 0.020	0.33 ± 0.082	0.01 ± 0.003	ND
6PG-DH				
12 h	0.08 ± 0.001	ND	ND	0.11 ± 0.002
OD_{600} of 1.5	0.07 ± 0.005	<0.001 ± 0.000	<0.001 ± 0.000	ND

[a] Cells were cultivated in mannitol medium at 15% dissolved oxygen and pH 6 in a bioreactor.
[b] G6P-DH, glucose-6-phosphate dehydrogenase; 6PG-DH, 6-phosphogluconate dehydrogenase. The sample time is the time when the cell extracts were prepared (either at an OD_{600} of 1.5 or after 12 h of growth).
[c] The mean values ± standard deviations for three biological replicates are shown. ND, not determined.

nounced in *G. oxydans* Δ*upp* Δ*edd* Δ*eda* mutant strain (Fig. 2C). Whereas the growth rates of the two strains were almost identical in growth phase I (0.43 h^{-1} and 0.44 h^{-1}), the mutant grew faster than the parent strain in growth phase II and reached a 24% higher final OD_{600} (Table 2). Determination of the cell weight (dry weight) verified that the higher OD_{600} value correlated with an increased biomass formation by the mutant (2.63 g of cells [dry weight] liter^{-1} versus 1.92 g of cells [dry weight] liter^{-1}, respectively). In growth phase I, the cell yield (gram of cells [dry weight] per gram of mannitol consumed intracellularly) of the Δ*upp* Δ*edd* Δ*eda* mutant was increased by 43%, whereas in growth phase II, the cell yield (gram of cells [dry weight] per gram of fructose consumed intracellularly) of the mutant was nearly identical (Table 2). As shown in Fig. 2F, the kinetics of mannitol consumption and fructose formation in growth phase I were identical for both strains, but fructose consumption by the Δ*upp* Δ*edd* Δ*eda* mutant in growth phase II was faster than by the Δ*upp* strain, leading to an increased total consumption. At the end of cultivation, the mutant had consumed 22 mM more fructose than the reference strain. This correlates with the increased biomass formation by the mutant, which also produced 37% more CO_2 than the reference strain (Fig. 3C and Tables 2 and 3). The kinetics of 5-keto-fructose formation in growth phase II and the final titer were very similar for the two strains. The final acetate titers were also similar, but acetate production started several hours later in the Δ*edd* Δ*eda* mutant than in the parent strain (Fig. 2F). The ratio of acetate to carbon dioxide formation was much lower in the Δ*upp* Δ*edd* Δ*eda* mutant than in the reference strain (Table 2). The carbon balance of the Δ*upp* Δ*edd* Δ*eda* mutant amounted to 94% (Table 3).

The specific activities of glucose-6-phosphate dehydrogenase (Zwf) and 6-phosphogluconate dehydrogenase (Gnd) in cell extracts were determined 12 h after inoculation. The Δ*upp* Δ*edd* Δ*eda* mutant had a 13% higher glucose-6-phosphate dehydrogenase activity and a 38% higher 6-phosphogluconate dehydrogenase activity than the reference strain (Table 4).

Effects of plasmid-encoded *gnd* or *edd eda* genes on growth. In order to confirm that the effects of the *gnd* deletion and the *edd eda* deletion on growth are in fact due to the deletions rather than to secondary mutations, the expression plasmids pBBR1p384-*gnd*

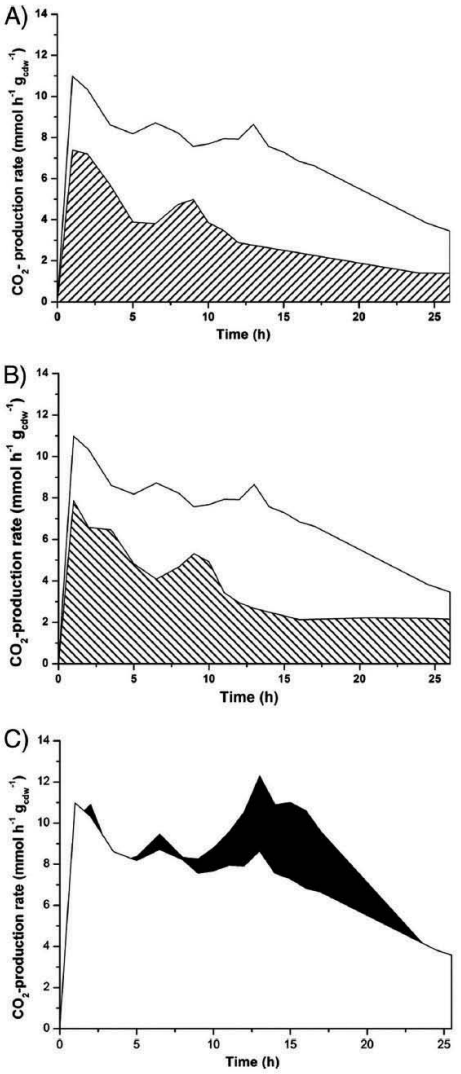

FIG 3 Specific carbon dioxide production of *G. oxydans* deletion strains and the reference strain (*G. oxydans* Δ*upp* strain) (white area). *G. oxydans* Δ*upp* Δ*gnd* (A), Δ*upp* Δ*gnd zwf** (B), and Δ*upp* Δ*edd* Δ*eda* (C) deletion strains were studied. The cells were cultivated in mannitol medium at 15% dissolved oxygen at pH 6. The mean values of three independent cultures are shown. g_{cdw}, gram of cells (dry weight).

TABLE 5 Specific activity of glucose-6-phosphate dehydrogenase and 6-phosphogluconate dehydrogenase in cell extracts of the *G. oxydans* strains[a]

G. oxydans strain[b]	Enzyme activity (μmol min^{-1} mg of protein^{-1})[c]	
	G6P-DH	6PG-DH
Δ*upp*(pBBRp384)	0.29 ± 0.03	0.07 ± 0.01
Δ*upp*(pBBRp384-*gnd*)	0.28 ± 0.02	0.38 ± 0.03
Δ*upp* Δ*gnd*	0.26 ± 0.01	<0.001 ± 0.00
Δ*upp* Δ*gnd*(pBBRp384-*gnd*)	0.04 ± 0.00	0.40 ± 0.00
Δ*upp* Δ*edd* Δ*eda*(pBBRp384)	0.32 ± 0.05	0.08 ± 0.01
Δ*upp* Δ*edd* Δ*eda*(pBBRp384-*gnd*)	0.32 ± 0.04	0.44 ± 0.02

[a] Cells were cultivated in mannitol medium in a baffled shaking flask at pH 6 and 140 rpm and used for the preparation of cell extracts at an OD_{600} of 1.5.
[b] *G. oxydans* strains carrying a plasmid (pBBRp384 or pBBRp384-*gnd*) or not carrying a plasmid.
[c] G6P-DH, glucose-6-phosphate dehydrogenase; 6PG-DH, 6-phosphogluconate dehydrogenase. The mean values ± standard deviations for three biological replicates are shown.

and pBBR1p384-*edd-eda* were constructed. The presence of the control plasmid pBBR1p384 had no influence on the growth of the Δ*upp* and Δ*upp* Δ*edd* Δ*eda* strains but inhibited the growth of the Δ*upp* Δ*gnd* strain. Since the growth of the Δ*upp* Δ*gnd* mutant is already hampered, the introduction of a plasmid carrying no beneficial genes and the presence of kanamycin in the medium presumably stresses these cells much more than cells of a healthy strain. The presence of pBBR1p384-*gnd* significantly improved growth of the Δ*upp* Δ*gnd* mutant and of the reference strain (Δ*upp*). This indicates that an increased carbon flux through the PPP and a reduced flux through EDP have a positive effect on growth. The presence of pBBR1p384-*gnd* led to an increase in the 6-phosphogluconate dehydrogenase activity from 0.07 ± 0.01 μmol min^{-1} mg of protein^{-1} to 0.38 ± 0.03 μmol min^{-1} mg of protein^{-1} in the reference strain and from <0.001 ± 0.00 μmol min^{-1} mg of protein^{-1} to 0.40 ± 0.00 μmol min^{-1} mg of protein^{-1} in the Δ*upp* Δ*gnd* strain (Table 5). The latter strain showed a strongly reduced activity of G6P-DH. Sequencing of the *zwf* gene (GOX0145) revealed a point mutation in codon 222 resulting in an amino acid exchange from glycine to aspartate. Since the growth of this strain was similar to that of the reference strain, flux through the G6P-DH seems to be still sufficient.

Although the presence of the *gnd* expression plasmid in the Δ*upp* Δ*edd* Δ*eda* mutant led to an increased activity of 6-phosphogluconate dehydrogenase activity from 0.08 to 0.44 μmol min^{-1} mg of protein^{-1}, growth was not improved further (Table 5 and Fig. 4). The presence of the *edd eda* expression plasmid pBBR1p384-*edd-eda* on the other hand inhibited growth of the reference strain (Δ*upp* strain) and of the Δ*upp* Δ*edd* Δ*eda* mutant strain.

Transcriptome analysis. Transcriptome comparisons of the Δ*upp* Δ*gnd* and Δ*upp* Δ*gnd zwf** mutants versus the reference strain were performed using cells harvested at an OD_{600} of 1.5 (Fig. 2A and B). In the Δ*upp* Δ*gnd* mutant, 55 genes were differentially expressed; 38 of the genes had an mRNA ratio of ≥2, and 17 had an mRNA ratio of ≤0.5 (see Table S1 in the supplemental material). In total, 155 genes were differentially expressed in the Δ*upp* Δ*gnd zwf** mutant; 111 of the genes had an mRNA ratio of ≥2, and 44 had an mRNA ratio of ≤0.5 (Table S1). DNA microarray analyses of the Δ*upp* Δ*edd* Δ*eda* mutant versus the reference strain were performed using cells harvested in the second growth phase at an OD_{600} of 5.8 ± 0.3 and 5.1 ± 0.3, respectively (Table S1 and Fig. 2C). In total, 79 genes showed differential expression; 4 of these genes had an mRNA ratio of ≥2.0, and 75 had an mRNA ratio of ≤0.5. Selected genes that were regulated in at least two of the three DNA microarray experiments are listed in Table 6. The genes were grouped into four categories, and the most interesting genes are described in more detail below.

(**i**) **Genes involved in respiration.** In the Δ*upp* Δ*gnd* and Δ*upp*

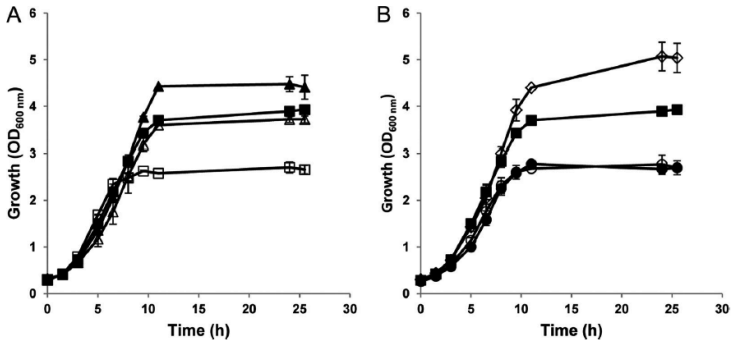

FIG 4 Complementation studies using the *gnd* expression plasmid pBBR1p384-*gnd*, the *edd eda* expression plasmid pBBR1p384-*edd-eda*, and the control plasmid pBBRp384. (A) The reference strain, *G. oxydans* Δ*upp* strain, carrying pBBR1p384 (■) or pBBR1p384-*gnd* (▲) and the PPP mutant *G. oxydans* Δ*upp* Δ*gnd* strain carrying no additional plasmid (○) or carrying pBBR1p384 (□) or pBBR1p384-*gnd* (△). (B) The reference strain, *G. oxydans* Δ*upp* strain, carrying pBBR1p384 (■) or pBBR1p384-*edd-eda* (●) and the EDP mutant *G. oxydans* Δ*upp* Δ*edd* Δ*eda* strain carrying pBBR1p384 (◇), pBBR1p384-*edd-eda* (○), or pBBR1p384-*gnd* (△). The strains were cultivated in shaking flasks with mannitol medium at 30°C and 140 rpm. After about 5 h, the dissolved oxygen concentration in the medium became zero (data not shown), leading to microaerobic growth conditions. This explains why the growth behavior in shaking flasks differed from that in the bioreactor, in which the dissolved oxygen concentration was kept constantly at 15%. The mean values and standard deviations for three independent cultures are shown. Cells were harvested at an OD_{600} of 1.5 for enzyme activity measurements.

TABLE 6 Transcriptome comparisons of four *G. oxydans* strains[a]

Functional category and annotation	Locus tag	mRNA ratio[b] of the following strain compared to the reference strain (Δ*upp*):		
		Δ*upp* Δ*gnd*	Δ*upp* Δ*gnd zwf**	Δ*upp* Δ*edd* Δ*eda*
Respiration				
NAD(P) transhydrogenase subunit α1	GOX0310	2.09	3.39	NR
NAD(P) transhydrogenase subunit α2	GOX0311	2.13	3.22	NR
NAD(P) transhydrogenase subunit b	GOX0312	2.26	2.92	NR
Alcohol:NAD^+ oxidoreductase	GOX0313	2.23	2.93	NR
Probable alcohol:$NAD(P)^+$ oxidoreductase	GOX0314	1.60	2.11	NR
Metabolism				
Carbonic anhydrase	GOX1785	NR	2.81	2.02
Glycerol-3-phosphate dehydrogenase	GOX2088	3.79	3.92	NR
Glycerol kinase	GOX2090	2.54	3.01	NR
Triosephosphate isomerase	GOX2217	7.34	6.96	0.37
Ribose-5-phosphate isomerase B	GOX2218	9.56	7.64	0.42
Dihydroxyacetone kinase	GOX2222	6.37	2.81	0.47
Transport				
Glycerol uptake facilitator protein	GOX2089	3.64	3.37	NR
Probable mannitol/sorbitol ABC transporter permease protein	GOX2184	3.07	2.10	NR
Periplasmic mannitol/sorbitol-binding protein	GOX2185	3.29	2.84	NR
Ribose ABC transporter, periplasmic binding protein	GOX2219	8.26	8.30	0.42
Ribose ABC transporter, ATP-binding protein	GOX2220	6.27	4.02	0.47
Ribose ABC transporter, permease protein	GOX2221	5.39	2.57	0.52
Stress				
DNA starvation/stationary-phase protection protein Dps	GOX0707	NR	3.36	0.49
Small heat shock protein	GOX1329	NR	2.55	0.21

[a] The transcriptomes of *G. oxydans* Δ*upp* Δ*gnd*, Δ*upp* Δ*gnd zwf**, and Δ*upp* Δ*edd* Δ*eda* mutants were compared to the transcriptome of the reference strain (*G. oxydans* Δ*upp* strain). The two PPP mutants and the reference strain were harvested in growth phase I at an OD_{600} of 1.5, and the ED mutant and the reference strain were harvested in growth phase II at an OD_{600} of 5.8 ± 0.3 and 5.1 ± 0.3, respectively. Cells were cultivated in mannitol medium at pH 6 and 15% dissolved oxygen. Selected genes with an mRNA ratio of ≥2.0 (lower ones allowed in the case of operons) or ≤0.5 (higher ones allowed in the case of operons) and a *P* value of ≤0.05 in at least two of three experiments are listed. The genes were grouped into different functional categories within which they were ordered according to their locus tag number. A list of all genes with an mRNA ratio of ≥2.0 or ≤0.5 is given in Table S1 in the supplemental material.

[b] The data shown represent mean values from three biological replicates. NR, not regulated.

Δ*gnd zwf** mutants, but not in the Δ*upp* Δ*edd* Δ*eda* mutant strain, the genes of a putative operon encoding the membrane-bound PntA1A2B transhydrogenase and two dehydrogenases showed increased expression (GOX0310 to GOX0314, mRNA ratios of 2.1 to 1.6 and 3.4 to 2.1, respectively).

(ii) Genes involved in metabolism. In the Δ*upp* Δ*gnd* and Δ*upp* Δ*gnd zwf** mutants, two genes involved in glycerol metabolism, glycerol-3-phosphate dehydrogenase (GOX2088) and glycerol kinase (GOX2090), as well as the genes for dihydroxyacetone kinase (GOX2222) and triosephosphate isomerase (GOX2217), displayed increased expression, although no glycerol had been added to the culture medium.

(iii) Genes involved in transport. The Δ*upp* Δ*gnd* and Δ*upp* Δ*gnd zwf** mutant strains showed an elevated mRNA ratio of the gene encoding the glycerol uptake protein (GOX2089), which presumably forms an operon with the genes for glycerol 3-phosphate dehydrogenase and glycerol kinase. The genes encoding a ribose ABC transporter (GOX2219 to GOX2221) were strongly upregulated in the two PPP mutants but downregulated in the ED mutant.

(iv) Genes involved in stress responses. The Δ*upp* Δ*gnd zwf** mutant showed increased expression of the genes encoding Dps (GOX0707) and a small heat shock protein (GOX1329). In the Δ*upp* Δ*gnd* mutant, these genes were expressed at the same level as in the reference strain, and in the Δ*upp* Δ*edd-eda* mutant, these genes displayed decreased expression.

DISCUSSION

In this study, the two functional pathways for cytoplasmic sugar degradation in *G. oxydans*, the pentose phosphate pathway and the Entner-Doudoroff pathway, were alternatively disabled by deletion of the *gnd* gene and by deletion of the *edd eda* genes, respectively. The results of growth experiments using media with mannitol as the source of energy and carbon and yeast extract as the supplement revealed that neither of the two pathways, PPP or EDP, is essential for survival of *G. oxydans*.

The absence of 6-phosphogluconate dehydrogenase imposed a selection pressure on the cells for secondary mutations in the *zwf* gene, causing inactivation of glucose-6-phosphate dehydrogenase. This suggests that a situation in which the EDP is the only pathway for sugar degradation causes a severe stress which is partially overcome by blocking access of glucose-6-phosphate to the EDP. It was shown for *Escherichia coli* that the addition of gluconate to a strain that lacked 2-keto-3-deoxy-6-phosphogluconate (KDPG) aldolase and overproduced 6-phosphogluconate dehydratase resulted in a rapid accumulation of KDPG within the cell, which was correlated with an immediate and significant decrease in growth (5). Mutants of *Pseudomonas cepacia* deficient in either

6-phosphogluconate dehydratase or KDPG aldolase also showed growth inhibition with glucose, gluconate, and fructose as carbon sources and e.g., citrate as supplement, presumably as a consequence of accumulation of 6-phosphogluconate, KDPG, or both (1). Based on these data, the selection pressure of the Δ*upp* Δ*gnd* mutant of *G. oxydans* for secondary *zwf* mutations inactivating glucose-6-phosphate dehydrogenase could be due to increased concentrations of 6-phosphogluconate or KDPG. The reasons for the inhibitory effects of these compounds are not yet known. However, the fact that three of the Δ*upp* Δ*gnd* mutants contained an intact *zwf* gene (at least at the time point when the gene was amplified for sequencing) and only slightly lowered glucose-6-phosphate dehydrogenase activities indicates that alternative possibilities for coping with increased concentrations of 6-phosphogluconate or KDPG exist.

The Δ*upp* Δ*gnd* and Δ*upp* Δ*gnd zwf** mutant strains showed reduced growth rates in comparison to the reference strain (Δ*upp* strain) in the first growth phase. The reasons for the reduced growth rates could be inhibitory effects of increased 6-phosphogluconate or KDPG concentrations, as discussed above, or insufficient availability of metabolites that are derived from intermediates of the PPP. The second growth phase observed in the reference strain (Δ*upp*) was absent in the Δ*upp* Δ*gnd* and Δ*upp* Δ*gnd zwf** strains, which correlates with the fact that only negligible amounts of fructose were metabolized by these strains in the cytoplasm (6 to 3 mM versus 50 mM by the reference strain). This behavior might be caused by an insufficient energy supply in the absence of the PPP and/or by an insufficient rate of fructose catabolism via the EDP.

In contrast to the PPP mutants, the absence of the EDP proved to be beneficial for growth for the Δ*upp* Δ*edd* Δ*eda* mutant. In growth phase I, the Δ*upp* Δ*edd* Δ*eda* mutant took up 9 mM less mannitol (or fructose) than the reference strain did but formed slightly more biomass and carbon dioxide (Table 2). This results in a 43% increased growth yield, which is in agreement with the sole operation of the energetically more efficient PPP. In growth phase II, the EDP mutant consumed 40% more fructose than the reference strain. In particular, the amount of fructose catabolized in the cytoplasm was 60% higher. The increased fructose consumption was accompanied by a 54% increase in biomass. Unexpectedly, growth yields in growth phase II did not differ between the EDP mutant and the reference strain, pointing to a predominance of the PPP in growth phase II in the reference strain. The longer period of almost unimpaired exponential growth of the EDP mutant is probably due to the lack of an adjustment phase during the transition from growth phase I to II. This transition is connected to *de novo* protein synthesis as was shown in an earlier study (17). Since improved growth of *G. oxydans* on mannitol was obtained not only by deletion of the *edd eda* genes but also by overexpression of the *gnd* gene, 6-phosphogluconate dehydrogenase appears to be the rate-limiting enzyme of the PPP. Both an increased 6-phosphogluconate dehydrogenase activity and a deletion of the *edd eda* genes presumably result in an increased flux through the PPP. Furthermore, the EDP intermediate KDPG might have an inhibitory effect on the activity of 6-phosphogluconate dehydrogenase that is eliminated by deletion of *edd* or weakened by overexpression of *gnd*.

An interesting difference between the usage of the PPP and the EDP is energetic efficiency. Conversion of 1 mol glucose-6-phosphate via the EDP yields 2 mol acetate or acetyl-CoA + 2 mol CO_2 + 4 mol NAD(P)H + 2 mol ATP (Fig. 1). In the absence of phosphofructokinase, the PPP operates cyclically, as fructose-6-phosphate formed by transaldolase or transketolase is converted to glucose-6-phosphate, which enters the oxidative PPP again. This has recently been shown for an *Escherichia coli* Δ*pfkA* mutant (23). Therefore, conversion of 1 mol glucose-6-phosphate via the PPP in the absence of phosphofructokinase yields 1 mol acetate or acetyl-CoA + 4 mol CO_2 + 8 mol NAD(P)H + 2 mol ATP (13) (Fig. 1). The two dehydrogenases of the oxidative PPP were shown to have dual coenzyme specificities (25), but based on the kinetic properties, it was proposed that *in vivo* glucose-6-phosphate dehydrogenase utilizes $NADP^+$ and 6-phosphogluconate dehydrogenase NAD^+ as cofactors (21). The acetaldehyde dehydrogenase of *G. oxydans* is NADP dependent (12). *G. oxydans* possesses a PntA1A2B transhydrogenase (GOX0310 to GOX0312) that can convert NADPH to NADH (8, 21), which is then reoxidized by the respiratory chain via NADH dehydrogenase and used for generating proton motive force and ATP by oxidative phosphorylation. The higher energy yield obtained by oxidizing glucose-6-phosphate by the PPP might contribute to increased biomass formation of the Δ*upp* Δ*edd* Δ*eda* mutant or the strain overexpressing 6-phosphogluconate dehydrogenase.

The transcriptome comparisons of the three mutant strains versus the reference strain revealed a number of interesting differences. In the PPP mutants, about two-thirds of the altered genes showed increased expression and about one-third showed decreased expression. In contrast, in the EDP mutant, 95% of the regulated genes showed decreased expression. In the EDP mutant, a group of about 20 genes involved in different types of stress responses showed a 2- to 3-fold reduced expression (see Table S1 in the supplemental material), suggesting that in the slower-growing reference strain, a weak general stress response is elicited in growth phase II. The increased expression in the PPP mutants of the GOX0310 to GOX0314 genes encoding the PntA1A2B transhydrogenase and two dehydrogenases might indicate an imbalanced redox state of the NAD(P)(H) cofactor pools, as upregulation of these genes was previously also observed in oxygen-limited cells of *G. oxydans* (7). The GOX2088 to GOX2090 genes involved in glycerol uptake (glycerol facilitator) and catabolism (glycerol kinase and glycerol 3-phosphate dehydrogenase) were upregulated in the PPP mutants, although glycerol was not added as a component of the medium. Upregulation of these genes might be caused by increased formation of glycerol 3-phosphate, which in *Escherichia coli* serves as the inducer of the GlpR repressor (15). As a homologous protein is present in *G. oxydans* and encoded immediately upstream of the gene encoding glycerol 3-phosphate dehydrogenase, a similar type of regulation as in *E. coli* can be anticipated. The genes showing the strongest upregulation in the PPP mutants were GOX2217 to GOX2122, which encode triosephosphate isomerase, ribose-5-phosphate isomerase, the three components of a ribose ABC transporter, and dihydroxyacetone kinase. These genes, which presumably form an operon, might be induced by a lack of building blocks for the synthesis of nucleic acids and aromatic amino acids due to the reduced activity of the PPP. Interestingly, the ribose ABC transporter of *Sinorhizobium meliloti* and of *Bifidobacterium longum* was shown to also import fructose (14, 26).

The results of this work show that neither of the two functional pathways for sugar degradation, PPP and EDP, is essential for growth of *G. oxydans* on mannitol and yeast extract and support

the view that the PPP is much more important than the EDP. Surprisingly, the absence of the EDP genes improved the growth yield in growth phase I and growth rate and biomass formation in growth phase II. Nonfunctionality of the PPP, on the other hand, led to a reduced growth rate and biomass formation in growth phase I and the lack of growth phase II. Future studies on the behavior of the PPP and EDP mutants on alternative carbon sources will be performed.

ACKNOWLEDGMENTS

We are most grateful to Armin Ehrenreich and Wolfgang Liebl (TU München) for providing the materials and protocols used for generating the *G. oxydans* deletion mutants and Uwe Deppenmeier (Universität Bonn) for providing plasmid pBBR1p384. We thank Dietmar Laudert, Günter Pappenberger, and Hans-Peter Hohmann (DSM Nutritional Products, Kaiseraugst, Switzerland) for their scientific input and helpful discussions.

We also thank DSM Nutritional Products (Kaiseraugst, Switzerland) for financial support. This work was funded by the German Ministry of Education and Research (BMBF) via the GenoMik-Transfer program (grant 0315632D).

REFERENCES

1. Allenza P, Lessie TG. 1982. *Pseudomonas cepacia* mutants blocked in the Entner-Doudoroff pathway. J. Bacteriol. 150:1340–1347.
2. Bertani G. 2004. Lysogeny at mid-twentieth century: P1, P2, and other experimental systems. J. Bacteriol. 186:595–600.
3. Bertani G. 1951. Studies on lysogenesis. I. The mode of phage liberation by lysogenic *Escherichia coli.* J. Bacteriol. 62:293–300.
4. Bradford MM. 1976. A rapid and sensitive method for the quantitation of microgram quantities of protein utilizing the principle of protein-dye binding. Anal. Biochem. 72:248–254.
5. Fuhrman LK, Wanken A, Nickerson KW, Conway T. 1998. Rapid accumulation of intracellular 2-keto-3-deoxy-6-phosphogluconate in an Entner-Doudoroff aldolase mutant results in bacteriostasis. FEMS Microbiol. Lett. 159:261–266.
6. Hanahan D, Jessee J, Bloom FR. 1991. Plasmid transformation of *Escherichia coli* and other bacteria. Methods Enzymol. 204:63–113.
7. Hanke T, et al. 2012. Influence of oxygen limitation, absence of the cytochrome bc_1 complex and low pH on global gene expression in *Gluconobacter oxydans* 621H using DNA microarray technology. J. Biotechnol. 157:359–372.
8. Jackson JB, White SA, Quirk PG, Venning JD. 2002. The alternating site, binding change mechanism for proton translocation by transhydrogenase. Biochemistry 41:4173–4185.
9. Katzen F, Becker A, Ielmini MV, Oddo CG, Ielpi L. 1999. New mobilizable vectors suitable for gene replacement in gram-negative bacteria and their use in mapping of the 3′ end of the *Xanthomonas campestris* pv. campestris *gum* operon. Appl. Environ. Microbiol. 65:278–282.
10. Kersters K, Lisdiyanti P, Komagata K, Swings J. 2006. The family *Acetobacteriaceae*: the genera *Acetobacter*, *Acidomonas*, *Asaia*, *Gluconacetobacter*, *Gluconobacter* and *Kozakia*, p 163–200. *In* Dworkin M, Falkow S, Rosenberg E, Schleifer K-H, Stackebrandt E (ed), The prokaryotes, vol 5, 3rd ed. Springer-Verlag GmbH, Heidelberg, Germany.
11. Kovach ME, et al. 1995. Four new derivatives of the broad-host-range cloning vector pBBR1MCS, carrying different antibiotic-resistance cassettes. Gene 166:175–176.
12. Krajewski V, et al. 2010. Metabolic engineering of *Gluconobacter oxydans* for improved growth rate and growth yield on glucose by elimination of gluconate formation. Appl. Environ. Microbiol. 76:4369–4376.
13. Kruger NJ, von Schaewen A. 2003. The oxidative pentose phosphate pathway: structure and organisation. Curr. Opin. Plant Biol. 6:236–246.
14. Lambert A, Osteras M, Mandon K, Poggi MC, Le Rudulier D. 2001. Fructose uptake in *Sinorhizobium meliloti* is mediated by a high-affinity ATP-binding cassette transport system. J. Bacteriol. 183:4709–4717.
15. Larson TJ, Ye S, Weissenborn DL, Hoffmann HJ, Schweizer H. 1987. Purification and characterization of the repressor for the *sn*-glycerol 3-phosphate regulon of *Escherichia coli* K12. J. Biol. Chem. 262:15869–15874.
16. Moritz B, Striegel K, De Graaf AA, Sahm H. 2000. Kinetic properties of the glucose-6-phosphate and 6-phosphogluconate dehydrogenases from *Corynebacterium glutamicum* and their application for predicting pentose phosphate pathway flux *in vivo*. Eur. J. Biochem. 267:3442–3452.
17. Olijve W, Kok JJ. 1979. Analysis of growth of *Gluconobacter oxydans* in glucose containing media. Arch. Microbiol. 121:283–290.
18. Parmentier S, Beauprez J, Arnaut F, Soetaert W, Vandamme EJ. 2005. *Gluconobacter oxydans* NAD-dependent, D-fructose reducing, polyol dehydrogenases activity: screening, medium optimisation and application for enzymatic polyol production. Biotechnol. Lett. 27:305–311.
19. Prust C, et al. 2005. Complete genome sequence of the acetic acid bacterium *Gluconobacter oxydans*. Nat. Biotechnol. 23:195–200.
20. Raspor PP, Goranovič D. 2008. Biotechnological applications of acetic acid bacteria. Crit. Rev. Biotechnol. 28:101–124.
21. Rauch B, Pahlke J, Schweiger P, Deppenmeier U. 2010. Characterization of enzymes involved in the central metabolism of *Gluconobacter oxydans*. Appl. Microbiol. Biotechnol. 88:711–718.
22. Sambrook J, Russell DW. 2001. Molecular cloning: a laboratory manual, 3rd ed. Cold Spring Harbor Laboratory Press, Cold Spring Harbor, NY.
23. Siedler S, Bringer S, Blank LM, Bott M. 2012. Engineering yield and rate of reductive biotransformation in *Escherichia coli* by partial cyclization of the pentose phosphate pathway and PTS-independent glucose transport. Appl. Microbiol. Biotechnol. 93:1459–1467.
24. Simon R, Priefer U, Pühler A. 1983. A broad host range mobilization system for *in vivo* genetic engineering: transposon mutagenesis in Gram-negative bacteria. Nat. Biotechnol. 1:784–791.
25. Tonouchi N, Sugiyama M, Yokozeki K. 2003. Coenzyme specificity of enzymes in the oxidative pentose phosphate pathway of *Gluconobacter oxydans*. Biosci. Biotechnol. Biochem. 67:2648–2651.
26. Wei X, et al. 2012. Fructose uptake in *Bifidobacterium longum* NCC2705 is mediated by an ATP-binding cassette transporter. J. Biol. Chem. 287: 357–367.

Supplementary Material

Table S1 Genome-wide comparison of mRNA levels of *G. oxydans* Δ*upp* Δ*edd-eda* versus *G. oxydans* Δ*upp* (reference), second growth phase as well as *G. oxydans* Δ*upp* Δ*gnd* and *G. oxydans* Δ*upp* Δ*gnd zwf** versus *G. oxydans* Δ*upp* (reference) during growth in mannitol medium at pH 6 and 15% dissolved oxygen. Genes with an mRNA ratio ≥2.0 or ≤0.5 and a p-value of ≤0.05 are listed. The data shown represent mean values from three biological replicates. The genes were grouped into different functional categories within which they were ordered according to their locus tag.

***G. oxydans* Δ*upp* Δ*edd-eda* versus *G. oxydans* Δ*upp* (reference); mRNA ratio of 75 genes ≤0.5, second growth phase**

Gene	Annotation	Gene name	mRNA ratio	n	*p*-Value
GOX0049	DnaJ family protein		0.47	3	3.26E-02
GOX0090	Putative sugar kinase		0.50	3	2.85E-02
GOX0182	Hypothetical protein GOX0182		0.48	3	1.04E-02
GOX0235	Hypothetical protein GOX0235		0.48	3	1.69E-02
GOX0278	Cytochrome *bd* ubiquinol oxidase subunit I	*cydA*	0.40	3	2.25E-04
GOX0337	Hypothetical protein GOX0337		0.47	3	2.20E-02
GOX0347	Hypothetical protein GOX0347		0.40	3	4.69E-03
GOX0430	KDPG aldolase	*eda*	0.08	3	2.16E-03
GOX0431	Phosphogluconate dehydratase	*edd*	0.06	3	1.38E-03
GOX0478	Putative oxidoreductase		0.50	3	2.17E-02
GOX0502	Putative oxidoreductase		0.39	3	5.62E-03
GOX0503	Hypothetical protein GOX0503		0.32	3	2.27E-03
GOX0506	RNA polymerase factor sigma factor H (sigma-32)	*rpoH*	0.33	3	1.93E-04
GOX0570	Hypothetical protein GOX0570		0.40	3	1.24E-02
GOX0576	Hypothetical protein GOX0576		0.28	3	1.53E-03
GOX0608	ATP-dependent Clp protease adaptor protein ClpS	*clpS*	0.35	3	1.45E-02
GOX0626	Thioredoxin		0.39	3	4.78E-03
GOX0673	Ferrous iron transport protein A (FeoA)	*feoA*	0.40	3	9.68E-03
GOX0707	DNA starvation/stationary phase protection protein Dps	*dps*	0.49	3	4.01E-02
GOX0726	Hypothetical protein GOX0726		0.43	3	2.33E-02
GOX0734	Hypothetical protein GOX0734		0.30	3	5.05E-03
GOX0762	Thioredoxin		0.30	3	1.17E-02
GOX0763	ATP-dependent protease La		0.44	3	1.40E-02
GOX0820	GrpE protein (HSP-70 cofactor)		0.30	3	6.56E-03
GOX0833	Cold shock protein		0.39	3	3.02E-03

GOX0857	Chaperone protein DnaK		0.32	3	5.60E-03
GOX0858	Chaperone protein DnaJ		0.48	3	4.21E-02
GOX0875	AtsE protein		0.32	3	6.25E-04
GOX0880	Hypothetical protein GOX0880		0.48	3	1.38E-02
GOX0889	Peptidyl-prolyl cis-trans isomerase		0.46	3	1.33E-02
GOX0890	Hypothetical protein GOX0890		0.18	3	4.60E-03
GOX1024	Heat shock protein 90	*hsp90*	0.40	3	7.25E-03
GOX1095	Aminomethyltransferase (Glycine cleavage system T protein)		0.41	3	3.27E-02
GOX1096	Glycine cleavage system H protein		0.35	3	1.85E-02
GOX1299	Hypothetical protein GOX1299		0.37	3	1.50E-03
GOX1328	Hypothetical protein GOX1328		0.42	3	2.04E-02
GOX1329	Small heat shock protein	*hsd*	0.21	3	1.55E-03
GOX1410	Hypothetical protein GOX1410		0.50	3	9.16E-03
GOX1414	Chaperone protein DnaJ	*dnaJ*	0.49	3	1.66E-02
GOX1459	Transcriptional regulator		0.42	3	3.68E-02
GOX1463	ATP-dependent Clp protease, ATP-binding subunit ClpV	*clpV*	0.43	3	3.05E-03
GOX1500	Hypothetical protein GOX1500		0.50	3	1.02E-02
GOX1615	Putative oxidoreductase		0.49	3	5.54E-03
GOX1617	Hypothetical protein GOX1617		0.42	3	4.52E-03
GOX1633	Hypothetical protein GOX1633		0.31	3	4.61E-03
GOX1660	Hypothetical protein GOX1660		0.49	3	1.25E-02
GOX1661	Bacterioferritin comigratory protein		0.50	3	2.90E-02
GOX1735	Hypothetical protein GOX1735		0.44	3	3.90E-04
GOX1745	Hypothetical protein GOX1745		0.35	3	9.46E-05
GOX1751	HesB family protein		0.48	3	9.77E-03
GOX1836	N-formylmethionylaminoacyl-tRNA deformylase		0.38	3	6.22E-03
GOX1837	Small heat shock protein HspA		0.32	3	4.60E-03
GOX1838	Hypothetical protein GOX1838		0.29	3	7.05E-03
GOX1839	Putative translation initiation inhibitor		0.44	3	1.74E-02
GOX1841	Hypothetical protein GOX1841		0.23	3	3.39E-03
GOX1901	Co-chaperonin GroES		0.33	3	2.17E-02
GOX1902	Chaperonin GroEL		0.42	3	4.35E-03
GOX1910	Hypothetical protein GOX1910		0.50	3	1.40E-02
GOX1946	Two component response regulator		0.50	3	1.04E-02
GOX2079	Hypothetical protein GOX2079		0.44	3	1.29E-02
GOX2086	Hypothetical protein GOX2086		0.49	3	3.02E-03
GOX2109	Hypothetical protein GOX2109		0.37	3	9.72E-03
GOX2186	Ribulokinase		0.48	3	4.76E-03
GOX2217	Triosephosphate isomerase		0.37	3	9.11E-03
GOX2218	Ribose-5-phosphate isomerase B		0.42	3	1.05E-02
GOX2219	Ribose ABC transporter, periplasmic binding protein		0.42	3	1.50E-02

GOX2220	Ribose ABC transporter, ATP-binding protein		0.47	3	4.22E-02
GOX2222	Dihydroxyacetone kinase		0.47	3	3.19E-02
GOX2257	Hypothetical protein GOX2257		0.37	3	1.19E-03
GOX2272	Membrane-bound dipeptidase		0.41	3	2.33E-02
GOX2305	Hypothetical protein GOX2305		0.49	3	2.82E-02
GOX2306	Glutaredoxin		0.50	3	2.35E-02
GOX2397	Small heat shock protein	*hsd*	0.29	3	1.20E-02
GOX2493	Peptide methionine sulfoxide reductase		0.33	3	2.31E-03
GOX2685	Transposase		0.48	3	2.78E-02

***G. oxydans* Δ*upp* Δ*gnd zwf** versus *G. oxydans* Δ*upp* (reference); mRNA ratio of 44 genes ≤0.5**

Gene	Annotation	Gene name	mRNA ratio	n	*p*-Value
GOX0035	Hypothetical protein GOX0035		0.49	3	4.47E-03
GOX0103	Carboxypeptidase-related protein		0.49	3	6.64E-03
GOX0155	Phospho-N-acetylmuramoyl-pentapeptide-transferase		0.49	3	8.77E-03
GOX0197	Signal recognition particle protein	*ffh*	0.50	3	9.16E-03
GOX0351	Putative outer membrane drug efflux protein		0.50	3	2.33E-03
GOX0405	TonB-dependent outer membrane receptor		0.40	3	2.56E-04
GOX0424	Flagellar MS-ring protein		0.45	3	1.77E-02
GOX0440	Ornithine decarboxylase		0.41	3	5.96E-03
GOX0452	50S Ribosomal protein L13		0.49	3	2.28E-05
GOX0585	Cytochrome c subunit of aldehyde dehydrogenase		0.18	3	7.44E-03
GOX0694	Hypothetical protein GOX0694		0.50	3	2.11E-02
GOX0695	Hypothetical protein GOX0695		0.47	3	2.81E-02
GOX0743	Ammonium transporter AmtB		0.43	3	6.30E-04
GOX0744	Nitrogen regulatory protein P-II, GlnK		0.48	3	2.18E-03
GOX0907	TonB-dependent outer membrane receptor		0.40	3	8.96E-03
GOX0928	Phosphoadenosine phosphosulfate reductase		0.44	3	6.85E-03
GOX0945	TonB-dependent outer membrane receptor		0.18	3	4.33E-04
GOX1017	TonB-dependent outer membrane receptor		0.30	3	2.16E-03
GOX1029	Hypothetical protein GOX1029		0.42	2	6.69E-04
GOX1114	Vitamin B12-dependent ribonucleotide reductase		0.43	3	9.52E-04
GOX1363	Hypothetical protein GOX1363		0.44	3	5.82E-03
GOX1365	ABC transporter permease protein		0.42	2	2.40E-02
GOX1366	ABC transporter ATP-binding protein		0.44	3	1.70E-03
GOX1525	Flagellar biosynthetic protein FliQ	*fliQ*	0.39	3	4.65E-02
GOX1526	Flagellar hook-basal body protein FleE	*fleE*	0.44	3	3.70E-02

GOX1527	Flagellar basal body rod protein FlgC	*flgC*	0.41	3	3.83E-02
GOX1528	Flagellar basal-body rod protein FlgB	*flgB*	0.43	3	3.42E-02
GOX1569	Tricorn protease homolog		0.37	3	7.89E-05
GOX1648	Cytochrome *c*-type biogenesis protein CycL precursor		0.44	3	2.63E-02
GOX1650	Cytochrome *c*-type biogenesis protein CysK		0.49	3	1.27E-03
GOX1651	Cytochrome *c*-type biogenesis protein CcmE		0.46	3	4.53E-03
GOX1652	Heme exporter protein C		0.50	3	1.23E-03
GOX1705	6-phosphogluconate dehydrogenase-like protein	*gnd*	0.04	3	1.37E-03
GOX1781	Bacterial Peptide Chain Release Factor 3 (RF-3)		0.45	3	2.73E-02
GOX1830	Hypothetical protein GOX1830		0.42	3	5.88E-03
GOX1903	TonB-dependent receptor protein		0.17	3	1.17E-03
GOX1982	Hypothetical protein GOX1982		0.50	3	1.85E-02
GOX2544	Transcriptional regulator protein		0.50	3	2.43E-04
GOX2668	MucR family transcriptional regulator		0.10	3	5.09E-03
GOX2674	Death on curing protein		0.10	3	8.56E-04
GOX2675	Transposase		0.06	3	2.37E-03
GOX2676	Putative alcohol/aldehyde dehydrogenase		0.04	3	2.89E-03
GOX2684	NAD(P)H-dependent 2-cyclohexen-1-one reductase		0.04	3	3.58E-04
GOX2694	ParA-like protein		0.04	3	7.88E-04

***G. oxydans* Δ*upp* Δ*gnd* versus *G. oxydans* Δ*upp* (reference); mRNA ratio of 17 genes ≤0.5**

Gene	**Annotation**	**Gene name**	**mRNA ratio**	**n**	***p*-Value**
GOX1705	6-phosphogluconate dehydrogenase-like protein	*gnd*	0.13	3	2.11E-03
GOX2676	Putative alcohol/aldehyde dehydrogenase		0.14	3	5.62E-03
GOX2684	NAD(P)H-dependent 2-cyclohexen-1-one reductase		0.16	3	6.15E-04
GOX2694	ParA-like protein		0.18	3	7.94E-04
GOX2675	Transposase		0.20	3	3.49E-04
GOX1525	Flagellar biosynthetic protein FliQ	*fliQ*	0.37	3	4.26E-03
GOX0788	Flagellin assembly protein	*mviN*	0.41	3	5.25E-03
GOX1528	Flagellar basal-body rod protein FlgB	*flgB*	0.43	3	1.98E-06
GOX0787	Flagellin B		0.44	3	4.32E-03
GOX1026	Flagellar hook-associated protein 1 FlgK	*flgK*	0.44	3	5.91E-03
GOX1526	Flagellar hook-basal body protein FleE	*fleE*	0.46	3	6.20E-03
GOX1613	Protein with GGDEF and EAL domain		0.46	3	2.19E-03
GOX1527	Flagellar basal body rod protein FlgC	*flgC*	0.47	3	2.32E-03
GOX1027	Flagellar hook protein FlgE	*flgE*	0.49	3	2.76E-03
GOX0127	Chemotaxis MotB protein		0.49	3	1.25E-02

GOX1870	Hypothetical protein GOX1870		0.49	3	1.44E-02
GOX0426	Hypothetical protein GOX0426		0.50	3	1.79E-02

Category: Respiration and Energy Metabolism

***G. oxydans* Δ*upp*Δ*edd-eda* versus *G. oxydans* Δ*upp* (reference), second growth phase**

Gene	Annotation	Gene name	mRNA ratio	n	*p*-Value
GOX0278	Cytochrome *bd* ubiquinol oxidase subunit I	*cydA*	0.40	3	2.25E-04

***G. oxydans* Δ*upp*Δ*gnd zwf** versus *G. oxydans* Δ*upp* (reference)**

Gene	Annotation	Gene name	mRNA ratio	n	*p*-Value
GOX0201	NAD(P)H-flavin oxidoreductase		2.24	3	6.27E-03
GOX0310	NAD(P) transhydrogenase subunit α1	*pntA1*	3.39	3	1.33E-02
GOX0311	NAD(P) transhydrogenase subunit α2	*pntA2*	3.22	3	8.22E-03
GOX0312	NAD(P) transhydrogenase subunit b	*pntB*	2.92	3	3.88E-03
GOX0313	Alcohol:NAD^+ oxidoreductase		2.93	3	1.21E-03
GOX0314	Probable alcohol:$NAD(P)^+$ oxidoreductase		2.11	3	3.62E-02
GOX0585	Cytochrome *c* subunit of aldehyde dehydrogenase		0.18	3	7.44E-03
GOX1648	Cytochrome *c*-type biogenesis protein CycL precursor		0.44	3	2.63E-02
GOX1650	Cytochrome *c*-type biogenesis protein CysK		0.49	3	1.27E-03
GOX1651	Cytochrome *c*-type biogenesis protein CcmE		0.46	3	4.53E-03

***G. oxydans* Δ*upp*Δ*gnd* versus *G. oxydans* Δ*upp* (reference)**

Gene	Annotation	Gene name	mRNA ratio	n	*p*-Value
GOX0310	NAD(P) transhydrogenase subunit α1	*pntA1*	2.09	3	1.41E-02
GOX0311	NAD(P) transhydrogenase subunit α2	*pntA2*	2.13	3	2.83E-02
GOX0312	NAD(P) transhydrogenase subunit b	*pntB*	2.26	3	1.70E-03
GOX0313	Alcohol:NAD^+ oxidoreductase		2.23	3	1.45E-03

Category: Metabolism

***G. oxydans* Δ*upp*Δ*edd-eda* versus *G. oxydans* Δ*upp* (reference). second growth phase**

Gene	Annotation	Gene name	mRNA ratio	n	*p*-Value
GOX0430	KDPG aldolase	*eda*	0.08	3	2.16E-03
GOX0431	Phosphogluconate dehydratase	*edd*	0.06	3	1.38E-03
GOX0626	Thioredoxin		0.39	3	4.78E-03
GOX0762	Thioredoxin	*trxA*	0.30	3	1.17E-02
GOX0875	AtsE protein		0.32	3	6.25E-04
GOX1095	Aminomethyltransferase (Glycine cleavage system T protein)		0.41	3	3.27E-02
GOX1096	Glycine cleavage system H protein		0.35	3	1.85E-02

GOX1751	HesB family protein		0.48	3	9.77E-03
GOX1785	Carbonic anhydrase	*cynT*	2.02	3	3.31E-04
GOX1836	N-formylmethionylaminoacyl-tRNA deformylase		0.38	3	6.22E-03
GOX2186	Ribulokinase		0.48	3	4.76E-03
GOX2217	Triosephosphate isomerase		0.37	3	9.11E-03
GOX2218	Ribose-5-phosphate isomerase B		0.42	3	1.05E-02
GOX2222	Dihydroxyacetone kinase		0.47	3	3.19E-02
GOX2272	Membrane-bound dipeptidase		0.41	3	2.33E-02
GOX2306	Glutaredoxin		0.50	3	2.35E-02
GOX2493	Peptide methionine sulfoxide reductase		0.33	3	2.31E-03
GOX2685	Transposase		0.48	3	2.78E-02

***G. oxydans* Δ*upp*Δ*gnd zwf** versus *G. oxydans* Δ*upp* (reference)**

Gene	**Annotation**	**Gene name**	**mRNA ratio**	**n**	***p*-Value**
GOX0103	Carboxypeptidase-related protein		0.49	3	6.64E-03
GOX0155	Phospho-N-acetylmuramoyl-pentapeptide-transferase		0.49	3	8.77E-03
GOX0165	UDP-3-O-acyl-N-acetylglucosamine deacetylase		2.94	3	1.82E-02
GOX0438	Rare lipoprotein A		2.46	3	1.43E-02
GOX0440	Ornithine decarboxylase		0.41	3	5.96E-03
GOX0875	AtsE protein		3.32	3	3.46E-03
GOX0881	Arylesterase		2.28	3	2.41E-02
GOX0928	Phosphoadenosine phosphosulfate reductase		0.44	3	6.85E-03
GOX1050	dTDP-4-dehydrorhamnose reductase		2.07	3	2.17E-03
GOX1114	Vitamin B12-dependent ribonucleotide reductase		0.43	3	9.52E-04
GOX1118	Trehalose-phosphatase		2.26	3	1.08E-02
GOX1119	Alpha,alpha-trehalose-phosphate synthase		2.59	3	1.94E-03
GOX1276	Secreted protein of amidohydrolase family		2.27	3	2.90E-03
GOX1432	NADP-dependent D-sorbitol dehydrogenase		2.50	3	1.98E-03
GOX1497	Acyl-CoA dehydrogenase		2.06	3	1.86E-02
GOX1516	Fructose-1,6-bisphosphatase II	*fbp*	2.36	3	5.57E-03
GOX1540	Fructose-1,6-bisphosphate aldolase		2.86	3	2.44E-03
GOX1569	Tricorn protease homolog		0.37	3	7.89E-05
GOX1705	6-phosphogluconate dehydrogenase-like protein	*gnd*	0.04	3	1.37E-03
GOX1712	Aldehyde dehydrogenase		2.83	3	3.55E-03
GOX1713	Putative protease of DJ-1/Pfpl family	*pfpI*	2.32	3	9.33E-03
GOX1766	Non-heme chloroperoxidase		2.90	3	5.16E-04
GOX1785	Carbonic anhydrase	*cynT*	2.81	3	5.07E-03
GOX1953	5-Methylcytosine-specific restriction		2.09	3	1.11E-02

	enzyme				
GOX2088	Glycerol-3-phosphate dehydrogenase	*glpD*	3.92	3	2.10E-02
GOX2090	Glycerol kinase	*glpK*	3.01	3	5.94E-03
GOX2186	Ribulokinase		2.69	3	1.77E-02
GOX2197	N-formylglutamate deformylase		2.01	3	3.46E-02
GOX2217	Triosephosphate isomerase		6.96	3	4.76E-02
GOX2218	Ribose-5-phosphate isomerase B		7.64	3	4.38E-02
GOX2222	Dihydroxyacetone kinase		2.81	3	8.41E-03
GOX2675	Transposase		0.06	3	2.37E-03
GOX2684	NAD(P)H-dependent 2-cyclohexen-1-one reductase		0.04	3	3.58E-04
GOX2694	ParA-like protein		0.04	3	7.88E-04
GOX2719	Transposase		2.17	3	3.81E-02

***G. oxydans* Δ*upp*Δ*gnd* versus *G. oxydans* Δ*upp* (reference)**

Gene	Annotation	Gene name	mRNA ratio	n	*p*-Value
GOX1705	6-phosphogluconate dehydrogenase-like protein	*gnd*	0.13	3	2.11E-03
GOX2684	NAD(P)H-dependent 2-cyclohexen-1-one reductase		0.16	3	6.15E-04
GOX2694	ParA-like protein		0.18	3	7.94E-04
GOX2675	Transposase		0.20	3	3.49E-04
GOX1704	Bifunctional transaldolase/phosoglucose isomerase	*pgi/tal*	2.08	3	3.19E-03
GOX2719	Transposase		2.16	3	1.07E-03
GOX1540	Fructose-1,6-bisphosphate aldolase		2.26	3	2.56E-03
GOX1703	Transketolase	*tkt*	2.36	3	4.74E-03
GOX2090	Glycerol kinase	*glpK*	2.54	3	3.37E-03
GOX2088	Glycerol-3-phosphate dehydrogenase	*glpD*	3.79	3	4.75E-04
GOX2222	Dihydroxyacetone kinase		6.37	3	2.74E-03
GOX2217	Triosephosphate isomerase		7.34	3	3.26E-03
GOX2218	Ribose-5-phosphate isomerase B		9.56	3	2.52E-03
GOX2186	Ribulokinase		2.60	3	2.14E-04

Category: Regulation and signal transduction

***G. oxydans* Δ*upp*Δ*edd-eda* versus *G. oxydans* Δ*upp* (reference), second growth phase**

Gene	Annotation	Gene name	mRNA ratio	n	*p*-Value
GOX0506	RNA polymerase factor sigma factor H (sigma-32)	*rpoH*	0.33	3	1.93E-04
GOX1459	Transcriptional regulator		0.42	3	3.68E-02
GOX1946	Two component response regulator		0.50	3	1.04E-02

***G. oxydans* Δ*upp*Δ*gnd zwf** versus *G. oxydans* Δ*upp* (reference)**

Gene	Annotation	Gene name	mRNA ratio	n	*p*-Value
GOX0197	Signal recognition particle protein	*ffh*	0.50	3	9.16E-03
GOX0744	Nitrogen regulatory protein P-II, GlnK		0.48	3	2.18E-03
GOX2544	Transcriptional regulator protein		0.50	3	2.43E-04
GOX2668	MucR family transcriptional regulator		0.10	3	5.09E-03

***G. oxydans* Δ*upp*Δ*gnd* versus *G. oxydans* Δ*upp* (reference)**

Gene	Annotation	Gene name	mRNA ratio	n	*p*-Value
GOX1613	Protein with GGDEF and EAL domain		0.46	3	2.19E-03

Category: Transport

***G. oxydans* Δ*upp*Δ*edd-eda* versus *G. oxydans* Δ*upp* (reference). second growth phase**

Gene	Annotation	Gene name	mRNA ratio	n	*p*-Value
GOX0673	Ferrous iron transport protein A (FeoA)	*feoA*	0.40	3	9.68E-03
GOX2219	Ribose ABC transporter, periplasmic binding protein		0.42	3	1.50E-02
GOX2220	Ribose ABC transporter, ATP-binding protein		0.47	3	4.22E-02

***G. oxydans* Δ*upp*Δ*gnd zwf** versus *G. oxydans* Δ*upp* (reference)**

Gene	Annotation	Gene name	mRNA ratio	n	*p*-Value
GOX0405	TonB-dependent outer membrane receptor		0.40	3	2.56E-04
GOX0649	Sugar-proton symporter		2.13	3	2.26E-02
GOX0743	Ammonium transporter AmtB		0.43	3	6.30E-04
GOX0907	TonB-dependent outer membrane receptor		0.40	3	8.96E-03
GOX0945	TonB-dependent outer membrane receptor		0.18	3	4.33E-04
GOX1017	TonB-dependent outer membrane receptor		0.30	3	2.16E-03
GOX1365	ABC transporter permease protein		0.42	2	2.40E-02
GOX1366	ABC transporter ATP-binding protein		0.44	3	1.70E-03
GOX1652	Heme exporter protein C		0.50	3	1.23E-03
GOX1661	Bacterioferritin comigratory protein		3.63	3	8.22E-03
GOX1903	TonB-dependent receptor protein		0.17	3	1.17E-03
GOX2089	Glycerol uptake facilitator protein	*glpF*	3.37	3	1.37E-02
GOX2184	Probable mannitol/sorbitol ABC transporter permease protein		2.10	3	2.18E-02
GOX2185	Periplasmic mannitol/sorbitol binding protein		2.84	3	2.78E-02
GOX2219	Ribose ABC transporter. periplasmic binding protein		8.30	3	2.87E-02

GOX2220	Ribose ABC transporter, ATP-binding protein		4.02	3	1.86E-02
GOX2221	Ribose ABC transporter, permease protein		2.57	3	3.76E-03

***G. oxydans* Δ*upp*Δ*gnd* versus *G. oxydans* Δ*upp* (reference)**

Gene	Annotation	Gene name	mRNA ratio	n	*p*-Value
GOX0649	Sugar-proton symporter		2.16	3	1.73E-02
GOX2183	Probable mannitol/sorbitol ABC transporter ATP-binding protein		2.49	3	7.47E-03
GOX2182	Probable mannitol/sorbitol ABC transporter permease protein		2.91	3	1.67E-03
GOX2184	Probable mannitol/sorbitol ABC transporter permease protein		3.07	3	3.04E-03
GOX2185	Periplasmic mannitol/sorbitol binding protein		3.29	3	3.92E-08
GOX2231	Putative sugar transporter		3.49	3	2.18E-03
GOX2089	Glycerol uptake facilitator protein	*glpF*	3.64	3	2.42E-03
GOX2221	Ribose ABC transporter, permease protein		5.39	3	1.90E-05
GOX2220	Ribose ABC transporter, ATP-binding protein		6.27	3	2.24E-04
GOX2219	Ribose ABC transporter, periplasmic binding protein		8.26	3	4.52E-03

Category: Motility

***G. oxydans* Δ*upp*Δ*edd-eda* versus *G. oxydans* Δ*upp* (reference), second growth phase**

Gene	Annotation	Gene name	mRNA ratio	n	*p*-Value
GOX0787	Flagellin B		2.90	3	5.86E-03
GOX0953	Flagellar basal body rod protein FlgG	*flgG*	2.17	3	9.38E-03
GOX1027	Flagellar hook protein FlgE	*flgE*	2.07	3	1.96E-02

***G. oxydans* Δ*upp*Δ*gnd zwf** versus *G. oxydans* Δ*upp* (reference)**

Gene	Annotation	Gene name	mRNA ratio	n	*p*-Value
GOX0424	Flagellar MS-ring protein		0.45	3	1.77E-02
GOX1525	Flagellar biosynthetic protein FliQ	*fliQ*	0.39	3	4.65E-02
GOX1526	Flagellar hook-basal body protein FleE	*fleE*	0.44	3	3.70E-02
GOX1527	Flagellar basal body rod protein FlgC	*flgC*	0.41	3	3.83E-02
GOX1528	Flagellar basal-body rod protein FlgB	*flgB*	0.43	3	3.42E-02

***G. oxydans* Δ*upp*Δ*gnd* versus *G. oxydans* Δ*upp* (reference)**

Gene	Annotation	Gene name	mRNA ratio	n	*p*-Value
GOX1525	Flagellar biosynthetic protein FliQ	*fliQ*	0.37	3	4.26E-03
GOX0788	Flagellin assembly protein	*mviN*	0.41	3	5.25E-03
GOX1528	Flagellar basal-body rod protein FlgB	*flgB*	0.43	3	1.98E-06
GOX0787	Flagellin B		0.44	3	4.32E-03

GOX1026	Flagellar hook-associated protein 1 FlgK	*flgK*	0.44	3	5.91E-03
GOX1526	Flagellar hook-basal body protein FleE	*fleE*	0.46	3	6.20E-03
GOX1527	Flagellar basal body rod protein FlgC	*flgC*	0.47	3	2.32E-03
GOX1027	Flagellar hook protein FlgE	*flgE*	0.49	3	2.76E-03
GOX0127	Chemotaxis MotB protein		0.49	3	1.25E-02

Category: Stress

***G. oxydans* Δ*upp* Δ*edd-eda* versus *G. oxydans* Δ*upp* (reference). second growth phase**

Gene	Annotation	Gene name	mRNA ratio	n	*p*-Value
GOX0049	DnaJ family protein		0.47	3	3.26E-02
GOX0608	ATP-dependent Clp protease adaptor protein ClpS	*clpS*	0.35	3	1.45E-02
GOX0707	DNA starvation/stationary phase protection protein Dps	*dps*	0.49	3	4.01E-02
GOX0763	ATP-dependent protease La		0.44	3	1.40E-02
GOX0820	GrpE protein (HSP-70 cofactor)		0.30	3	6.56E-03
GOX0833	Cold shock protein		0.39	3	3.02E-03
GOX0857	Chaperone protein DnaK		0.32	3	5.60E-03
GOX0858	Chaperone protein DnaJ		0.48	3	4.21E-02
GOX1024	Heat shock protein 90	*hsp90*	0.40	3	7.25E-03
GOX1329	Small heat shock protein	*hsd*	0.21	3	1.55E-03
GOX1414	Chaperone protein DnaJ	*dnaJ*	0.49	3	1.66E-02
GOX1463	ATP-dependent Clp protease. ATP-binding subunit ClpV	*clpV*	0.43	3	3.05E-03
GOX1661	Bacterioferritin comigratory protein		0.50	3	2.90E-02
GOX1837	Small heat shock protein HspA		0.32	3	4.60E-03
GOX1901	Co-chaperonin GroES		0.33	3	2.17E-02
GOX1902	Chaperonin GroEL		0.42	3	4.35E-03
GOX2397	Small heat shock protein	*hsd*	0.29	3	1.20E-02

***G. oxydans* Δ*upp*Δ*gnd zwf* versus *G. oxydans* Δ*upp* (reference)**

Gene	Annotation	Gene name	mRNA ratio	n	*p*-Value
GOX0329	Stress response protein CsbD		2.69	3	1.54E-02
GOX0707	DNA starvation/stationary phase protection protein Dps	*dps*	3.36	3	2.41E-03
GOX0798	Trypsin-like serine protease. (HtrA/DegQ/DegS family) with two PDZ domains		2.14	3	1.65E-03
GOX1138	Catalase	*katG*	2.61	3	4.55E-04
GOX1329	Small heat shock protein	*hsd*	2.55	3	6.79E-03
GOX1859	Excinuclease ABC subunit B		2.20	3	1.38E-02
GOX1992	Osmotically inducible protein C, peroxyredoxin	*osmC*	3.78	3	4.89E-03

GOX2674	Death on curing protein		0.10	3	8.56E-04

Category: Tanscriptional and translational machinery

***G. oxydans* Δ*upp*Δ*edd-eda* versus *G. oxydans* Δ*upp* (reference). second growth phase**

Gene	Annotation	Gene name	mRNA ratio	n	*p*-Value
GOX0889	Peptidyl-prolyl cis-trans isomerase	*ppi*	0.46	3	1.33E-02

***G. oxydans* Δ*upp*Δ*gnd zwf** versus *G. oxydans* Δ*upp* (reference)**

Gene	Annotation	Gene name	mRNA ratio	n	*p*-Value
GOX0452	50S Ribosomal protein L13		0.49	3	2.28E-05
GOX1781	Bacterial Peptide Chain Release Factor 3 (RF-3)		0.45	3	2.73E-02

Category: Predicted functions

***G. oxydans* Δ*upp*Δ*edd-eda* versus *G. oxydans* Δ*upp* (reference), second growth phase**

Gene	Annotation	Gene name	mRNA ratio	n	*p*-Value
GOX0090	Putative sugar kinase		0.50	3	2.85E-02
GOX0478	Putative oxidoreductase		0.50	3	2.17E-02
GOX0502	Putative oxidoreductase		0.39	3	5.62E-03
GOX1615	Putative oxidoreductase		0.49	3	5.54E-03
GOX1839	Putative translation initiation inhibitor		0.44	3	1.74E-02

***G. oxydans* Δ*upp*Δ*gnd zwf** versus *G. oxydans* Δ*upp* (reference)**

Gene	Annotation	Gene name	mRNA ratio	n	*p*-Value
GOX0290	Putative oxidoreductase		2.06	3	1.11E-03
GOX0351	Putative outer membrane drug efflux protein		0.50	3	2.33E-03
GOX0417	Putative 2-hydroxyacid dehydrogenase		2.04	3	7.12E-03
GOX0458	Putative oxidoreductase		2.07	3	1.03E-04
GOX0470	Putative peroxidase	*efeB*	3.08	3	5.96E-03
GOX0471	Putative 4-hydroxyphenylpyruvate dioxygenase		3.02	3	6.85E-04
GOX0502	Putative oxidoreductase		2.34	3	5.25E-03
GOX0644	Putative 2,5-diketo-D-gluconic acid reductase		2.46	3	6.87E-04
GOX0646	Putative oxidoreductase		2.39	3	6.65E-03
GOX1122	Putative NAD-dependent aldehyde dehydrogenase		2.99	3	1.12E-02
GOX1139	Putative oxidoreductase		3.12	3	5.88E-03
GOX1351	Putative isomerase		2.65	3	1.55E-02
GOX1494	Putative oxidoreductase		2.45	3	4.96E-03
GOX1495	Oxidoreductase, iron-sulphur binding subunit		2.48	3	1.95E-02
GOX1538	Short chain dehydrogenase		3.16	3	3.60E-03

GOX1615	Putative oxidoreductase		2.16	3	4.45E-03
GOX1801	Putative oxidoreductase		2.58	3	7.12E-08
GOX1849	Putative oxidoreductase		4.03	3	3.26E-03
GOX1857	Uncharacterized PQQ-containing dehydrogenase 1		2.85	3	3.16E-02
GOX1865	Putative transmembrane protein		2.32	3	2.67E-03
GOX1899	Putative oxidoreductase		2.24	3	4.96E-03
GOX1900	Putative carboxymethylenebutenolidase		2.17	3	5.83E-03
GOX2181	Putative polyol dehydrogenase		2.34	3	9.60E-03
GOX2199	Probable myosin-crossreactive antigen		2.69	3	3.69E-03
GOX2200	Probable myosin-crossreactive antigen		3.30	3	6.87E-03
GOX2376	Putative aldehyde dehydrogenase		2.33	3	1.78E-03
GOX2676	Putative alcohol/aldehyde dehydrogenase		0.04	3	2.89E-03

***G. oxydans* Δ*upp*Δ*gnd* versus *G. oxydans* Δ*upp* (reference)**

Gene	Annotation	Gene name	mRNA ratio	n	*p*-Value
GOX2676	Putative alcohol/aldehyde dehydrogenase		0.14	3	5.62E-03
GOX2200	Probable myosin-crossreactive antigen		2.04	3	4.07E-03
GOX2181	Putative polyol dehydrogenase		2.58	3	4.46E-03
GOX1857	Uncharacterized PQQ-containing dehydrogenase 1		4.22	3	3.12E-04
GOX0471	Putative 4-hydroxyphenylpyruvate dioxygenase		2.21	3	1.31E-03
GOX1357	Putative electron transport protein		2.33	3	8.82E-03
GOX1849	Putative oxidoreductase		2.23	3	1.29E-02

Category: Hypothetical proteins

***G. oxydans* Δ*upp* Δ*edd-eda* versus *G. oxydans* Δ*upp* (reference), second growth phase**

Gene	Annotation	Gene name	mRNA ratio	n	*p*-Value
GOX0182	Hypothetical protein GOX0182		0.48	3	1.04E-02
GOX0235	Hypothetical protein GOX0235		0.48	3	1.69E-02
GOX0337	Hypothetical protein GOX0337		0.47	3	2.20E-02
GOX0347	Hypothetical protein GOX0347		0.40	3	4.69E-03
GOX0503	Hypothetical protein GOX0503		0.32	3	2.27E-03
GOX0570	Hypothetical protein GOX0570		0.40	3	1.24E-02
GOX0576	Hypothetical protein GOX0576		0.28	3	1.53E-03
GOX0726	Hypothetical protein GOX0726		0.43	3	2.33E-02
GOX0734	Hypothetical protein GOX0734		0.30	3	5.05E-03
GOX0880	Hypothetical protein GOX0880		0.48	3	1.38E-02

GOX0890	Hypothetical protein GOX0890		0.18	3	4.60E-03
GOX1299	Hypothetical protein GOX1299		0.37	3	1.50E-03
GOX1328	Hypothetical protein GOX1328		0.42	3	2.04E-02
GOX1410	Hypothetical protein GOX1410		0.50	3	9.16E-03
GOX1500	Hypothetical protein GOX1500		0.50	3	1.02E-02
GOX1617	Hypothetical protein GOX1617		0.42	3	4.52E-03
GOX1633	Hypothetical protein GOX1633		0.31	3	4.61E-03
GOX1660	Hypothetical protein GOX1660		0.49	3	1.25E-02
GOX1735	Hypothetical protein GOX1735		0.44	3	3.90E-04
GOX1745	Hypothetical protein GOX1745		0.35	3	9.46E-05
GOX1838	Hypothetical protein GOX1838		0.29	3	7.05E-03
GOX1841	Hypothetical protein GOX1841		0.23	3	3.39E-03
GOX1910	Hypothetical protein GOX1910		0.50	3	1.40E-02
GOX2079	Hypothetical protein GOX2079		0.44	3	1.29E-02
GOX2086	Hypothetical protein GOX2086		0.49	3	3.02E-03
GOX2109	Hypothetical protein GOX2109		0.37	3	9.72E-03
GOX2257	Hypothetical protein GOX2257		0.37	3	1.19E-03
GOX2305	Hypothetical protein GOX2305		0.49	3	2.82E-02

***G. oxydans* Δ*upp*Δ*gnd zwf** versus *G. oxydans* Δ*upp* (reference)**

Gene	**Annotation**	**Gene name**	**mRNA ratio**	**n**	***p*-Value**
GOX0035	Hypothetical protein GOX0035		0.49	3	4.47E-03
GOX0198	Hypothetical protein GOX0198		2.04	3	9.80E-03
GOX0244	Hypothetical membrane-spanning protein		2.21	3	1.71E-03
GOX0347	Hypothetical protein GOX0347		3.02	3	1.86E-02
GOX0404	Hypothetical protein GOX0404		2.07	3	1.45E-05
GOX0453	Hypothetical protein GOX0453		2.13	3	4.21E-03
GOX0472	Hypothetical protein GOX0472		2.45	3	1.93E-02
GOX0474	Hypothetical protein GOX0474		2.46	3	2.48E-03
GOX0475	Hypothetical protein GOX0475		2.36	3	1.60E-03
GOX0503	Hypothetical protein GOX0503		2.16	3	4.85E-03
GOX0568	Hypothetical protein GOX0568		2.02	3	1.11E-02
GOX0643	Hypothetical protein GOX0643		2.21	3	1.26E-02
GOX0694	Hypothetical protein GOX0694		0.50	3	2.11E-02
GOX0695	Hypothetical protein GOX0695		0.47	3	2.81E-02
GOX0726	Hypothetical protein GOX0726		4.38	3	1.10E-02
GOX0734	Hypothetical protein GOX0734		2.39	3	8.61E-03
GOX0741	Hypothetical protein GOX0741		2.19	3	3.49E-03
GOX0827	Hypothetical protein GOX0827		2.11	3	5.64E-03
GOX0975	Hypothetical protein GOX0975		2.33	3	2.93E-02
GOX1007	Hypothetical protein GOX1007		2.62	3	6.81E-04
GOX1008	Hypothetical protein GOX1008		2.01	3	1.72E-02

GOX1029	Hypothetical protein GOX1029		0.42	2	6.69E-04
GOX1072	Hypothetical protein GOX1072		2.00	3	3.43E-02
GOX1094	Hypothetical protein GOX1094		2.41	3	8.51E-03
GOX1299	Hypothetical protein GOX1299		2.55	3	1.06E-02
GOX1363	Hypothetical protein GOX1363		0.44	3	5.82E-03
GOX1534	Hypothetical protein GOX1534		3.20	3	3.83E-03
GOX1633	Hypothetical protein GOX1633		3.92	3	5.81E-04
GOX1655	Hypothetical protein GOX1655		2.04	3	1.89E-02
GOX1660	Hypothetical protein GOX1660		4.95	3	2.70E-03
GOX1735	Hypothetical protein GOX1735		2.36	3	2.25E-02
GOX1736	Hypothetical protein GOX1736		2.72	3	2.03E-02
GOX1749	Hypothetical protein GOX1749		3.59	3	2.98E-02
GOX1784	Hypothetical protein GOX1784		2.72	3	2.01E-03
GOX1830	Hypothetical protein GOX1830		0.42	3	5.88E-03
GOX1841	Hypothetical protein GOX1841		3.61	3	2.15E-03
GOX1850	Hypothetical protein GOX1850		2.20	3	1.50E-02
GOX1910	Hypothetical protein GOX1910		2.76	3	8.39E-05
GOX1982	Hypothetical protein GOX1982		0.50	3	1.85E-02
GOX2017	Hypothetical protein GOX2017		2.88	3	1.02E-03
GOX2028	Hypothetical protein GOX2028		2.05	3	6.34E-04
GOX2064	Hypothetical protein GOX2064		4.88	3	6.72E-03
GOX2079	Hypothetical protein GOX2079		5.26	3	2.92E-03
GOX2109	Hypothetical protein GOX2109		2.66	3	2.36E-03
GOX2216	Hypothetical protein GOX2216		3.35	2	4.49E-02
GOX2257	Hypothetical protein GOX2257		3.41	3	3.42E-04
GOX2734	Hypothetical protein GOX2734		2.00	3	1.27E-02

***G. oxydans* Δ*upp*Δ*gnd* versus *G. oxydans* Δ*upp* (reference)**

Gene	**Annotation**	**Gene name**	**mRNA ratio**	**n**	***p*-Value**
GOX0352	Hypothetical protein GOX0352		2.00	3	5.06E-08
GOX0426	Hypothetical protein GOX0426		0.50	3	1.79E-02
GOX0475	Hypothetical protein GOX0475		2.51	3	3.68E-03
GOX0576	Hypothetical protein GOX0576		2.09	3	3.47E-02
GOX1633	Hypothetical protein GOX1633		2.94	3	1.57E-02
GOX1660	Hypothetical protein GOX1660		2.86	3	1.44E-02
GOX1841	Hypothetical protein GOX1841		2.05	3	1.93E-02
GOX1870	Hypothetical protein GOX1870		0.49	3	1.44E-02
GOX2028	Hypothetical protein GOX2028		3.03	3	1.01E-02
GOX2064	Hypothetical protein GOX2064		2.32	3	1.25E-02

3.2. Glucose metabolism of *G. oxydans* 621H

Own contribution to this manuscript: about 70 %. I performed all experimental work described in the manuscript and wrote a draft. I am first author of the manuscript.

Published in Applied Microbiology and Biotechnology; DOI 10.1007/s00253-013-4707-2

Impact factor: 3.583

Role of the pentose phosphate pathway and the Entner–Doudoroff pathway in glucose metabolism of *Gluconobacter oxydans* 621H

Janine Richhardt · Stephanie Bringer · Michael Bott

Received: 13 November 2012 / Revised: 9 January 2013 / Accepted: 10 January 2013

Abstract Glucose catabolism by the obligatory aerobic acetic acid bacterium *Gluconobacter oxydans* 621H proceeds in two phases comprising rapid periplasmic oxidation of glucose to gluconate (phase I) and oxidation of gluconate to 2-ketogluconate or 5-ketogluconate (phase II). Only a small amount of glucose and part of the gluconate is taken up into the cells. To determine the roles of the pentose phosphate pathway (PPP) and the Entner–Doudoroff pathway (EDP) for intracellular glucose and gluconate catabolism, mutants defective in either the PPP (Δ*gnd*, Δ*gnd zwf**) or the EDP (Δ*edd–eda*) were characterized under defined conditions of pH 6 and 15 % dissolved oxygen. In the presence of yeast extract, neither of the two pathways was essential for growth with glucose. However, the PPP mutants showed a reduced growth rate in phase I and completely lacked growth in phase II. In contrast, the EDP mutant showed the same growth behavior as the reference strain. These results demonstrate that the PPP is of major importance for cytoplasmic glucose and gluconate catabolism, whereas the EDP is dispensable. Reasons for this difference are discussed.

Keywords *Gluconobacter oxydans* · *gnd* · *zwf* · *edd* · *eda* · Glucose

Introduction

Gluconobacter oxydans, a gram-negative, strictly aerobic, rod-shaped bacterium, belongs to the family of acetic acid bacteria (Kersters et al. 2006) and is used in industry for decades, with its main application being the production of vitamin C and of 6-amino-L-sorbose, an intermediate in the synthesis of the antidiabetic drug miglitol (Raspor and Goranovič 2008). *G. oxydans* 621H, whose genome has been sequenced (Prust et al. 2005), possesses two spatially separated modes of sugar catabolism. The majority of the sugar or sugar alcohol is oxidized in the periplasm by membrane-bound dehydrogenases feeding electrons directly into the respiratory chain. A minor part of the sugar is catabolized in the cytoplasm, either in the nonphosphorylated state by soluble dehydrogenases forming sugar acids or keto sugar acids or after phosphorylation by the pentose phosphate pathway (PPP) or the Entner–Doudoroff pathway (EDP) (Fig. 1). The absence of 6-phosphofructokinase (Pfk) renders the Embden–Meyerhof pathway nonfunctional (Prust et al. 2005). Furthermore, the tricarboxylic acid cycle is incomplete because the genes for succinate dehydrogenase and also succinyl-CoA synthetase are lacking (Prust et al. 2005).

In a recent study on the intracellular mannitol/fructose catabolism of *G. oxydans* 621H (Richhardt et al. 2012), we showed that the absence of the EDP caused by deletion of the genes *edd–eda* led to an increased biomass yield in the first growth phase and to a 24 % increased final OD_{600}. In contrast, inactivation of the PPP by deletion of the *gnd* gene for 6-phosphogluconate dehydrogenase (6PG-DH) caused a complete loss of the second growth phase and led to a reduced final OD_{600}. Furthermore, deletion of *gnd* resulted in the formation of spontaneous mutations in the *zwf* gene, encoding glucose 6-phosphate dehydrogenase (G6P-DH). These Δ*gnd zwf** mutants were completely disabled in intracellular fructose metabolism, but reached the same final OD_{600} as the Δ*gnd* mutant (Richhardt et al. 2012). These results showed that neither of the two pathways is essential for the growth of *G. oxydans* in a medium containing yeast extract and that the absence of the PPP is growth inhibitory, whereas the absence of the EDP is beneficial for growth with mannitol as carbon source.

Electronic supplementary material The online version of this article (doi:10.1007/s00253-013-4707-2) contains supplementary material, which is available to authorized users.

J. Richhardt · S. Bringer (✉) · M. Bott (✉)
Institut für Bio- und Geowissenschaften, IBG-1: Biotechnologie, Forschungszentrum Jülich, Jülich 52425 Germany
e-mail: st.bringer-meyer@fz-juelich.de
e-mail: m.bott@fz-juelich.de

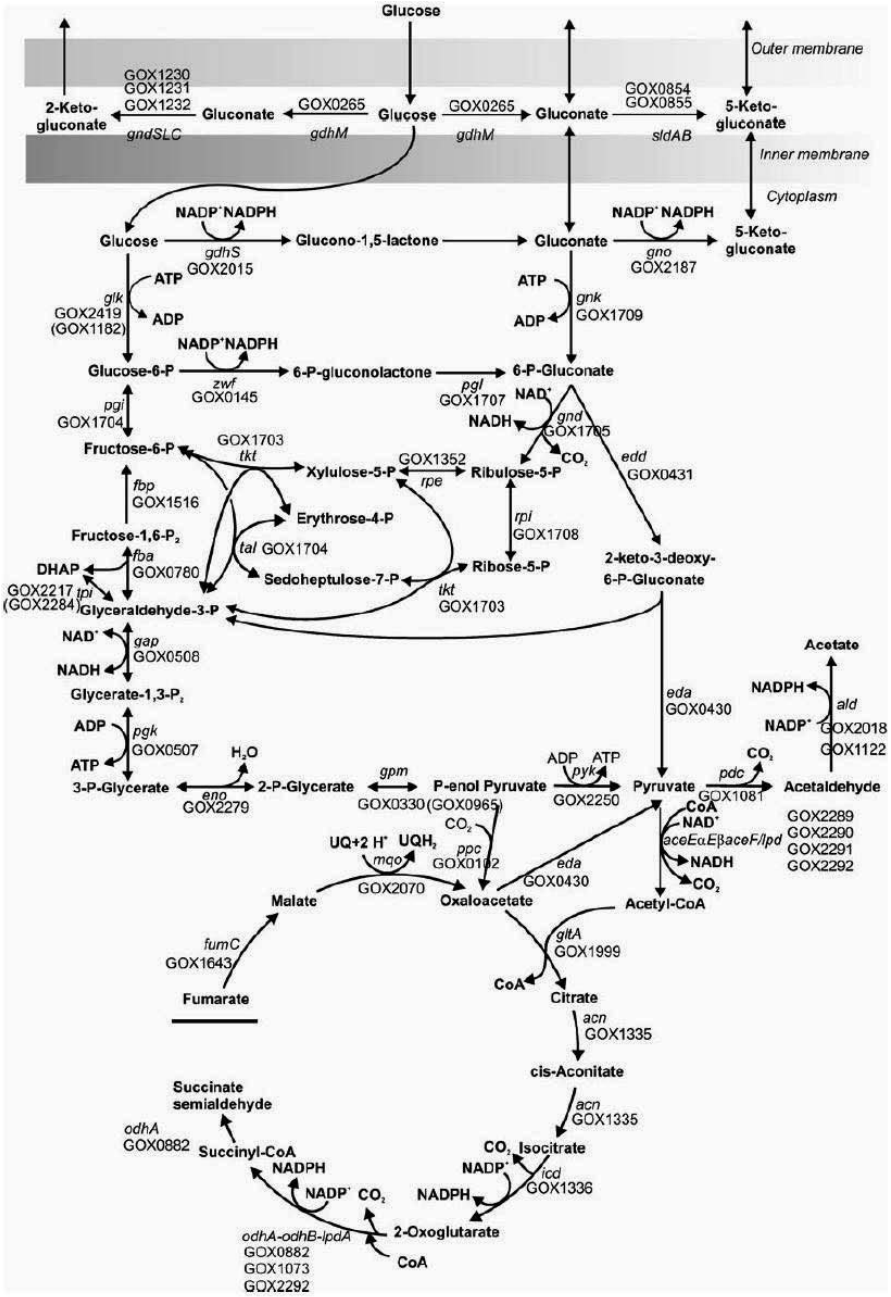

Fig. 1 Scheme of the central carbon metabolism of *G. oxydans* with the substrate glucose

Table 1 Bacterial strains used in this work

Strain *G. oxydans*	Description	Source
Δ*upp*	Δ*upp* derivative of *G. oxydans* 621H (deletion of GOX0327), reference strain in this study	Peters et al. (2012)
Δ*upp* Δ*gnd*	Δ*gnd* derivative of *G. oxydans* 621H Δ*upp* (deletion of GOX1705)	Richhardt et al. (2012)
Δ*upp* Δ*gnd zwf**	Δ*gnd* derivative of *G. oxydans* 621H Δ*upp* (deletion of GOX1705) with a mutation in *zwf* (GOX0145)	Richhardt et al. (2012)
Δ*upp* Δ*edd–eda*	Δ*edd–eda* derivative of *G. oxydans* 621H Δ*upp* (deletion of GOX0430 and GOX0431)	Richhardt et al. (2012)

In this study, using the three *G. oxydans* mutants described previously, we analyzed the role of PPP and EDP for growth, with glucose as carbon and energy source.

Materials and methods

Materials

Chemicals were obtained from Sigma-Aldrich (Taufirchen, Germany), Qiagen (Hilden, Germany), Merck (Darmstadt, Germany), and Roche Diagnostics (Mannheim, Germany).

Bacterial strains, plasmids, media, and growth conditions

The bacterial strains used in this study are listed in Table 1. *G. oxydans* ATCC 621H Δ*upp* (ATCC 621H is identical to DSM2343), which lacks the *upp* gene for uracil phosphoribosyltransferase, was obtained from Dr. Armin Ehrenreich, Technical University of Munich, Munich, Germany. *G. oxydans* strains were cultivated on complex medium containing 5 gL^{-1} yeast extract, 2.5 gL^{-1} $MgSO_4 \cdot 7H_2O$, 1 gL^{-1} $(NH_4)_2SO_4$, 1 gL^{-1} KH_2PO_4, 220 mM (4 % *w/v*) mannitol or 222 mM (4 % *w/v*) glucose, and 10 mM thymidine. The initial pH value of the medium was 6.0. *G. oxydans* possesses a natural resistance towards cefoxitin; as a precaution to prevent bacterial contaminations, cefoxitin was added to the media at a concentration of 50 $\mu g ml^{-1}$. Precultures were grown with the carbon source mannitol in baffled shaking flasks at 30 °C and 140 rpm. For the determination of growth parameters and enzyme activity measurements, cells were cultivated in 250 ml of the same medium with glucose instead of mannitol as the carbon source in a parallel bioreactor system (DASGIP, Jülich, Germany) composed of four 400-ml vessels, each equipped with electrodes for measuring the dissolved oxygen (DO) concentration and the pH. The system allows for constant control of these two parameters. The carbon dioxide concentration in the exhaust gas was measured continuously by an infrared spectrometer and the oxygen concentration was measured with a zirconium dioxide sensor. The pH was kept at pH 6.0 by automatic titration with 2 M NaOH and 2 M HCl. The oxygen availability was kept constant at 15 % DO by mixing air, O_2, and N_2. Calibration was performed by gassing with air (100 % DO) and N_2 (0 % DO). The agitation speed was kept constant at 900 rpm. Control and recording of all data were carried out by the software "Fedbatch Pro" (DASGIP, Jülich, Germany).

Determination of products by high-performance liquid chromatography (HPLC) analysis

One milliliter culture was centrifuged for 5 min at 13,000×*g* and the supernatant was filtered through a 0.2-μm filter (Millipore, Billerica, MA, USA) prior to HPLC analysis. Gluconate, 2-ketogluconate, 5-ketogluconate, and acetate were quantified with a Shodex RSpak DE-413L 250 × 4.6 mm ID column (CS Chromatographie Service GmbH, Langerwehe, Germany) at 40 °C using 2 mM $HClO_4$ as the eluent at a flow rate of 0.4 $ml\,min^{-1}$. Gluconate, 2-ketogluconate, and 5-ketogluconate were detected by an ultraviolet detector at 210 nm, and acetate was detected with a refraction index detector. Retention times for 2-ketogluconate, gluconate, 5-ketogluconate, and acetate were 5.4, 5.9, 6.4, and 12.3 min, respectively. Calibration curves were made using different metabolite concentrations, ranging from 0 to 20.4 mM gluconate, from 0 to 20.6 mM 2-ketogluconate, and from 0 to 20.6 mM 5-ketogluconate or from 0 to 50 mM acetate.

Enzymatic determination of glucose concentrations

One milliliter culture was centrifuged for 5 min at 13,000×*g* and the supernatant was filtered through a 0.2-μm filter (Millipore, Billerica, MA, USA) prior to the glucose assay. Glucose concentrations were determined photometrically at 340 nm using two different appropriate dilutions of the supernatant. Forty microliters of the diluted supernatant was added to 200 μl of a ready-to-use master mix. The master mix contained 1.2 mM adenosine triphosphate (ATP; disodium salt), 1.2 mM $NADP^+ \cdot 2H_2O$, 2.2 mM $MgSO_4 \cdot 7H_2O$, 1.6 U

ml^{-1} hexokinase (Roche Diagnostics Deutschland, Mannheim, Germany), and 1.8 Uml^{-1} G6P-DH (Roche Diagnostics Deutschland, Mannheim, Germany) in Tris–maleate buffer, pH 6.8. After incubation for 45 min at 37 °C with shaking, the absorption at 340 nm was measured with an MTP-Reader (Tecan, Crailsheim, Germany). Finally, the concentration of glucose was calculated using standard linear regression ranging from 0 to 0.75 $mgml^{-1}$ glucose.

Preparation of cell-free extracts and enzyme assays

For in vitro determinations of enzyme activities, culture samples (10 ml) were taken after 12 h of cultivation (Δ*upp* and Δ*upp* Δ*edd–eda*) or at an OD_{600} of 1.5 (Δ*upp*, Δ*upp* Δ*gnd*, and Δ*upp* Δ*gnd zwf**) and centrifuged at 10,414×*g* for 3 min. Cells were resuspended in 800 µl 50 mM Tris–HCl, pH 7.5 and disrupted at 4 °C by three times 15-s bead-beating with 0.1 mm diameter glass beads using a Silamat S5 (Ivoclar Vivadent GmbH, Germany). The resulting crude extracts were centrifuged at 16,000×*g* (4 °C, 30 min) to remove intact cells and cell debris. The supernatants were used as cell-free extracts. Enzyme activities were measured photometrically at 340 nm using three different dilutions of the cell-free extract.

G6P-DH and 6PG-DH activities were measured at 30 °C by standard methods (Moritz et al. 2000). Protein concentrations were determined according to Bradford (1976) using bovine serum albumin as the standard.

Results

Glucose catabolism in *G. oxydans*

The present study was conducted to clarify the relative impacts and functions of the PPP and EDP for cytoplasmic degradation of glucose and gluconate. A scheme of the central carbon metabolism of *G. oxydans*, including the reactions involved in glucose catabolism, is shown in Fig. 1. In Figs. 2, 3, and 4 and Tables 2 and 3, growth in glucose medium, substrate consumption, product formation, and carbon balances are shown for the reference strain *G. oxydans* Δ*upp* and the deletion mutants described in the succeeding paragraphs. Growth of *G. oxydans* on glucose proceeds in two phases. In phase I, glucose is rapidly oxidized in the periplasm by the membrane-bound, pyrroloquinoline quinone-containing glucose dehydrogenase (GOX0265, *gdhM*) to gluconate, resulting in a high demand for oxygen and in a strong acidification of the culture medium. Only a small fraction of glucose is transported into the cell via an unknown transporter. The phosphoenolpyruvic acid-dependent phosphotransferase system of *G. oxydans* is considered to be inactive as a transport system since it lacks the EII^B and EII^C components and the function of the remaining components EI, HPr, EIIA, and HPr kinase is not yet clear. Gluconate is taken up by a putative gluconate permease (GOX2188, *gntP*) (Prust et al. 2005).

In growth phase II, a major part of gluconate is oxidized in the periplasm by the membrane-bound gluconate 2-dehydrogenase (GOX1230–1232) to 2-ketogluconate. In contrast to a number of other *Gluconobacter* species (e.g., DSM3504), the strain used in this study (DSM2343) does not oxidize 2-ketogluconate to 2,5-di-keto-gluconate due to the lack of the gene encoding the membrane-bound 2-ketogluconate dehydrogenase (Shinagawa and Ameyama 1982; Weenk et al. 1984). In principle, gluconate could also be oxidized in the periplasm to 5-ketogluconate by the membrane-bound major polyol dehydrogenase (GOX0854 and GOX0855). However, this probably does not occur at pH 6 applied in the present work, as the enzyme has its optimum activity for 5-ketogluconate formation at acidic pH values of 3.5–4.0 (Ano et al. 2011; Matsushita et al. 2003; Miyazaki et al. 2002). Whereas 5-ketogluconate can be formed in the cytoplasm (see the succeeding paragraphs), 2-ketogluconate production is confined to the periplasm since no cytoplasmic enzyme with gluconate 2-dehydrogenase activity exists.

Cytoplasmic glucose catabolism can occur via a soluble $NADP^+$-dependent glucose dehydrogenase (GOX2015, *gdhS*) or via glucose kinases (GOX2419, *glkA* and GOX1182, *glkB*). The intracellular gluconate can be converted to 5-ketogluconate by a soluble $NADP^+$-dependent gluconate 5-dehydrogenase (GOX2187, *gno*) or phosphorylated by gluconate kinase (GOX1709, *gnk*). Glucose 6-phosphate and 6-phosphogluconate are catabolized in the cytoplasm either through the PPP or the EDP. At the onset of growth phase II, defined here as the time point when the primary substrate glucose is totally oxidized to gluconate, growth changes from a rapid, exponential fashion to a slow, linear fashion. The intracellular formation of 5-ketogluconate decreases in growth phase II. Moreover, acetate is formed in phase II from pyruvate via pyruvate decarboxylase (GOX1081, *pdc*) and acetaldehyde dehydrogenases (GOX1122 and GOX2018) (Fig. 1) (Krajewski et al. 2010; Peters et al. 2012; Schweiger et al. 2007).

Characterization of *G. oxydans* Δ*upp* Δ*gnd* and Δ*upp* Δ*gnd zwf** lacking 6PG-DH or additionally G6P-DH

In order to test the role of the oxidative part of the PPP in glucose/gluconate catabolism, two mutants, one lacking only the *gnd* gene encoding 6PG-DH and one carrying an additional mutation in the *zwf* gene causing inactivation of the encoded G6P-DH, were cultivated under controlled conditions in a parallel bioreactor system with glucose as the

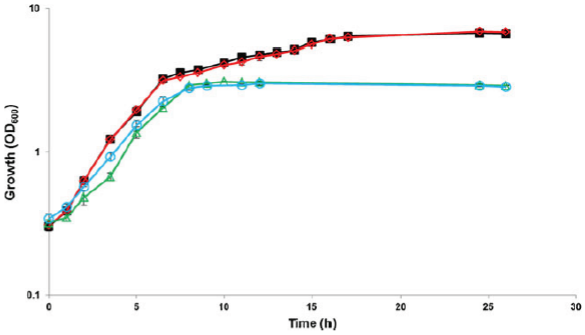

Fig. 2 Growth of *G. oxydans* reference strain Δ*upp* (*black squares*) and mutants Δ*upp* Δ*gnd* (*blue circles*), Δ*upp* Δ*gnd zwf** (*green triangles*), and Δ*upp* Δ*edd–eda* (*red diamonds*). Cells were cultivated under controlled conditions (15 % DO, pH 6) in a bioreactor using glucose as carbon and energy source. Mean values and standard deviations of three independent cultures are shown

carbon source. The latter mutant (Δ*upp* Δ*gnd zwf**) is in principle still able to catabolize glucose via the EDP by oxidation to gluconate with the soluble glucose dehydrogenase and subsequent phosphorylation of gluconate to 6-phosphogluconate with gluconate kinase. The mutants were characterized with respect to growth and enzyme activities and compared to the reference strain *G. oxydans* Δ*upp*.

The two mutant strains Δ*upp* Δ*gnd* and Δ*upp* Δ*gnd zwf** showed nearly the same growth behavior, indicating that the lack of G6P-DH activity in the Δ*gnd* background was not an additional hindrance for the cells. However, growth of both strains was significantly impaired compared to the reference strain with 30 and 35 % reduced growth rates and 57 and 56 % reduced final OD_{600} values (Fig. 2,

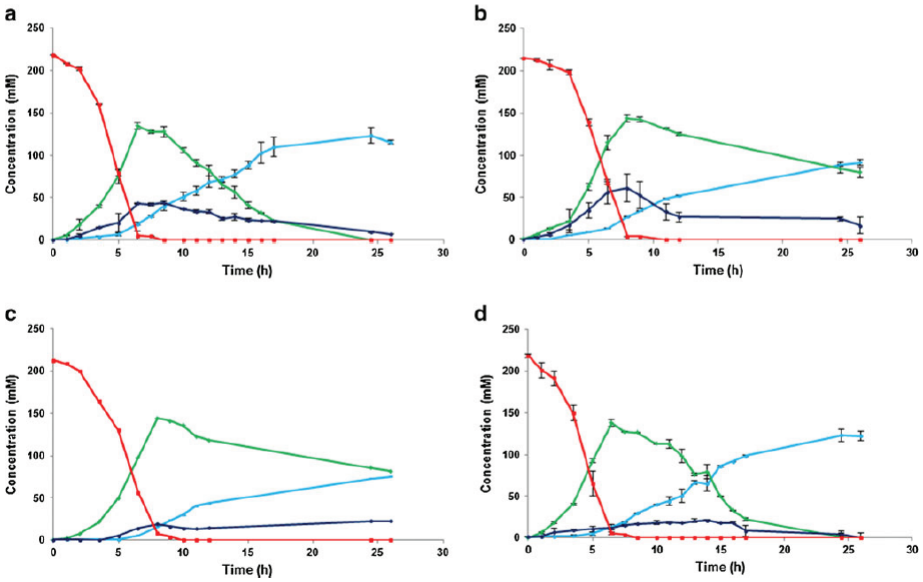

Fig. 3 Substrate consumption and product formation by the *G. oxydans* reference strain Δ*upp* (**a**) and mutants Δ*upp* Δ*gnd* (**b**), Δ*upp* Δ*gnd zwf** (**c**), and Δ*upp* Δ*edd–eda* (**d**). Cells were cultivated in glucose medium with 15 % DO and at pH 6. Glucose is indicated in *red*, gluconate is indicated in *green*, 2-ketogluconate is indicated in *light blue*, and 5-ketogluconate is indicated in *dark blue*. Mean values of two biological replicates (Δ*upp* Δ*gnd zwf**) or mean values and standard deviations of three biological replicates (Δ*upp*, Δ*upp* Δ*gnd*, and Δ*upp* Δ*edd–eda*) are shown

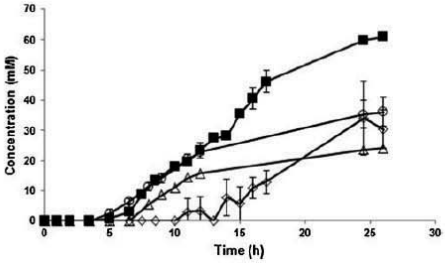

Fig. 4 Acetate formation of *G. oxydans* reference strain Δ*upp* (*filled squares*) and mutants Δ*upp* Δ*gnd* (*open circles*), Δ*upp* Δ*gnd zwf** (*open triangles*), and Δ*upp* Δ*edd–eda* (*open diamonds*). Cells were cultivated in glucose medium at pH 6 with 15 % DO. Mean values of two biological replicates (Δ*upp* Δ*gnd zwf**) or mean values and standard deviations of three biological replicates (Δ*upp*, Δ*upp* Δ*gnd*, and Δ*upp* Δ*edd–eda*) are shown

Table 2). In particular, the second growth phase was absent (Fig. 2). Both mutants completely consumed glucose, but not as rapidly as the reference strain, due to the slower growth. The reference strain required about 8 h for complete glucose consumption, the Δ*upp* Δ*gnd* strain about 11 h, and the Δ*upp* Δ*gnd zwf** strain about 10 h (Fig. 3). In contrast to the complete consumption of gluconate by the reference strain in growth phase II, only about 50 % of the maximal gluconate concentration observed at the end of phase I was oxidized to 2-ketogluconate and the rest of around 80 mM was left in the culture supernatants of the Δ*upp* Δ*gnd* and the Δ*upp* Δ*gnd zwf** strains (Fig. 3). The final 2-ketogluconate concentrations in the culture supernatants of strains Δ*upp* Δ*gnd* and Δ*upp* Δ*gnd zwf** were 24 and 37 % lower than that of the reference strain, respectively. On the other hand, the final 5-ketogluconate titer was increased by more than 100 % (Table 2).

The overall amount of sugar metabolized within the cell, except the fraction converted to 5-ketogluconate, was reduced by 71 and 63 % in strains Δ*upp* Δ*gnd* and Δ*upp* Δ*gnd zwf**, respectively. This correlated with strong decreases in carbon dioxide formation by 81 % (Δ*upp* Δ*gnd*) and 87 % (Δ*upp* Δ*gnd zwf**) and in acetate formation by 41 % (Δ*upp* Δ*gnd*) and 61 % (Δ*upp* Δ*gnd zwf**) (Fig. 4, Table 2). The ratio of acetate to CO_2 was nearly the same in the deletion mutants (Table 2), indicating that it was derived from pyruvate catabolism. The carbon balances were closed to more than 94 % for the reference strain and mutants Δ*upp* Δ*gnd* and Δ*upp* Δ*gnd zwf** (Table 3).

The enzyme activities of G6P-DH and 6PG-DH were tested in cell-free extracts of the glucose-grown strains harvested in the mid-exponential growth phases (Table 4, Fig. 2). The reference strain showed a G6P-DH activity of 0.48± 0.024 $\mu molmin^{-1}mg_{protein}^{-1}$ and a 6PG-DH activity of 0.03± 0.004 $\mu molmin^{-1}mg_{protein}^{-1}$ (Table 4). As expected, no 6PG-DH activity (≤0.001 $\mu molmin^{-1}mg_{protein}^{-1}$) was detectable in the Δ*upp* Δ*gnd* and Δ*upp* Δ*gnd zwf** mutants, confirming that *gnd* is the only gene coding for this activity. Interestingly, G6P-DH activity was reduced by 42 % in the Δ*upp* Δ*gnd* strain compared to the reference strain.

In Fig. 5, the amounts of base and acid required to keep the pH constantly at 6 are shown. Comparable volumes of 2 M NaOH were used in growth phase I, showing that the periplasmic oxidation of glucose to gluconic acid was largely unaffected in Δ*upp* Δ*gnd* and Δ*upp* Δ*gnd zwf** mutants. In growth phase II, the reference strain consumed some HCl to balance cytoplasmic gluconate consumption, whereas the Δ*upp* Δ*gnd* and Δ*upp* Δ*gnd zwf** mutants did not consume any HCl, in accordance with the fact that gluconate was not metabolized in the cytoplasm by these strains.

Table 2 Growth parameters of the indicated *G. oxydans* strains

G. oxydans strain	Final OD_{600}	μ (h^{-1})	Glucose consumed (mM)	Gluconate (mM)	2-KGA (mM)	5-KGA (mM)	Acetate (mM)	CO_2 (mM)	Acetate/ CO_2	Sugar taken up by the cells[a] (mM)
Δ*upp*	6.68±0.14	0.46±0.00	219±3	0±0	119±6	8±2	61±1	280±10	0.22	92
Δ*upp* Δ*gnd*	2.90±0.10	0.32±0.03	215±0	80±6	91±3	17±10	36±5	53±9	0.68	27
Δ*upp* Δ*gnd zwf**	2.93	0.30	213	81	75	23	24	37	0.65	34
Δ*upp* Δ*edd–eda*	6.83±0.07	0.47±0.01	218±2	0±0	126±7	9±6	31±5	290±23	0.11	83

Cells were cultivated in glucose medium at 15 % DO and pH 6 in a bioreactor. Values for OD_{600}, gluconate, 2-KGA, 5-KGA, acetate, and CO_2 were measured after 26 h of growth. Mean values of two (Δ*upp* Δ*gnd zwf**) or mean values and standard deviations of three (Δ*upp*, Δ*upp* Δ*gnd*, and Δ*upp* Δ*edd–eda*) biological replicates are shown

2-KGA 2-ketogluconate, *5-KGA* 5-ketogluconate

[a] This value was determined as the concentration difference between glucose consumed and periplasmic products formed: Glucose−(Gluconate+2-KGA+5-KGA)

Table 3 Carbon balances of the indicated *G. oxydans* strains

Parameter	*G. oxydans* strain							
	Δ*upp*		Δ*upp* Δ*gnd*		Δ*upp* Δ*gnd zwf**		Δ*upp* Δ*edd–eda*	
	(mmol C)	%	(mmol C)	%	(mmol C)	%	(mmol C)	%
Glucose consumed	1,313±18	100	1,290±0	100	1,278	100	1,305±11	100
Biomass formed[a]	90±2	7	38±1	3	39	3	92±2	7
Metabolites formed	887±45	68	1,198±65	93	1,119	88	866±74	66
CO_2 formed	279±9	21	53±9	4	37	3	290±23	22
Percent carbon found in products		96		100		94		97

Cells were cultivated in glucose medium at pH 6 with 15 % DO in a bioreactor. All parameters were calculated after 26 h of growth. Mean values of two (Δ*gnd zwf**) or mean values and standard deviations of three (reference, Δ*gnd* and Δ*edd–eda*) biological replicates are shown

[a] The carbon content of the biomass was calculated by first converting OD_{600} values to cell dry weight (CDW) values using an experimentally determined conversion factor: OD_{600}=1 corresponds to 0.32 g $CDWL^{-1}$. CDW was assumed to contain 50 % carbon and, therefore, mmol C= CDW× 0.5/12×1,000

Characterization of *G. oxydans* strain Δ*edd–eda* lacking the EDP

In a complementary approach, the role of the EDP in glucose/gluconate catabolism was studied using the recently described Δ*upp* Δ*edd–eda* mutant lacking 6-phosphogluconate dehydratase and 2-keto-3-deoxy-6-phosphogluconate aldolase. The reference strain Δ*upp* and the Δ*upp* Δ*edd–eda* strain did not show any differences in growth behavior (Fig. 2). Both the growth rate (0.46±0.00 and 0.47±0.01) and the final OD_{600} (6.72±0.2 and 6.92±0.16) were comparable (Table 2). Furthermore, the strains differed only slightly in their sugar metabolism (Fig. 3, Table 2). Both strains consumed glucose within the first 8 h, resulting in comparable amounts of gluconate, 2-ketogluconate, and 5-ketogluconate. In growth phase II, gluconate was completely metabolized by both the reference strain and the Δ*upp* Δ*edd–eda* mutant. The final titers of ketogluconates (126±7 mM 2-ketogluconate, 9±6 mM 5-ketogluconate) of the EDP mutant were 8 mM higher than that of the reference strain (119± 6 mM 2-ketogluconate, 8±2 mM 5-ketogluconate). As a consequence, the overall sugar uptake by the EDP mutant (83 mM) was 9 mM lower than that by the reference strain (92 mM). Acetate formation by the EDP mutant was reduced by 50 % (31±5 mM) compared to the reference strain (61±1 mM), while CO_2 formation was slightly increased (290 vs. 280 mM) (Fig. 4, Table 2). As the biomass formed by the two strains was comparable (Table 3), a larger fraction of the sugar taken up by the EDP mutant is presumably converted to biomass and less to acetate and CO_2. This might contribute to the decreased acetate formation and the only slightly increased CO_2 formation by the EDP mutant. Acetate formation by the Δ*upp* Δ*edd–eda* mutant started 6 h later compared to the reference strain. The carbon balance of the Δ*upp* Δ*edd–eda* mutant was closed to 97 % (Table 3). The G6P-DH and 6PG-DH activities of the Δ*edd–eda* strain were similar to that of the reference strain (Table 4).

An interesting difference between the Δ*upp* Δ*edd–eda* mutant and the reference strain was the observation that the

Table 4 Specific activity of G6P-DH and 6PG-DH in cell-free extracts of the indicated *G. oxydans* strains

Enzyme	Enzyme activity ($\mu molmin^{-1}mg_{protein}^{-1}$)			
	G. oxydans Δ*upp*	*G. oxydans* Δ*upp* Δ*gnd*	*G. oxydans* Δ*upp* Δ*gnd zwf**	*G. oxydans* Δ*upp* Δ*edd–eda*
G6P-DH (OD_{600} 1.5)	0.48±0.024	0.28±0.126	0.01±0.004	n.d.
G6P-DH (12 h)	0.68±0.010	n.d.	n.d.	0.61±0.009
6PG-DH (OD_{600} 1.5)	0.03±0.004	< 0.001±0.000	<0.001±0.000	n.d.
6PG-DH (12 h)	0.08±0.014	n.d.	n.d.	0.08±0.009

Cells were cultivated in glucose medium at 15 % DO and pH 6 in a bioreactor and used for the preparation of cell-free extracts, either at an OD_{600} of 1.5 or after 12 h. Mean values of three biological replicates and standard deviations are shown

n.d. not determined

EDP mutant required about twice the volume of 2 M HCl in the second growth phase to keep the pH at 6, presumably caused by the decreased acetate formation. In contrast, the volume of 2 M NaOH titrated in the first growth phase was the same for both strains (Fig. 5).

Discussion

The roles of the PPP and the EDP for the growth of *G. oxydans* under controlled conditions (15 % DO, pH 6) in a medium containing glucose as carbon and energy source and yeast extract as supplement were studied using mutants lacking the oxidative PPP (Δ*upp* Δ*gnd* and Δ*upp* Δ*gnd zwf**) or the EDP (Δ*upp* Δ*edd–eda*). Compared to the reference strain Δ*upp*, mutants Δ*upp* Δ*gnd* and Δ*upp* Δ*gnd zwf*, which behaved essentially similar, showed reduced growth rates in phase I, whereas the second growth phase starting after the oxidation of glucose to gluconate was completely lost. This correlated with the fact that only negligible amounts of gluconate were taken up by the PPP mutants in this phase (0–4 mM). Consequently, the PPP is apparently essential for growth on gluconate. A similar phenotype of the PPP mutants was also observed during growth on mannitol, which in phase I is oxidized to fructose and in phase II partially to ketofructose (Richhardt et al. 2012). In both cases, the behavior might be caused by the inhibitory effects of potentially increased concentrations of 6-phosphogluconate and/or KDPG (2-keto-3-deoxy-6-phosphogluconate), by an insufficient rate of gluconate or fructose catabolism via the EDP, or by an insufficient energy supply in the absence of the PPP. As outlined by Richhardt et al. (2012), conversion of 1 mol glucose 6-phosphate via the EDP yields 2 mol acetate or acetyl-CoA, 2 mol CO_2, 2 mol ATP, and 4 mol NAD(P)H, whereas conversion via the PPP in the absence of phosphofructokinase yields 1 mol acetate or acetyl-CoA, 4 mol CO_2, 2 mol ATP, and 8 mol NAD(P)H (Kruger and Von Schaewen 2003; Richhardt et al. 2012). The doubled amount of NAD(P)H should allow an increased formation of proton-motive force and of ATP by oxidative phosphorylation.

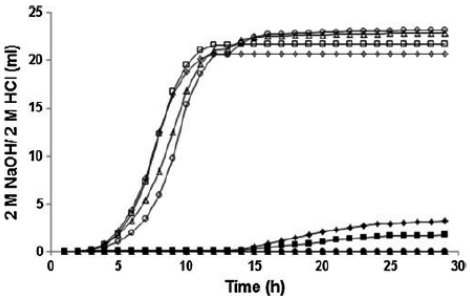

Fig. 5 Volumes of 2 M NaOH (*open symbols*) or 2 M HCl (*closed symbols*) consumed to keep the pH constantly at 6 during cultivation of different *G. oxydans* strains with glucose: *filled and open squares* Δ*upp*, *filled and open diamonds* Δ*upp* Δ*edd–eda*, *filled and open triangles* Δ*upp* Δ*gnd*, *filled and open circles* Δ*upp* Δ*gnd zwf**. Mean values of two biological replicates are shown

During growth on mannitol, the mutants Δ*upp* Δ*gnd* and Δ*upp* Δ*gnd zwf** showed different acetate/CO_2 ratios, which might be caused by the fact that the Δ*upp* Δ*gnd* mutant, but not the Δ*upp* Δ*gnd zwf** strain, could still metabolize glucose 6-phosphate via the EDP (Richhardt et al. 2012). During growth on glucose, the situation is different, as the Δ*upp* Δ*gnd zwf** mutant is also able to metabolize glucose via the EDP after oxidation to gluconate and phosphorylation to 6-phosphogluconate (Fig. 1). This might explain why the acetate/CO_2 ratios of both PPP-defective strains were comparable during growth on glucose (Table 2).

In contrast to the PPP mutants, the Δ*edd–eda* strain showed the same growth behavior as the reference strain (Fig. 2), indicating that the EDP is dispensable for glucose and gluconate metabolism. The 50 % reduced formation of acetate by the Δ*edd–eda* strain (Table 2) is presumably not only caused by a reduced carbon flux through the EDP, but also by an increased utilization of the sugar taken up for biomass synthesis. The reduced formation of acetate by the Δ*edd–eda* strain correlated with a doubled amount of HCl required to keep the pH at 6 in growth phase II. In an experiment without pH control in the second growth phase, it was observed that the pH of the Δ*edd–eda* strain increased much faster and to a higher value compared to the reference strain (Fig. S1).

The unaltered growth characteristics of the EDP mutant on glucose/gluconate differ from the beneficial effect observed previously for the growth of the Δ*upp* Δ*edd–eda* mutant on mannitol (Richhardt et al. 2012). On mannitol, the absence of the EDP caused an improved growth yield in phase I and a 40 % increased fructose utilization in phase II. In particular, the amount of fructose catabolized in the cytoplasm was 60 % higher than in the reference strain and was accompanied by a 54 % increase in biomass (Richhardt et al. 2012). In the case of gluconate, such an improvement by the EDP mutant was not possible, as the reference strain had already metabolized gluconate completely. Thus, no further increase was possible.

In summary, the present study showed that the PPP, rather than the EDP, is of prime importance for the growth of *G. oxydans* on glucose and thus confirmed previous results with mannitol (Richhardt et al. 2012). To answer the

question for the physiological role of the EDP in *G. oxydans*, further investigations are required.

Acknowledgments We are most grateful to Armin Ehrenreich and Wolfgang Liebl (TU München) for providing the strain and protocol used for generating the *G. oxydans* deletion mutants. We also thank DSM Nutritional Products (Kaiseraugst, Switzerland) for the financial support and Dietmar Laudert, Günter Pappenberger, and Hans-Peter Hohmann (DSM Nutritional Products) for their scientific input and their continued disposition for discussion. This work was funded by the German Ministry of Education and Research (BMBF) within the GenoMik-Transfer program (grant 0315632D).

References

Ano Y, Shinagawa E, Adachi O, Toyama H, Yakushi T, Matsushita K (2011) Selective, high conversion of D-glucose to 5-keto-D-gluconate by *Gluconobacter suboxydans*. Biosci Biotechnol Biochem 75:586–589

Bradford MM (1976) A rapid and sensitive method for the quantitation of microgram quantities of protein utilizing the principle of protein-dye binding. Anal Biochem 72:248–254

Kersters K, Lisdiyanti P, Komagata K, Swings J (2006) The family *Acetobacteriaceae*: the genera *Acetobacter*, *Acidomonas*, *Asaia*, *Gluconacetobacter*, *Gluconobacter* and *Kozakia*. In: Dworkin M, Falkow S, Rosenberg E, Schleifer K-H, Stackebrandt E (eds) The prokaryotes, vol. 5, 3rd edn. Springer, Heidelberg, pp 163–200

Krajewski V, Simić P, Mouncey NJ, Bringer S, Sahm H, Bott M (2010) Metabolic engineering of *Gluconobacter oxydans* for improved growth rate and growth yield on glucose by elimination of gluconate formation. Appl Environ Microbiol 76:4369–4376

Kruger NJ, Von Schaewen A (2003) The oxidative pentose phosphate pathway: structure and organisation. Curr Opin Plant Biol 6:236–246

Matsushita K, Fujii Y, Ano Y, Toyama H, Shinjoh M, Tomiyama N, Miyazaki T, Sugisawa T, Hoshino T, Adachi O (2003) 5-keto-D-gluconate production is catalyzed by a quinoprotein glycerol dehydrogenase, major polyol dehydrogenase, in *Gluconobacter* species. Appl Environ Microbiol 69:1959–1966

Miyazaki T, Tomiyama N, Shinjoh M, Hoshino T (2002) Molecular cloning and functional expression of D-sorbitol dehydrogenase from *Gluconobacter suboxydans* IF03255, which requires pyrroloquinoline quinone and hydrophobic protein SldB for activity development in *E. coli*. Biosci Biotechnol Biochem 66:262–270

Moritz B, Striegel K, De Graaf AA, Sahm H (2000) Kinetic properties of the glucose-6-phosphate and 6-phosphogluconate dehydrogenases from *Corynebacterium glutamicum* and their application for predicting pentose phosphate pathway flux in vivo. Eur J Biochem 267:3442–3452

Peters B, Junker A, Brauer K, Mühlthaler B, Kostner D, Mientus M, Liebl W, Ehrenreich A (2012) Deletion of pyruvate decarboxylase by a new method for efficient markerless gene deletions in *Gluconobacter oxydans*. Appl Microbiol Biotechnol. doi:10.1007/s00253-00012-04354-z

Prust C, Hoffmeister M, Liesegang H, Wiezer A, Fricke WF, Ehrenreich A, Gottschalk G, Deppenmeier U (2005) Complete genome sequence of the acetic acid bacterium *Gluconobacter oxydans*. Nat Biotechnol 23:195–200

Raspor PP, Goranovič D (2008) Biotechnological applications of acetic acid bacteria. Crit Rev Biotechnol 28:101–124

Richhardt J, Bringer S, Bott M (2012) Mutational analysis of the pentose phosphate and Entner–Doudoroff pathways in *Gluconobacter oxydans* reveals improved growth of a Δ*edd* Δ*eda* mutant on mannitol. Appl Environ Microbiol 78:6975–6986

Schweiger P, Volland S, Deppenmeier U (2007) Overproduction and characterization of two distinct aldehyde-oxidizing enzymes from *Gluconobacter oxydans* 621H. J Mol Microbiol Biotechnol 13:147–155

Shinagawa E, Ameyama M (1982) 2-Keto-D-gluconate dehydrogenase from *Gluconobacter melanogenus*, membrane-bound. Meth Enzymol 89:194–198

Weenk G, Olijve W, Harder W (1984) Ketogluconate formation by *Gluconobacter* species. Appl Microbiol Biotechnol 20:400–405

Supplementary Material

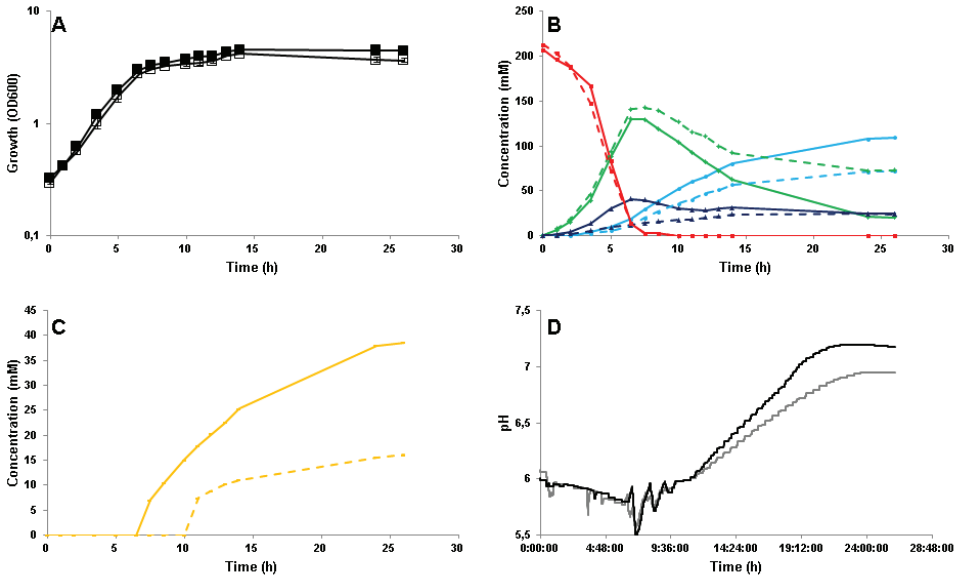

Fig. S1 Cultivation of the *G. oxydans* reference strain Δ*upp* and the Δ*upp* Δ*edd-eda* mutant in glucose medium at 15% dissolved oxygen. Acification of the medium in growth phase I was prevented by titration of 2 M NaOH to keep the pH at 6, whereas alkalinization of the medium in growth phase II was not prevented by addition of HCl. A: Growth of the reference strain Δ*upp* (closed symbols) and the Δ*upp* Δ*edd-eda* mutant (open symbols), B: Sugar concentration of the reference strain (closed line) and the Δ*upp* Δ*edd-eda* mutant (dashed line); glucose is shown in red, gluconate in green, 5-ketogluconate in dark blue, and 2-ketogluconate in light blue. C: Acetate formation by the reference strain (closed line) and the Δ*upp* Δ*edd-eda* mutant (dashed line). D: pH during cultivation of the reference strain (grey line) and the Δ*upp* Δ*edd-eda* mutant (black line). Mean values and standard deviations of three independent cultures are shown for A and mean values of two independent cultures for D; values for B and C are shown for one exemplary culture.

3.3. Global gene expression in *G. oxydans* 621H

Own contribution to this manuscript: about 20%. I performed the cultivation and the comparative DNA-microarray comparison of the *G. oxydans* reference strain and the Δ*qcrABC* mutant at pH 4 (chapters 3.2 and 3.3 of the results section). Moreover, I wrote a draft of the part of the manuscript part dealing with the Δ*qcrABC* mutant. I am second author of the published work.

Published in: Journal of Biotechnology, Vol. 157, pp. 359-372

Impact factor: 3.045

Influence of oxygen limitation, absence of the cytochrome bc_1 complex and low pH on global gene expression in *Gluconobacter oxydans* 621H using DNA microarray technology

Tanja Hanke, Janine Richhardt, Tino Polen, Hermann Sahm, Stephanie Bringer*, Michael Bott*

Institut für Bio- und Geowissenschaften, IBG-1: Biotechnologie, Forschungszentrum Jülich, D-52425 Jülich, Germany

ARTICLE INFO

Article history:
Received 11 August 2011
Received in revised form
20 December 2011
Accepted 21 December 2011
Available online 29 December 2011

Keywords:
Acetic acid bacterium
Cytochrome bc_1 complex
Genome-wide transcription profiling
Oxygen supply
pH of medium

ABSTRACT

The genome-wide transcriptional responses of the strictly aerobic α-proteobacterium *Gluconobacter oxydans* 621H to oxygen limitation, to the absence of the cytochrome bc_1 complex, and to low pH were studied using DNA microarray analyses. Oxygen limitation caused expression changes of 486 genes, representing 20% of the chromosomal genes. Genes with an increased mRNA level included those for terminal oxidases, the cytochrome bc_1 complex, transhydrogenase, two alcohol dehydrogenases, heme biosynthesis, PTS proteins, proteins involved in cyclic diGMP synthesis and degradation, two sigma factors, flagella and chemotaxis proteins, several stress proteins, and a putative exporter protein. The downregulated genes comprised those for respiratory dehydrogenases, enzymes of central metabolism, PQQ biosynthesis, outer membrane receptors, Sec proteins, and proteins involved in transcription and translation. A Δ*qrcABC* mutant of *G. oxydans* showed a growth defect during cultivation on mannitol at pH 4 under oxygen saturation. Comparison of the transcriptomes of this mutant versus the wild type under these conditions revealed 51 differentially expressed genes. Interestingly, almost all of the 45 genes with increased expression in the Δ*qrcABC* mutant at pH 4 were also upregulated in the wild type grown at pH 6 under oxygen limitation. These results support an active role of the cytochrome bc_1 complex in *G. oxydans* respiration. The transcriptome comparison of *G. oxydans* wild type at pH 4 versus pH 6 in mannitol medium under oxygen-saturated conditions uncovered only 72 differentially expressed genes. The 35 upregulated genes included those for cytochrome *bd* oxidase, major polyol dehydrogenase, iron storage and oxidative stress proteins. Among the 37 downregulated genes were some encoding enzymes dealing with carbon dioxide, such as biotin carboxylase, biotin carboxyl carrier protein, and carboanhydrase. These results give first insights into global transcriptional responses of *G. oxydans*.

1. Introduction

The strictly aerobic α-proteobacterium *Gluconobacter oxydans* is used for a variety of industrial applications due to its unusual metabolic capabilities, in particular the incomplete oxidation of organic substrates. Main industrial applications of *G. oxydans* are the production of vitamin C, dihydroxyacetone and 6-amino-L-sorbose, a key intermediate for the synthesis of the anti-diabetic drug miglitol (Raspor and Goranovič, 2008). Habitats of *Gluconobacter* strains are sugary niches, e.g. ripe grapes, apples, dates, other fruits, garden soil, cider, beer, and wine (Gupta et al., 2001). Furthermore, *Gluconobacter* species occur on honeybees which probably act as vectors in the dissemination of these bacteria (Crotti et al., 2010; Kersters et al., 2006).

A set of membrane-integral dehydrogenases enable *G. oxydans* to oxidize diverse sugars, sugar alcohols and other reduced compounds in one or more steps in the periplasm. The resulting products accumulate in the culture medium, often causing its acidification. The catalytic centres of these dehydrogenases are located in the periplasm and deliver electrons or electrons and protons to the respiratory chain (Levering et al., 1988; Matsushita et al., 1994). The rate of these oxidations is usually quite high, resulting in a high demand of *G. oxydans* for oxygen. Only a small fraction of the sugars or sugar alcohols is transported into the cell and catabolized in the cytoplasm via the pentose phosphate pathway (PPP) and the Entner–Doudoroff pathway (EDP). Due to the absence of a gene encoding 6-phosphofructokinase, the Embden–Meyerhof–Parnas pathway (EMP) is non-functional (Prust et al., 2005). Likewise, the tricarboxylic acid (TCA) cycle is incomplete because the genes for succinate dehydrogenase and also succinyl-CoA synthetase are lacking (Prust et al., 2005).

Besides the above-mentioned membrane-bound substrate dehydrogenases, the respiratory chain of *G. oxydans* contains a

* Corresponding authors. Tel.: +49 2461 613476/3294; fax: +49 2461 612710.
E-mail addresses: st.bringer-meyer@fz-juelich.de (S. Bringer), m.bott@fz-juelich.de (M. Bott).

non-proton pumping NADH dehydrogenase II, a cytochrome bo_3-type ubiquinol oxidase and a cytochrome *bd*-type quinol oxidase. In addition, *G. oxydans* also possesses the genes *qcrABC* (GOX0565-0567) for a cytochrome bc_1 complex and *cycA* (GOX0258) for a soluble cytochrome c_{552} (Prust et al., 2005). However, genes for a terminal cytochrome *c* oxidase are absent in the genome and therefore, the function of the cytochrome bc_1 complex is unclear. A possible role of the cytochrome bc_1 complex might be the detoxification of H_2O_2. *G. oxydans* contains a gene (GOX0998) for a periplasmic cytochrome *c* peroxidase which could use reduced cytochrome c_{552} as electron donor and convert H_2O_2 to water. However, in other bacteria, these enzymes are usually present in addition to other terminal electron acceptors from reduced cytochrome *c* (Atack and Kelly, 2007; Yamada et al., 2007) rather than functioning as the main acceptor. Further organisms containing the genes for a cytochrome bc_1 complex but lacking the genes for a cytochrome *c* oxidase are *Zymomonas mobilis* (Charoensuk et al., 2011; Sootsuwan et al., 2008), *Acetobacter pasteurianus* (Azuma et al., 2009) and *Acetobacter aceti* (Azuma et al., 2009; Sakurai et al., 2011), all of which belong to the α-proteobacteria.

The periplasmatic oxidation of sugars to sugar acids by *G. oxydans* leads to an acidification of the medium to pH values below 4. The organism is able to grow under such acidic conditions with only little reduction of growth rate. Indirect evidence for of a pH-dependent regulation of respiratory chain components has been reported (Matsushita et al., 1989) indicating that the concentration of the cytochrome *bd* oxidase increased when the pH dropped from 6 to 4 (Matsushita et al., 1989). In other bacteria like *E. coli*, respiratory chain components and especially the cytochrome *bd* oxidase are usually regulated by oxygen availability rather than by pH (Gennis and Stewart, 1996).

As described above, the oxygen dependency and the ability to adapt to low pH values are key characteristics of *G. oxydans*. In this study, we used genome-wide DNA microarrays to study the influence of oxygen availability and low pH on global gene expression in *G. oxydans* in order to obtain a global view on the corresponding responses. Moreover, we created a deletion mutant lacking the *qcrABC* genes for the cytochrome bc_1 complex, characterized the growth properties of this mutant and compared its global gene expression with that of the wild type. In this case, the aim was to get hints on the physiological function of the cytochrome bc_1 complex. To our knowledge, this is the first study applying transcriptomics to *G. oxydans*.

2. Materials and methods

2.1. Chemicals and enzymes

Chemicals were obtained from Sigma–Aldrich (Taufkirchen, Germany), Operon (Munich, Germany), Qiagen (Hilden, Germany), or Merck (Darmstadt, Germany).

2.2. Bacterial strains and culture conditions

G. oxydans DSM 2343 (ATCC 621H) was obtained from the Deutsche Sammlung von Mikroorganismen und Zellkulturen (Braunschweig, Germany). Precultures of *G. oxydans* were grown in shaking flasks at 30 °C and 220 rpm in complex medium (mannitol medium) containing 80 g l^{-1} mannitol, 5 g l^{-1} yeast extract, 2.5 g l^{-1} $MgSO_4 \times 7H_2O$, and 0.5 g l^{-1} glycerol. The initial pH of the medium was 6.0. For DNA microarray analysis, cells were cultivated in 200 ml of the same medium in a bioreactor system (DASGIP, Jülich, Germany) composed of four 400-ml vessels, each equipped with electrodes for measuring the dissolved oxygen concentration (DO) and the pH. The system allows to constantly control these two parameters. The carbon dioxide concentration in the exhaust air was measured continuously by an infrared spectrometer. The pH values and oxygen levels used are given in the respective results sections. The pH was kept at pH 6.0 or pH 4.0 by automatic titration of 2 M NaOH and 2 M HCl. The oxygen availability was kept constant at 15% DO by mixing air, O_2 and N_2. Oxygen-limited conditions were achieved by gassing the culture with 2% O_2/98% N_2, resulting in a DO concentration of 0%. Calibration was performed by gassing with air (100% DO) and N_2 (0% DO). Control and recording of all data was carried out by the software "Fedbatch Pro" (DASGIP, Jülich, Germany).

2.3. Determination of mannitol and fructose by HPLC analysis

Mannitol and fructose were quantified with a Rezex RCM-Monosaccharide 300 mm × 7.8 mm column (Phenomenex, Aschaffenburg, Germany) at 85 °C using H_2O as the eluent at a flow rate of 0.6 ml min^{-1}. Substances were detected by a refractive index detector. Retention times for fructose and mannitol were 12.50 and 15.82 min, respectively. A calibration curve was made using ten different metabolite concentrations, ranging from 1 to 10 g l^{-1} mannitol and fructose, respectively.

2.4. General cloning techniques

Recombinant DNA work was performed according to standard protocols (Sambrook and Russell, 2001). For PCRs, genomic DNA isolated from *G. oxydans* 621H was used as template. Phusion DNA polymerase (New England Biolabs, Ipswich, MA, USA) was used for PCR amplification of DNA fragments required for cloning and for analytical PCR assays according to the instructions of the manufacturer. The oligonucleotides used for PCR are given below.

2.5. Plasmid construction for marker-free deletion of the qcrABC genes

To generate a plasmid for marker-free deletion of the *qcrABC* genes, pK19*mobsacB* was used (Schäfer et al., 1994). For the in-frame deletion of the entire *qcrABC* operon, around 600 bp each of the upstream region of *qcrA* (GOX0565) and of the downstream region of *qcrC* (GOX0567) were amplified using the oligonucleotide pairs qcrA-for/qcrA-rev (5′-TATATAGTCGACGATCACATGAGCCGT-CTGAAGGGCGG-3′/5′-CCCATCCACTAAACTTA AACACTGGGTCATG-CGGAACCTCTGCCG-3′) and qcrC-for/qcrC-rev (5′-AGTTTAGTGGAT-GGGCGCCGCTGACCGAGCTGAACTACATC-3′/5′-TATATATCTAGAGA CAGCCGTCAGCCGCATCGTTTC-3′). The two resulting PCR fragments were fused by overlap extension PCR using the oligonucleotides qcrA-for and qcrC-rev and the resulting 1.2 kb DNA fragments were cut with XbaI and SalI and cloned into pK19*mobsacB* cut with the same enzymes, resulting in pK19*mobsacB*-**Δ***qcrABC*. The 1.2 kb insert of this plasmid was sequenced for proof of correctness.

2.6. Conjugational plasmid transfer into G. oxydans and isolation of the ΔqcrABC mutant

E. coli S17-1 was transformed with pK19*mobsacB*-**Δ***qcrAB* and then served as donor strain to transfer the plasmid to *G. oxydans* by conjugation. For the biparental mating *E. coli* was cultivated in 50 ml LB medium with 50 μg ml^{-1} kanamycin, *G. oxydans* in 50 ml mannitol medium with 50 μg ml^{-1} cefoxitin. When the cultures had reached an OD_{600} of about 0.6, the cells were harvested by centrifugation, washed twice in LB medium (*E. coli*) or mannitol medium (*G. oxydans*), resuspended in 0.5 ml of the respective medium, and mixed in a 1:1 ratio (v/v). The mixed cell suspension was applied on mannitol medium agar and incubated overnight at 30 °C. The cell patches were scraped from the plates with 2 ml

mannitol medium, resuspended, diluted 10^2- to 10^5-fold, and streaked on selective mannitol medium agar containing cefoxitin and kanamycin (each 50 μg ml^{-1}). Only *G. oxydans* cells harbouring pK19*mobsacB* can grow on these plates, as they are cefoxitin-resistant in contrast to *E. coli*. The agar plates were incubated at 30 °C for 2–3 days until colonies had formed. Five kanamycin-resistant colonies were chosen and cultivated overnight in 100 ml non-selective mannitol medium at 30 °C and 220 rpm. Afterwards, 100 μl of the culture was plated on selective (with kanamycin) and non-selective (without kanamycin) mannitol medium agar plates containing 10% (w/v) sucrose and cultivated for 2–3 days at 30 °C. 30 kanamycin-sensitive and sucrose-resistant colonies were picked and plated as a control on kanamycin mannitol medium agar. The selected colonies were analysed by colony PCR using the oligonucleotides ΔqcrABC-for (5′-GAATGAACGCAGCTAGTCAG-3′) and ΔqcrABC-rev (5′-CTGCACGGCCAGGTG-3′). In 27 clones a 4 kb fragment was formed, which corresponds to the wild-type situation, whereas in three clones a 1.5 kb fragment was observed, which corresponds to the size expected for a *qcrABC* deletion. Of one of these three clones the upstream and downstream regions of the 21 bp linker were amplified by PCR and sequenced to confirm the correctness of the deletion. The corresponding strain was named *G. oxydans* 621H-Δ*qcrABC*.

2.7. RNA preparation and cDNA labeling

25 ml of a *G. oxydans* culture was added to 25 g of crushed ice in a Falcon tube which had been pre-cooled in liquid nitrogen. The cells were sedimented by centrifugation for 3 min at 4 °C and 10,397 × *g* and after removal of the supernatant the tube with the cell pellet was immersed in liquid nitrogen and then stored at −70 °C. For total RNA preparation, the RNeasy system (Qiagen, Hilden, Germany) was used. The cell pellet was resuspended in 700 μl of RLT buffer containing 7 μl β-mercaptoethanol and transferred to two vials each containing 0.5 g of 0.1-mm diameter zirconium silica beads (Roth, Karlsruhe, Germany). Cells were disrupted by 4 × 30 s bead beating using a Silamat S5 (Ivoclar Vivadent, Ellwangen, Germany). The lysate was centrifuged at 8000 × *g* for 2 min and the supernatant was mixed with 250 μl ethanol (−20 °C). RNA was extracted with two RNeasy mini-columns following the manufacturer's instructions. DNA digestion was performed for 20 min on column by adding 30 Kuniz U RNase-free DNase. RNA concentration and quality were checked photometrically and on formaldehyde-containing agarose gels according to standard procedures (Sambrook and Russell, 2001). cDNA synthesis for DNA microarray analysis was performed as described (Polen et al., 2007). 25 μg RNA was used for random hexamer-primed synthesis of fluorescently labeled cDNA with the fluorescent nucleotide analogues Cy3-dUTP and Cy5-dUTP (GE Healthcare, Freiburg, Germany). The mixture contained 3 μl 1 mM Cy3-dUTP or Cy5-dUTP, 3 μl 0.1 M DTT, 6 μl 5× first strand buffer (Invitrogen, Karlsruhe, Germany), 0.6 μl dNTP-mix (25 mM each of dATP, dCTP, and dGTP and 10 mM dTTP) and 2 μl Superscript II reverse transcriptase (Invitrogen, Darmstadt, Germany). The mixture was incubated for 10 min at room temperature and 110 min at 42 °C, stopped by addition of 10 μl 0.1 N NaOH, incubated for 10 min at 70 °C, and then neutralized by addition of 10 μl 0.1 N HCl. The sensors were purified by washing three times with water on a Microcon column (Millipore, YM-30).

2.8. Quantitative real time PCR

For quantitative real time PCR experiments, 500 ng RNA were transcribed into cDNA using the Omniscript RT kit (Qiagen, Hilden, Germany) and specific primers for the genes under investigation (5′-CTCCGCCATGCCAGCGTC for GOX0278; 5′-CATGAGCCG-TCTGAAGGG for GOX0564, 5′-CCAGATCAGGTTTGACCGGCG for GOX1675, 5′-GCGGGACATCATGTTGATGG for GOX1914). The cDNA products were quantified using the QuantiTect SYBR Green PCR kit (Qiagen, Hilden, Germany) and a LightCycler instrument 1.0 (Roche Diagnostics, Mannheim, Germany) according to the instructions of the supplier. The following oligonucleotides were used: 5′-CCCCGCTGCTGTTCTTCTCCTTCC/5′-GAAGCCCGCA-GGCGACATGAAC for GOX0278; 5′-GGGGACTTTTCCTCCGCTTG/ 5′-GCGGAATGAGGGCATGAATC for GOX0564; 5′-GACCGGTTTCA-GCCTCAAATCCGG/5′-CCTGCGTGGTCTGAAGCGTGGTG for GOX1675; 5′-ACCCAGGCTCCTACCACCACG/5′-CGATGATGACGAT-CACCGATGCC for GOX1914. To quantify the amount of cDNA a calibration curve was generated using eight known DNA concentrations of the genes of interest. These DNA fragments were processed in parallel with the cDNA probes. For each concentration of cDNA, the "no amplification" control was subtracted, which was obtained in reactions containing water instead of reverse transcriptase.

2.9. G. oxydans DNA microarrays

The *G. oxydans* DNA microarrays were obtained from Eurofins MWG Operon (Ebersberg, Germany). The array design comprises 3864 sequence-specific longmer oligonucleotide probes (70mer). 2731 oligonucleotides represent all annotated protein coding genes from *G. oxydans* 621H genomic DNA (NC_006677) and the five plasmids found in this strain (NC_006672, NC_006673, NC_006674, NC_006675, NC_006676). 67 genes represent structural RNAs. 939 selected oligonucleotides represent intergenic regions. For intergenic regions >100 bp one probe was designed, for intergenic regions >500 bp two probes. 127 further oligonucleotide probes (from *B. subtilis* 168, alien spike controls, *lacI*, *lacZ*, *tetA*, *cat*, *aph*) were included as negative and positive controls to check for quality and specificity of hybridization. The set of 3864 oligonucleotides was spotted in duplicate on glass slides resulting in two identical sub-arrays of 2 cm × 2 cm each having spot sizes of 80–100 μm and about 225 μm spot distance.

2.10. Hybridization of the DNA microarrays

Preparation of the slides was performed in 50 ml Falcon tubes. All reagents were from the OpArray system from Eurofins MWG Operon. Slides were incubated at 42 °C in Pre-Hyb solution for 1 h, then the slides were transferred to Wash 1 solution (1.25 ml Wash B and 48.75 ml H_2O) and incubated for 5 min at 37 °C. Slides were washed with H_2O and dried in a centrifuge (Sigma Laboratory Centrifuge 4K15C, 5 min, 521 × *g*). Hybridization was carried out for 16–18 h at 42 °C using a MAUI hybridization system (BioMicro Systems, Salt Lake City, USA). For post-hybridization, slides were washed at 37 °C in Wash 2 solution (5 ml Wash A, 2.5 ml Wash B and 42.5 ml H_2O) and Wash 3 solution (5 ml Wash A and 45 ml H_2O) for 10 min each. Slides were rotated in Wash 4 solution (1 ml Wash A and 49 ml H_2O) for 5 min at room temperature. Finally, the slides were dried by centrifugation (Sigma Laboratory Centrifuge 4K15C, 5 min, 521 × *g*).

2.11. DNA microarray analysis

Fluorescence of the hybridized DNA microarrays was determined at 532 nm (Cy3-dUTP) and 635 nm (Cy5-dUTP) at 10 μm resolution with a GenePix 4000B laser scanner (Molecular Devices, Sunnyvale, CA, USA). Quantitative image analysis was carried out using GenePix image analysis software and results were saved as GPR-file (GenePix Pro 6.0). For data normalization, GPR-files were processed using the BioConductor/R-packages limma and marray

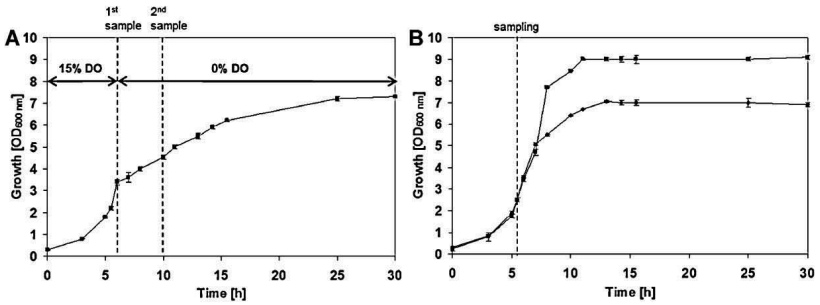

Fig. 1. Influence of oxygen and pH on growth of *G. oxydans* 621H. (A) Cells were cultivated at pH 6 (constant) in mannitol medium at 15% dissolved oxygen (DO) for 6 h, when the first sample for DNA microarray analysis (oxygen saturated cells) was taken. Then, the remaining culture was gassed with 2% O_2/98% N_2, resulting in a DO concentration of 0% and the second sample for microarray analysis (oxygen limited cells) was taken 4 h after the shift to oxygen limitation. Mean values and standard deviations of 4 independent cultures are shown. (B) Cells were cultivated in mannitol medium at 15% DO either at pH 6 (squares) or at pH 4 (rhombs). Mean values and standard deviations of 3 independent cultures are shown. In A and B dashed vertical lines show the times when samples for DNA microarray analysis or qRT-PCR were taken.

(http://www.bioconductor.org). For further analysis, the processed and loess-normalized data as well as detailed experimental information according to MIAME (Brazma et al., 2001) were stored in the in-house microarray database (Polen and Wendisch, 2004).

DNA microarray experiments were repeated independently three times for *G. oxydans* Δ*qrcABC* versus wild type and *G. oxydans* grown at pH 4 versus pH 6 and four times for *G. oxydans* grown at oxygen limitation versus oxygen saturation in biological replicates. To filter for differentially expressed genes, the following criteria had to be fulfilled: (i) flags ≥0 (GenePix Pro 6.0), (ii) signal/noise ≥5 for Cy5 (F635Median/B635Median, GenePix Pro 6.0) or Cy3 (F532Median/B532Median, GenePix Pro 6.0), (iii) mRNA ratio ≥2.0 (lower ones allowed in the case of operons) or ≤0.5 (higher ones allowed in the case of operons), (iv) in a paired Student's *t*-test, relative RNA levels had to be significantly different from all spots ($p < 0.05$).

3. Results and discussion

3.1. Effects of oxygen limitation on global gene expression in G. oxydans 621H

In its natural habitat *G. oxydans* is likely subject to low-oxygen stress conditions, due to the rapid oxygen consumption by its own metabolism. Therefore, the organism's reaction to oxygen deprivation on the transcriptional level was investigated. For this purpose wild-type cells were cultivated in a bioreactor system in mannitol medium for 6 h at constantly 15% dissolved oxygen and at a constant pH of 6. After this time, the culture had reached an OD_{600} of 3.5 and a sample was taken and used for RNA isolation (Fig. 1A). Immediately afterwards, gassing of the remaining culture was changed by using a mixture composed of 2% O_2 and 98% N_2, which caused the dissolved oxygen concentration to drop to zero. By decreasing the oxygen availability, the previously exponentially growing cells immediately entered linear growth and were harvested for RNA isolation 4 h after reducing the oxygen concentration at an OD_{600} of 4.5 (Fig. 1A). The cultivations were performed in triplicate starting from independent precultures. RNA was prepared from the six samples and used for comparative DNA microarray analysis as described in Section 2. In total, 486 genes showed differential expression: 215 genes had an mRNA ratio (oxygen limitation/oxygen excess) of ≥2.0 and 271 genes had an mRNA ratio of ≤0.5. These genes are listed in Table S1. Selected genes (including operons) are described in the following paragraphs based on a functional categorization (Table 1).

(i) *Genes involved in respiration and energy metabolism.* Many of the genes whose expression was influenced by oxygen limitation are involved in respiration and ATP synthesis. Several proteins directly or indirectly involved in feeding electrons into the respiratory chain showed decreased mRNA levels under oxygen limitation, such as the genes for the membrane-bound PQQ-containing glucose dehydrogenase (*gdhM*, GOX0265, mRNA ratio 0.5), the PQQ-containing major polyol dehydrogenase (*sldAB*, GOX0854-0855, mRNA ratio 0.1) and the type II NADH dehydrogenase (*ndh*, GOX1675, mRNA ratio 0.37). The major polyol dehydrogenase SldAB is responsible for the oxidation of mannitol to fructose. In contrast, the components responsible for transferring electrons from ubiquinol to oxygen were upregulated under oxygen limitation, which are the genes encoding the two terminal ubiquinol oxidases cytochrome bo_3 (*cyoBACD*, GOX1911-1914, mRNA ratio 2.7–3.8) and cytochrome *bd* (*cydAB*, GOX0278-0279, mRNA ratio 1.9–3.6). Interestingly, also the genes encoding the cytochrome bc_1 complex (*qcrABC*, GOX0565-0567, mRNA ratio 1.8–2.5) had increased mRNA levels, whereas the soluble cytochrome c_{552} (*cycA*, GOX0258) showed similar mRNA levels under oxygen excess and oxygen limitation.

The opposite regulation of genes for membrane-bound and in part PQQ-dependent dehydrogenases and terminal oxidases represents an adequate response to oxygen limitation. It probably allows the cells to reduce the electron flux into the respiratory chain on the one hand and to increase the capability to capture the limiting oxygen on the other hand.

Remarkably, the genes encoding pyridine nucleotide transhydrogenase (*pntA1A2B*, GOX0310-0312, mRNA ratio 10.4–14.7) belonged to the most strongly up-regulated genes under oxygen limitation. Transhydrogenase PntAB is located in the cytoplasmic membrane of many bacteria and couples the redox reaction between NAD(H) and NADP(H) to the translocation of protons across the membrane. Transhydrogenase can operate reversibly, i.e. either consumes the electrochemical proton gradient Δp for $NADP^+$ reduction or generates Δp at the expense of NADPH oxidation (Jackson et al., 2002). The genes downstream of *pntB*, GOX0313-0314, encode putative zink-containing alcohol dehydrogenases and showed mRNA ratios (13.6 and 14.6) similar to the *pntA1A2B* genes, suggesting

Table 1
Genome-wide comparison of mRNA levels in *G. oxydans* during growth under oxygen limitation and oxygen excess. Cells were cultivated for 6 h in mannitol medium at a constant pH of 6 and oxygen excess (constantly 15% dissolved oxygen) and then shifted to oxygen limitation for 4.5 h by gassing with 2% O_2/98% N_2, resulting in a dissolved oxygen concentration of 0%. Selected genes with an mRNA ratio ≥2.0 (lower ones allowed in the case of operons) or ≤0.5 (higher ones allowed in the case of operons) and a *p*-value of ≤0.05 are listed. The data shown represent mean values from four biological replicates. The genes were grouped into different functional categories within which they were ordered according to their mRNA ratios except in the case of operons, which were ordered according to their locus tag. A list of all genes with an mRNA ratio ≥2.0 or ≤0.5 in the respective functional categories is given in Table S1.

Locus tag	Annotation	Gene	mRNA ratio O_2 limitation/ O_2 saturation	*p*-Value
	Respiration and energy metabolism			
	mRNA ratio of 23 genes ≥ 2.0, of 9 genes ≤ 0.5			
	Selected genes			
GOX0310	NAD(P) transhydrogenase subunit α2	*pntA2*	10.37	3.76×10^{-4}
GOX0311	NAD(P) transhydrogenase subunit α1	*pntA1*	14.70	1.36×10^{-3}
GOX0312	NAD(P) transhydrogenase subunit β	*pntB*	12.04	4.33×10^{-4}
GOX0313	Alcohol:NAD^+ oxidoreductase		13.58	7.09×10^{-4}
GOX0314	Probable alcohol:NAD(P)$^+$ oxidoreductase		14.63	2.35×10^{-3}
GOX1911	Cytochrome bo_3 ubiquinol oxidase subunit II	*cyoB*	2.82	1.63×10^{-3}
GOX1912	Cytochrome bo_3 ubiquinol oxidase subunit I	*cyoA*	2.70	1.05×10^{-2}
GOX1913	Cytochrome bo_3 ubiquinol oxidase subunit III	*cyoC*	3.56	2.53×10^{-5}
GOX1914	Cytochrome bo_3 ubiquinol oxidase subunit IV	*cyoD*	3.81	4.04×10^{-3}
GOX2167	F_1F_0-ATP synthase subunit β	*atpD*	2.81	4.36×10^{-3}
GOX2168	F_1F_0-ATP synthase subunit ε	*atpC*	3.14	3.49×10^{-3}
GOX2169	F_1F_0-ATP synthase subunit q	*atpQ**	2.79	4.94×10^{-3}
GOX2170	F_1F_0-ATP synthase subunit r	*atpR**	3.13	$1,39 \times 10^{-2}$
GOX2171	F_1F_0-ATP synthase subunit a	*atpB*	3.30	7.59×10^{-3}
GOX2172	F_1F_0-ATP synthase subunit c	*atpE*	2.99	7.50×10^{-4}
GOX2173	F_1F_0-ATP synthase subunit b	*atpF*	2.64	6.25×10^{-3}
GOX2174	F_1F_0-ATP synthase subunit α	*atpA*	2.38	8.40×10^{-3}
GOX2175	F_1F_0-ATP synthase subunit γ	*atpG*	1.96	8.40×10^{-3}
GOX0564	Cytochrome *c*	*cycA*	2.02	1.22×10^{-3}
GOX0565	Ubiquinol-cytochrome *c* oxidoreductase FeS protein	*qrcA*	2.49	3.64×10^{-3}
GOX0566	Ubiquinol-cytochrome *c* oxidoreductase cytochrome *b*	*qrcB*	2.20	1.23×10^{-2}
GOX0567	Ubiquinol-cytochrome-*c* oxidoreductase cytochrome c_1	*qrcC*	1.80	1.66×10^{-3}
GOX2409	ABC transporter, cytochrome *bd* biogenesis CydD	*cydD*	2.26	4.23×10^{-6}
GOX2410	ABC transporter, cytochrome *bd* biogenesis CydC	*cydC*	2.48	3.04×10^{-3}
GOX0278	Cytochrome *bd* ubiquinol oxidase subunit I	*cydA*	3.64	7.17×10^{-5}
GOX0279	Cytochrome *bd* ubiquinol oxidase subunit II	*cydB*	1.94	8.94×10^{-3}
GOX1310	F_1F_0-ATP synthase subunit δ	*atpH*	0.58	5.62×10^{-3}
GOX1311	F_1F_0-ATP synthase subunit α	*atpA*	0.62	5.54×10^{-3}
GOX1312	F_1F_0-ATP synthase subunit γ	*atpG*	0.62	5.77×10^{-3}
GOX1313	F_1F_0-ATP synthase subunit β	*atpD*	0.51	1.17×10^{-2}
GOX1314	F_1F_0-ATP synthase subunit ε	*atpC*	0.50	3.20×10^{-3}
GOX1110	F_1F_0-ATP synthase subunit b′	*atpF*′	0.48	3.37×10^{-3}
GOX1111	F_1F_0-ATP synthase subunit b	*atpF*	0.40	5.79×10^{-3}
GOX1112	F_1F_0-ATP synthase subunit c	*atpE*	0.51	2.83×10^{-3}
GOX1113	F_1F_0-ATP synthase subunit a	*atpB*	0.57	6.00×10^{-3}
GOX0265	Membrane-bound glucose dehydrogenase (PQQ)	*gdhM*	0.50	1.79×10^{-5}
GOX1675	NADH dehydrogenase type II	*ndh*	0.37	1.02×10^{-5}
GOX1230	Gluconate 2-dehydrogenase cytochrome *c* subunit	*gndA*	0.23	3.32×10^{-4}
GOX1231	Gluconate 2-dehydrogenase subunit α	*gndB*	0.19	1.30×10^{-4}
GOX1232	Gluconate 2-dehydrogenase subunit γ	*gndC*	0.26	2.47×10^{-4}
GOX0854	Major polyol dehydrogenase large subunit	*sldA*	0.10	4.81×10^{-6}
GOX0855	Major polyol dehydrogenase small subunit	*sldB*	0.10	6.38×10^{-5}
	Metabolism			
	mRNA ratio of 44 genes ≥ 2.0, of 79 genes ≤ 0.5,			
	Selected genes			
GOX1896	Coproporphyrinogen III oxidase		6.43	1.73×10^{-3}
GOX1636	5-Aminolevulinate synthase		4.60	1.55×10^{-3}
GOX2308	Delta-aminolevulinic acid dehydratase		3.08	2.77×10^{-7}
GOX1864	Protoheme IX farnesyltransferase		2.97	1.63×10^{-3}
GOX1883	Porphobilinogen deaminase		2.13	1.06×10^{-3}
GOX0874	Ferrochelatase		2.21	2.71×10^{-4}
GOX1190	Glucose-1-phosphatase	*yihX*	2.07	3.58×10^{-3}
GOX0983	Coenzyme PQQ synthesis protein E	*pqqE*	0.86	4.38×10^{-2}
GOX0984	Coenzyme PQQ synthesis protein D	*pqqD*	0.51	2.29×10^{-5}
GOX0985	Coenzyme PQQ synthesis protein C	*pqqC*	0.63	3.63×10^{-3}
GOX0986	Coenzyme PQQ synthesis protein B	*pqqB*	0.37	1.82×10^{-7}
GOX0987	Coenzyme PQQ synthesis protein A	*pqqA*	0.44	4.04×10^{-3}
GOX1703	Transketolase	*tkt*	0.47	9.40×10^{-3}
GOX1704	Bifunctional transaldolase/phosphoglucose isomerase	*pgi/tal*	0.44	1.71×10^{-2}
GOX1705	6-Phosphogluconate dehydrogenase-like protein	*gnd*	0.44	2.38×10^{-2}
GOX1432	NADP-dependent D-sorbitol dehydrogenase		0.46	1.41×10^{-3}
GOX0145	Glucose-6-phosphate 1-dehydrogenase	*zwf*	0.45	$4.46\ 10^{-5}$
GOX0849	NADPH-dependent L-sorbose reductase		0.44	2.14×10^{-3}
GOX2015	NAD(P)-dependent glucose 1-dehydrogenase	*gdh*	0.44	3.10×10^{-3}
GOX2187	Gluconate 5-dehydrogenase		0.44	5.90×10^{-4}

Table 1 (*Continued*)

Locus tag	Annotation	Gene	mRNA ratio O_2 limitation/ O_2 saturation	*p*-Value
GOX1381	Gluconolactonase		0.39	3.13×10^{-4}
GOX1516	Fructose 1,6-bisphosphatase II	*fbp*	0.38	3.98×10^{-3}
GOX0748	Aldose 1-epimerase		0.35	3.49×10^{-6}
GOX1336	Isocitrate dehydrogenase	*icd*	0.17	2.05×10^{-4}
GOX1335	Aconitate hydratase	*aco*	0.13	1.85×10^{-4}
	Transport			
	mRNA ratio of 5 genes ≥ 2.0, of 32 genes ≤ 0.5			
	Selected genes			
GOX0812	Phosphoenolpyruvate-protein phosphotransferase	*ptsI*	1.83	8.79×10^{-4}
GOX0813	Phosphocarrier protein HPr	*ptsH*	2.20	5.21×10^{-3}
GOX0814	PTS system IIA component	*ptsIIA*	4.10	1.53×10^{-4}
GOX0815	Hypothetical protein GOX0815		6.53	1.81×10^{-4}
GOX0816	HPr kinase	*ptsK*	1.27	3.93×10^{-3}
GOX0673	Ferrous iron transport protein A (FeoA)	*feoA*	5.86	4.80×10^{-3}
GOX0674	Ferrous iron transport protein B (FeoB)	*feoB*	3.24	1.35×10^{-2}
GOX0970	Outer membrane channel lipoprotein		0.49	1.46×10^{-4}
GOX2401	Protein translocase subunit SecF	*secF*	0.48	2.41×10^{-4}
GOX1173	TonB-dependent outer membrane receptor		0.39	1.39×10^{-3}
GOX0360	Preprotein translocase subunit SecY	*secY*	0.39	5.58×10^{-3}
GOX0197	Signal recognition particle protein	*ffh*	0.34	8.69×10^{-4}
GOX2402	Preprotein translocase subunit SecD	*secD*	0.39	2.54×10^{-3}
GOX0758	Porin		0.19	2.03×10^{-3}
	Regulation and signal transduction (except chemotaxis)			
	mRNA ratio of 8 genes ≥ 2, of 8 genes ≤ 0.5			
GOX0506	RNA polymerase sigma factor H (σ^{32})	*rpoH*	4.04	3.77×10^{-5}
GOX1613	Protein with GGDEF and EAL domain		3.78	1.86×10^{-3}
GOX2069	Transcriptional regulator, DeoR family		2.94	1.38×10^{-3}
GOX0135	Transcriptional regulator, Ros/MucR family		2.80	3.66×10^{-3}
GOX2406	RNA polymerase sigma factor E (σ^{24})	*rpoE*	2.53	3.37×10^{-3}
GOX2471	Transcriptional regulator, XRE family		2.32	9.96×10^{-3}
GOX0960	Protein with GGDEF and EAL domain		2.32	3.49×10^{-5}
GOX0683	Protein with GGDEF domain		2.13	6.88×10^{-3}
GOX0771	Ferric uptake regulation protein	*fur*	0.49	3.24×10^{-4}
GOX1022	Transcriptional regulator		0.41	5.98×10^{-3}
GOX0772	Transcriptional regulator, Ros/MucR family		0.16	9.12×10^{-5}
GOX1192	Transcriptional regulator, MarR/AsnC family		0.49	7.02×10^{-3}
GOX0778	Two component sensor histidine kinase		0.42	6.51×10^{-3}
GOX0513	Transcriptional regulator, AsnC family		0.39	1.05×10^{-3}
GOX0522	Transcriptional regulator		0.33	2.09×10^{-3}
GOX0132	Transcriptional regulator		0.27	1.22×10^{-6}
	Motility			
	mRNA ratio of 20 genes ≥ 2.0, of 0 genes ≤ 0.5			
GOX0952	Flagellar basal body P-ring biosynthesis protein FlgA	*flgA*	2.79	2.03×10^{-4}
GOX0953	Flagellar basal body rod protein FlgG	*flgG*	3.54	1.01×10^{-4}
GOX0954	Flagellar basal-body rod protein FlgF	*flgF*	4.26	1.39×10^{-3}
GOX0787	Flagellin B		3.44	2.00×10^{-3}
GOX0788	Flagellin assembly protein		4.23	1.42×10^{-3}
GOX1025	Flagellar hook-associated protein FlgL	*flgL*	3.69	4.32×10^{-3}
GOX1026	Flagellar hook-associated protein 1 FlgK	*flgK*	2.76	4.93×10^{-3}
GOX1525	Flagellar biosynthetic protein FliQ	*fliQ*	2.18	2.99×10^{-3}
GOX1526	Flagellar hook-basal body protein FleE	*fleE*	2.55	6.27×10^{-4}
GOX1527	Flagellar basal body rod protein FlgC	*flgC*	2.65	3.05×10^{-3}
GOX1528	Flagellar basal-body rod protein FlgB	*flgB*	3.41	6.18×10^{-3}
GOX0425	Basal-body rod modification protein FlgD	*flgD*	3.04	4.05×10^{-4}
GOX1027	Flagellar hook protein FlgE	*flgE*	2.83	2.24×10^{-3}
GOX0620	Chemotactic signal-response protein CheL	*cheL*	2.54	7.18×10^{-5}
GOX0697	Flagellar FliL protein	*fliL*	2.40	1.97×10^{-3}
GOX1550	Chemotaxis protein CheX	*cheX*	2.32	3.27×10^{-4}
GOX1551	Chemotaxis protein CheY	*cheY*	2.16	7.08×10^{-5}
GOX0421	Flagellar motor switch protein		2.18	2.53×10^{-3}
GOX0126	Flagellar motor protein MotA	*motA*	2.08	1.75×10^{-3}
GOX1549	Methyl-accepting chemotaxis protein		2.06	6.42×10^{-4}
	Stress			
	mRNA ratio of 11 genes ≥ 2.0, of 0 genes ≤ 0.5			
GOX1329	Small heat shock protein	*hsd*	5.29	3.2210^{-4}
GOX1463	ATP-dependent Clp protease ATP-binding subunit ClpV	*clpV*	3.42	1.09×10^{-3}
GOX2163	Cold shock protein	*csp*	3.04	8.24×10^{-5}
GOX0609	ATP-dependent Clp protease ATP-binding subunit ClpA	*clpA*	2.85	1.16×10^{-4}
GOX1577	ATP-dependent Clp protease ATP-binding subunit ClpB	*clpB*	2.82	1.08×10^{-5}
GOX1992	Osmotically inducible protein C	*osmC*	2.73	1.53×10^{-5}
GOX1024	Heat shock protein 90	*hsp90*	2.63	1.72×10^{-5}
GOX2397	Small heat shock protein	*hsd*	2.32	4.25×10^{-4}
GOX1414	Chaperone protein DnaJ	*dnaJ*	2.18	5.18×10^{-3}

Table 1 (*Continued*)

Locus tag	Annotation	Gene	mRNA ratio O_2 limitation/ O_2 saturation	*p*-Value
GOX1302	Paraquat-inducible protein A		2.16	2.75×10^{-3}
GOX0861	Flavohemoprotein	*hmp*	2.15	1.56×10^{-2}
	Transcriptional and translational machinery			
	mRNA ratio of 12 genes ≥ 2.0, of 70 genes ≤ 0.5			
	Selected genes			
GOX1106	Alanine tRNA		2.91	5.58×10^{-3}
GOX1722	Arginine tRNA		2.74	8.23×10^{-4}
GOX1445	Leucine tRNA		2.70	5.83×10^{-3}
GOX2486	Cysteine tRNA		2.54	1.21×10^{-3}
GOX0199	Serine tRNA		2.43	6.70×10^{-9}
GOX0172	Arginine tRNA		2.31	4.38×10^{-3}
GOX0872	Proline tRNA		2.00	2.01×10^{-2}
GOX0385	RNA polymerase, subunit β′	*rpoC*	0.40	3.14×10^{-3}
GOX0386	RNA polymerase, subunit β	*rpoB*	0.43	6.94×10^{-3}
GOX0356	RNA polymerase, subunit α	*rpoA*	0.37	2.83×10^{-3}
GOX0105	Elongation factor G	*fusA*	0.31	6.08×10^{-5}
GOX0382	Elongation factor Tu	*tuf*	0.30	2.28×10^{-3}
GOX0074	Elongation factor Ts	*tsf*	0.29	1.49×10^{-3}
GOX1780	30S ribosomal protein S4	*rpsD*	0.27	4.71×10^{-4}
	Predicted functions			
	mRNA ratio of 16 genes ≥ 2.0, of 24 genes ≤ 0.5			
	Selected genes			
GOX0647	Putative exporter protein, ArAE family	*fusB*	18.22	4.00×10^{-2}
GOX2199	Probable myosin-crossreactive antigen		5.62	4.82×10^{-5}
GOX2200	Probable myosin-crossreactive antigen		5.37	2.69×10^{-7}
GOX0090	Putative sugar kinase		5.14	8.89×10^{-4}
GOX0354	Putative sugar/polyol transporter		0.12	9.11×10^{-4}
	Hypothetical proteins			
	mRNA ratio of 76 genes ≥ 2.0, of 49 genes ≤ 0.5			

that these five genes might form an operon. This points to a functional connection between transhydrogenase and the two alcohol dehydrogenases/aldehyde reductases. Increased levels of these enzymes might allow the cells a rapid exchange between NAD^+/NADH and $NADP^+$/NADPH and reoxidation of NAD(P)H via reduction of aldehydes/ketones to the corresponding alcohols, which could be favourable under oxygen limitation.

The *G. oxydans* genome contains three gene clusters coding for subunits of F_1F_O-ATP synthases. The clusters GOX1110-1113 and GOX1310-1314 encode the subunits of the F_O part and the F_1 part of an ATP synthase which is an ortholog of the ATP synthases of *Acetobacter pasteurianus* IFO 3283–01, *Gluconacetobacter diazotrophicus* PAl 5 and other α-proteobacteria. Both these clusters showed a decreased expression under oxygen limitation (mRNA ratio 0.40–0.62). The third cluster GOX2167-2175 might code for a Na^+-translocating F_1F_O-ATP synthase (Dibrova et al., 2010). Remarkably, the genes of this cluster showed an increased expression under oxygen limitation (mRNA ratio 1.96–3.30).

The ATP synthase encoded by GOX2167-2175 is an ortholog of the Na^+-translocating F_1F_O-ATP synthases, present in the archaea *Methanosarcina barkeri* and *M. acetivorans*, in a number of marine and halotolerant bacteria and in pathogenic *Burgholderia* species, occurring always in addition to the proton-translocating ATP synthases (Dibrova et al., 2010; Müller and Grüber, 2003; Saum et al., 2009). The sodium-dependent ATP synthase is absent in *Acetobacter pasteurianus* and *Gluconacetobacter diazotrophicus*, pointing to an acquisition of this operon by lateral gene transfer. The strict conservation of the gene order suggests that the whole operon is transferred as a single unit. The expression pattern of the genes for the two ATP synthases suggests that sodium ions might play an important role as coupling ions under oxygen limitation.

(ii) *Genes involved in metabolism.* Many genes encoding enzymes involved in heme biosynthesis, starting from glycine and succinyl-CoA, were upregulated under oxygen limitation: δ-aminolevulinate synthase (GOX1636, mRNA ratio 4.6), δ-aminolevulinic acid dehydratase (GOX2308, mRNA ratio 3.1), porphobilinogen deaminase (GOX1883, mRNA ratio 2.1), coproporphyrinogen III oxidase (GOX1896, mRNA ratio 6.4), ferrochelatase (GOX0874, mRNA ratio 2.2), and protoheme IX farnesyltransferase (GOX1864, mRNA ratio 3.0). Upregulation of heme biosynthesis is probably necessary due to the increased expression of the two terminal oxidases and the cytochrome bc_1 complex, all of which contain heme groups (see above).

Differentially expressed genes encoding enzymes involved in EMP, PPP, TCA cycle, and gluconeogenesis generally showed lower expression under oxygen limitation. A decreased mRNA level was also observed for the genes of the PQQ biosynthesis operon (*pqqABCDE*, GOX0983-GOX0987, mRNA ratio 0.4–0.9). This correlates with the decreased expression of several PQQ-containing dehydrogenases of the respiratory chain (see above). The cases of heme and PQQ show that the synthesis of prosthetic groups and the corresponding apo-proteins occurs in a coordinated fashion.

(iii) *Genes involved in transport.* Due to the lack of the EII^B and EII^C components, the PTS system in *G. oxydans* is considered to be inactive as a transport system (Prust et al., 2005) and the function of the remaining components EI, HPr, EIIA and HPr kinase is not yet clear. The genes encoding these latter proteins (GOX0812-0816) had increased expression levels under oxygen limitation (mRNA ratio 1.3–4.1), showing that they are subject to transcriptional regulation. The genes *feoA* and *feoB* (GOX0673 and 0674, mRNA ratios 5.9 and 3.3) encode ferrous iron transport proteins. Their increased expression could be related to an increased iron demand caused by increased heme biosynthesis (see above).

Among the downregulated genes encoding proteins involved in transport were several TonB-dependent outer membrane receptors (GOX0907, 0945, 1015, 1017, 1173, 1796, 1903, mRNA ratios 0.1–0.4) (Table S1) and other proteins associated with the outer membrane, e.g. an outer membrane channel lipoprotein (GOX0970, mRNA ratio 0.5), and a porin (GOX0785, mRNA ratio 0.2). Also several genes involved in protein secretion by the Sec system displayed decreased mRNA ratios, i.e. those encoding SecF (GOX2401, ratio 0.5), SecD (GOX2402, ratio 0.3), SecY (GOX0360, ratio 0.4) and the signal recognition particle protein (GOX0197, ratio 0.3).

(iv) *Genes involved in regulation and signal transduction.* Three genes coding for signal transduction proteins with GGDEF domains and in two cases also EAL domains showed an increased mRNA level (GOX1613, mRNA ratio 3.8; GOX0960, mRNA ratio 2.3; GOX0683, mRNA ratio 2.1). GGDEF and EAL domains are known to have diguanylate cyclase activity and diguanylate phosphodiesterase activity, respectively, and control the cellular level of the second messenger cyclic di-GMP (Schirmer and Jenal, 2009), which was first identified in *Gluconacetobacter xylinus* (Ross et al., 1987). It was recently reported that a protein of *Shewanella oneidensis* with GGDEF and EAL domains might function as an O_2/redox sensor (Sundararajan et al., 2011). Thus, one or several of the *G. oxydans* proteins with a GGDEF domain might have a similar function and could be involved in the regulation of genes of the respiratory chain. Five genes coding for transcriptional regulators had increased mRNA levels under oxygen limitation, three of them coding for transcriptional regulators of different families (GOX2069, GOX0135, GOX2471) and two coding for sigma factors, i.e. σ^{32} (GOX0506) and σ^{24} (GOX2406). Whereas the target genes of the transcriptional regulators and the stimuli they respond to have not been identified yet, σ^{32} and σ^{24} are known to be induced under different stress conditions and to activate expression of genes required to counteract these stresses (Österberg et al., 2011). As shown below, expression of several stress genes was induced under oxygen limitation, which might be due to the activity of σ^{32} and σ^{24}.

Six genes coding for transcriptional regulators displayed decreased expression under oxygen limitation (*fur*, GOX0772, GOX1192, GOX0513, GOX0522, GOX0132), but except for Fur protein the detailed function of the corresponding proteins is unknown. Fur functions as an iron-sensing global regulator of iron homeostasis controlling both the induction of iron uptake functions (under iron limitation) and the expression of iron storage proteins and iron-utilizing enzymes (under iron sufficiency) (Lee and Helmann, 2007). A gene (GOX0778) coding for a histidine kinase of a two-component regulatory system also had a lowered mRNA level under oxygen limitation, but the function of this system is also not known yet.

(v) *Genes involved in motility.* Of the 29 genes involved in flagella biosynthesis and function and of the 13 chemotaxis-assigned genes present in the genome of *G. oxydans* 621H 16 and 4 genes showed mRNA levels above 2.0 under oxygen limitation. This suggests an increased motility of the cells, allowing them to find better growth conditions more rapidly. Whether *G. oxydans* shows aerotaxis has not been studied yet.

(vi) *Genes involved in stress responses.* Several genes involved in different types of stress responses, such as heat shock (GOX1329, ratio 5.3; GOX2397, ratio 2.3), cold shock (GOX2163, ratio 3.0), or oxidative stress (GOX1302, ratio 2.2; GOX0861, ratio 2.15), the chaperons Hsp90 (GOX1024, ratio 2.6) and DnaJ (GOX1414, ratio 2.2) as well as three Clp ATPases (GOX1463, ratio 3.4; GOX0609, ratio 2.9; GOX1577, ratio 2.8) were found to have increased mRNA levels under oxygen limitation, which might be related to the increased expression of σ^{32} and σ^{24}. As the cells obviously face neither heat nor cold stress under the cultivation conditions used, the induction of these genes might represent a kind of general stress response triggered by the decreased growth rate under oxygen limitation.

(vii) *Genes involved in the transcriptional and translational machinery.* Many genes encoding proteins involved in transcription and translation showed lower expression under oxygen limitation (Table S1). These included three subunits of the RNA polymerase (GOX0385, 0386, mRNA ratios 0.4, GOX0356, mRNA ratio 0.4), elongation factors G (GOX0105, mRNA ratio 0.3), Tu (GOX0382, mRNA ratio 0.3) and Ts (GOX0074, mRNA ratio 0.3), and 45 ribosomal proteins. This response probably presents an adaptation to the reduced, linear growth observed after shifting the cells from oxygen excess to oxygen limitation. On the other hand, seven genes coding for tRNAs were stronger expressed under oxygen limitation (GOX 1106, 1722, 1445, 2486, 0199, 0172, 0872, mRNA ratios 2.0–3.0) which is not yet understood.

(viii) *Genes with predicted functions.* The *fus* gene (GOX0647), originally annotated as fusaric acid resistance protein, was strongly overexpressed (mRNA ratio 18.2) under oxygen limitation (as well as during growth at pH 4, see below). It has orthologs in *Acetobacter pasteurianus* IFO 3283–01 and *Gluconacetobacter diazotrophicus* PAI 5. Fusaric acid, a picolinic acid derivative, is a phytotoxin produced by *Fusarium oxysporum* (Fakhouri et al., 2003). Since no fusaric acid was present in the culture medium, the physiological function of this membrane protein is not clear. The GOX0647 protein shows similarity to proteins of the aromatic acid exporter family (ArAE family, TCDB 2.A.85) (Saier et al., 2009), indicating that it could be involved in the export of a metabolite that accumulates to toxic levels under conditions of low oxygen or acidic pH. Two genes for putative myosin-crossreactive antigens (GOX2199-2200, mRNA ratio 5.4–5.6), which are flanked by transposases and thus might constitute a mobile DNA element, showed increased expression. Also a conserved gene coding for a protein with an N-terminal YjeF_N domain and a C-terminal sugar kinase domain (GOX0090, mRNA ratio 5.1) displayed a high mRNA level under oxygen limitation. Among the downregulated genes with predicted functions were a number of genes encoding putative transport proteins, e.g. GOX0354, whose product is a putative sugar/polyol transporter (mRNA ratio 0.1).

(ix) *Genes with unknown functions.* In total, 125 genes with unknown functions encoding hypothetical proteins were differentially expressed.

In order to confirm the results of the DNA microarray analysis, the expression ratios (oxygen limitation versus oxygen excess) of three selected genes (GOX1914 = *cyoD*, GOX1675 = *ndh*, and GOX0564 = *cycA*) were determined by qRT-PCR. As shown in Table 2, the mRNA ratios obtained by qRT-PCR were in good agreement with the data of the DNA microarray analysis, confirming the reliability of the latter method.

3.2. Growth phenotype of a G. oxydans ΔqrcABC mutant lacking the cytochrome bc_1 complex

As described in Section 1, the function of the cytochrome bc_1 complex in *G. oxydans* is unclear, since this organism lacks genes for a cytochrome *c* oxidase that usually transfers the electrons from the bc_1 complex to oxygen. The *qcrABC* genes were found to be expressed at increased levels under oxygen limitation (see above), showing that they are subject to transcriptional regulation and suggesting a physiological role of the bc_1 complex. In order to find hints for the function of this respiratory complex, a deletion mutant was constructed which lacks the *qcrABC* genes (for details see Section

Table 2
Ratio of mRNA levels of selected genes in *G. oxydans* 621H under different growth conditions determined by qRT-PCR. The data represent mean values and standard deviations based on three independent biological experiments.

Condition and gene	Gene product	qRT-PCR ratio	DNA microarray ratio
O_2 limitation/O_2 saturation			
GOX1914	Cytochrome bo_3 ubiquinol oxidase subunit IV	3.5 ± 0.91	3.8 ± 1.21
GOX1675	NADH dehydrogenase II	0.5 ± 0.05	0.4 ± 0.02
GOX0564	Cytochrome c_{552}	1.8 ± 0.35	2.0 ± 0.42
pH 4/pH 6			
GOX0278	Cytochrome *bd* ubiquinol oxidase subunit I	1.7 ± 0.32	2.2 ± 0.44

2). During cultivation with mannitol as the carbon source at pH 6 and 15% dissolved oxygen growth and product formation was identical for the wild type and the Δ*qrcABC* mutant. In contrast, the growth characteristics of the two strains were distinctly different from each other when the pH value of the medium was kept at 4. In comparison to the wild type, the deletion mutant showed delayed substrate consumption and product formation, however, the same final fructose concentration accumulated in the medium (Fig. 2A). The growth rate of the Δ*qrcABC* mutant was 18% slower than that of the wild type ($\mu = 0.46\,h^{-1}$ compared to $\mu = 0.56\,h^{-1}$) and the final OD_{600} was 13% lower (4.83 ± 0.05 versus 5.56 ± 0.17). The delay in substrate consumption and product formation was paralleled by the oxygen consumption and carbon dioxide production rates (Fig. 2B). These results clearly suggest that the cytochrome bc_1 complex has a physiological function in *G. oxydans*, at least at acidic pH.

3.3. Genome-wide comparison of mRNA levels in the G. oxydans ΔqrcABC mutant and the wild type during growth in mannitol medium at pH 4

For comparing global gene expression of the Δ*qrcABC* deletion mutant and the wild type, both strains were cultivated in mannitol medium at pH 4 and 15% dissolved oxygen and harvested in the exponential growth phase after 5.5 h at an OD_{600} of 2.5 (Fig. 2A). In total, 51 genes showed differential expression (Δ*qcrABC*/wild type), 45 with an mRNA ratio ≥2 and 6 with an mRNA ratio ≤0.5 (Table 3). About 75% of these genes also showed differential expression during oxygen limitation described above (Venn diagram Fig. S1 and Table S2).

(i) *Genes involved in respiration and energy metabolism.* The mRNA levels of the gene cluster comprising the *pntA1A2B* genes and two genes for alcohol dehydrogenases/aldehyde reductase (GOX0310-0314, ratio 3.1–4.0) and the *cyoBACD* cluster (GOX1911-1914, ratio 2.1–2.3) encoding the cytochrome bo_3 terminal oxidase were higher in the Δ*qrcABC* mutant than in the wild type. Interestingly, these genes also showed an increased expression in the wild type under oxygen limitation (Table 1). An increased mRNA level of *cyoBACD* suggests that the capacity to transfer electrons to oxygen is insufficient in the Δ*qrcABC* mutant, which argues in favour of an active participation of the cytochrome bc_1 complex in respiration at pH 4. The mRNA ratio of the *qcrABC* genes was very low, as expected for the comparison of the Δ*qrcABC* mutant and the wild type.

(ii) *Genes involved in metabolism.* A gene encoding a protein of the Rieske non-heme iron oxygenase family, which might function as ring-hydroxylating dioxygenase, displayed increased expression in the deletion mutant (GOX2373, mRNA ratio 2.8). The same gene was also upregulated in the wild type under oxygen limitation (Table S1).

(iii) *Genes involved in transport.* Under acidic conditions the Δ*qrcABC* mutant showed an enhanced transcription of the *exbBD-tonB* genes (GOX0530-0532, mRNA ratio 1.7–5.0). The wild type also showed elevated mRNA ratios of these genes under oxygen deprivation (Table S1). The protein complex encoded by these genes is anchored to the cytoplasmic membrane and is involved in energization of outer membrane transport (Noinaj et al., 2010). Increased expression was also observed for the genes *feoAB* (GOX0673-0674, mRNA ratio 3.0 and 1.7), which encode proteins of the cytoplasmic membrane involved in transport of Fe^{2+}. Again, the wild type also displayed elevated mRNA ratios of the *feoAB* genes under oxygen deprivation (Table 1). Two genes (GOX2180, GOX1246) encoding TonB-dependent outer membrane receptors showed increased mRNA levels, while two others (GOX0945, GOX1903) showed decreased mRNA levels.

(iv) *Gene involved in regulation and signal transduction.* The gene GOX1613 coding for a protein with a GGDEF and an EAL domain and thus involved in synthesis and degradation of cyclic diGMP, showed an increased expression in the Δ*qrcABC* mutant. Again, such a response was also observed in the wild type under oxygen limitation (Table 1).

(v) *Genes involved in motility.* Many genes encoding proteins involved in flagella synthesis or in chemotaxis were

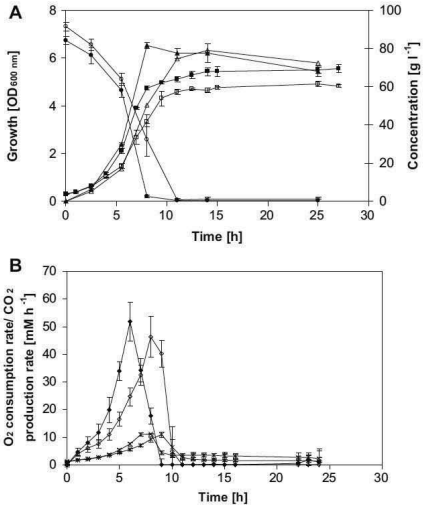

Fig. 2. (A) Growth (■, □), mannitol consumption (●, ○) and fructose formation (▲, △) of *G. oxydans* 621H (filled symbols) and its Δ*qrcABC* deletion mutant (open symbols) at pH 4 and 15% dissolved oxygen. (B) Oxygen consumption rates (♦, ◊) and carbon dioxide formation rates (×, *) of the cultures shown in panel A. Wild type, filled rhombs and crosses; Δ*qcrABC* mutant, open rhombs and stars. Mean values and standard deviations of 3 independent cultures are shown.

Table 3
Genome-wide comparison of mRNA levels of the Δ*qcrABC* mutant of *G. oxydans* with the wild type during growth in mannitol medium at pH 4 and 15% dissolved oxygen. Samples for RNA isolation were taken after 5.5 h cultivation at an OD_{600} of 2.5. Genes with an mRNA ratio ≥2.0 (lower ones allowed in the case of operons) or ≤0.5 (higher ones allowed in the case of operons) and a *p*-value of ≤0.05 are listed. The data shown represent mean values from three biological replicates. The genes were grouped into different functional categories within which they were ordered according to their mRNA ratios except in the case of operons, which were ordered according to their locus tag.

Locus tag	Annotation	Gene	mRNA ratio Δ*qcrABC*/Wt	*p*-Value
	Respiration and energy metabolism			
GOX0310	NAD(P) transhydrogenase subunit α2	*pntA2*	3.14	1.53×10^{-3}
GOX0311	NAD(P) transhydrogenase subunit α1	*pntA1*	3.80	4.77×10^{-3}
GOX0312	NAD(P) transhydrogenase subunit β	*pntB*	3.44	2.76×10^{-3}
GOX0313	Alcohol:NAD^+ oxidoreductase		4.00	3.19×10^{-3}
GOX0314	Probable alcohol:$NAD(P)^+$ oxidoreductase		3.58	5.43×10^{-3}
GOX1911	Cytochrome bo_3 ubiquinol oxidase subunit II	*cyoB*	2.09	7.68×10^{-3}
GOX1912	Cytochrome bo_3 ubiquinol oxidase subunit I	*cyoA*	2.28	6.81×10^{-3}
GOX1913	Cytochrome bo_3 ubiquinol oxidase subunit III	*cyoC*	2.10	2.34×10^{-3}
GOX1914	Cytochrome bo_3 ubiquinol oxidase subunit IV	*cyoD*	2.15	2.94×10^{-3}
GOX0565	Ubiquinol-cytochrome *c* oxidoreductase, FeS protein	*qrcA*	0.05	3.19×10^{-3}
GOX0566	Ubiquinol-cytochrome *c* oxidoreductase, cytochrome *b*	*qrcB*	0.03	6.97×10^{-4}
GOX0567	Ubiquinol-cytochrome *c* oxidoreductase, cytochrome c_1	*qrcC*	0.05	3.38×10^{-3}
	Metabolism			
GOX2373	Protein of Rieske non-heme iron oxygenase family, putative ring-hydroxylating dioxygenase		2.81	6.17×10^{-4}
	Transport			
GOX0530	TonB protein	*tonB*	1.70	1.00×10^{-2}
GOX0531	ExbD protein	*exbD*	2.98	3.42×10^{-3}
GOX0532	ExbB protein	*exbB*	4.97	5.36×10^{-3}
GOX2180	TonB-dependent receptor (disrupted by IS element)		3.38	7.71×10^{-3}
GOX0673	Ferrous iron transport protein A (FeoA)	*feoA*	3.04	3.21×10^{-4}
GOX0674	Ferrous iron transport protein B (FeoB)	*feoB*	1.73	$0.00 \times 10^{-}$
GOX1246	TonB-dependent receptor protein		2.34	8.93×10^{-4}
GOX0945	TonB-dependent outer membrane receptor		0.47	1.77×10^{-2}
GOX1903	TonB-dependent receptor protein		0.38	1.70×10^{-3}
	Regulation and signal transduction (except chemotaxis)			
GOX1613	Protein with GGDEF and EAL domain		2.36	1.61×10^{-3}
	Motility			
GOX1025	Flagellar hook-associated protein FlgL	*flgL*	2.73	1.36×10^{-2}
GOX1026	Flagellar hook-associated protein 1 FlgK	*flgK*	2.66	1.22×10^{-3}
GOX1027	Flagellar hook protein FlgE	*flgE*	2.81	3.85×10^{-3}
GOX0787	Flagellin B		2.73	1.34×10^{-3}
GOX0788	Flagellin assembly protein		2.06	3.11×10^{-3}
GOX0952	Flagellar basal body P-ring biosynthesis protein FlgA	*flgA*	1.66	1.69×10^{-2}
GOX0953	Flagellar basal body rod protein FlgG	*flgG*	2.33	1.22×10^{-2}
GOX0954	Flagellar basal-body rod protein FlgF	*flgF*	2.28	9.07×10^{-4}
GOX1525	Flagellar biosynthetic protein FliQ	*fliQ*	1.79	9.44×10^{-3}
GOX1526	Flagellar hook-basal body protein FleE	*fleE*	1.72	1.89×10^{-2}
GOX1527	Flagellar basal body rod protein FlgC	*flgC*	1.83	1.23×10^{-2}
GOX1528	Flagellar basal-body rod protein FlgB	*flgB*	2.03	1.82×10^{-3}
GOX1549	Methyl-accepting chemotaxis protein		1.93	3.00×10^{-2}
GOX1550	Chemotaxis protein CheX	*cheX*	2.01	1.61×10^{-2}
GOX1551	Chemotaxis protein CheY	*cheY*	1.95	1.61×10^{-3}
GOX1552	Chemotaxis protein CheA	*cheA*	1.88	3.94×10^{-2}
	Stress			
GOX0798	Trypsin-like serine protease (HtrA/DegQ/DegS family) with two PDZ domains		2.24	1.18×10^{-2}
	Predicted functions			
GOX2199	Probable myosin-crossreactive antigen		2.33	1.51×10^{-3}
GOX2200	Probable myosin-crossreactive antigen		2.01	6.60×10^{-3}
	Hypothetical proteins			
GOX0442	Hypothetical protein GOX0442		2.22	2.65×10^{-3}
GOX0890	Hypothetical protein GOX0890		2.19	5.92×10^{-2}
GOX0053	Hypothetical protein GOX0053		2.15	5.62×10^{-3}
GOX1841	Hypothetical protein GOX1841		2.14	8.91×10^{-3}
GOX0426	Hypothetical protein GOX0426		2.06	1.10×10^{-2}
GOX0635	Hypothetical protein GOX0635		2.02	6.78×10^{-3}
GOX1870	Hypothetical protein GOX1870		2.00	2.40×10^{-2}
GOX2379	Hypothetical protein GOX2379		2.00	2.55×10^{-2}
GOX1982	Hypothetical protein GOX1982		0.46	4.35×10^{-4}

Table 4
Genome-wide comparison of mRNA levels in *G. oxydans* during growth at pH 4 and pH 6. Cells were cultivated for 5.5 h (OD_{600} = 2.5) in mannitol medium with pH control and at constantly 15% dissolved oxygen. Genes with an mRNA ratio ≥2.0 (lower ones allowed in the case of operons) or ≤0.5 (higher ones allowed in the case of operons) and a *p*-value of ≤0.05 are listed. The data shown represent mean values from three biological replicates. The genes were grouped into different functional categories within which they were ordered according to their mRNA ratios except in the case of operons, which were ordered according to their locus tag.

Locus tag	Annotation	Gene	mRNA ratio pH4/pH6	*p*-Value
	Respiration and energy metabolism			
GOX0278	Cytochrome *bd* ubiquinol oxidase subunit I	*cydA*	2.22	1.11×10^{-2}
GOX0279	Cytochrome *bd* ubiquinol oxidase subunit II	*cydB*	1.59	5.11×10^{-2}
GOX2096	Major polyol dehydrogenase large subunit	*sldA*	2.21	1.64×10^{-3}
GOX2097	Major polyol dehydrogenase small subunit	*sldB*	2.22	1.28×10^{-2}
	Metabolism			
GOX1748	Bacterioferritin	*bfr*	3.37	1.99×10^{-3}
GOX1712	Aldehyde dehydrogenase		2.15	4.88×10^{-3}
GOX1713	Putative protease of DJ-1/PfpI family	*pfpI*	2.08	$0.00 \times 10^{-}$
GOX1276	Secreted protein of aminohydrolase family		2.02	1.38×10^{-3}
GOX1335	Aconitate hydratase	*acnA*	0.49	1.98×10^{-3}
GOX1336	Isocitrate dehydrogenase	*icd*	0.45	2.23×10^{-2}
GOX0216	N-Methylhydantoinase A		0.48	7.45×10^{-4}
GOX0212	Biotin carboxyl carrier protein of acetyl-CoA carboxylase	*accB*	0.44	6.16×10^{-3}
GOX0213	Biotin carboxylase	*accC*	0.47	1.62×10^{-3}
GOX1851	Glutamate synthase	*gltD*	0.39	3.54×10^{-4}
GOX1852	Glutamate synthase	*gltB*	0.35	4.01×10^{-3}
GOX1785	Carbonic anhydrase	*cynT*	0.37	8.75×10^{-4}
GOX0652	Xanthine dehydrogenase accessory protein XdhC	*xdhC*	0.34	2.76×10^{-2}
GOX0653	Xanthine dehydrogenase, large subunit XdhB	*xdhB*	0.34	9.25×10^{-4}
	Transport			
GOX1903	TonB-dependent outer membrane receptor		0.42	4.62×10^{-4}
GOX1173	TonB-dependent outer membrane receptor		0.40	4.90×10^{-2}
GOX0945	TonB-dependent outer membrane receptor		0.35	2.36×10^{-2}
GOX0907	TonB-dependent outer membrane receptor		0.34	2.01×10^{-3}
GOX1017	TonB-dependent outer membrane receptor		0.31	4.86×10^{-3}
GOX0207	TonB-dependent outer membrane receptor		0.22	2.27×10^{-3}
GOX0524	TonB-dependent outer membrane receptor		0.19	8.69×10^{-3}
	Regulators			
GOX0768	Transcriptional regulator		0.49	2.14×10^{-2}
	Stress			
GOX0707	DNA starvation/stationary phase protection protein Dps	*dps*	3.47	4.21×10^{-2}
GOX1138	Catalase	*kat*	2.10	1.68×10^{-3}
GOX1992	Osmotically inducible protein C, peroxiredoxin	*osmC*	2.01	7.16×10^{-3}
	Transcriptional and translational machinery			
GOX1374	DNA topoisomerase I	*topA*	3.02	3.62×10^{-3}
	Predicted functions			
GOX0647	Putative exporter protein, ArAE family	*fus*	12.91	1.52×10^{-3}
GOX0679	Conserved protein of the SAM superfamily		3.20	4.43×10^{-2}
GOX1615	Putative oxidoreductase		2.54	1.50×10^{-2}
GOX2676	Putative alcohol/aldehyde dehydrogenase		2.45	2.47×10^{-2}
GOX0291	Putative ferredoxin subunit of ring-hydroxylating dioxygenase	*hca*	2.34	9.20×10^{-4}
GOX0470	Putative peroxidase	*efeB*	2.24	3.39×10^{-2}
GOX1351	Putative isomerase		2.10	2.93×10^{-2}
GOX1462	Putative oxidoreductase		2.10	5.42×10^{-3}
GOX1538	Short chain dehydrogenase		2.02	2.90×10^{-2}
GOX1225	Putative phage tail protein		0.47	8.08×10^{-3}
GOX0905	Putative oxidoreductase		0.45	4.13×10^{-4}
GOX0210	Putative carboxylase		0.44	4.92×10^{-3}
GOX0208	Putative glucarate/galactarate transporter		0.43	4.73×10^{-2}
GOX2256	Putative aminotransferase		0.41	8.74×10^{-3}
GOX1857	Uncharacterized PQQ-containing dehydrogenase 1		0.40	9.72×10^{-3}
	Hypothetical proteins			
GOX0890	Hypothetical protein GOX0890		4.93	4.87×10^{-3}
GOX1841	Hypothetical protein GOX1841		3.36	2.55×10^{-2}
GOX0943	Hypothetical protein GOX0943		3.13	9.41×10^{-3}
GOX0726	Hypothetical protein GOX0726		2.76	8.76×10^{-3}
GOX0553	Hypothetical protein GOX0553		2.75	6.48×10^{-3}
GOX0433	Hypothetical protein GOX0433		2.50	4.50×10^{-3}
GOX0944	Hypothetical protein GOX0944		2.48	1.99×10^{-2}
GOX0497	Hypothetical protein GOX0497		2.31	5.22×10^{-4}
GOX1951	Hypothetical protein GOX1951		2.27	1.86×10^{-3}
GOX0352	Hypothetical protein GOX0352		2.20	2.62×10^{-2}
GOX0244	Hypothetical membrane-spanning protein		2.19	4.58×10^{-2}
GOX2083	Hypothetical protein GOX2083		2.15	2.36×10^{-2}
GOX2079	Hypothetical protein GOX2079		2.13	1.51×10^{-3}
GOX0576	Hypothetical protein GOX0576		2.11	2.50×10^{-2}
GOX0902	Hypothetical protein GOX0902		0.47	2.82×10^{-2}
GOX0904	Hypothetical protein GOX0904		0.44	2.10×10^{-3}

Table 4 (*Continued*)

Locus tag	Annotation	Gene	mRNA ratio pH4/pH6	*p*-Value
GOX0209	Hypothetical protein GOX0209		0.42	3.59×10^{-3}
GOX0211	Hypothetical protein GOX0211		0.40	3.27×10^{-3}
GOX0204	Hypothetical protein GOX0204		0.39	3.49×10^{-2}
GOX1749	Hypothetical protein GOX1749		0.37	1.40×10^{-2}
GOX1982	Hypothetical protein GOX1982		0.36	3.88×10^{-3}
GOX1209	Hypothetical protein GOX1209		0.36	1.82×10^{-2}
GOX1660	Hypothetical protein GOX1660		0.35	3.91×10^{-2}
GOX0903	Hypothetical protein GOX0903		0.33	1.81×10^{-3}
GOX1784	Hypothetical protein GOX1784		0.33	1.55×10^{-3}
GOX2017	Hypothetical protein GOX2017		0.31	1.17×10^{-2}
GOX1210	Hypothetical protein GOX1210		0.25	4.60×10^{-2}

upregulated in the Δ*qrcABC* mutant. This parallels the situation in oxygen-limited wild type cells (Table 1).

(vi) *Gene involved in stress responses*. A periplasmic serine protease belonging to the HtrA/DegQ/DegS family showed an increased mRNA ratio (GOX0798). This gene was not differentially regulated in the wild type, neither at pH 4 nor under oxygen limitation.

(vii) *Genes with predicted functions*. Genes GOX2199 and 2200, annotated as putative myosin-crossreactive antigens (MCRA), showed increased mRNA levels in the Δ*qrcABC* mutant. The same pattern was also observed in the wild type under oxygen limitation. Recently, a *Streptococcus pyogenes* MCRA was characterized as an FAD-containing fatty acid double bond hydratase (Volkov et al., 2010).

(viii) *Genes with unknown functions*. Nine genes encoding hypothetical proteins of unknown function were differentially expressed in the Δ*qrcABC* deletion mutant.

3.4. Effect of decreased pH on global gene expression in G. oxydans 621H

For comparing global gene expression at pH 4 and pH 6, cultures were grown in bioreactors with mannitol medium at the indicated pH values and a constant dissolved oxygen concentration of 15%. As shown in Fig. 1B, the growth rates were identical at pH 4 and pH 6 and samples were harvested for RNA isolation after 5.5 h in the exponential growth phase at an OD_{600} of 2.5. Differences were observed in the final ODs reached, which were about 9 at pH 6, but only about 7 at pH 4. In total, only 72 genes showed differential expression, 35 with an mRNA ratio ≥2 and 37 with an mRNA ratio ≤0.5 (Table 4).

(i) *Genes involved in respiration and energy metabolism*. The *cydAB* genes encoding cytochrome *bd* ubichinol oxidase (GOX0278, mRNA ratio 2.2; GOX0279, mRNA ratio 1.6) and the *sldAB* genes encoding the major polyol dehydrogenase (GOX2096-2097, mRNA ratios 2.2) were upregulated at pH 4. In agreement with this result, earlier studies had already provided evidence for an increased concentration of cytochrome *bd* oxidase at lower pH values (Matsushita et al., 1989).

(ii) *Genes involved in metabolism*. The genes for bacterioferritin (GOX1748, mRNA ratio 3.4), an aldehyde dehydrogenase (GOX1712, mRNA ratio 2.2), a protease (GOX1713, mRNA ratio 2.1) and a protein with an amidohydrolase domain (GOX1276, mRNA ratio 2.0) displayed increased expression. Bacterioferritin functions as an iron storage protein (Andrews et al., 2003), suggesting an increased iron uptake and an increased iron content under acidic conditions. Among the downregulated genes were two of the TCA cycle (*acn*, GOX1335, mRNA ratio 0.5; *icd*, GOX1336, mRNA ratio 0.5), two involved in nitrogen assimilation (*gltBD*, GOX1852 and 1851, mRNA ratios 0.4), two involved in xanthine oxidation (*xdhBC*, GOX0653 and 0652, mRNA ratios 0.3), two involved in fatty acid biosynthesis (*accBC*, GOX0212 and 0213, mRNA ratios 0.4–0.5), and one encoding carboanhydrase (*cynT*, GOX1785, mRNA ratio 0.4). The lowered expression of the latter three genes might be related to an increased concentration of dissolved CO_2 at low pH.

(iii) *Genes involved in transport*. Transcription of genes for seven TonB-dependent outer membrane receptors was reduced at acidic pH. As the majority of these proteins are involved in the uptake of iron complexes (Noinaj et al., 2010), the lowered expression might reflect a better availability of iron at pH 4 due to the increased solubility.

(iv) *Gene involved in regulation*. Only one gene for a transcriptional regulator of the XRE family showed a reduced expression at pH 4 (GOX0768, mRNA ratio 0.5). The function of this regulator is unknown.

(v) *Genes involved in stress responses*. The gene *dps* (DNA-binding protein in starved cells, GOX0707, mRNA ratio 3.5), showed a high transcript level at pH 4. Dps protects DNA from acid damage by binding to DNA in *E. coli* (Jeong et al., 2008) and simultaneously functions as an iron storage protein which oxidizes Fe^{2+} to Fe^{3+} with H_2O_2 (Zhao et al., 2002). As besides *dps* also the *kat* gene for catalase had an increased mRNA level (GOX1138, mRNA ratio 2.1), a stronger production of H_2O_2 at low pH can be inferred. The *osmC* gene, which also showed increased expression at pH 4 (GOX1992, mRNA ratio 2.0), encodes a peroxiredoxin presumably involved in the defense against oxidative stress caused by exposure to organic hydroperoxides (Lesniak et al., 2003).

(vi) *Genes involved in the transcriptional and translational machinery*. The DNA topoisomerase I gene *topA* displayed a significantly increased expression at pH 4 (GOX1374, mRNA ratio 3.0). This enzyme degrades the RNA component of RNA:DNA hybrids and is important in nucleic acid metabolism (Kim et al., 2011). In *E. coli topA* expression is activated in response to oxidative stress (Weinstein-Fischer and Altuvia, 2007).

(vii) *Genes with predicted functions*. The gene with the most strongly increased mRNA level at pH 4 was the *fus* gene (GOX0647, ratio12.9) encoding a putative exporter protein of the aromatic acid exporter family. This gene also showed strongly increased expression in oxygen-limited cells (Table 1). The gene for an uncharacterized PQQ-containing dehydrogenase showed a decreased mRNA level (GOX1857, ratio 0.40).

(viii) *Genes with unknown functions*. In total, 27 genes with unknown functions encoding hypothetical proteins were differentially expressed at pH 4.

In order to confirm the results of the DNA microarray analysis, the mRNA ratio (pH 4 versus pH 6) of the *cydA* gene (GOX0278) was determined by qRT-PCR. As shown in Table 2, the data obtained by

qRT-PCR were again in good agreement with the data of the DNA microarray analysis.

4. Conclusions

In this work, first insights into the global responses of *G. oxydans* to two particularly important environmental parameters were obtained, oxygen availability and pH. In its natural habitat, oxygen deprivation due to the rapid oxygen consumption by *G. oxydans* itself and acidic conditions due to the action of sugar fermenting organisms and the incomplete oxidation of substrates by *G. oxydans* are likely to occur very often. Our results show that oxygen deprivation causes expression changes of about 500 genes, many of which are certainly due to non-exponential growth observed after the switch to oxygen limitation. Many interesting questions arise from this oxygen starvation stimulon, such as to the functions of the two, inversely regulated F_1F_O-ATP synthases. Moreover, evidence was obtained that despite the apparent absence of a cytochrome *c* oxidase the cytochrome bc_1 complex seems to play a role as an electron transfer component under oxygen limitation, where the *qcrABC* genes were upregulated in the wild type, and under acidic conditions, where the Δ*qcrABC* mutant showed a growth defect. Surprisingly, the transcriptional changes observed in the comparison of wild type cells grown at pH 4 and pH 6 were quite limited and did not include typical acid response proteins known from other bacteria (Booth et al., 2002; Foster, 2004; Krulwich et al., 2011). This indicates that *G. oxydans* either uses other proteins and mechanisms to adapt to lower pH or that its standard enzymatic equipment is adapted for growth at both pH 6 and pH 4.

Acknowledgements

This work was funded by the German Ministry of Education and Research (BMBF) within the GenoMik-Plus program (grant 0313751H). We thank DSM Nutritional Products (Kaiseraugst, Switzerland) for financial support and Petra Simić and Hans-Peter Hohmann (DSM Nutritional Products) for their scientific input and their continued disposition for discussion. We are indebted to Volker Müller (Frankfurt am Main, Germany) for his assistance in the interpretation of results on F_1F_o-ATP synthases.

Appendix A. Supplementary data

Supplementary data associated with this article can be found, in the online version, at doi:10.1016/j.jbiotec.2011.12.020.

References

Andrews, S.C., Robinson, A.K., Rodriguez-Quinones, F., 2003. Bacterial iron homeostasis. FEMS Microbiol. Rev. 27, 215–237.

Atack, J.M., Kelly, D.J., 2007. Structure, mechanism and physiological roles of bacterial cytochrome *c* peroxidases. Adv. Microb. Physiol. 52, 73–106.

Azuma, Y., Hosoyama, A., Matsutani, M., Furuya, N., Horikawa, H., Harada, T., Hirakawa, H., Kuhara, S., Matsushita, K., Fujita, N., Shirai, M., 2009. Whole-genome analyses reveal genetic instability of *Acetobacter pasteurianus*. Nucleic Acids Res. 37, 5768–5783.

Booth, I.R., Cash, P., O'Byrne, C., 2002. Sensing and adapting to acid stress. Antonie Van Leeuwenhoek 81, 33–42.

Brazma, A., Hingamp, P., Quackenbush, J., Sherlock, G., Spellman, P., Stoeckert, C., Aach, J., Ansorge, W., Ball, C.A., Causton, H.C., Gaasterland, T., Glenisson, P., Holstege, F.C., Kim, I.F., Markowitz, V., Matese, J.C., Parkinson, H., Robinson, A., Sarkans, U., Schulze-Kremer, S., Stewart, J., Taylor, R., Vilo, J., Vingron, M., 2001. Minimum information about a microarray experiment (MIAME)-toward standards for microarray data. Nat. Genet. 29, 365–371.

Charoensuk, K., Irie, A., Lertwattanasakul, N., Sootsuwan, K., Thanonkeo, P., Yamada, M., 2011. Physiological importance of cytochrome *c* peroxidase in ethanologenic thermotolerant *Zymomonas mobilis*. J. Mol. Microbiol. Biotechnol. 20, 70–82.

Crotti, E., Rizzi, A., Chouaia, B., Ricci, I., Favia, G., Alma, A., Sacchi, L., Bourtzis, K., Mandrioli, M., Cherif, A., Bandi, C., Daffonchio, D., 2010. Acetic acid bacteria, newly emerging symbionts of insects. Appl. Environ. Microbiol. 76, 6963–6970.

Volkov, A., Liavonchanka, A., Kamneva, O., Fiedler, T., Goebel, C., Kreikemeyer, B., Feussner, I., 2010. Myosin cross-reactive antigen of *Streptococcus pyogenes* M49 encodes a fatty acid double bond hydratase that plays a role in oleic acid detoxification and bacterial virulence. J. Biol. Chem. 285, 10353–10361.

Weinstein-Fischer, D., Altuvia, S., 2007. Differential regulation of *Escherichia coli* topoisomerase I by Fis. Mol. Microbiol. 63, 1131–1144.

Dibrova, D.V., Galperin, M., Mulkidjanian, A., 2010. Characterization of the N-ATPase, a distinct, laterally transferred Na^+-translocating form of the bacterial F-type membrane ATPase. Bioinformatics 26, 1473–1476.

Fakhouri, W., Walker, F., Armbruster, W., Buchenauer, H., 2003. Detoxification of fusaric acid by a nonpathogenic *Colletotrichum* sp. Physiol. Mol. Plant Pathol. 63, 263–269.

Foster, J.W., 2004. Escherichia coli acid resistance: tales of an amateur acidophile. Nat. Rev. Microbiol. 2, 898–907.

Gennis, R.B., Stewart, V., 1996. Respiration. In: *Escherichia coli* and *Salmonella typhimurium*. Cell. Mol. Biol., 217–261.

Gupta, A., Singh, V.K., Qazi, G.N., Kumar, A., 2001. Gluconobacter oxydans: its biotechnological applications. J. Mol. Microbiol. Biotechnol. 3, 445–456.

Jackson, J.B., White, S.A., Quirk, P.G., Venning, J.D., 2002. The alternating site, binding change mechanism for proton translocation by transhydrogenase. Biochemistry 41, 4173–4185.

Jeong, K.C., Hung, K.F., Baumler, D.J., Byrd, J.J., Kaspar, C.W., 2008. Acid stress damage of DNA is prevented by Dps binding in *Escherichia coli* O157:H7. BMC Microbiol. 8, 181.

Kersters, K., Lisdiyanti, P., Komagata, K., Swings, J., 2006. The family *Acetobacteriaceae*: the genera *Acetobacter*, *Acidomonas*, *Asaia*, *Gluconacetobacter*, *Gluconobacter*, and *Kozakia*. In: Dworkin, M., Falkow, S., Rosenberg, E., Schleifer, K-H., Stackebrandt, E. (Eds.), The Prokaryotes, vol. 5, 3rd ed. Springer-Verlag GmbH, Heidelberg, pp. 163–200.

Kim, N., Huang, S.Y., Williams, J.S., Li, Y.C., Clark, A.B., Cho, J.E., Kunkel, T.A., Pommier, Y., Jinks-Robertson, S., 2011. Mutagenic processing of ribonucleotides in DNA by yeast topoisomerase I. Science 332, 1561–1564.

Krulwich, T.A., Sachs, G., Padan, E., 2011. Molecular aspects of bacterial pH sensing and homeostasis. Nat. Rev. Microbiol. 9, 330–343.

Lee, J.W., Helmann, J.D., 2007. Functional specialization within the Fur family of metalloregulators. Biometals 20, 485–499.

Lesniak, J., Barton, W.A., Nikolov, D.B., 2003. Structural and functional features of the *Escherichia coli* hydroperoxide resistance protein OsmC. Protein Sci. 12, 2838–2843.

Levering, P.R., Weenk, G., Olijve, W., Dijkhuizen, L., Harder, W., 1988. Regulation of gluconate and ketogluconate production in *Gluconobacter oxydans* ATCC 621H. Arch. Microbiol. 149, 534–539.

Matsushita, K., Nagatani, Y., Shinagawa, E., Adachi, O., Ameyama, M., 1989. Effect of extracellular pH on the respiratory chain and energetics of *Gluconobacter suboxydans*. Agric. Biol. Chem. 53, 2895–2902.

Matsushita, K., Toyama, H., Adachi, O., 1994. Respiratory chains and bioenergetics of acetic acid bacteria. Adv. Microb. Physiol. 36, 247–301.

Müller, V., Grüber, G., 2003. ATP synthases: structure, function and evolution of unique energy converters. Cell. Mol. Life Sci. 60, 474–494.

Noinaj, N., Guillier, M., Barnard, T.J., Buchanan, S.K., 2010. TonB-dependent transporters: regulation, structure, and function. Annu. Rev. Microbiol. 64, 43–60.

Österberg, S., Del Peso-Santos, T., Shingler, V., 2011. Regulation of alternative sigma factor use. Annu. Rev. Microbiol. 65, 37–55.

Polen, T., Schluesener, D., Poetsch, A., Bott, M., Wendisch, V.F., 2007. Characterization of citrate utilization in *Corynebacterium glutamicum* by transcriptome and proteome analysis. FEMS Microbiol. Lett. 273, 109–119.

Polen, T., Wendisch, V.F., 2004. Genomewide expression analysis in amino acid-producing bacteria using DNA microarrays. Appl. Biochem. Biotechnol. 118, 215–232.

Prust, C., Hoffmeister, M., Liesegang, H., Wiezer, A., Fricke, W.F., Ehrenreich, A., Gottschalk, G., Deppenmeier, U., 2005. Complete genome sequence of the acetic acid bacterium *Gluconobacter oxydans*. Nat. Biotechnol. 23, 195–200.

Raspor, P.P., Goranovič, D., 2008. Biotechnological applications of acetic acid bacteria. Crit. Rev. Biotechnol. 28, 101–124.

Ross, P., Weinhouse, H., Aloni, Y., Michaeli, D., Weinberger-Ohana, P., Mayer, R., Braun, S., de Vroom, E., van der Marel, G.A., van Boom, J.H., Benziman, M., 1987. Regulation of cellulose synthesis in *Acetobacter xylinum* by cyclic diguanylic acid. Nature 325, 279–281.

Saier Jr., M.H., Yen, M.R., Noto, K., Tamang, D.G., Elkan, C., 2009. The Transporter Classification Database: recent advances. Nucleic Acids Res. 37, D274–D278.

Sakurai, K., Arai, H., Ishii, M., Igarashi, Y., 2011. Transcriptome response to different carbon sources in *Acetobacter aceti*. Microbiology 157, 899–910.

Sambrook, J., Russell, D.W., 2001. Molecular Cloning: A Laboratory Manual, 3rd ed. Cold Spring Harbor Laboratory Press, Cold Spring Harbor, NY.

Saum, R., Schlegel, K., Meyer, B., Müller, V., 2009. The F_1F_OATP synthase genes in *Methanosarcina acetivorans* are dispensable for growth and ATP synthesis. FEMS Microbiol. Lett. 300, 230–236.

Schäfer, A., Tauch, A., Jäger, W., Kalinowski, J., Thierbach, G., Pühler, A., 1994. Small mobilizable multi-purpose cloning vectors derived from the *Escherichia coli* plasmids pK18 and pK19: selection of defined deletions in the chromosome of *Corynebacterium glutamicum*. Gene 145, 69–73.

Schirmer, T., Jenal, U., 2009. Structural and mechanistic determinants of c-di-GMP signalling. Nat. Rev. Microbiol. 7, 724–735.

Sootsuwan, K., Lertwattanasakul, N., Thanonkeo, P., Matsushita, K., Yamada, M., 2008. Analysis of the respiratory chain in ethanologenic *Zymomonas mobilis* with a cyanide-resistant *bd*-type ubiquinol oxidase as the only terminal oxidase and its possible physiological roles. J. Mol. Microbiol. Biotechnol. 14, 163–175.

Sundararajan, A., Kurowski, J., Yan, T., Klingeman, D.M., Joachimiak, M.P., Zhou, J., Naranjo, B., Gralnick, J.A., Fields, M.W., 2011. Shewanella oneidensis MR-1 sensory box protein involved in aerobic and anoxic growth. Appl. Environ. Microbiol. 77, 4647–4656.

Yamada, H., Takashima, E., Konishi, K., 2007. Molecular characterization of the membrane-bound quinol peroxidase functionally connected to the respiratory chain. FEBS J. 274, 853–866.

Zhao, G., Ceci, P., Ilari, A., Giangiacomo, L., Laue, T.M., Chiancone, E., Chasteen, N.D., 2002. Iron and hydrogen peroxide detoxification properties of DNA-binding protein from starved cells. A ferritin-like DNA-binding protein of *Escherichia coli*. J. Biol. Chem. 277, 27689–27696.

Supplementary material

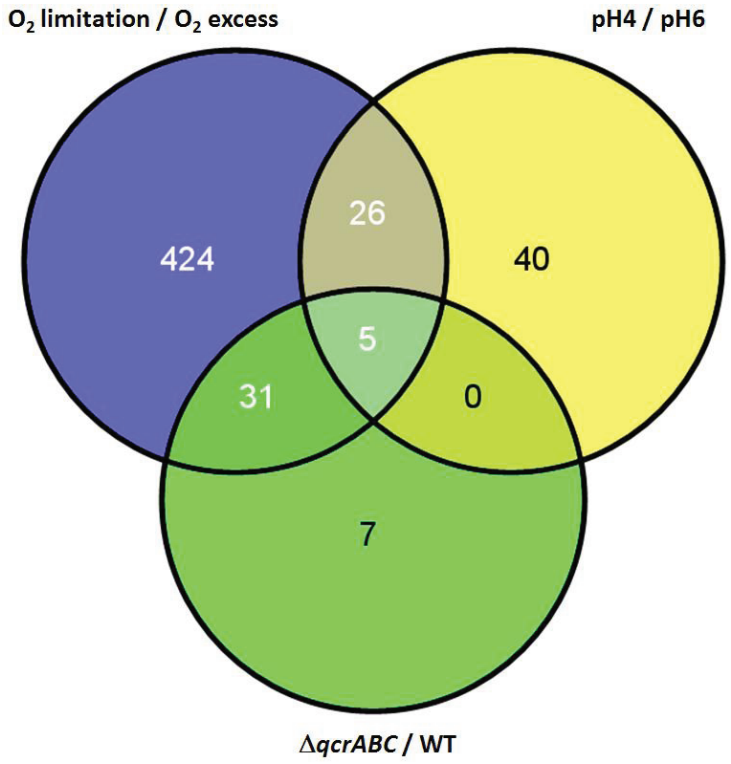

Fig. S1. Venn diagram showing the overlaps by the number of genes ≥ 2-fold differentially expressed in the conditions tested. The diagram was created by the online tool Venny (bioinfogp.cnb.csic.es/tools/venny/index.html).

Table S1 Genome-wide comparison of mRNA levels in *G. oxydans* during growth under oxygen limitation and oxygen excess (see Fig. 1 and Table 1). A list of all genes with an mRNA ratio ≥2.0 or ≤0.5 is shown. The data shown represent mean values from four biological replicates. The genes were grouped into different functional categories within which they were ordered according to their locus tags.

Oxygen limitation versus oxygen saturation; mRNA ratio of 215 genes ≥ 2.0

Gene	Annotation	mRNA ratio	n	*p*-value
GOX0031	Hypothetical protein GOX0031	2.16	4	1.90E-03
GOX0053	Hypothetical protein GOX0053	3.71	4	3.40E-04
GOX0090	Putative sugar kinase	5.14	4	8.89E-04
GOX0126	Flagellar motor protein MotA	2.08	4	1.75E-03
GOX0135	Transcriptional regulator Ros/MucR family	2.80	4	3.66E-03
GOX0137	Hypothetical membrane-spanning protein	2.86	4	1.90E-04
GOX0172	Arginine tRNA	2.31	4	4.38E-03
GOX0198	Hypothetical protein GOX0198	2.17	4	5.99E-04
GOX0199	Serine tRNA	2.43	2	6.70E-09
GOX0204	Hypothetical protein GOX0204	2.45	4	1.10E-03
GOX0278	Cytochrome bd ubiquinol oxidase subunit I	3.64	4	7.58E-05
GOX0310	NAD(P) transhydrogenase subunit alpha2	10.37	4	3.76E-04
GOX0311	NAD(P) transhydrogenase subunit alpha1	14.70	4	1.36E-03
GOX0312	NAD(P) transhydrogenase subunit beta	12.04	4	4.33E-04
GOX0313	Alcohol:NAD oxidoreductase	13.58	4	7.09E-04
GOX0314	Probable Alcohol:NAD(P) oxidoreductase	14.63	4	2.35E-03
GOX0333	Hypothetical protein GOX0333	2.24	4	1.64E-03
GOX0334	Probable (di) nucleoside polyphosphate hydrolase	2.21	4	1.33E-04
GOX0421	Flagellar motor switch protein	2.18	4	2.53E-03
GOX0422	Hypothetical protein GOX0422	2.17	4	1.93E-02
GOX0425	Basal-body rod modification protein FlgD	3.04	4	4.05E-04
GOX0426	Hypothetical protein GOX0426	3.42	4	2.34E-03
GOX0442	Hypothetical protein GOX0442	2.21	4	1.94E-02
GOX0443	Molybdopterin (MPT) converting factor, subunit 2	2.27	4	3.28E-04
GOX0444	Bifunctional molybdenum cofactor biosynthesis protein (Molybdopterin-guanine dinucleotide biosynthesis protein A and MoaD)	2.28	4	2.48E-03

GOX0445	Molybdenum cofactor biosynthesis protein C	3.07	4	5.58E-05
GOX0475	Hypothetical protein GOX0475	2.16	4	1.25E-03
GOX0506	RNA polymerase factor sigma factor H (sigma-32)	4.04	4	3.77E-05
GOX0549	Hypothetical protein GOX0549	2.51	4	1.37E-03
GOX0564	Cytochrome c552	2.02	4	1.22E-03
GOX0565	Ubiquinol-cytochrome *c* oxidoreductase FeS protein	2.49	4	3.81E-03
GOX0566	Ubiquinol-cytochrome *c* oxidoreductase cytochrome *b*	2.20	4	1.29E-02
GOX0570	Hypothetical protein GOX0570	2.37	4	3.04E-05
GOX0571	Hypothetical protein GOX0571	2.62	4	4.14E-03
GOX0572	Putative oxidoreductase	3.61	4	1.73E-03
GOX0573	Metallo-beta-lactamase superfamily protein	4.81	4	1.68E-03
GOX0576	Hypothetical protein GOX0576	2.80	4	2.68E-03
GOX0585	Cytochrome *c* subunit of aldehyde dehydrogenase	2.02	4	5.61E-04
GOX0586	Membrane-bound aldehyde dehydrogenase, small subunit	2.01	4	1.17E-03
GOX0607	D-Aalanyl-D-alanine carboxypeptidase	2.51	4	7.26E-06
GOX0609	ATP-dependent Clp protease ATP-binding subunit ClpA	2.85	4	1.16E-04
GOX0618	Hemolysin-related protein	2.46	4	1.50E-02
GOX0619	Hypothetical protein GOX0619	2.56	4	7.14E-04
GOX0620	Chemotactic signal-response protein CheL	2.54	4	7.18E-05
GOX0635	Hypothetical protein GOX0635	2.01	4	2.78E-02
GOX0647	Putative exporter protein. ArAE family	18.22	4	4.00E-02
GOX0673	Ferrous iron transport protein A (FeoA)	5.86	4	4.91E-03
GOX0674	Ferrous iron transport protein B (FeoB)	3.24	4	1.40E-02
GOX0683	Protein with GGDEF domain	2.13	4	6.88E-03
GOX0694	Hypothetical protein GOX0694	2.53	4	4.97E-04
GOX0695	Hypothetical protein GOX0695	2.56	4	1.57E-03
GOX0697	Flagellar FliL protein	2.40	4	1.97E-03
GOX0708	Hypothetical protein GOX0708	2.18	4	1.47E-02
GOX0746	FAD-dependent monooxygenase	2.03	4	5.97E-04
GOX0747	Serine O-acetyltransferase CysE	2.05	4	9.70E-03
GOX0755	Hypothetical protein in adhS 5' region	2.36	4	1.50E-03
GOX0762	Thioredoxin	2.10	4	3.79E-04
GOX0787	Flagellin B	3.44	4	2.00E-03
GOX0788	Flagellin assembly protein	4.23	4	1.42E-03
GOX0813	Phosphocarrier protein HPr	2.20	4	5.48E-03
GOX0814	PTS system, IIA component	4.10	4	1.59E-04

GOX0815	Hypothetical protein GOX0815	6.53	4	1.86E-04
GOX0861	Flavohemoprotein	2.15	4	1.56E-02
GOX0872	Proline tRNA	2.00	3	2.01E-02
GOX0874	Ferrochelatase	2.21	4	2.71E-04
GOX0875	AtsE protein	2.42	4	1.24E-04
GOX0880	Hypothetical protein GOX0880	3.00	4	1.54E-02
GOX0886	Hypothetical protein GOX0886	3.46	4	1.15E-03
GOX0890	Hypothetical protein GOX0890	9.60	4	2.78E-03
GOX0915	Hypothetical protein GOX0915	2.94	4	9.15E-03
GOX0946	Putative oxidoreductase	2.29	4	2.93E-03
GOX0952	Flagellar basal body P-ring biosynthesis protein FlgA	2.79	4	2.03E-04
GOX0953	Flagellar basal body rod protein FlgG	3.54	4	1.01E-04
GOX0954	Flagellar basal-body rod protein FlgF	4.26	4	1.39E-03
GOX0960	Protein with GGDEF and EAL domain	2.32	4	3.49E-05
GOX0973	Outer membrane channel lipoprotein	3.39	4	1.41E-04
GOX0996	Transposase (class II)	2.34	4	1.70E-03
GOX1024	Heat shock protein 90	2.63	4	1.72E-05
GOX1025	Flagellar hook-associated protein FlgL	3.69	4	4.32E-03
GOX1026	Flagellar hook-associated protein 1 FlgK	2.76	4	4.93E-03
GOX1027	Flagellar hook protein FlgE	2.83	4	2.24E-03
GOX1106	Alanine tRNA	2.91	4	5.58E-03
GOX1107	O-antigen biosynthesis protein RfbC	3.16	4	8.54E-04
GOX1131	Pyrroline-5-carboxylate reductase	2.17	4	1.40E-04
GOX1132	Hypothetical protein GOX1132	3.01	4	1.47E-03
GOX1190	Glucose-1-phosphatase	2.07	4	3.58E-03
GOX1239	Hypothetical protein GOX1239	2.32	4	3.15E-03
GOX1248	Hypothetical protein GOX1248	2.28	4	1.42E-03
GOX1273	Hypothetical protein GOX1273	2.26	4	1.64E-03
GOX1302	Paraquat-inducible protein A	2.16	4	2.75E-03
GOX1322	Transposase (class I)	2.25	4	1.35E-02
GOX1329	Small heat shock protein	5.29	4	3.22E-04
GOX1355	Hypothetical protein GOX1355	2.27	4	1.02E-02
GOX1359	Excinuclease ABC subunit A	2.59	4	2.41E-03
GOX1414	Chaperone protein DnaJ	2.18	4	5.18E-03
GOX1424	Hypothetical protein GOX1424	2.26	4	4.51E-03
GOX1442	Hypothetical protein GOX1442	8.96	4	7.48E-04
GOX1445	Leucine tRNA	2.70	4	5.83E-03
GOX1462	Putative oxidoreductase	2.69	4	5.10E-03
GOX1463	ATP-dependent Clp protease, ATP-binding subunit ClpV	3.42	4	1.09E-03
GOX1500	Hypothetical protein GOX1500	4.07	4	3.07E-04

GOX1501	Hypothetical protein GOX1501	3.88	4	5.38E-06
GOX1521	Hypothetical protein GOX1521	2.07	4	1.24E-03
GOX1525	Flagellar biosynthetic protein FliQ	2.18	4	2.99E-03
GOX1526	Flagellar hook-basal body protein FleE	2.55	4	6.27E-04
GOX1527	Flagellar basal body rod protein FlgC	2.65	4	3.05E-03
GOX1528	Flagellar basal-body rod protein FlgB	3.41	4	6.18E-03
GOX1549	Methyl-accepting chemotaxis protein	2.06	4	6.42E-04
GOX1550	Chemotaxis protein CheX	2.32	4	3.27E-04
GOX1551	Chemotaxis protein CheY	2.16	4	7.08E-05
GOX1576	Transposase (class II)	2.70	4	2.28E-03
GOX1577	ATP-dependent Clp protease ATP-binding subunit ClpB	2.82	4	1.08E-05
GOX1578	Hypothetical protein GOX1578	2.92	4	1.46E-03
GOX1613	Protein with GGDEF and EAL domain	3.78	4	1.86E-03
GOX1617	Hypothetical protein GOX1617	2.32	4	3.64E-04
GOX1636	5-Aminolevulinate synthase	4.60	4	1.55E-03
GOX1654	Hypothetical protein GOX1654	2.39	4	4.40E-04
GOX1664	Recombination factor protein RarA	2.22	4	2.16E-03
GOX1688	Peptidoglycan-associated lipoprotein	3.06	4	1.22E-06
GOX1697	Hypothetical protein GOX1697	2.44	4	5.89E-03
GOX1698	Aminopeptidase	2.00	4	8.92E-03
GOX1722	Arginine tRNA	2.74	2	8.23E-04
GOX1742	Hypothetical protein GOX1742	2.37	4	9.42E-03
GOX1745	Hypothetical protein GOX1745	2.13	4	2.59E-03
GOX1752	Deoxyguanosinetriphosphate triphosphohydrolase	2.27	4	1.03E-04
GOX1768	Alkylated DNA repair protein AlkB	2.22	4	3.84E-03
GOX1773	Putative LacX protein	3.29	4	1.92E-03
GOX1774	Putative ATP-sensitive potassium channel protein	4.03	4	1.78E-04
GOX1779	Putative LysM domain protein	6.93	4	3.03E-05
GOX1841	Hypothetical protein GOX1841	3.32	4	2.38E-04
GOX1858	Hypothetical protein GOX1858	2.02	4	6.72E-04
GOX1863	Hypothetical protein GOX1863	3.42	4	2.94E-04
GOX1864	Protoheme IX farnesyltransferase	2.97	4	1.63E-03
GOX1870	Hypothetical protein GOX1870	2.32	4	3.20E-02
GOX1875	Hypothetical protein GOX1875	2.05	4	1.21E-03
GOX1883	Porphobilinogen deaminase	2.13	4	1.06E-03
GOX1895	Hypothetical protein GOX1895	4.12	4	1.45E-03
GOX1896	Coproporphyrinogen III oxidase	6.43	4	1.73E-03
GOX1898	Hypothetical protein GOX1898	2.08	4	1.19E-03
GOX1900	Putative carboxymethylenebutenolidase	2.09	4	1.63E-02
GOX1911	Cytochrome bo_3 ubiquinol oxidase subunit II	2.82	4	1.63E-03

GOX1912	Cytochrome bo_3 ubiquinol oxidase subunit I	2.70	4	1.05E-02
GOX1913	Cytochrome bo_3 ubiquinol oxidase subunit III	3.56	4	2.53E-05
GOX1914	Cytochrome bo_3 ubiquinol oxidase subunit IV	3.81	4	4.04E-03
GOX1917	ATP-dependent DNA helicase	2.12	4	1.52E-02
GOX1923	Hypothetical protein GOX1923	2.06	4	1.58E-03
GOX1928	Hypothetical protein GOX1928	2.94	4	7.39E-10
GOX1942	Hypothetical protein GOX1942	2.25	4	8.45E-04
GOX1951	Hypothetical protein GOX1951	2.42	4	3.61E-03
GOX1953	5-Methylcytosine-specific restriction enzyme	7.10	4	3.92E-04
GOX1988	Pyridoxamine 5'-phosphate oxidase	5.54	4	6.45E-04
GOX1992	Osmotically inducible protein C. peroxyredoxin	2.73	4	1.53E-05
GOX1995	Hypothetical protein GOX1995	2.52	4	1.60E-03
GOX2051	Hypothetical protein GOX2051	2.52	4	2.42E-03
GOX2052	Hypothetical protein GOX2052	2.83	4	6.38E-03
GOX2053	Hypothetical protein GOX2053	2.34	4	3.39E-02
GOX2063	Hypothetical protein GOX2063	2.38	4	1.79E-04
GOX2066	Glutaminase	8.58	4	1.26E-03
GOX2069	Transcriptional regulator. DeoR family	2.94	4	1.38E-03
GOX2152	Hypothetical protein GOX2152	2.58	4	6.82E-04
GOX2153	Hypothetical protein GOX2153	2.63	4	1.96E-03
GOX2163	Cold shock protein	3.04	4	8.24E-05
GOX2165	Transposase (class II)	2.11	4	9.00E-03
GOX2167	F1Fo ATP synthase subunit beta	2.81	4	4.36E-03
GOX2168	F1Fo ATP synthase subunit epsilon	3.14	4	3.49E-03
GOX2169	F1Fo ATP synthase subunit q	2.79	4	4.94E-03
GOX2170	F1Fo ATO synthase subunit r	3.13	4	1.39E-02
GOX2171	F1Fo ATP synthase subunit a	3.30	4	7.59E-03
GOX2172	F1Fo ATP synthase subunit c	2.99	4	7.50E-04
GOX2173	F1Fo ATP synthase subunit b	2.64	4	6.25E-03
GOX2174	F1Fo ATP synthase subunit alpha	2.38	4	8.40E-03
GOX2199	Probable myosin-crossreactive antigen	5.62	4	4.82E-05
GOX2200	Probable myosin-crossreactive antigen	5.37	4	2.69E-07
GOX2205	Hypothetical protein GOX2205	2.02	4	8.34E-03
GOX2207	Methylenetetrahydrofolate reductase	2.20	4	1.19E-02
GOX2209	Truncated transposase (class I)	2.05	4	2.18E-02
GOX2225	Thiamine biosynthesis protein ThiC	2.10	4	1.21E-04
GOX2246	Hypothetical protein GOX2246	3.52	4	8.30E-05
GOX2252	Hypothetical protein GOX2252	2.60	4	1.28E-04
GOX2253	Putative oxidoreductase	2.46	4	6.82E-05

GOX2272	Membrane-bound dipeptidase	2.51	4	1.98E-04
GOX2274	CDP-diacylglycerol--glycerol-3-phosphate 3-phosphatidyltransferase	2.83	4	5.93E-05
GOX2278	Hypothetical protein GOX2278	2.53	4	5.58E-05
GOX2308	Delta-aminolevulinic acid dehydratase	3.08	4	2.77E-07
GOX2311	Hypothetical protein GOX2311	2.03	4	1.39E-03
GOX2326	Hypothetical protein GOX2326	3.03	4	2.69E-04
GOX2366	Hypothetical protein GOX2366	2.04	3	1.48E-02
GOX2373	Protein of Riske non-heme iron oxygenase family. putative ring-hydroxylating dioxygenase	3.72	4	1.79E-03
GOX2379	Hypothetical protein GOX2379	3.62	4	3.45E-04
GOX2397	Small heat shock protein	2.32	4	4.25E-04
GOX2406	RNA polymerase sigma factor E (sigma-24)	2.53	4	3.37E-03
GOX2409	ABC transporter. cytochrome bd biogenesis CydD	2.26	4	4.23E-06
GOX2410	ABC transporter. cytochrome bd biogenesis CydC	2.48	4	3.04E-03
GOX2413	Hypothetical protein GOX2413	3.24	4	3.29E-04
GOX2455	Putative phage-related protein	2.55	4	3.56E-03
GOX2457	Phage DNA Packaging Protein	2.75	4	6.38E-04
GOX2461	Hypothetical protein GOX2461	2.19	3	7.04E-03
GOX2470	Hypothetical protein GOX2470	2.54	4	4.78E-03
GOX2471	Transcriptional regulator. XRE family	2.32	4	9.96E-03
GOX2486	Cyteine tRNA	2.54	4	1.21E-03
GOX2487	Outer membrane protein TolC	3.80	4	7.60E-04
GOX2488	Hypothetical protein GOX2488	2.35	4	1.60E-04
GOX2500	Formamidopyrimidine-DNA glycosylase	2.13	4	1.09E-03
GOX2520	Hypothetical protein GOX2520	4.15	4	1.04E-03
GOX2646	DNA integration/recombination/invertion protein	3.15	4	2.08E-03
GOX2647	Hydroxyacylglutathione hydrolase	2.15	4	1.51E-05
GOX2659	Transposase	2.38	4	9.18E-04
GOX2675	Transposase	2.47	4	3.08E-04
GOX2684	NAD(P)H-dependent 2-cyclohexen-1-one reductase	3.17	4	6.71E-05
GOX2685	Transposase	2.77	4	2.06E-03
GOX2699	Hypothetical protein GOX2699	2.17	4	1.72E-05
GOX2719	Transposase	10.98	4	5.65E-05
GOX2720	Hypothetical protein GOX2720	12.34	4	2.03E-04
GOX2733	Hypothetical protein GOX2733	2.00	4	7.37E-03
GOX2734	Hypothetical protein GOX2734	2.07	4	1.12E-02

Oxygen limitation versus oxygen saturation; mRNA ratio of 271 genes ≤ 0.5

Gene	Annotation	mRNA ratio	n	*p*-value
GOX0013	Hypothetical protein GOX0013	0.15	4	5.55E-05
GOX0024	Undecaprenyl pyrophosphate phosphatase	0.40	4	2.22E-03
GOX0035	Hypothetical protein GOX0035	0.42	4	3.68E-03
GOX0036	Enoyl[acyl-carrier-protein] reductase	0.41	4	2.37E-03
GOX0039	Putative hemagglutinin-related protein	0.42	4	3.20E-03
GOX0074	Elongation factor Ts	0.29	4	1.49E-03
GOX0075	30SRibosomal protein S2	0.27	4	1.44E-04
GOX0088	Trigger factor	0.40	4	7.07E-04
GOX0103	Carboxypeptidase-related protein	0.23	4	1.23E-04
GOX0105	Elongation factor G	0.31	4	6.08E-05
GOX0106	50S Ribosomal protein L28	0.28	4	3.11E-04
GOX0115	3-Oxoacyl-[acyl-carrier-protein] synthase	0.40	4	2.01E-03
GOX0116	Fatty acid/phospholipid synthesis protein	0.24	4	2.87E-03
GOX0117	50S Ribosomal protein L32	0.37	4	5.93E-04
GOX0132	Transcriptional regulator	0.27	4	1.22E-06
GOX0140	50SRibosomal protein L27	0.44	4	5.89E-04
GOX0143	Hypothetical protein GOX0143	0.45	4	3.59E-03
GOX0145	Glucose-6-phosphate 1-dehydrogenase	0.45	4	4.46E-05
GOX0190	Aspartate aminotransferase A	0.47	4	7.33E-06
GOX0191	3-Isopropylmalate dehydrogenase	0.35	4	4.03E-04
GOX0192	3-Isopropylmalate dehydratase. small subunit	0.32	4	1.80E-04
GOX0193	Isopropylmalate isomerase large subunit	0.24	4	4.42E-04
GOX0194	50S Ribosomal protein L19	0.28	4	2.52E-04
GOX0195	tRNA (Guanine-N(1)-)-methyltransferase	0.27	4	2.11E-04
GOX0196	30S Ribosomal protein S16	0.36	4	4.06E-04
GOX0197	Signal recognition particle protein	0.34	4	8.69E-04
GOX0200	ATP-dependent RNA helicase	0.10	4	1.38E-04
GOX0207	TonB-dependent outer membrane receptor	0.18	4	3.56E-04
GOX0213	Biotin carboxylase	0.46	4	1.02E-04
GOX0254	Putative Fe-S-cluster redox enzyme	0.44	4	1.65E-03
GOX0262	Phenylalanyl-tRNA synthetase alpha chain	0.45	4	1.72E-03
GOX0263	50S Ribosomal protein L20	0.34	4	1.89E-04
GOX0264	LSU Ribosomal protein L35P	0.47	4	1.05E-03
GOX0265	Membrane-bound glucose dehydrogenase (PQQ)	0.50	4	1.97E-05
GOX0304	50S Ribosomal protein L9	0.35	4	8.21E-04
GOX0305	30S Ribosomal protein S18	0.38	4	1.89E-04
GOX0306	SSU Ribosomal protein S6P	0.34	4	1.38E-03
GOX0321	Carbamoyl phosphate synthase small subunit	0.30	4	9.80E-05
GOX0322	Carbamoyl phosphate synthase large subunit	0.32	4	4.33E-05
GOX0326	Hypothetical protein GOX0326	0.35	4	1.51E-04
GOX0345	Ribonuclease HII	0.41	4	1.61E-04

GOX0352	Hypothetical protein GOX0352	0.36	4	8.60E-04
GOX0354	Putative sugar/polyol transporter	0.12	4	9.11E-04
GOX0355	LSU Ribosomal protein L17P	0.36	4	3.03E-03
GOX0356	RNA polymerase subunit alpha	0.37	4	2.83E-03
GOX0357	30S Ribosomal protein S11	0.37	4	6.30E-03
GOX0359	Adenylate kinase	0.39	4	1.77E-03
GOX0360	Preprotein translocase subunit SecY	0.39	4	5.58E-03
GOX0361	LSU Ribosomal protein L15P	0.45	4	2.28E-02
GOX0362	LSU Ribosomal protein L30P	0.37	4	4.83E-03
GOX0363	30S Ribosomal protein S5	0.29	4	1.57E-03
GOX0364	50S Ribosomal protein L18	0.25	4	4.10E-03
GOX0365	50S Ribosomal protein L6	0.27	4	4.85E-04
GOX0366	30S Ribosomal protein S8	0.27	4	5.51E-03
GOX0367	30S Ribosomal protein S14	0.42	4	4.48E-03
GOX0368	50S Ribosomal protein L5	0.16	4	7.52E-04
GOX0369	LSU Ribosomal protein L24P	0.29	4	9.99E-04
GOX0370	LSU Ribosomal protein L14P	0.31	4	1.85E-03
GOX0371	SSU Ribosomal protein S17P	0.40	4	3.15E-05
GOX0372	LSU Ribosomal protein L29P	0.35	4	6.62E-04
GOX0373	50S Ribosomal protein L16	0.26	4	3.79E-04
GOX0374	30S Ribosomal protein S3	0.25	4	3.44E-03
GOX0375	50S Ribosomal protein L22	0.26	4	3.08E-03
GOX0376	SSU Ribosomal protein S19P	0.24	4	1.11E-03
GOX0377	50S Ribosomal protein L2	0.25	4	1.12E-04
GOX0378	LSU Ribosomal protein L23P	0.30	4	2.28E-04
GOX0379	50S Ribosomal protein L4	0.28	4	1.91E-04
GOX0380	50S Ribosomal protein L3	0.30	4	3.61E-05
GOX0381	30S Ribosomal protein S10	0.26	4	2.86E-03
GOX0382	Elongation factor Tu	0.30	4	2.28E-03
GOX0383	30S Ribosomal protein S7	0.16	4	2.46E-03
GOX0384	30S Ribosomal protein S12	0.22	4	1.13E-05
GOX0385	RNA polymerase. subunit beta'	0.40	4	3.14E-03
GOX0386	RNA polymerase. subunit beta	0.43	4	6.94E-03
GOX0387	50S Ribosomal protein L7/L12	0.21	4	2.90E-04
GOX0388	LSU Ribosomal protein L10P	0.20	4	5.22E-04
GOX0389	50S Ribosomal protein L1	0.31	4	3.90E-03
GOX0390	50S Ribosomal protein L11	0.43	4	1.37E-03
GOX0392	Putative transport transmembrane protein	0.46	4	7.36E-04
GOX0393	Putative transport transmembrane protein	0.43	4	5.02E-04
GOX0396	DNA recombination protein RmuC-like protein	0.40	4	4.71E-03
GOX0397	Hypothetical protein GOX0397	0.46	4	1.56E-04
GOX0404	Hypothetical protein GOX0404	0.13	4	1.57E-04
GOX0405	TonB-dependent outer membrane receptor	0.09	4	1.69E-04

GOX0413	Acetyl-coenzyme A synthetase	0.48	4	5.74E-03
GOX0415	Putative transport protein	0.30	4	2.99E-04
GOX0416	Protein-tyrosine phosphatase	0.33	4	1.17E-04
GOX0435	Acetyl-CoA carboxylase biotin carboxylase subunit	0.49	4	4.09E-04
GOX0440	Ornithine decarboxylase	0.31	4	9.08E-04
GOX0451	30S Ribosomal protein S9	0.22	4	1.89E-04
GOX0452	50S Ribosomal protein L13	0.31	4	1.04E-02
GOX0474	Hypothetical protein GOX0474	0.48	4	1.85E-02
GOX0497	Hypothetical protein GOX0497	0.41	4	2.76E-04
GOX0512	Amino acid transport protein	0.32	4	1.31E-03
GOX0513	Transcriptional regulator. AsnC family	0.39	4	1.05E-03
GOX0515	Hypothetical protein GOX0515	0.18	4	1.00E-04
GOX0516	Uncharacterized PQQ-dependent dehydrogenase 4	0.49	4	5.09E-03
GOX0522	Transcriptional regulator	0.33	4	2.09E-03
GOX0524	TonB-dependent outer membrane receptor	0.13	4	4.00E-04
GOX0562	Putative siderophore receptor protein	0.32	4	1.67E-03
GOX0568	Hypothetical protein GOX0568	0.33	4	9.58E-05
GOX0596	30S Ribosomal protein S1	0.41	4	5.43E-05
GOX0599	Hypothetical protein GOX0599	0.39	4	6.00E-04
GOX0600	Hypothetical protein GOX0600	0.40	4	6.32E-03
GOX0610	Hypothetical protein GOX0610	0.47	4	1.95E-03
GOX0689	Probable outer membrane efflux lipoprotein	0.41	4	8.87E-04
GOX0690	Acriflavin resistance protein B (mulitdrug efflux system)	0.40	4	7.85E-04
GOX0691	Acriflavin resistance protein A (mulitdrug efflux system)	0.39	4	2.28E-04
GOX0699	L-Asparagine permease	0.16	4	1.95E-13
GOX0745	Hypothetical protein GOX0745	0.29	4	2.31E-03
GOX0748	Aldose 1-epimerase	0.35	4	3.49E-06
GOX0758	Porin	0.19	4	2.03E-03
GOX0767	Hypothetical protein GOX0767	0.49	4	3.71E-03
GOX0771	Ferric uptake regulation protein	0.49	4	3.24E-04
GOX0772	Transcriptional regulator, Ros/MucR family	0.16	4	9.12E-05
GOX0774	Ribosomal-protein-alanine acetyltransferase	0.49	3	3.70E-02
GOX0775	Hypothetical protein GOX0775	0.46	4	4.78E-03
GOX0778	Two component sensor histidine kinase	0.42	4	6.51E-03
GOX0797	Hypothetical protein GOX0797	0.46	4	5.38E-04
GOX0805	Hypothetical protein GOX0805	0.45	4	5.84E-04
GOX0806	Hypothetical protein GOX0806	0.34	4	3.92E-03
GOX0807	Hypothetical protein GOX0807	0.33	4	6.11E-03
GOX0823	Threonyl-tRNA synthetase	0.48	4	3.21E-04
GOX0827	Hypothetical protein GOX0827	0.46	4	6.29E-05
GOX0828	Hypothetical protein GOX0828	0.49	4	1.05E-04
GOX0834	Putative oxidoreductase	0.50	4	2.40E-03
GOX0835	Adenine phosphoribosyltransferase	0.30	4	1.65E-03

GOX0845	Hypothetical protein GOX0845	0.44	4	1.52E-03
GOX0846	Hypothetical protein GOX0846	0.36	4	1.13E-03
GOX0849	NADPH-dependent L-sorbose reductase	0.44	4	2.14E-03
GOX0854	D-Sorbitol dehydrogenase subunit SldA	0.10	4	4.81E-06
GOX0855	D-Sorbitol dehydrogenase subunit SldB	0.10	4	6.38E-05
GOX0859	Shikimate 5-dehydrogenase	0.31	4	3.82E-04
GOX0866	S-Adenosylmethionine synthetase	0.18	4	1.16E-03
GOX0867	SAM-dependent methyltransferase	0.21	4	1.27E-04
GOX0868	Electron transfer flavoprotein-ubiquinone oxidoreductase/ putative oxidoreductase	0.28	4	1.40E-04
GOX0901	Xanthine/uracil permease	0.43	4	1.81E-04
GOX0902	Hypothetical protein GOX0902	0.45	4	7.20E-06
GOX0903	Hypothetical protein GOX0903	0.46	4	1.44E-04
GOX0905	Putative oxidoreductase	0.37	4	7.09E-04
GOX0907	TonB-dependent outer membrane receptor	0.23	4	1.36E-04
GOX0909	Thiol:disulfide interchange protein DsbD	0.45	4	9.81E-04
GOX0943	Hypothetical protein GOX0943	0.30	4	1.21E-07
GOX0944	Hypothetical protein GOX0944	0.42	4	5.39E-04
GOX0945	TonB-dependent outer membrane receptor	0.11	4	2.49E-04
GOX0969	Hypothetical protein GOX0969	0.32	4	3.62E-05
GOX0970	Outer membrane channel lipoprotein	0.49	4	1.46E-04
GOX0971	Cation efflux system protein CzcA	0.49	4	6.62E-04
GOX0972	Cation efflux system protein CzcB	0.44	4	1.21E-03
GOX0978	Bifunctional riboflavin biosynthesis protein RibD	0.33	4	2.03E-03
GOX0979	Riboflavin synthase subunit alpha	0.43	4	1.46E-03
GOX0980	3,4-Dihydroy-2-butanone 4-phosphate synthase/GTP cyclohydrolase II	0.35	4	2.31E-03
GOX0981	6,7-Dimethyl-8-ribityllumazine synthase	0.44	4	7.57E-04
GOX0986	Coenzyme PQQ synthesis protein B	0.37	4	3.42E-07
GOX0987	Coenzyme PQQ synthesis protein A	0.44	4	3.84E-03
GOX1003	Septum formation associated protein (Maf-like protein)	0.44	4	1.44E-03
GOX1015	TonB-dependent receptor of ferrichrome transport system	0.42	4	1.30E-03
GOX1017	TonB-dependent outer membrane receptor	0.11	4	6.32E-05
GOX1022	Transcriptional regulator	0.41	4	5.98E-03
GOX1029	Hypothetical protein GOX1029	0.47	4	4.09E-03
GOX1070	Transcription termination factor Rho	0.46	4	7.53E-03
GOX1087	Acetolactate synthase large subunit	0.34	4	2.64E-04
GOX1088	Acetolactate synthase 3 regulatory subunit	0.35	4	8.20E-05
GOX1089	Ketol-acid reductoisomerase	0.37	4	6.30E-04
GOX1090	S-Adenosylmethionine decarboxylase proenzyme	0.27	4	6.47E-04
GOX1091	Spermidine synthase	0.11	4	3.05E-04
GOX1108	Hypothetical protein GOX1108	0.49	4	6.79E-04
GOX1110	F_1F_o ATP synthase subunit b'	0.48	4	3.19E-03
GOX1111	F_1F_o ATP synthase subunit b	0.40	4	5.54E-03

GOX1114	Vitamin B12-dependent ribonucleotide reductase	0.31	4	1.10E-04
GOX1137	Probable lipopolysaccharide modification acyltransferase	0.44	4	1.43E-03
GOX1141	LSU Ribosomal protein L25P	0.31	4	2.32E-04
GOX1142	Peptidyl-tRNA hydrolase	0.31	4	7.95E-04
GOX1173	TonB-dependent outer membrane receptor	0.39	4	1.39E-03
GOX1174	Purine-cytosine permease	0.49	4	7.94E-03
GOX1179	Putative sugar uptake ABC transporter permease protein	0.44	4	2.94E-04
GOX1192	Transcriptional regulator, MarR/AsnC family	0.49	4	7.02E-03
GOX1197	Hypothetical protein GOX1197	0.22	4	6.10E-04
GOX1198	Sulfite reductase (Ferredoxin)	0.25	4	3.23E-04
GOX1199	Putative oxidoreductase	0.35	4	1.41E-03
GOX1230	Gluconate 2-dehydrogenase, cytochrome $_c$ subunit	0.23	4	3.24E-04
GOX1231	Gluconate 2-dehydrogenase alpha chain	0.19	4	1.27E-04
GOX1232	Gluconate 2-dehydrogenase gamma chain	0.26	4	2.41E-04
GOX1236	Ornithine carbamoyltransferase	0.33	4	8.54E-04
GOX1237	Acetylornithine aminotransferase	0.35	4	1.01E-03
GOX1244	Putative enolase-phosphatase	0.44	4	4.40E-04
GOX1245	Riboflavin kinase	0.45	4	3.41E-03
GOX1269	Hypothetical protein GOX1269	0.29	4	2.39E-04
GOX1282	Ribonuclease PH	0.48	4	3.82E-04
GOX1286	Hypothetical protein GOX1286	0.16	4	3.74E-04
GOX1287	Biopolymer transport ExbB protein	0.12	4	4.26E-04
GOX1288	Biopolymer transport ExbD protein	0.16	4	8.95E-06
GOX1289	Biopolymer transport ExbD protein	0.18	4	3.66E-04
GOX1290	Hypothetical protein GOX1290	0.39	4	3.61E-05
GOX1335	Aconitate hydratase	0.13	4	1.85E-04
GOX1336	Isocitrate dehydrogenase	0.17	4	2.05E-04
GOX1351	Putative isomerase	0.29	4	1.87E-04
GOX1365	ABC transporter permease protein	0.33	4	1.00E-05
GOX1366	ABC transporter ATP-binding protein	0.33	4	6.90E-06
GOX1381	Gluconolactonase	0.39	4	3.13E-04
GOX1392	Hypothetical protein GOX1392	0.49	4	2.92E-05
GOX1416	Porin B precursur	0.15	4	3.36E-04
GOX1418	Carbohydrate-selective porin	0.19	4	4.06E-05
GOX1432	NADP-D-sorbitol dehydrogenase	0.46	4	1.41E-03
GOX1436	Adenosine deaminase	0.44	4	3.91E-04
GOX1440	S-Adenosylmethionine:tRNA ribosyltransferase-isomerase	0.49	4	2.35E-03
GOX1455	ATP-dependent RNA helicase	0.27	4	3.89E-04
GOX1483	Capsule polysaccharide export protein	0.50	4	1.87E-04
GOX1490	Putative glycosyltransferase	0.50	4	1.09E-04
GOX1516	Fructose 1,6-bisphosphatase II	0.38	4	3.98E-03

GOX1542	Putative aluminum resistance protein	0.40	4	1.50E-04
GOX1543	Hypothetical protein GOX1543	0.43	4	1.11E-03
GOX1563	Hypothetical protein GOX1563	0.21	4	4.36E-03
GOX1567	DedA family protein	0.48	4	7.86E-04
GOX1569	Tricorn protease homolog	0.40	4	3.22E-04
GOX1572	Amino acid ABC transporter ATP-binding protein	0.43	4	3.87E-04
GOX1579	Hypothetical protein associated with nus operon	0.39	4	1.49E-03
GOX1642	Carboxypeptidase-related protein	0.20	4	6.54E-06
GOX1662	Hypothetical protein GOX1662	0.39	4	6.65E-03
GOX1671	O-Succinylhomoserine sulfhydrylase	0.29	4	4.11E-03
GOX1675	NADH dehydrogenase type II	0.37	4	1.12E-05
GOX1699	Hypothetical protein GOX1699	0.27	4	3.57E-04
GOX1703	Transketolase	0.47	4	8.92E-03
GOX1704	Bifunctional transaldolase/phosoglucose isomerase	0.44	4	1.63E-02
GOX1705	6-Phosphogluconate dehydrogenase-like protein	0.44	4	2.28E-02
GOX1736	Hypothetical protein GOX1736	0.47	4	3.20E-03
GOX1780	30S ribosomal protein S4	0.27	4	4.71E-04
GOX1781	Bacterial Peptide Chain Release Factor 3 (RF-3)	0.18	4	8.97E-04
GOX1796	TonB-dependent outer membrane receptor	0.45	4	4.86E-03
GOX1815	Phosphatidate cytidylyltransferase	0.45	4	1.11E-02
GOX1828	GTPase EngB	0.44	4	8.15E-05
GOX1829	Acetylglutamate kinase	0.49	4	2.11E-03
GOX1832	Succinyl-diaminopimelate desuccinylase	0.43	4	1.32E-03
GOX1851	Putative oxidoreductase	0.19	4	1.73E-04
GOX1852	Glutamate synthase	0.23	4	4.24E-04
GOX1857	Uncharacterized PQQ-containing dehydrogenase 1	0.12	4	1.34E-04
GOX1873	DNA mismatch repair protein	0.41	4	6.59E-04
GOX1903	TonB-dependent outer membrane receptor	0.12	4	9.50E-05
GOX1957	Putative thiol:disulfide interchange protein II	0.40	4	2.21E-05
GOX1971	Galactose-proton symporter	0.26	4	9.13E-04
GOX1972	Putative transport protein	0.27	4	9.18E-04
GOX1982	Hypothetical protein GOX1982	0.25	4	8.64E-05
GOX2010	1-Acyl-sn-glycerol-3-phosphate acyltransferase	0.40	3	4.54E-02
GOX2015	NAD(P)-dependent glucose 1-dehydrogenase	0.44	4	3.10E-03
GOX2028	Hypothetical protein GOX2028	0.17	4	1.27E-04
GOX2030	Chaperone protein DnaK	0.16	4	4.49E-03
GOX2039	Acyl-carrier-protein S-malonyltransferase	0.41	4	2.38E-03
GOX2041	Acyl carrier protein	0.47	4	8.08E-04
GOX2073	Formyltetrahydrofolate deformylase	0.39	4	3.07E-03
GOX2074	5-Methyltetrahydrofolate-S-homocysteine methyltransferase	0.41	4	7.53E-07
GOX2134	Peptidyl-dipeptidase DCP	0.40	4	5.01E-05
GOX2135	Hypothetical protein GOX2135	0.47	4	1.37E-05
GOX2136	Aminopeptidase	0.47	4	9.68E-04

GOX2142	Hypothetical protein GOX2142	0.45	4	3.90E-05
GOX2143	ABC transporter ATP-binding protein	0.38	4	1.16E-03
GOX2151	Hypothetical protein GOX2151	0.42	4	2.11E-03
GOX2187	Gluconate 5-dehydrogenase	0.44	4	5.90E-04
GOX2258	Putative phytoene synthase	0.45	4	3.67E-04
GOX2260	Squalene-hopene cyclase	0.42	4	4.83E-04
GOX2299	Adenylosuccinate lyase	0.49	4	2.73E-03
GOX2376	Putative aldehyde dehydrogenase	0.44	4	3.31E-03
GOX2401	Protein translocase subunit SecF	0.48	4	2.41E-04
GOX2402	Preprotein translocase subunit SecD	0.39	4	2.54E-03
GOX2491	Dihydroxy-acid dehydratase	0.35	4	1.81E-04
GOX2546	Replication protein A	0.42	4	3.86E-03
GOX2560	RND-type multidrug efflux pump, membrane permease	0.49	4	2.93E-03
GOX2561	RND-type multidrug efflux pump. outer membrane protein	0.50	2	1.16E-03
GOX2578	Putative isochorismatase	0.46	4	1.87E-03
GOX2580	Hypothetical protein GOX2580	0.42	4	3.27E-04
GOX2603	Replicator initiator RepC	0.42	4	6.97E-04
GOX2616	DotI	0.35	4	4.13E-03

Oxygen limitation versus oxygen saturation; respiration and energy metabolism; mRNA ratio of 24 genes ≥ 2.0; mRNA ratio of 9 genes ≤ 0.5

Gene	Annotation	mRNA ratio	n	*p*-value
GOX0278	Cytochrome *bd* ubiquinol oxidase subunit I	3.64	4	7.58E-05
GOX0310	NAD(P) transhydrogenase subunit alpha2	10.37	4	3.76E-04
GOX0311	NAD(P) transhydrogenase subunit alpha1	14.70	4	1.36E-03
GOX0312	NAD(P) transhydrogenase subunit beta	12.04	4	4.33E-04
GOX0313	Alcohol:NAD oxidoreductase	13.58	4	7.09E-04
GOX0564	Cytochrome *c*552	2.02	4	1.22E-03
GOX0565	Ubiquinol-cytochrome *c* oxidoreductase FeS protein	2.49	4	3.81E-03
GOX0566	Ubiquinol-cytochrome *c* oxidoreductase cytochrome *b*	2.20	4	1.29E-02
GOX0585	Cytochrome *c* subunit of aldehyde dehydrogenase	2.02	4	5.61E-04
GOX0586	Membrane-bound aldehyde dehydrogenase. small subunit	2.01	4	1.17E-03
GOX1911	Cytochrome bo_3 ubiquinol oxidase subunit II	2.82	4	1.63E-03
GOX1912	Cytochrome bo_3 ubiquinol oxidase subunit I	2.70	4	1.05E-02
GOX1913	Cytochrome bo_3 ubiquinol oxidase subunit III	3.56	4	2.53E-05
GOX1914	Cytochrome bo_3 ubiquinol oxidase subunit IV	3.81	4	4.04E-03
GOX2167	F_1F_o ATP synthase subunit beta	2.81	4	4.36E-03
GOX2168	F_1F_o ATP synthase subunit epsilon	3.14	4	3.49E-03
GOX2169	F_1F_o ATP synthase subunit q	2.79	4	4.94E-03
GOX2170	F_1F_o ATP synthase subunit r	3.13	4	1.39E-02
GOX2171	F_1F_o ATP synthase subunit a	3.30	4	7.59E-03
GOX2172	F_1F_o ATP synthase subunit c	2.99	4	7.50E-04

GOX2173	F_1F_o ATP synthase subunit b	2.64	4	6.25E-03
GOX2174	F_1F_o ATP synthase subunit alpha	2.38	4	8.40E-03
GOX2409	ABC transporter, cytochrome *bd* biogenesis CydD	2.26	4	4.23E-06
GOX2410	ABC transporter, cytochrome *bd* biogenesis CydC	2.48	4	3.04E-03
GOX0265	Membrane-bound glucose dehydrogenase (PQQ)	0.50	4	1.97E-05
GOX0854	D-Sorbitol dehydrogenase subunit SldA	0.10	4	4.81E-06
GOX0855	D-Sorbitol dehydrogenase subunit SldB	0.10	4	6.38E-05
GOX1110	F_1F_o ATP synthase subunit b'	0.48	4	3.19E-03
GOX1111	F_1F_o ATP synthase subunit b	0.40	4	5.54E-03
GOX1230	Gluconate 2-dehydrogenase. cytochrome c subunit	0.23	4	3.24E-04
GOX1231	Gluconate 2-dehydrogenase alpha chain	0.19	4	1.27E-04
GOX1232	Gluconate 2-dehydrogenase gamma chain	0.26	4	2.41E-04
GOX1675	NADH dehydrogenase type II	0.37	4	1.12E-05

Oxygen limitation versus oxygen saturation; metabolism; mRNA ratio of 44 genes ≥ 2.0; mRNA ratio of 79 genes ≤ 0.5

Gene	**Annotation**	**mRNA ratio**	**n**	***p*-value**
GOX0443	Molybdopterin (MPT) converting factor, subunit 2	2.27	4	3.28E-04
GOX0444	Bifunctional molybdenum cofactor biosynthesis protein (Molybdopterin-guanine dinucleotide biosynthesis protein A and MoaD)	2.28	4	2.48E-03
GOX0445	Molybdenum cofactor biosynthesis protein C	3.07	4	5.58E-05
GOX0573	Metallo-beta-lactamase superfamily protein	4.81	4	1.68E-03
GOX0607	D-Aalanyl-D-alanine carboxypeptidase	2.51	4	7.26E-06
GOX0618	Hemolysin-related protein	2.46	4	1.50E-02
GOX0746	FAD-dependent monooxygenase	2.03	4	5.97E-04
GOX0747	Serine O-acetyltransferase CysE	2.05	4	9.70E-03
GOX0762	Thioredoxin	2.10	4	3.79E-04
GOX0874	Ferrochelatase	2.21	4	2.71E-04
GOX0875	AtsE protein	2.42	4	1.24E-04
GOX0996	Transposase (class II)	2.34	4	1.70E-03
GOX1107	O-antigen biosynthesis protein RfbC	3.16	4	8.54E-04
GOX1131	Pyrroline-5-carboxylate reductase	2.17	4	1.40E-04
GOX1190	Glucose-1-phosphatase	2.07	4	3.58E-03
GOX1322	Transposase (class I)	2.25	4	1.35E-02
GOX1576	Transposase (class II)	2.70	4	2.28E-03
GOX1636	5-Aminolevulinate synthase	4.60	4	1.55E-03
GOX1688	Peptidoglycan-associated lipoprotein	3.06	4	1.22E-06
GOX1698	Aminopeptidase	2.00	4	8.92E-03
GOX1752	Deoxyguanosinetriphosphate triphosphohydrolase	2.27	4	1.03E-04
GOX1864	Protoheme IX farnesyltransferase	2.97	4	1.63E-03
GOX1883	Porphobilinogen deaminase	2.13	4	1.06E-03
GOX1896	Coproporphyrinogen III oxidase	6.43	4	1.73E-03
GOX1953	5-Methylcytosine-specific restriction enzyme	7.10	4	3.92E-04

GOX1988	Pyridoxamine 5'-phosphate oxidase	5.54	4	6.45E-04
GOX2066	Glutaminase	8.58	4	1.26E-03
GOX2165	Transposase (class II)	2.11	4	9.00E-03
GOX2207	Methylenetetrahydrofolate reductase	2.20	4	1.19E-02
GOX2209	Truncated transposase (class I)	2.05	4	2.18E-02
GOX2225	Thiamine biosynthesis protein ThiC	2.10	4	1.21E-04
GOX2272	Membrane-bound dipeptidase	2.51	4	1.98E-04
GOX2274	CDP-diacylglycerol--glycerol-3-phosphate 3-phosphatidyltransferase	2.83	4	5.93E-05
GOX2308	Delta-aminolevulinic acid dehydratase	3.08	4	2.77E-07
GOX2373	Protein of Riske non-heme iron oxygenase family. putative ring-hydroxylating dioxygenase	3.72	4	1.79E-03
GOX2457	Phage DNA Packaging Protein	2.75	4	6.38E-04
GOX2487	Outer membrane protein TolC	3.80	4	7.60E-04
GOX2500	Formamidopyrimidine-DNA glycosylase	2.13	4	1.09E-03
GOX2647	Hydroxyacylglutathione hydrolase	2.15	4	1.51E-05
GOX2659	Transposase	2.38	4	9.18E-04
GOX2675	Transposase	2.47	4	3.08E-04
GOX2684	NAD(P)H-dependent 2-cyclohexen-1-one reductase	3.17	4	6.71E-05
GOX2685	Transposase	2.77	4	2.06E-03
GOX2719	Transposase	10.98	4	5.65E-05
GOX0024	Undecaprenyl pyrophosphate phosphatase	0.40	4	2.22E-03
GOX0036	Enoyl[acyl-carrier-protein] reductase	0.41	4	2.37E-03
GOX0103	Carboxypeptidase-related protein	0.23	4	1.23E-04
GOX0115	3-Oxoacyl-[acyl-carrier-protein] synthase	0.40	4	2.01E-03
GOX0116	Fatty acid/phospholipid synthesis protein	0.24	4	2.87E-03
GOX0145	Glucose-6-phosphate 1-dehydrogenase	0.45	4	0.00
GOX0190	Aspartate aminotransferase A	0.47	4	7.33E-06
GOX0191	3-Isopropylmalate dehydrogenase	0.35	4	4.03E-04
GOX0192	3-Isopropylmalate dehydratase, small subunit	0.32	4	1.80E-04
GOX0193	Isopropylmalate isomerase large subunit	0.24	4	4.42E-04
GOX0207	TonB-dependent outer membrane receptor	0.18	4	3.56E-04
GOX0213	Biotin carboxylase	0.46	4	1.02E-04
GOX0321	Carbamoyl phosphate synthase small subunit	0.30	4	9.80E-05
GOX0322	Carbamoyl phosphate synthase large subunit	0.32	4	4.33E-05
GOX0359	Adenylate kinase	0.39	4	1.77E-03
GOX0405	TonB-dependent outer membrane receptor	0.09	4	1.69E-04
GOX0413	Acetyl-coenzyme A synthetase	0.48	4	5.74E-03
GOX0416	Protein-tyrosine phosphatase	0.33	4	1.17E-04
GOX0435	Acetyl-CoA carboxylase biotin carboxylase subunit	0.49	4	4.09E-04
GOX0440	Ornithine decarboxylase	0.31	4	9.08E-04
GOX0524	TonB-dependent outer membrane receptor	0.13	4	4.00E-04
GOX0690	Acriflavin resistance protein B (mulitdrug efflux system)	0.40	4	7.85E-04

GOX0691	Acriflavin resistance protein A (mulitdrug efflux system)	0.39	4	2.28E-04
GOX0748	Aldose 1-epimerase	0.35	4	3.49E-06
GOX0835	Adenine phosphoribosyltransferase	0.30	4	1.65E-03
GOX0849	NADPH-dependent L-sorbose reductase	0.44	4	2.14E-03
GOX0859	Shikimate 5-dehydrogenase	0.31	4	3.82E-04
GOX0866	S-Adenosylmethionine synthetase	0.18	4	1.16E-03
GOX0867	SAM-dependent methyltransferase	0.21	4	1.27E-04
GOX0909	Thiol:disulfide interchange protein DsbD	0.45	4	9.81E-04
GOX0978	Bifunctional riboflavin biosynthesis protein RibD	0.33	4	2.03E-03
GOX0979	Riboflavin synthase subunit alpha	0.43	4	1.46E-03
GOX0980	3,4-Dihydroy-2-butanone 4-phosphate synthase/GTP cyclohydrolase II	0.35	4	2.31E-03
GOX0981	6,7-Dimethyl-8-ribityllumazine synthase	0.44	4	7.57E-04
GOX0986	Coenzyme PQQ synthesis protein B	0.37	4	3.42E-07
GOX0987	Coenzyme PQQ synthesis protein A	0.44	4	3.84E-03
GOX1003	Septum formation associated protein (Maf-like protein)	0.44	4	1.44E-03
GOX1087	Acetolactate synthase large subunit	0.34	4	2.64E-04
GOX1088	Acetolactate synthase 3 regulatory subunit	0.35	4	8.20E-05
GOX1089	Ketol-acid reductoisomerase	0.37	4	6.30E-04
GOX1090	S-Adenosylmethionine decarboxylase proenzyme	0.27	4	6.47E-04
GOX1091	Spermidine synthase	0.11	4	3.05E-04
GOX1114	Vitamin B12-dependent ribonucleotide reductase	0.31	4	1.10E-04
GOX1137	Probable lipopolysaccharide modification acyltransferase	0.44	4	1.43E-03
GOX1198	Sulfite reductase (Ferredoxin)	0.25	4	3.23E-04
GOX1236	Ornithine carbamoyltransferase	0.33	4	8.54E-04
GOX1237	Acetylornithine aminotransferase	0.35	4	1.01E-03
GOX1245	Riboflavin kinase	0.45	4	3.41E-03
GOX1335	Aconitate hydratase	0.13	4	1.85E-04
GOX1336	Isocitrate dehydrogenase	0.17	4	2.05E-04
GOX1381	Gluconolactonase	0.39	4	3.13E-04
GOX1432	NADP-D-sorbitol dehydrogenase	0.46	4	1.41E-03
GOX1436	Adenosine deaminase	0.44	4	3.91E-04
GOX1516	Fructose 1,6-bisphosphatase II	0.38	4	3.98E-03
GOX1567	DedA family protein	0.48	4	7.86E-04
GOX1569	Tricorn protease homolog	0.40	4	3.22E-04
GOX1642	Carboxypeptidase-related protein	0.20	4	6.54E-06
GOX1671	O-Succinylhomoserine sulfhydrylase	0.29	4	4.11E-03
GOX1703	Transketolase	0.47	4	8.92E-03
GOX1704	Bifunctional transaldolase/phosoglucose isomerase	0.44	4	1.63E-02
GOX1705	6-Phosphogluconate dehydrogenase-like protein	0.44	4	2.28E-02
GOX1815	Phosphatidate cytidylyltransferase	0.45	4	1.11E-02
GOX1828	GTPase EngB	0.44	4	8.15E-05

GOX1829	Acetylglutamate kinase	0.49	4	2.11E-03
GOX1832	Succinyl-diaminopimelate desuccinylase	0.43	4	1.32E-03
GOX1852	Glutamate synthase	0.23	4	4.24E-04
GOX2010	1-Acyl-sn-glycerol-3-phosphate acyltransferase	0.40	3	4.54E-02
GOX2015	NAD(P)-dependent glucose 1-dehydrogenase	0.44	4	3.10E-03
GOX2039	Acyl-carrier-protein S-malonyltransferase	0.41	4	2.38E-03
GOX2041	Acyl carrier protein	0.47	4	8.08E-04
GOX2073	Formyltetrahydrofolate deformylase	0.39	4	3.07E-03
GOX2074	5-Methyltetrahydrofolate-S-homocysteine methyltransferase	0.41	4	7.53E-07
GOX2134	Peptidyl-dipeptidase DCP	0.40	4	5.01E-05
GOX2136	Aminopeptidase	0.47	4	9.68E-04
GOX2187	Gluconate 5-dehydrogenase	0.44	4	5.90E-04
GOX2260	Squalene-hopene cyclase	0.42	4	4.83E-04
GOX2299	Adenylosuccinate lyase	0.49	4	2.73E-03
GOX2491	Dihydroxy-acid dehydratase	0.35	4	1.81E-04
GOX2616	DotI	0.35	4	4.13E-03

Oxygen limitation versus oxygen saturation; regulation and signal transduction; mRNA ratio of 8 genes ≥ 2.0; mRNA ratio of 8 genes ≤ 0.5

Gene	Annotation	mRNA ratio	n	*p*-value
GOX0135	Transcriptional regulator, Ros/MucR family	2.80	4	3.66E-03
GOX0506	RNA polymerase factor sigma factor H (sigma-32)	4.04	4	3.77E-05
GOX1613	Protein with GGDEF and EAL domain	3.78	4	1.86E-03
GOX0683	Protein with GGDEF domain	2.13	4	6.88E-03
GOX2069	Transcriptional regulator, DeoR family	2.94	4	1.38E-03
GOX2406	RNA polymerase sigma factor E (sigma-24)	2.53	4	3.37E-03
GOX2471	Transcriptional regulator, XRE family	2.32	4	9.96E-03
GOX0960	Protein with GGDEF and EAL domain	2.32	4	3.49E-05
GOX0132	Transcriptional regulator	0.27	4	1.22E-06
GOX0513	Transcriptional regulator, AsnC family	0.39	4	1.05E-03
GOX0522	Transcriptional regulator	0.33	4	2.09E-03
GOX0771	Ferric uptake regulation protein	0.49	4	3.24E-04
GOX0772	Transcriptional regulator, Ros/MucR family	0.16	4	9.12E-05
GOX0778	Two component sensor histidine kinase	0.42	4	6.51E-03
GOX1022	Transcriptional regulator	0.41	4	5.98E-03
GOX1192	Transcriptional regulator, MarR/AsnC family	0.49	4	7.02E-03

Oxygen limitation versus oxygen saturation; transport; mRNA ratio of 5 genes ≥ 2.0; mRNA ratio of 32 genes ≤ 0.5

Gene	Annotation	mRNA ratio	n	*p*-value

GOX0673	Ferrous iron transport protein A (FeoA)	5.86	4	4.91E-03
GOX0674	Ferrous iron transport protein B (FeoB)	3.24	4	1.40E-02
GOX0813	Phosphocarrier protein HPr	2.20	4	5.48E-03
GOX0814	PTS system, IIA component	4.10	4	1.59E-04
GOX0973	Outer membrane channel lipoprotein	3.39	4	1.41E-04
GOX0197	Signal recognition particle protein	0.34	4	8.69E-04
GOX0360	Preprotein translocase subunit SecY	0.39	4	5.58E-03
GOX0512	Amino acid transport protein	0.32	4	1.31E-03
GOX0699	L-Asparagine permease	0.16	4	1.95E-13
GOX0758	Porin	0.19	4	2.03E-03
GOX0901	Xanthine/uracil permease	0.43	4	1.81E-04
GOX0907	TonB-dependent outer membrane receptor	0.23	4	1.36E-04
GOX0945	TonB-dependent outer membrane receptor	0.11	4	2.49E-04
GOX0970	Outer membrane channel lipoprotein	0.49	4	1.46E-04
GOX0971	Cation efflux system protein CzcA	0.49	4	6.62E-04
GOX0972	Cation efflux system protein CzcB	0.44	4	1.21E-03
GOX1015	TonB-dependent receptor of ferrichrome transport system	0.42	4	1.30E-03
GOX1017	TonB-dependent outer membrane receptor	0.11	4	6.32E-05
GOX1173	TonB-dependent outer membrane receptor	0.39	4	1.39E-03
GOX1174	Purine-cytosine permease	0.49	4	7.94E-03
GOX1287	Biopolymer transport ExbB protein	0.12	4	4.26E-04
GOX1288	Biopolymer transport ExbD protein	0.16	4	8.95E-06
GOX1289	Biopolymer transport ExbD protein	0.18	4	3.66E-04
GOX1365	ABC transporter permease protein	0.33	4	1.00E-05
GOX1366	ABC transporter ATP-binding protein	0.33	4	6.90E-06
GOX1416	Porin B precursur	0.15	4	3.36E-04
GOX1418	Carbohydrate-selective porin	0.19	4	4.06E-05
GOX1483	Capsule polysaccharide export protein	0.50	4	1.87E-04
GOX1572	Amino acid ABC transporter ATP-binding protein	0.43	4	3.87E-04
GOX1796	TonB-dependent outer membrane receptor	0.45	4	4.86E-03
GOX1903	TonB-dependent outer membrane receptor	0.12	4	9.50E-05
GOX1971	Galactose-proton symporter	0.26	4	9.13E-04
GOX2143	ABC transporter ATP-binding protein	0.38	4	1.16E-03
GOX2401	Protein translocase subunit SecF	0.48	4	2.41E-04
GOX2402	Preprotein translocase subunit SecD	0.39	4	2.54E-03
GOX2560	RND-type multidrug efflux pump, membrane permease	0.49	4	2.93E-03
GOX2561	RND-type multidrug efflux pump, outer membrane protein	0.50	2	1.16E-03

Oxygen limitation versus oxygen saturation; motility; mRNA ratio of 20 genes ≥ 2.0; mRNA ratio of 0 genes ≤ 0.5

Gene	Annotation	mRNA ratio	n	*p*-value

GOX0126	Flagellar motor protein MotA	2.08	4	1.75E-03
GOX0421	Flagellar motor switch protein	2.18	4	2.53E-03
GOX0425	Basal-body rod modification protein FlgD	3.04	4	4.05E-04
GOX0620	Chemotactic signal-response protein CheL	2.54	4	7.18E-05
GOX0697	Flagellar FliL protein	2.40	4	1.97E-03
GOX0787	Flagellin B	3.44	4	2.00E-03
GOX0788	Flagellin assembly protein	4.23	4	1.42E-03
GOX0952	Flagellar basal body P-ring biosynthesis protein FlgA	2.79	4	2.03E-04
GOX0953	Flagellar basal body rod protein FlgG	3.54	4	1.01E-04
GOX0954	Flagellar basal-body rod protein FlgF	4.26	4	1.39E-03
GOX1025	Flagellar hook-associated protein FlgL	3.69	4	4.32E-03
GOX1026	Flagellar hook-associated protein 1 FlgK	2.76	4	4.93E-03
GOX1027	Flagellar hook protein FlgE	2.83	4	2.24E-03
GOX1525	Flagellar biosynthetic protein FliQ	2.18	4	2.99E-03
GOX1526	Flagellar hook-basal body protein FleE	2.55	4	6.27E-04
GOX1527	Flagellar basal body rod protein FlgC	2.65	4	3.05E-03
GOX1528	Flagellar basal-body rod protein FlgB	3.41	4	6.18E-03
GOX1549	Methyl-accepting chemotaxis protein	2.06	4	6.42E-04
GOX1550	Chemotaxis protein CheX	2.32	4	3.27E-04
GOX1551	Chemotaxis protein CheY	2.16	4	7.08E-05

Oxygen limitation versus oxygen saturation; stress; mRNA ratio of 11 genes ≥ 2.0; mRNA ratio of 0 genes ≤ 0.5

Gene	**Annotation**	**mRNA ratio**	**n**	***p*-value**
GOX0609	ATP-dependent Clp protease ATP-binding subunit ClpA	2.85	4	1.16E-04
GOX0861	Flavohemoprotein	2.15	4	1.56E-02
GOX1024	Heat shock protein 90	2.63	4	1.72E-05
GOX1302	Paraquat-inducible protein A	2.16	4	2.75E-03
GOX1329	Small heat shock protein	5.29	4	3.22E-04
GOX1414	Chaperone protein DnaJ	2.18	4	5.18E-03
GOX1463	ATP-dependent Clp protease. ATP-binding subunit ClpV	3.42	4	1.09E-03
GOX1577	ATP-dependent Clp protease ATP-binding subunit ClpB	2.82	4	1.08E-05
GOX1992	Osmotically inducible protein C. peroxyredoxin	2.73	4	1.53E-05
GOX2163	Cold shock protein	3.04	4	8.24E-05
GOX2397	Small heat shock protein	2.32	4	4.25E-04

Oxygen limitation versus oxygen saturation; transcriptional and translational machinery; mRNA ratio of 12 genes ≥ 2.0; mRNA ratio of 70 genes ≤ 0.5

Gene	Annotation	mRNA ratio	n	*p*-value
GOX0172	Arginine tRNA	2.31	4	4.38E-03
GOX0199	Serine tRNA	2.43	2	6.70E-09
GOX0872	Proline tRNA	2.00	3	2.01E-02
GOX1106	Alanine tRNA	2.91	4	5.58E-03
GOX1359	Excinuclease ABC subunit A	2.59	4	2.41E-03
GOX1445	Leucine tRNA	2.70	4	5.83E-03
GOX1664	Recombination factor protein RarA	2.22	4	2.16E-03
GOX1722	Arginine tRNA	2.74	2	8.23E-04
GOX1768	Alkylated DNA repair protein AlkB	2.22	4	3.84E-03
GOX1917	ATP-dependent DNA helicase	2.12	4	1.52E-02
GOX2486	Cyteine tRNA	2.54	4	1.21E-03
GOX2646	DNA integration/recombination/invertion protein	3.15	4	2.08E-03
GOX0074	Elongation factor Ts	0.29	4	1.49E-03
GOX0075	30SRibosomal protein S2	0.27	4	1.44E-04
GOX0088	Trigger factor	0.40	4	7.07E-04
GOX0105	Elongation factor G	0.31	4	6.08E-05
GOX0106	50S Ribosomal protein L28	0.28	4	3.11E-04
GOX0117	50S Ribosomal protein L32	0.37	4	5.93E-04
GOX0140	50SRibosomal protein L27	0.44	4	5.89E-04
GOX0194	50S Ribosomal protein L19	0.28	4	2.52E-04
GOX0195	tRNA (Guanine-N(1)-)-methyltransferase	0.27	4	2.11E-04
GOX0196	30S Ribosomal protein S16	0.36	4	4.06E-04
GOX0200	ATP-dependent RNA helicase	0.10	4	1.38E-04
GOX0262	Phenylalanyl-tRNA synthetase alpha chain	0.45	4	1.72E-03
GOX0263	50S Ribosomal protein L20	0.34	4	1.89E-04
GOX0264	LSU Ribosomal protein L35P	0.47	4	1.05E-03
GOX0304	50S Ribosomal protein L9	0.35	4	8.21E-04
GOX0305	30S Ribosomal protein S18	0.38	4	1.89E-04
GOX0306	SSU Ribosomal protein S6P	0.34	4	1.38E-03
GOX0345	Ribonuclease HII	0.41	4	1.61E-04
GOX0355	LSU Ribosomal protein L17P	0.36	4	3.03E-03
GOX0356	RNA polymerase subunit alpha	0.37	4	2.83E-03
GOX0357	30S Ribosomal protein S11	0.37	4	6.30E-03
GOX0361	LSU Ribosomal protein L15P	0.45	4	2.28E-02
GOX0362	LSU Ribosomal protein L30P	0.37	4	4.83E-03
GOX0363	30S Ribosomal protein S5	0.29	4	1.57E-03
GOX0364	50S Ribosomal protein L18	0.25	4	4.10E-03
GOX0365	50S Ribosomal protein L6	0.27	4	4.85E-04
GOX0366	30S Ribosomal protein S8	0.27	4	5.51E-03

GOX0367	30S Ribosomal protein S14	0.42	4	4.48E-03
GOX0368	50S Ribosomal protein L5	0.16	4	7.52E-04
GOX0369	LSU Ribosomal protein L24P	0.29	4	9.99E-04
GOX0370	LSU Ribosomal protein L14P	0.31	4	1.85E-03
GOX0371	SSU Ribosomal protein S17P	0.40	4	3.15E-05
GOX0372	LSU Ribosomal protein L29P	0.35	4	6.62E-04
GOX0373	50S Ribosomal protein L16	0.26	4	3.79E-04
GOX0374	30S Ribosomal protein S3	0.25	4	3.44E-03
GOX0375	50S Ribosomal protein L22	0.26	4	3.08E-03
GOX0376	SSU Ribosomal protein S19P	0.24	4	1.11E-03
GOX0377	50S Ribosomal protein L2	0.25	4	1.12E-04
GOX0378	LSU Ribosomal protein L23P	0.30	4	2.28E-04
GOX0379	50S Ribosomal protein L4	0.28	4	1.91E-04
GOX0380	50S Ribosomal protein L3	0.30	4	3.61E-05
GOX0381	30S Ribosomal protein S10	0.26	4	2.86E-03
GOX0382	Elongation factor Tu	0.30	4	2.28E-03
GOX0383	30S Ribosomal protein S7	0.16	4	2.46E-03
GOX0384	30S Ribosomal protein S12	0.22	4	1.13E-05
GOX0385	RNA polymerase. subunit beta'	0.40	4	3.14E-03
GOX0386	RNA polymerase. subunit beta	0.43	4	6.94E-03
GOX0387	50S Ribosomal protein L7/L12	0.21	4	2.90E-04
GOX0388	LSU Ribosomal protein L10P	0.20	4	5.22E-04
GOX0389	50S Ribosomal protein L1	0.31	4	3.90E-03
GOX0390	50S Ribosomal protein L11	0.43	4	1.37E-03
GOX0396	DNA recombination protein RmuC-like protein	0.40	4	4.71E-03
GOX0451	30S Ribosomal protein S9	0.22	4	1.89E-04
GOX0452	50S Ribosomal protein L13	0.31	4	1.04E-02
GOX0596	30S Ribosomal protein S1	0.41	4	5.43E-05
GOX0774	Ribosomal-protein-alanine acetyltransferase	0.49	3	3.70E-02
GOX0823	Threonyl-tRNA synthetase	0.48	4	3.21E-04
GOX0835	Adenine phosphoribosyltransferase	0.30	4	1.65E-03
GOX1070	Transcription termination factor Rho	0.46	4	7.53E-03
GOX1141	LSU Ribosomal protein L25P	0.31	4	2.32E-04
GOX1142	Peptidyl-tRNA hydrolase	0.31	4	7.95E-04
GOX1282	Ribonuclease PH	0.48	4	3.82E-04
GOX1440	S-Adenosylmethionine:tRNA ribosyltransferase-isomerase	0.49	4	2.35E-03
GOX1455	ATP-dependent RNA helicase	0.27	4	3.89E-04
GOX1780	30S ribosomal protein S4	0.27	4	4.71E-04
GOX1781	Bacterial Peptide Chain Release Factor 3 (RF-3)	0.18	4	8.97E-04
GOX1873	DNA mismatch repair protein	0.41	4	6.59E-04
GOX2030	Chaperone protein DnaK	0.16	4	4.49E-03
GOX2546	Replication protein A	0.42	4	3.86E-03

GOX2603	Replicator initiator RepC	0.42	4	6.97E-04

Oxygen limitation versus oxygen saturation; predicted functions; mRNA ratio of 15 genes ≥ 2.0; mRNA ratio of 24 genes ≤ 0.5

Gene	Annotation	mRNA ratio	n	*p*-value
GOX0090	Putative sugar kinase	5.14	4	8.89E-04
GOX0314	Probable Alcohol:NAD(P) oxidoreductase	14.63	4	2.35E-03
GOX0334	Probable (di) nucleoside polyphosphate hydrolase	2.21	4	1.33E-04
GOX0572	Putative oxidoreductase	3.61	4	1.73E-03
GOX0647	Putative exporter protein. ArAE family	18.22	4	4.00E-02
GOX0946	Putative oxidoreductase	2.29	4	2.93E-03
GOX1462	Putative oxidoreductase	2.69	4	5.10E-03
GOX1773	Putative LacX protein	3.29	4	1.92E-03
GOX1774	Putative ATP-sensitive potassium channel protein	4.03	4	1.78E-04
GOX1779	Putative LysM domain protein	6.93	4	3.03E-05
GOX1900	Putative carboxymethylenebutenolidase	2.09	4	1.63E-02
GOX2199	Probable myosin-crossreactive antigen	5.62	4	4.82E-05
GOX2200	Probable myosin-crossreactive antigen	5.37	4	2.69E-07
GOX2253	Putative oxidoreductase	2.46	4	6.82E-05
GOX2455	Putative phage-related protein	2.55	4	3.56E-03
GOX0039	Putative hemagglutinin-related protein	0.42	4	3.20E-03
GOX0254	Putative Fe-S-cluster redox enzyme	0.44	4	1.65E-03
GOX0354	Putative sugar/polyol transporter	0.12	4	9.11E-04
GOX0392	Putative transport transmembrane protein	0.46	4	7.36E-04
GOX0393	Putative transport transmembrane protein	0.43	4	5.02E-04
GOX0415	Putative transport protein	0.30	4	2.99E-04
GOX0516	Uncharacterized PQQ-dependent dehydrogenase 4	0.49	4	5.09E-03
GOX0562	Putative siderophore receptor protein	0.32	4	1.67E-03
GOX0689	Probable outer membrane efflux lipoprotein	0.41	4	8.87E-04
GOX0834	Putative oxidoreductase	0.50	4	2.40E-03
GOX0868	Electron transfer flavoprotein-ubiquinone oxidoreductase/ putative oxidoreductase	0.28	4	1.40E-04
GOX0905	Putative oxidoreductase	0.37	4	7.09E-04
GOX1179	Putative sugar uptake ABC transporter permease protein	0.44	4	2.94E-04
GOX1199	Putative oxidoreductase	0.35	4	1.41E-03
GOX1244	Putative enolase-phosphatase	0.44	4	4.40E-04
GOX1351	Putative isomerase	0.29	4	1.87E-04
GOX1542	Putative aluminum resistance protein	0.40	4	1.50E-04
GOX1851	Putative oxidoreductase	0.19	4	1.73E-04
GOX1857	Uncharacterized PQQ-containing dehydrogenase 1	0.12	4	1.34E-04
GOX1957	Putative thiol:disulfide interchange protein II	0.40	4	2.21E-05
GOX1972	Putative transport protein	0.27	4	9.18E-04

GOX2258	Putative phytoene synthase	0.45	4	3.67E-04
GOX2376	Putative aldehyde dehydrogenase	0.44	4	3.31E-03
GOX2578	Putative isochorismatase	0.46	4	1.87E-03

Oxygen limitation versus oxygen saturation; hypothetical proteins; mRNA ratio of 76 genes ≥ 2.0; mRNA ratio of 49 genes ≤ 0.5

Gene	Annotation	mRNA ratio	n	*p*-value
GOX0031	Hypothetical protein GOX0031	2.16	4	1.90E-03
GOX0053	Hypothetical protein GOX0053	3.71	4	3.40E-04
GOX0137	Hypothetical membrane-spanning protein	2.86	4	1.90E-04
GOX0198	Hypothetical protein GOX0198	2.17	4	5.99E-04
GOX0204	Hypothetical protein GOX0204	2.45	4	1.10E-03
GOX0333	Hypothetical protein GOX0333	2.24	4	1.64E-03
GOX0422	Hypothetical protein GOX0422	2.17	4	1.93E-02
GOX0426	Hypothetical protein GOX0426	3.42	4	2.34E-03
GOX0442	Hypothetical protein GOX0442	2.21	4	1.94E-02
GOX0475	Hypothetical protein GOX0475	2.16	4	1.25E-03
GOX0549	Hypothetical protein GOX0549	2.51	4	1.37E-03
GOX0570	Hypothetical protein GOX0570	2.37	4	3.04E-05
GOX0571	Hypothetical protein GOX0571	2.62	4	4.14E-03
GOX0576	Hypothetical protein GOX0576	2.80	4	2.68E-03
GOX0619	Hypothetical protein GOX0619	2.56	4	7.14E-04
GOX0635	Hypothetical protein GOX0635	2.01	4	2.78E-02
GOX0694	Hypothetical protein GOX0694	2.53	4	4.97E-04
GOX0695	Hypothetical protein GOX0695	2.56	4	1.57E-03
GOX0708	Hypothetical protein GOX0708	2.18	4	1.47E-02
GOX0755	Hypothetical protein in adhS 5' region	2.36	4	1.50E-03
GOX0815	Hypothetical protein GOX0815	6.53	4	1.86E-04
GOX0880	Hypothetical protein GOX0880	3.00	4	1.54E-02
GOX0886	Hypothetical protein GOX0886	3.46	4	1.15E-03
GOX0890	Hypothetical protein GOX0890	9.60	4	2.78E-03
GOX0915	Hypothetical protein GOX0915	2.94	4	9.15E-03
GOX1132	Hypothetical protein GOX1132	3.01	4	1.47E-03
GOX1239	Hypothetical protein GOX1239	2.32	4	3.15E-03
GOX1248	Hypothetical protein GOX1248	2.28	4	1.42E-03
GOX1273	Hypothetical protein GOX1273	2.26	4	1.64E-03
GOX1355	Hypothetical protein GOX1355	2.27	4	1.02E-02
GOX1424	Hypothetical protein GOX1424	2.26	4	4.51E-03
GOX1442	Hypothetical protein GOX1442	8.96	4	7.48E-04
GOX1500	Hypothetical protein GOX1500	4.07	4	3.07E-04
GOX1501	Hypothetical protein GOX1501	3.88	4	5.38E-06
GOX1521	Hypothetical protein GOX1521	2.07	4	1.24E-03

GOX1578	Hypothetical protein GOX1578	2.92	4	1.46E-03
GOX1617	Hypothetical protein GOX1617	2.32	4	3.64E-04
GOX1654	Hypothetical protein GOX1654	2.39	4	4.40E-04
GOX1697	Hypothetical protein GOX1697	2.44	4	5.89E-03
GOX1742	Hypothetical protein GOX1742	2.37	4	9.42E-03
GOX1745	Hypothetical protein GOX1745	2.13	4	2.59E-03
GOX1841	Hypothetical protein GOX1841	3.32	4	2.38E-04
GOX1858	Hypothetical protein GOX1858	2.02	4	6.72E-04
GOX1863	Hypothetical protein GOX1863	3.42	4	2.94E-04
GOX1870	Hypothetical protein GOX1870	2.32	4	3.20E-02
GOX1875	Hypothetical protein GOX1875	2.05	4	1.21E-03
GOX1895	Hypothetical protein GOX1895	4.12	4	1.45E-03
GOX1898	Hypothetical protein GOX1898	2.08	4	1.19E-03
GOX1923	Hypothetical protein GOX1923	2.06	4	1.58E-03
GOX1928	Hypothetical protein GOX1928	2.94	4	7.39E-10
GOX1942	Hypothetical protein GOX1942	2.25	4	8.45E-04
GOX1951	Hypothetical protein GOX1951	2.42	4	3.61E-03
GOX1995	Hypothetical protein GOX1995	2.52	4	1.60E-03
GOX2051	Hypothetical protein GOX2051	2.52	4	2.42E-03
GOX2052	Hypothetical protein GOX2052	2.83	4	6.38E-03
GOX2053	Hypothetical protein GOX2053	2.34	4	3.39E-02
GOX2063	Hypothetical protein GOX2063	2.38	4	1.79E-04
GOX2152	Hypothetical protein GOX2152	2.58	4	6.82E-04
GOX2153	Hypothetical protein GOX2153	2.63	4	1.96E-03
GOX2205	Hypothetical protein GOX2205	2.02	4	8.34E-03
GOX2246	Hypothetical protein GOX2246	3.52	4	8.30E-05
GOX2252	Hypothetical protein GOX2252	2.60	4	1.28E-04
GOX2278	Hypothetical protein GOX2278	2.53	4	5.58E-05
GOX2311	Hypothetical protein GOX2311	2.03	4	1.39E-03
GOX2326	Hypothetical protein GOX2326	3.03	4	2.69E-04
GOX2366	Hypothetical protein GOX2366	2.04	3	1.48E-02
GOX2379	Hypothetical protein GOX2379	3.62	4	3.45E-04
GOX2413	Hypothetical protein GOX2413	3.24	4	3.29E-04
GOX2461	Hypothetical protein GOX2461	2.19	3	7.04E-03
GOX2470	Hypothetical protein GOX2470	2.54	4	4.78E-03
GOX2488	Hypothetical protein GOX2488	2.35	4	1.60E-04
GOX2520	Hypothetical protein GOX2520	4.15	4	1.04E-03
GOX2699	Hypothetical protein GOX2699	2.17	4	1.72E-05
GOX2720	Hypothetical protein GOX2720	12.34	4	2.03E-04
GOX2733	Hypothetical protein GOX2733	2.00	4	7.37E-03
GOX2734	Hypothetical protein GOX2734	2.07	4	1.12E-02
GOX0013	Hypothetical protein GOX0013	0.15	4	5.55E-05
GOX0035	Hypothetical protein GOX0035	0.42	4	3.68E-03

GOX0143	Hypothetical protein GOX0143	0.45	4	3.59E-03
GOX0326	Hypothetical protein GOX0326	0.35	4	1.51E-04
GOX0352	Hypothetical protein GOX0352	0.36	4	8.60E-04
GOX0397	Hypothetical protein GOX0397	0.46	4	1.56E-04
GOX0404	Hypothetical protein GOX0404	0.13	4	1.57E-04
GOX0474	Hypothetical protein GOX0474	0.48	4	1.85E-02
GOX0497	Hypothetical protein GOX0497	0.41	4	2.76E-04
GOX0515	Hypothetical protein GOX0515	0.18	4	1.00E-04
GOX0568	Hypothetical protein GOX0568	0.33	4	9.58E-05
GOX0599	Hypothetical protein GOX0599	0.39	4	6.00E-04
GOX0600	Hypothetical protein GOX0600	0.40	4	6.32E-03
GOX0610	Hypothetical protein GOX0610	0.47	4	1.95E-03
GOX0745	Hypothetical protein GOX0745	0.29	4	2.31E-03
GOX0767	Hypothetical protein GOX0767	0.49	4	3.71E-03
GOX0775	Hypothetical protein GOX0775	0.46	4	4.78E-03
GOX0797	Hypothetical protein GOX0797	0.46	4	5.38E-04
GOX0805	Hypothetical protein GOX0805	0.45	4	5.84E-04
GOX0806	Hypothetical protein GOX0806	0.34	4	3.92E-03
GOX0807	Hypothetical protein GOX0807	0.33	4	6.11E-03
GOX0827	Hypothetical protein GOX0827	0.46	4	6.29E-05
GOX0828	Hypothetical protein GOX0828	0.49	4	1.05E-04
GOX0845	Hypothetical protein GOX0845	0.44	4	1.52E-03
GOX0846	Hypothetical protein GOX0846	0.36	4	1.13E-03
GOX0902	Hypothetical protein GOX0902	0.45	4	7.20E-06
GOX0903	Hypothetical protein GOX0903	0.46	4	1.44E-04
GOX0943	Hypothetical protein GOX0943	0.30	4	1.21E-07
GOX0944	Hypothetical protein GOX0944	0.42	4	5.39E-04
GOX0969	Hypothetical protein GOX0969	0.32	4	3.62E-05
GOX1029	Hypothetical protein GOX1029	0.47	4	4.09E-03
GOX1108	Hypothetical protein GOX1108	0.49	4	6.79E-04
GOX1197	Hypothetical protein GOX1197	0.22	4	6.10E-04
GOX1269	Hypothetical protein GOX1269	0.29	4	2.39E-04
GOX1286	Hypothetical protein GOX1286	0.16	4	3.74E-04
GOX1290	Hypothetical protein GOX1290	0.39	4	3.61E-05
GOX1392	Hypothetical protein GOX1392	0.49	4	2.92E-05
GOX1543	Hypothetical protein GOX1543	0.43	4	1.11E-03
GOX1563	Hypothetical protein GOX1563	0.21	4	4.36E-03
GOX1579	Hypothetical protein associated with nus operon	0.39	4	1.49E-03
GOX1662	Hypothetical protein GOX1662	0.39	4	6.65E-03
GOX1699	Hypothetical protein GOX1699	0.27	4	3.57E-04
GOX1736	Hypothetical protein GOX1736	0.47	4	3.20E-03
GOX1982	Hypothetical protein GOX1982	0.25	4	8.64E-05
GOX2028	Hypothetical protein GOX2028	0.17	4	1.27E-04

GOX2135	Hypothetical protein GOX2135	0.47	4	1.37E-05
GOX2142	Hypothetical protein GOX2142	0.45	4	3.90E-05
GOX2151	Hypothetical protein GOX2151	0.42	4	2.11E-03
GOX2580	Hypothetical protein GOX2580	0.42	4	3.27E-04

Table S2 Gene sets and expression data of common genes and of specific genes of a condition when using cut-off values two-fold differential expression and $p < 0.05$. Missing values indicate low signals which were not taken into account (see Materials & Methods).

			pO2 lim. / pO2 sat.		D*qrcABC* / Wt		pH 4 / pH 6	
Locus_Tag	**Annotation**	**mRNA-level**	**p-value**	**mRNA-level**	**p-value**	**mRNA-level**	**p-value**
GOX0890	Hypothetical protein GOX0890	9.60	2.78E-03	2.19	5.92E-02	4.93	4.87E-03
GOX0945	TonB-dependent outer membrane receptor	0.11	2.49E-04	0.47	1.77E-02	0.35	2.36E-02
GOX1841	Hypothetical protein GOX1841	3.32	2.38E-04	2.14	8.91E-03	3.36	2.55E-02
GOX1903	TonB-dependent outer membrane receptor	0.12	9.50E-05	0.38	1.70E-03	0.42	4.62E-04
GOX1982	Hypothetical protein GOX1982	0.25	8.64E-05	0.46	4.35E-04	0.36	3.88E-03
GOX0053	Hypothetical protein GOX0053	3.71	3.40E-04	2.15	5.62E-03	1.22	3.74E-02
GOX0310	NAD(P) transhydrogenase subunit alpha2	10.37	3.76E-04	3.14	1.53E-03	1.19	1.53E-01
GOX0311	NAD(P) transhydrogenase subunit alpha1	14.70	1.36E-03	3.80	4.77E-03	1.39	5.29E-02
GOX0312	NAD(P) transhydrogenase subunit beta	12.04	4.33E-04	3.44	2.76E-03	1.19	1.01E-02
GOX0313	Alcohol:NAD oxidoreductase	13.58	7.09E-04	4.00	3.19E-03	1.22	3.14E-02
GOX0314	Probable Alcohol:NAD(P) oxidoreductase	14.63	2.35E-03	3.58	5.43E-03	1.04	1.33E-01
GOX0426	Hypothetical protein GOX0426	3.42	2.34E-03	2.06	1.10E-02	1.08	2.18E-01
GOX0442	Hypothetical protein GOX0442	2.21	1.94E-02	2.22	2.65E-03	0.91	2.35E-01
GOX0565	Ubiquinol-cytochrome *c* oxidoreductase FeS protein	2.49	3.81E-03	0.05	3.19E-03	0.94	3.32E-01
GOX0566	Ubiquinol-cytochrome *c* oxidoreductase cytochrome *b*	2.20	1.29E-02	0.03	6.97E-04	1.02	4.40E-01
GOX0635	Hypothetical protein GOX0635	2.01	2.78E-02	2.02	6.78E-03	1.19	2.08E-01
GOX0673	Ferrous iron transport protein A (FeoA)	5.86	4.91E-03	3.04	3.21E-04	0.98	4.78E-01
GOX0787	Flagellin B	3.44	2.00E-03	2.73	1.34E-03	1.20	5.60E-03
GOX0788	Flagellin assembly protein	4.23	1.42E-03	2.06	3.11E-03	1.48	3.24E-02
GOX0953	Flagellar basal body rod protein FlgG	3.54	1.01E-04	2.33	1.22E-02	1.18	2.83E-02

GOX0954		Flagellar basal-body rod protein FlgF		4.26	1.39E-03		2.28	9.07E-04		1.24	1.18E-01
GOX1025		Flagellar hook-associated protein FlgL		3.69	4.32E-03		2.73	1.36E-02		1.22	2.28E-02
GOX1026		Flagellar hook-associated protein 1 FlgK		2.76	4.93E-03		2.66	1.22E-03		1.42	6.98E-02
GOX1027		Flagellar hook protein FlgE		2.83	2.24E-03		2.81	3.85E-03		1.29	1.74E-03
GOX1528		Flagellar basal-body rod protein FlgB		3.41	6.18E-03		2.03	1.82E-03		1.15	2.68E-01
GOX1550		Chemotaxis protein CheX		2.32	3.27E-04		2.01	1.61E-02		1.07	2.18E-01
GOX1613		Protein with GGDEF and EAL domain		3.78	1.86E-03		2.36	1.61E-03		1.29	1.10E-01
GOX1870		Hypothetical protein GOX1870		2.32	3.20E-02		2.00	2.40E-02		1.39	1.18E-01
GOX1911		Cytochrome bo_3 ubiquinol oxidase subunit II		2.82	1.63E-03		2.09	7.68E-03		1.12	1.70E-01
GOX1912		Cytochrome bo_3 ubiquinol oxidase subunit I		2.70	1.05E-02		2.28	6.81E-03		1.12	1.39E-01
GOX1913		Cytochrome bo_3 ubiquinol oxidase subunit III		3.56	2.53E-05		2.10	2.34E-03		1.13	1.03E-01
GOX1914		Cytochrome bo_3 ubiquinol oxidase subunit IV		3.81	4.04E-03		2.15	2.94E-03		1.31	1.44E-01
GOX2199		Probable myosin-crossreactive antigen		5.62	4.82E-05		2.33	1.51E-03		1.07	2.26E-01
GOX2200		Probable myosin-crossreactive antigen		5.37	2.69E-07		2.01	6.60E-03		1.04	3.56E-01
GOX2373		Protein of Riske non-heme iron oxygenase Family, putative ring-hydroxylating dioxygenase		3.72	1.79E-03		2.81	6.17E-04		1.84	4.07E-03
GOX2379		Hypothetical protein GOX2379		3.62	3.45E-04		2.00	2.55E-02		1.40	3.87E-02
GOX0204		Hypothetical protein GOX0204		2.45	1.10E-03		0.73	1.82E-02		0.39	3.49E-02
GOX0207		TonB-dependent outer membrane receptor		0.18	3.56E-04		0.83	1.28E-01		0.22	2.27E-03
GOX0213		Biotin carboxylase		0.46	1.02E-04		0.92	1.74E-01		0.47	1.62E-03
GOX0278		Cytochrome *bd* ubiquinol oxidase subunit I		3.64	7.58E-05		1.11	6.93E-02		2.22	1.11E-02
GOX0352		Hypothetical protein GOX0352		0.36	8.60E-04		0.58	5.20E-02		2.20	2.62E-02
GOX0497		Hypothetical protein GOX0497		0.41	2.76E-04		1.01	4.91E-01		2.31	5.22E-04
GOX0524		TonB-dependent outer membrane receptor		0.13	4.00E-04		0.92	1.24E-01		0.19	8.69E-03
GOX0576		Hypothetical protein GOX0576		2.80	2.68E-03		1.48	3.65E-02		2.11	2.50E-02
GOX0647		Putative exporter protein. ArAE family		18.22	4.00E-02		1.40	2.34E-02		12.91	1.53E-03
GOX0902		Hypothetical protein GOX0902		0.45	7.20E-06		0.88	6.05E-02		0.47	2.82E-02
GOX0903		Hypothetical protein GOX0903		0.46	1.44E-04		0.94	2.91E-01		0.33	1.81E-03

GOX0905		Putative oxidoreductase		0.37	7.09E-04		0.83	5.63E-02	0.45	4.13E-04
GOX0907		TonB-dependent outer membrane receptor		0.23	1.36E-04		0.73	1.05E-01	0.34	2.01E-03
GOX0943		Hypothetical protein GOX0943		0.30	1.21E-07		0.83	4.82E-02	3.13	9.41E-03
GOX0944		Hypothetical protein GOX0944		0.42	5.39E-04		0.89	9.01E-02	2.48	1.99E-02
GOX1017		TonB-dependent outer membrane receptor		0.11	6.32E-05		0.72	3.72E-02	0.31	4.86E-03
GOX1173		TonB-dependent outer membrane receptor		0.39	1.39E-03		0.92	3.48E-01	0.40	4.90E-02
GOX1335		Aconitate hydratase		0.13	1.85E-04		0.78	4.41E-02	0.49	1.98E-03
GOX1336		Isocitrate dehydrogenase		0.17	2.05E-04		0.75	5.89E-03	0.45	2.23E-02
GOX1351		Putative isomerase		0.29	1.87E-04		0.98	4.00E-01	2.10	2.93E-02
GOX1462		Putative oxidoreductase		2.69	5.10E-03		1.34	3.84E-02	2.10	5.42E-03
GOX1851		Putative oxidoreductase		0.19	1.73E-04		0.92	2.86E-01	0.39	3.54E-04
GOX1852		Glutamate synthase		0.23	4.24E-04		0.94	1.53E-01	0.35	4.01E-03
GOX1857		Uncharacterized PQQ-containing dehydrogenase 1		0.12	1.34E-04		0.93	3.10E-01	0.40	9.72E-03
GOX1951		Hypothetical protein GOX1951		2.42	3.61E-03		0.82	1.51E-01	2.27	1.86E-03
GOX1992		Osmotically inducible protein C, peroxyredoxin		2.73	1.53E-05		1.38	5.61E-02	2.01	7.16E-03
GOX0530		TonB protein		2.12	1.41E-01		1.70	9.16E-03	0.78	2.60E-01
GOX0531		ExbD protein		2.82	7.30E-02		2.98	3.42E-03	0.59	1.76E-01
GOX0532		ExbB protein		3.22	9.32E-02		4.97	5.36E-03	0.27	1.08E-01
GOX0567		Ubiquinol-cytochrome-c reductase		1.80	1.79E-03		0.05	3.38E-03	0.97	2.84E-01
GOX0798		Serine proteasem, HtrA/DegQ/DegS family		0.57	1.19E-04		2.24	1.18E-02	1.05	1.73E-01
GOX1246		TonB-dependent receptor protein		2.33	8.17E-02		2.34	2.36E-03	0.97	4.66E-01
GOX2180		TonB-dependent receptor (disrupted by IS element)		0.92	3.16E-01		3.38	7.71E-03	0.43	1.03E-01
GOX0208		Putative glucarate/galactarate transporter		0.66	2.78E-02		0.95	2.63E-01	0.43	4.73E-02
GOX0209		Hypothetical protein GOX0209		0.62	1.08E-03		0.96	2.70E-01	0.42	3.59E-03
GOX0210		Putative carboxylase		0.55	3.71E-04		0.92	1.81E-01	0.44	4.92E-03
GOX0211		Hypothetical protein GOX0211		0.54	3.68E-05		0.96	5.24E-02	0.40	3.27E-03

GOX0212		Biotin carboxyl carrier protein of acetyl-CoA carboxylase		0.63	7.39E-04		0.90	1.26E-02		0.44	6.16E-03
GOX0216		N-Methylhydantoinase A		0.51	3.06E-03		0.98	2.39E-01		0.48	7.45E-04
GOX0244		Hypothetical membrane-spanning protein		0.64	4.70E-05		1.22	1.52E-03		2.19	4.58E-02
GOX0291		Putative ferredoxin subunit of ring-hydroxylating dioxygenase		1.51	5.08E-04		1.04	3.97E-01		2.34	9.20E-04
GOX0433		Hypothetical protein GOX0433		0.88	7.81E-02		1.89	7.08E-03		2.50	4.50E-03
GOX0470		Putative peroxidase		0.60	1.80E-03		1.12	1.97E-03		2.24	3.39E-02
GOX0553		Hypothetical protein GOX0553		0.66	1.76E-02		0.79	2.65E-03		2.75	6.48E-03
GOX0652		Xanthine dehydrogenase XdhC protein					0.98	4.19E-01		0.34	2.76E-02
GOX0653		Xanthine dehydrogenase XdhB protein		0.59	2.65E-03		0.90	1.60E-01		0.34	9.25E-04
GOX0679		Conserved protein of the SAM superfamily		1.25	7.24E-02		1.14	1.07E-01		3.20	4.43E-02
GOX0707		DNA starvation/stationary phase protection protein Dps		1.21	5.09E-02		1.41	1.50E-01		3.47	4.21E-02
GOX0726		Hypothetical protein GOX0726		1.71	8.65E-03		1.31	7.86E-02		2.76	8.76E-03
GOX0768		Transcriptional regulator		1.66	4.58E-02		0.65	7.33E-02		0.49	2.14E-02
GOX0904		Hypothetical protein GOX0904		0.52	1.90E-03		0.84	1.18E-02		0.44	2.10E-03
GOX1138		Catalase		0.52	5.06E-03		0.98	4.35E-01		2.10	1.68E-03
GOX1209		Hypothetical protein GOX1209		1.01	4.03E-01		0.95	3.99E-01		0.36	1.82E-02
GOX1210		Hypothetical protein GOX1210		1.15	2.08E-01		0.87	1.73E-01		0.25	4.60E-02
GOX1225		Putative phage tail protein		0.84	1.38E-01		0.89	3.09E-01		0.47	8.08E-03
GOX1276		Organophosphate acid anhydrase		1.06	1.15E-01		1.12	1.79E-01		2.02	1.61E-02
GOX1374		DNA topoisomerase I		0.60	8.93E-04		0.93	2.24E-01		3.02	3.62E-03
GOX1538		Short chain dehydrogenase		0.64	4.14E-03		1.05	3.31E-01		2.02	2.90E-02
GOX1615		Putative oxidoreductase		1.16	2.91E-02		1.27	1.67E-02		2.54	1.50E-02
GOX1660		Hypothetical protein GOX1660		1.58	3.90E-02		1.16	3.44E-01		0.35	3.91E-02
GOX1712		Aldehyde dehydrogenase		1.31	3.53E-03		1.33	3.13E-02		2.15	4.88E-03
GOX1713		Protease I		1.50	1.20E-03		1.24	8.50E-02		2.08	1.38E-03
GOX1748		Bacterioferritin		0.69	7.79E-03		0.70	2.81E-02		3.37	1.99E-03

GOX1749		Hypothetical protein GOX1749		1.30	7.95E-03		1.09	2.74E-02		0.37	1.40E-02
GOX1784		Hypothetical protein GOX1784		0.69	1.76E-02		1.43	4.57E-03		0.33	1.55E-03
GOX1785		Carbonic anhydrase		0.82	3.88E-02		1.65	1.43E-02		0.37	8.75E-04
GOX2017		Hypothetical protein GOX2017		0.59	3.20E-03		1.33	9.56E-02		0.31	1.17E-02
GOX2079		Hypothetical protein GOX2079		0.64	2.19E-04		0.84	2.61E-01		2.13	1.51E-03
GOX2083		Hypothetical protein GOX2083		0.97	3.86E-01		1.19	4.08E-02		2.15	2.36E-02
GOX2096		Sorbitol dehydrogenase large subunit		0.99	4.74E-01		0.98	2.04E-01		2.21	1.64E-03
GOX2097		Sorbitol dehydrogenase small subunit		1.08	3.10E-01		1.01	4.87E-01		2.22	1.28E-02
GOX2256		Putative aminotransferase		0.52	4.03E-03		0.89	2.48E-01		0.41	8.74E-03
GOX2676		Putative alcohol/aldehyde dehydrogenase		0.92	2.11E-01		1.20	1.65E-01		2.45	2.47E-02
GOX0013		Hypothetical protein GOX0013		0.15	5.55E-05		0.66	2.33E-02		1.96	5.17E-03
GOX0024		Undecaprenyl pyrophosphate phosphatase		0.40	2.22E-03		0.87	7.20E-02		0.88	3.68E-02
GOX0031		Hypothetical protein GOX0031		2.16	1.90E-03		1.06	2.57E-01		0.92	2.51E-02
GOX0035		Hypothetical protein GOX0035		0.42	3.68E-03		0.76	5.32E-02		0.87	2.07E-01
GOX0036		Enoyl[acyl-carrier-protein] reductase		0.41	2.37E-03		0.78	6.35E-02		0.81	1.85E-01
GOX0039		Putative hemagglutinin-related protein		0.42	3.20E-03		0.95	2.15E-01		0.81	1.27E-01
GOX0074		Elongation factor Ts		0.29	1.49E-03		0.73	3.50E-02		1.02	4.32E-01
GOX0075		30SRibosomal protein S2		0.27	1.44E-04		0.69	8.70E-02		0.78	1.88E-01
GOX0088		Trigger factor		0.40	7.07E-04		0.76	9.89E-03		0.99	4.82E-01
GOX0090		Putative sugar kinase		5.14	8.89E-04		1.42	1.36E-02		1.07	3.49E-01
GOX0103		Carboxypeptidase-related protein		0.23	1.23E-04		0.74	2.33E-02		0.55	3.02E-03
GOX0105		Elongation factor G		0.31	6.08E-05		0.90	6.93E-02		1.20	2.08E-01
GOX0106		50S Ribosomal protein L28		0.28	3.11E-04		0.77	1.97E-03		1.21	1.16E-01
GOX0115		3-Oxoacyl-[acyl-carrier-protein] synthase		0.40	2.01E-03		0.75	4.73E-02		0.97	3.92E-01
GOX0116		Fatty acid/phospholipid synthesis protein		0.24	2.87E-03		0.76	5.73E-02		0.88	2.79E-01
GOX0117		50S Ribosomal protein L32		0.37	5.93E-04		0.83	6.91E-02		1.06	2.83E-01
GOX0126		Flagellar motor protein MotA		2.08	1.75E-03		1.42	4.21E-02		0.98	4.35E-01

GOX0132		Transcriptional regulator		0.27	1.22E-06		0.73	5.58E-03		0.73	2.32E-03
GOX0135		Transcriptional regulator. Ros/MucR family		2.80	3.66E-03		2.00	2.54E-03		0.69	1.13E-01
GOX0137		Hypothetical membrane-spanning protein		2.86	1.90E-04		1.06	7.24E-02		1.03	3.24E-01
GOX0140		50SRibosomal protein L27		0.44	5.89E-04		0.63	1.16E-02		0.95	3.52E-01
GOX0143		Hypothetical protein GOX0143		0.45	3.59E-03		0.81	8.46E-03		0.77	1.32E-01
GOX0145		Glucose-6-phosphate 1-dehydrogenase		0.45	4.46E-05		1.14	8.16E-02		1.23	2.22E-01
GOX0172		Arginine tRNA		2.31	4.38E-03		0.81	3.00E-01		0.78	3.56E-02
GOX0190		Aspartate aminotransferase A		0.47	7.33E-06		0.89	1.16E-01		0.62	1.67E-02
GOX0191		3-Isopropylmalate dehydrogenase		0.35	4.03E-04		0.79	5.71E-02		0.99	2.44E-01
GOX0192		3-Isopropylmalate dehydratase, small subunit		0.32	1.80E-04		0.69	7.65E-03		0.85	1.11E-01
GOX0193		Isopropylmalate isomerase large subunit		0.24	4.42E-04		0.59	6.11E-02		1.01	4.77E-01
GOX0194		50S Ribosomal protein L19		0.28	2.52E-04		0.73	4.67E-04		0.91	1.03E-01
GOX0195		tRNA (Guanine-N(1)-)-methyltransferase		0.27	2.11E-04		0.73	2.41E-02		0.97	3.69E-01
GOX0196		30S Ribosomal protein S16		0.36	4.06E-04		0.73	1.27E-01		0.82	1.60E-01
GOX0197		Signal recognition particle protein		0.34	8.69E-04		0.64	5.84E-03		0.74	1.88E-02
GOX0198		Hypothetical protein GOX0198		2.17	5.99E-04		1.17	2.27E-01		0.64	8.46E-03
GOX0199		Serine tRNA		2.43	6.70E-09						
GOX0200		ATP-dependent RNA helicase		0.10	1.38E-04		0.88	2.46E-01		0.69	2.71E-03
GOX0254		Putative Fe-S-cluster redox enzyme		0.44	1.65E-03		0.71	1.12E-02		1.18	3.23E-02
GOX0262		Phenylalanyl-tRNA synthetase alpha chain		0.45	1.72E-03		0.85	4.67E-02		1.03	4.27E-01
GOX0263		50S Ribosomal protein L20		0.34	1.89E-04		1.03	4.66E-01		0.98	4.43E-01
GOX0264		LSU Ribosomal protein L35P		0.47	1.05E-03		0.91	3.55E-01		1.03	2.26E-01
GOX0265		Membrane-bound glucose dehydrogenase (PQQ)		0.50	1.97E-05		0.67	5.39E-02		0.97	4.30E-01
GOX0304		50S Ribosomal protein L9		0.35	8.21E-04		0.74	1.84E-01		1.13	2.33E-01
GOX0305		30S Ribosomal protein S18		0.38	1.89E-04		0.82	5.39E-03		1.09	2.25E-01
GOX0306		SSU Ribosomal protein S6P		0.34	1.38E-03		0.78	5.23E-03		1.06	2.07E-01
GOX0321		Carbamoyl phosphate synthase small subunit		0.30	9.80E-05		0.84	1.56E-01		1.14	2.44E-01

GOX0322		Carbamoyl phosphate synthase large subunit		0.32	4.33E-05		0.85	8.03E-02		1.10	1.59E-01
GOX0326		Hypothetical protein GOX0326		0.35	1.51E-04		0.96	3.43E-01		1.43	1.09E-03
GOX0333		Hypothetical protein GOX0333		2.24	1.64E-03		1.26	8.69E-02		0.94	3.21E-01
GOX0334		Probable (di) nucleoside polyphosphate hydrolase		2.21	1.33E-04		1.20	2.27E-02		0.99	3.83E-01
GOX0345		Ribonuclease HII		0.41	1.61E-04		0.77	1.92E-02		1.16	1.46E-01
GOX0354		Putative sugar/polyol transporter		0.12	9.11E-04		0.61	9.87E-03		0.85	4.75E-02
GOX0355		LSU Ribosomal protein L17P		0.36	3.03E-03		0.78	5.81E-02		0.81	1.13E-01
GOX0356		RNA polymerase subunit alpha		0.37	2.83E-03		0.84	1.91E-01		0.81	1.50E-01
GOX0357		30S Ribosomal protein S11		0.37	6.30E-03		0.79	8.98E-03		0.86	2.68E-01
GOX0359		Adenylate kinase		0.39	1.77E-03		0.72	1.18E-03		0.87	2.07E-01
GOX0360		Preprotein translocase subunit SecY		0.39	5.58E-03		0.76	2.54E-02		0.96	2.87E-01
GOX0361		LSU Ribosomal protein L15P		0.45	2.28E-02		0.65	1.02E-02		0.85	3.16E-01
GOX0362		LSU Ribosomal protein L30P		0.37	4.83E-03		0.55	5.90E-03		0.81	1.86E-01
GOX0363		30S Ribosomal protein S5		0.29	1.57E-03		0.61	3.61E-03		1.13	2.93E-01
GOX0364		50S Ribosomal protein L18		0.25	4.10E-03		0.61	1.52E-02		0.86	2.71E-01
GOX0365		50S Ribosomal protein L6		0.27	4.85E-04		0.69	4.07E-02		0.91	3.17E-01
GOX0366		30S Ribosomal protein S8		0.27	5.51E-03		0.64	2.57E-02		0.96	4.42E-01
GOX0367		30S Ribosomal protein S14		0.42	4.48E-03		0.73	4.80E-02		0.95	4.05E-01
GOX0368		50S Ribosomal protein L5		0.16	7.52E-04		0.63	1.86E-02		0.84	1.63E-01
GOX0369		LSU Ribosomal protein L24P		0.29	9.99E-04		0.59	5.28E-03		0.82	1.61E-01
GOX0370		LSU Ribosomal protein L14P		0.31	1.85E-03		0.61	5.08E-03		0.94	3.81E-01
GOX0371		SSU Ribosomal protein S17P		0.40	3.15E-05		0.66	1.58E-02		1.01	4.35E-01
GOX0372		LSU Ribosomal protein L29P		0.35	6.62E-04		0.67	4.41E-03		1.04	3.69E-01
GOX0373		50S Ribosomal protein L16		0.26	3.79E-04		0.73	5.82E-02		1.06	2.47E-01
GOX0374		30S Ribosomal protein S3		0.25	3.44E-03		0.72	5.49E-03		1.02	4.53E-01
GOX0375		50S Ribosomal protein L22		0.26	3.08E-03		0.77	1.20E-02		1.08	2.87E-01

GOX0376		SSU Ribosomal protein S19P		0.24	1.11E-03		0.74	2.69E-02		0.94	2.27E-01
GOX0377		50S Ribosomal protein L2		0.25	1.12E-04		0.81	6.32E-03		1.00	4.79E-01
GOX0378		LSU Ribosomal protein L23P		0.30	2.28E-04		0.81	5.28E-02		0.97	2.85E-01
GOX0379		50S Ribosomal protein L4		0.28	1.91E-04		0.88	1.37E-01		0.91	1.69E-01
GOX0380		50S Ribosomal protein L3		0.30	3.61E-05		0.86	1.07E-01		1.20	1.23E-01
GOX0381		30S Ribosomal protein S10		0.26	2.86E-03		0.73	1.14E-01		0.97	4.37E-01
GOX0382		Elongation factor Tu		0.30	2.28E-03		0.81	6.38E-02		1.50	1.87E-01
GOX0383		30S Ribosomal protein S7		0.16	2.46E-03		0.75	1.95E-02		0.93	3.30E-01
GOX0384		30S Ribosomal protein S12		0.22	1.13E-05		0.74	1.07E-01		1.61	1.83E-01
GOX0385		RNA polymerase, subunit beta'		0.40	3.14E-03		0.81	4.22E-02		0.78	1.75E-01
GOX0386		RNA polymerase, subunit beta		0.43	6.94E-03		0.80	1.67E-02		0.98	4.74E-01
GOX0387		50S Ribosomal protein L7/L12		0.21	2.90E-04		0.58	5.32E-02		1.08	2.74E-01
GOX0388		LSU Ribosomal protein L10P		0.20	5.22E-04		0.63	7.77E-02		0.93	1.84E-01
GOX0389		50S Ribosomal protein L1		0.31	3.90E-03		0.57	7.44E-04		1.28	3.19E-01
GOX0390		50S Ribosomal protein L11		0.43	1.37E-03		0.60	8.37E-03		1.05	4.08E-01
GOX0392		Putative transport transmembrane protein		0.46	7.36E-04		0.88	4.97E-02		1.45	1.51E-02
GOX0393		Putative transport transmembrane protein		0.43	5.02E-04		0.87	3.83E-02		1.27	3.50E-02
GOX0396		DNA recombination protein RmuC-like protein		0.40	4.71E-03		0.77	5.89E-03		0.87	2.67E-01
GOX0397		Hypothetical protein GOX0397		0.46	1.56E-04		0.68	1.60E-02		0.73	1.99E-02
GOX0404		Hypothetical protein GOX0404		0.13	1.57E-04		0.79	1.44E-01		1.35	2.96E-02
GOX0405		TonB-dependent outer membrane receptor		0.09	1.69E-04		0.55	1.94E-03		0.76	1.03E-01
GOX0413		Acetyl-coenzyme A synthetase		0.48	5.74E-03		0.85	3.56E-02		0.73	1.45E-01
GOX0415		Putative transport protein		0.30	2.99E-04		0.78	9.60E-02		0.62	1.34E-02
GOX0416		Protein-tyrosine phosphatase		0.33	1.17E-04		0.92	1.28E-01		1.30	9.85E-02
GOX0421		Flagellar motor switch protein		2.18	2.53E-03		1.23	5.62E-02		1.14	1.26E-02
GOX0422		Hypothetical protein GOX0422		2.17	1.93E-02		1.19	1.72E-01		1.04	3.76E-01
GOX0425		Basal-body rod modification protein FlgD		3.04	4.05E-04		1.69	7.22E-04		1.22	2.09E-02

GOX0435		Acetyl-CoA carboxylase biotin carboxylase subunit		0.49	4.09E-04		0.91	9.97E-02		0.81	1.93E-01
GOX0440		Ornithine decarboxylase		0.31	9.08E-04		0.72	1.96E-02		0.95	1.08E-01
GOX0443		Molybdopterin (MPT) converting factor. subunit 2		2.27	3.28E-04		1.16	5.15E-02		0.95	3.39E-01
GOX0444		Bifunctional molybdenum cofactor biosynthesis protein (Molybdopterin-guanine dinucleotide biosynthesis protein A and MoaD)		2.28	2.48E-03		1.27	4.35E-02		0.96	3.81E-01
GOX0445		Molybdenum cofactor biosynthesis protein C		3.07	5.58E-05		1.30	9.68E-03		1.06	2.70E-01
GOX0451		30S Ribosomal protein S9		0.22	1.89E-04		0.84	2.08E-01		0.89	1.13E-01
GOX0452		50S Ribosomal protein L13		0.31	1.04E-02		0.76	6.39E-02		0.83	2.61E-01
GOX0474		Hypothetical protein GOX0474		0.48	1.85E-02		0.96	3.36E-01		1.65	2.95E-03
GOX0475		Hypothetical protein GOX0475		2.16	1.25E-03		1.40	3.85E-02		1.53	8.06E-03
GOX0506		RNA polymerase factor sigma factor H (sigma-32)		4.04	3.77E-05		1.34	7.08E-02		1.06	3.67E-01
GOX0512		Amino acid transport protein		0.32	1.31E-03		0.90	1.65E-01		0.68	8.19E-03
GOX0513		Transcriptional regulator. AsnC family		0.39	1.05E-03		0.96	1.42E-01		0.79	2.82E-02
GOX0515		Hypothetical protein GOX0515		0.18	1.00E-04		0.78	7.14E-02		1.30	5.52E-02
GOX0516		Uncharacterized PQQ-dependent dehydrogenase 4		0.49	5.09E-03		0.91	2.12E-01		0.75	4.33E-02
GOX0522		Transcriptional regulator		0.33	2.09E-03		0.93	3.67E-01		0.58	3.89E-03
GOX0549		Hypothetical protein GOX0549		2.51	1.37E-03		1.17	7.29E-02		0.82	6.10E-02
GOX0562		Putative siderophore receptor protein		0.32	1.67E-03		0.80	1.52E-02		0.96	4.04E-01
GOX0564		Cytochrome *c*552		2.02	1.22E-03		1.16	3.54E-02		0.99	3.77E-01
GOX0568		Hypothetical protein GOX0568		0.33	9.58E-05		0.99	4.63E-01		1.62	1.97E-02
GOX0570		Hypothetical protein GOX0570		2.37	3.04E-05		1.19	7.51E-04		1.26	1.14E-01
GOX0571		Hypothetical protein GOX0571		2.62	4.14E-03		0.92	1.55E-01		1.12	3.36E-01
GOX0572		Putative oxidoreductase		3.61	1.73E-03		0.96	1.57E-01		1.01	4.58E-01
GOX0573		Metallo-beta-lactamase superfamily protein		4.81	1.68E-03		1.05	3.47E-02		0.93	2.78E-01
GOX0585		Cytochrome *c* subunit of aldehyde		2.02	5.61E-04		1.23	6.61E-02		1.19	1.56E-01

		dehydrogenase									
GOX0586		Membrane-bound aldehyde dehydrogenase. small subunit		2.01	1.17E-03		1.17	2.13E-03		1.09	9.70E-02
GOX0596		30S Ribosomal protein S1		0.41	5.43E-05		0.81	6.54E-02		0.89	7.86E-02
GOX0599		Hypothetical protein GOX0599		0.39	6.00E-04		0.82	1.17E-01		0.83	4.49E-02
GOX0600		Hypothetical protein GOX0600		0.40	6.32E-03		0.86	2.73E-01		0.81	4.39E-02
GOX0607		D-Aalanyl-D-alanine carboxypeptidase		2.51	7.26E-06		1.35	3.82E-02		0.94	2.82E-01
GOX0609		ATP-dependent Clp protease ATP-binding subunit ClpA		2.85	1.16E-04		1.32	6.74E-02		0.77	1.62E-01
GOX0610		Hypothetical protein GOX0610		0.47	1.95E-03		0.88	2.17E-02		0.88	1.89E-01
GOX0618		Hemolysin-related protein		2.46	1.50E-02		1.15	1.45E-01		0.96	3.13E-01
GOX0619		Hypothetical protein GOX0619		2.56	7.14E-04		1.45	3.24E-03		1.15	3.09E-02
GOX0620		Chemotactic signal-response protein CheL		2.54	7.18E-05		1.52	2.06E-02		1.05	3.63E-01
GOX0674		Ferrous iron transport protein B (FeoB)		3.24	1.40E-02		1.73	8.93E-04		0.84	3.02E-01
GOX0683		Protein with GGDEF domain		2.13	6.88E-03		1.50	3.42E-03		1.01	4.44E-01
GOX0689		Probable outer membrane efflux lipoprotein		0.41	8.87E-04		0.86	5.38E-02		0.65	3.20E-02
GOX0690		Acriflavin resistance protein B (mulitdrug efflux system)		0.40	7.85E-04		0.85	5.84E-02		0.83	2.56E-02
GOX0691		Acriflavin resistance protein A (mulitdrug efflux system)		0.39	2.28E-04		0.79	5.21E-02		0.76	3.22E-02
GOX0694		Hypothetical protein GOX0694		2.53	4.97E-04		1.48	2.23E-02		0.97	3.55E-01
GOX0695		Hypothetical protein GOX0695		2.56	1.57E-03		1.43	6.39E-03		0.97	4.29E-01
GOX0697		Flagellar FliL protein		2.40	1.97E-03		1.50	7.66E-02		1.19	1.49E-01
GOX0699		L-Asparagine permease		0.16	1.95E-13		0.64	2.24E-03		0.68	1.19E-03
GOX0708		Hypothetical protein GOX0708		2.18	1.47E-02		1.22	5.76E-02		1.29	2.74E-02
GOX0745		Hypothetical protein GOX0745		0.29	2.31E-03		0.87	3.99E-02		1.51	2.89E-02
GOX0746		FAD-dependent monooxygenase		2.03	5.97E-04		1.09	3.07E-01		1.10	2.83E-01
GOX0747		Serine O-acetyltransferase CysE		2.05	9.70E-03		1.03	3.77E-01		0.96	2.38E-01
GOX0748		Aldose 1-epimerase		0.35	3.49E-06		0.93	1.37E-01		1.23	2.41E-02

GOX0755		Hypothetical protein in adhS 5' region		2.36	1.50E-03		1.04	3.97E-01		1.40	6.97E-02
GOX0758		Porin		0.19	2.03E-03		0.89	6.75E-02		0.68	9.67E-02
GOX0762		Thioredoxin		2.10	3.79E-04		1.29	1.98E-02		1.17	5.51E-02
GOX0767		Hypothetical protein GOX0767		0.49	3.71E-03		0.88	8.80E-02		0.99	4.55E-01
GOX0771		Ferric uptake regulation protein		0.49	3.24E-04		0.92	1.08E-01		0.97	3.05E-01
GOX0772		Transcriptional regulator. Ros/MucR family		0.16	9.12E-05		0.77	1.53E-02		0.97	1.63E-01
GOX0774		Ribosomal-protein-alanine acetyltransferase		0.49	3.70E-02		0.94	7.37E-02		1.28	7.41E-02
GOX0775		Hypothetical protein GOX0775		0.46	4.78E-03		0.92	2.44E-01		0.85	2.21E-01
GOX0778		Two component sensor histidine kinase		0.42	6.51E-03		1.00	4.79E-01		0.65	1.87E-02
GOX0797		Hypothetical protein GOX0797		0.46	5.38E-04		1.67	3.31E-03		1.41	5.76E-02
GOX0805		Hypothetical protein GOX0805		0.45	5.84E-04		0.90	2.74E-02		0.84	8.51E-02
GOX0806		Hypothetical protein GOX0806		0.34	3.92E-03		0.91	2.50E-01		0.76	5.83E-02
GOX0807		Hypothetical protein GOX0807		0.33	6.11E-03		0.78	2.74E-02		0.73	3.00E-02
GOX0813		Phosphocarrier protein HPr		2.20	5.48E-03		1.25	3.64E-02		1.29	7.87E-02
GOX0814		PTS system, IIA component		4.10	1.59E-04		1.28	1.10E-01		1.23	7.03E-02
GOX0815		Hypothetical protein GOX0815		6.53	1.86E-04		1.43	7.47E-02		1.03	3.23E-01
GOX0823		Threonyl-tRNA synthetase		0.48	3.21E-04		0.88	8.02E-02		0.93	3.00E-01
GOX0827		Hypothetical protein GOX0827		0.46	6.29E-05		1.15	1.43E-01		1.68	5.69E-04
GOX0828		Hypothetical protein GOX0828		0.49	1.05E-04		1.17	1.24E-01		1.42	4.43E-03
GOX0834		Putative oxidoreductase		0.50	2.40E-03		0.96	7.17E-02		0.87	4.83E-02
GOX0835		Adenine phosphoribosyltransferase		0.30	1.65E-03		0.84	7.10E-02		1.11	1.69E-01
GOX0845		Hypothetical protein GOX0845		0.44	1.52E-03		0.90	3.04E-02		1.80	3.62E-02
GOX0846		Hypothetical protein GOX0846		0.36	1.13E-03		0.81	1.67E-01		1.24	1.20E-01
GOX0849		NADPH-dependent L-sorbose reductase		0.44	2.14E-03		1.22	3.88E-02		1.50	1.55E-02
GOX0854		D-Sorbitol dehydrogenase subunit SldA		0.10	4.81E-06		0.93	2.22E-01		1.10	3.32E-01
GOX0855		D-Sorbitol dehydrogenase subunit SldB		0.10	6.38E-05		0.86	2.05E-01		1.94	9.18E-02
GOX0859		Shikimate 5-dehydrogenase		0.31	3.82E-04		0.87	8.32E-02		1.66	1.72E-04

GOX0861		Flavohemoprotein		2.15	1.56E-02		1.31	2.66E-03		1.29	1.59E-01
GOX0866		S-Adenosylmethionine synthetase		0.18	1.16E-03		0.99	4.62E-01		1.00	4.89E-01
GOX0867		SAM-dependent methyltransferase		0.21	1.27E-04		0.99	4.28E-01		1.10	9.29E-02
GOX0868		Electron transfer flavoprotein-ubiquinone oxidoreductase/ putative oxidoreductase		0.28	1.40E-04		1.05	3.33E-01		1.02	3.42E-01
GOX0872		Proline tRNA		2.00	2.01E-02						
GOX0874		Ferrochelatase		2.21	2.71E-04		1.11	2.98E-01		1.08	2.88E-01
GOX0875		AtsE protein		2.42	1.24E-04		1.31	1.14E-02		1.45	1.22E-02
GOX0880		Hypothetical protein GOX0880		3.00	1.54E-02		1.05	2.32E-01		1.26	5.70E-02
GOX0886		Hypothetical protein GOX0886		3.46	1.15E-03		1.07	2.52E-01		1.12	2.50E-01
GOX0901		Xanthine/uracil permease		0.43	1.81E-04		0.91	1.27E-01		0.54	2.25E-03
GOX0909		Thiol:disulfide interchange protein DsbD		0.45	9.81E-04		0.78	5.53E-02		0.63	1.07E-01
GOX0915		Hypothetical protein GOX0915		2.94	9.15E-03		1.35	3.25E-03		1.11	2.76E-01
GOX0946		Putative oxidoreductase		2.29	2.93E-03		1.10	2.91E-01		1.05	1.97E-01
GOX0952		Flagellar basal body P-ring biosynthesis protein FlgA		2.79	2.03E-04		1.66	1.69E-02		1.13	3.83E-02
GOX0960		Protein with GGDEF and EAL domain		2.32	3.49E-05		1.29	7.89E-05		1.03	2.27E-01
GOX0969		Hypothetical protein GOX0969		0.32	3.62E-05		0.83	1.72E-02		0.76	2.09E-02
GOX0970		Outer membrane channel lipoprotein		0.49	1.46E-04		0.80	2.10E-02		0.86	1.11E-01
GOX0971		Cation efflux system protein CzcA		0.49	6.62E-04		0.83	6.31E-02		0.79	1.35E-01
GOX0972		Cation efflux system protein CzcB		0.44	1.21E-03		0.81	1.81E-03		0.89	8.52E-02
GOX0973		Outer membrane channel lipoprotein		3.39	1.41E-04		1.22	3.92E-02		0.96	2.78E-01
GOX0978		Bifunctional riboflavin biosynthesis protein RibD		0.33	2.03E-03		0.84	6.26E-02		0.99	4.32E-01
GOX0979		Riboflavin synthase subunit alpha		0.43	1.46E-03		0.87	1.08E-02		1.03	4.12E-01
GOX0980		3,4-Dihydroy-2-butanone 4-phosphate synthase/GTP cyclohydrolase II		0.35	2.31E-03		0.74	7.83E-03		1.13	2.38E-01
GOX0981		6,7-Dimethyl-8-ribityllumazine synthase		0.44	7.57E-04		0.80	1.06E-01		0.88	1.26E-01
GOX0986		Coenzyme PQQ synthesis protein B		0.37	3.42E-07		0.86	9.08E-02		1.27	6.62E-05

GOX0987		Coenzyme PQQ synthesis protein A		0.44	3.84E-03		0.90	3.72E-01		1.20	8.45E-02
GOX0996		Transposase (class II)		2.34	1.70E-03		1.14	3.05E-01		0.99	4.59E-01
GOX1003		Septum formation associated protein (Maf-like protein)		0.44	1.44E-03		0.83	4.31E-02		0.93	3.26E-01
GOX1015		TonB-dependent receptor of ferrichrome transport system		0.42	1.30E-03		0.98	2.43E-01		1.12	1.43E-01
GOX1022		Transcriptional regulator		0.41	5.98E-03		1.10	2.80E-01		0.84	2.89E-02
GOX1024		Heat shock protein 90		2.63	1.72E-05		1.57	2.31E-02		1.21	3.60E-03
GOX1029		Hypothetical protein GOX1029		0.47	4.09E-03		0.99	3.57E-01		0.97	3.66E-01
GOX1070		Transcription termination factor Rho		0.46	7.53E-03		0.92	2.75E-01		0.94	3.84E-01
GOX1087		Acetolactate synthase large subunit		0.34	2.64E-04		0.73	5.28E-02		0.83	1.15E-01
GOX1088		Acetolactate synthase 3 regulatory subunit		0.35	8.20E-05		0.83	1.49E-02		0.86	5.61E-02
GOX1089		Ketol-acid reductoisomerase		0.37	6.30E-04		0.79	1.22E-01		0.76	4.68E-02
GOX1090		S-Adenosylmethionine decarboxylase proenzyme		0.27	6.47E-04		0.70	3.71E-03		0.84	9.11E-02
GOX1091		Spermidine synthase		0.11	3.05E-04		0.72	1.85E-03		0.88	1.02E-01
GOX1106		Alanine tRNA		2.91	5.58E-03		0.92	4.28E-01		0.83	2.02E-01
GOX1107		O-antigen biosynthesis protein RfbC		3.16	8.54E-04		1.46	1.13E-02		1.12	2.13E-01
GOX1108		Hypothetical protein GOX1108		0.49	6.79E-04		0.89	1.49E-01		1.10	2.73E-01
GOX1110		F_1F_o ATP synthase subunit b'		0.48	3.19E-03		0.92	5.08E-02		0.89	2.40E-01
GOX1111		F_1F_o ATP synthase subunit b		0.40	5.54E-03		0.92	1.83E-01		1.01	4.70E-01
GOX1114		Vitamin B12-dependent ribonucleotide reductase		0.31	1.10E-04		0.67	9.31E-02		0.93	2.47E-01
GOX1131		Pyrroline-5-carboxylate reductase		2.17	1.40E-04		1.09	2.13E-01		0.91	1.04E-01
GOX1132		Hypothetical protein GOX1132		3.01	1.47E-03		1.53	2.09E-04		0.99	4.67E-01
GOX1137		Probable lipopolysaccharide modification acyltransferase		0.44	1.43E-03		0.79	8.45E-02		0.67	6.86E-02
GOX1141		LSU Ribosomal protein L25P		0.31	2.32E-04		0.66	1.69E-02		0.98	3.49E-01
GOX1142		Peptidyl-tRNA hydrolase		0.31	7.95E-04		0.70	4.59E-03		0.94	1.72E-01

GOX1174		Purine-cytosine permease		0.49	7.94E-03		0.87	2.50E-01		0.63	4.61E-02
GOX1179		Putative sugar uptake ABC transporter permease protein		0.44	2.94E-04		0.95	3.16E-01		1.08	1.43E-01
GOX1190		Glucose-1-phosphatase		2.07	3.58E-03		1.02	3.26E-01		0.99	4.58E-01
GOX1192		Transcriptional regulator, MarR/AsnC family		0.49	7.02E-03		0.96	1.66E-01		1.16	1.41E-01
GOX1197		Hypothetical protein GOX1197		0.22	6.10E-04		0.87	2.54E-01		0.79	9.56E-02
GOX1198		Sulfite reductase (Ferredoxin)		0.25	3.23E-04		0.78	7.52E-02		0.92	1.94E-01
GOX1199		Putative oxidoreductase		0.35	1.41E-03		0.86	2.39E-01		0.88	1.83E-01
GOX1230		Gluconate 2-dehydrogenase, cytochrome *c* subunit		0.23	3.24E-04		0.97	1.18E-01		1.43	2.95E-02
GOX1231		Gluconate 2-dehydrogenase alpha chain		0.19	1.27E-04		1.05	1.24E-01		1.42	7.57E-03
GOX1232		Gluconate 2-dehydrogenase gamma chain		0.26	2.41E-04		1.13	3.32E-01		1.16	1.48E-01
GOX1236		Ornithine carbamoyltransferase		0.33	8.54E-04		0.84	1.33E-01		0.99	4.60E-01
GOX1237		Acetylornithine aminotransferase		0.35	1.01E-03		0.81	3.13E-02		0.84	5.89E-02
GOX1239		Hypothetical protein GOX1239		2.32	3.15E-03		1.13	5.17E-02		1.00	4.74E-01
GOX1244		Putative enolase-phosphatase		0.44	4.40E-04		0.96	3.18E-01		1.10	5.25E-02
GOX1245		Riboflavin kinase		0.45	3.41E-03		0.89	1.02E-01		0.98	3.92E-01
GOX1248		Hypothetical protein GOX1248		2.28	1.42E-03		1.08	2.07E-01		0.94	2.33E-01
GOX1269		Hypothetical protein GOX1269		0.29	2.39E-04		1.36	4.14E-02		1.31	8.38E-04
GOX1273		Hypothetical protein GOX1273		2.26	1.64E-03		1.19	3.69E-02		1.13	7.14E-02
GOX1282		Ribonuclease PH		0.48	3.82E-04		0.92	3.40E-02		0.89	3.24E-02
GOX1286		Hypothetical protein GOX1286		0.16	3.74E-04		0.60	3.68E-02		0.72	7.17E-02
GOX1287		Biopolymer transport ExbB protein		0.12	4.26E-04		0.68	2.11E-03		0.79	6.87E-02
GOX1288		Biopolymer transport ExbD protein		0.16	8.95E-06		0.66	8.03E-03		0.69	3.83E-03
GOX1289		Biopolymer transport ExbD protein		0.18	3.66E-04		0.73	1.03E-01		0.61	7.60E-03
GOX1290		Hypothetical protein GOX1290		0.39	3.61E-05		0.75	1.64E-02		0.66	1.06E-02
GOX1302		Paraquat-inducible protein A		2.16	2.75E-03		0.98	3.06E-01		1.27	2.42E-02
GOX1322		Transposase (class I)		2.25	1.35E-02		1.04	3.43E-01		1.11	3.32E-01

GOX1329		Small heat shock protein		5.29	3.22E-04		1.11	2.58E-01		1.06	2.68E-01
GOX1355		Hypothetical protein GOX1355		2.27	1.02E-02		1.58	9.34E-03		1.69	3.04E-02
GOX1359		Excinuclease ABC subunit A		2.59	2.41E-03		1.16	9.97E-02		1.85	4.63E-03
GOX1365		ABC transporter permease protein		0.33	1.00E-05		0.82	4.81E-02		0.68	1.81E-02
GOX1366		ABC transporter ATP-binding protein		0.33	6.90E-06		0.79	7.06E-02		0.81	9.88E-03
GOX1381		Gluconolactonase		0.39	3.13E-04		0.87	1.40E-01		1.42	9.08E-03
GOX1392		Hypothetical protein GOX1392		0.49	2.92E-05		0.88	3.53E-02		0.97	3.66E-01
GOX1414		Chaperone protein DnaJ		2.18	5.18E-03		1.21	8.12E-02		0.99	4.78E-01
GOX1416		Porin B precursur		0.15	3.36E-04		0.58	2.56E-02		0.80	2.00E-01
GOX1418		Carbohydrate-selective porin		0.19	4.06E-05		0.78	6.87E-02		0.95	2.86E-01
GOX1424		Hypothetical protein GOX1424		2.26	4.51E-03		1.29	3.03E-02		1.07	3.65E-01
GOX1432		NADP-D-sorbitol dehydrogenase		0.46	1.41E-03		1.00	4.69E-01		1.54	7.13E-03
GOX1436		Adenosine deaminase		0.44	3.91E-04		0.93	3.16E-01		0.55	1.42E-02
GOX1440		S-Adenosylmethionine:tRNA ribosyltransferase-isomerase		0.49	2.35E-03		0.83	2.74E-02		0.90	2.53E-01
GOX1442		Hypothetical protein GOX1442		8.96	7.48E-04		1.79	1.40E-02		1.02	3.47E-01
GOX1445		Leucine tRNA		2.70	5.83E-03		1.12	3.50E-01		0.92	2.93E-01
GOX1455		ATP-dependent RNA helicase		0.27	3.89E-04		0.71	4.95E-02		0.87	1.09E-01
GOX1463		ATP-dependent Clp protease. ATP-binding subunit ClpV		3.42	1.09E-03		1.52	4.82E-02		1.57	2.20E-02
GOX1483		Capsule polysaccharide export protein		0.50	1.87E-04		0.84	8.60E-02		0.89	7.81E-02
GOX1490		Putative glycosyltransferase		0.50	1.09E-04		0.79	7.87E-02		0.89	3.78E-02
GOX1500		Hypothetical protein GOX1500		4.07	3.07E-04		1.12	2.67E-01		0.96	1.25E-01
GOX1501		Hypothetical protein GOX1501		3.88	5.38E-06		1.16	1.31E-01		0.96	1.12E-01
GOX1516		Fructose 1,6-bisphosphatase II		0.38	3.98E-03		0.92	1.93E-01		1.20	2.35E-01
GOX1521		Hypothetical protein GOX1521		2.07	1.24E-03		1.25	9.02E-02		1.09	1.58E-01
GOX1525		Flagellar biosynthetic protein FliQ		2.18	2.99E-03		1.79	9.44E-03		1.20	1.06E-01
GOX1526		Flagellar hook-basal body protein FleE		2.55	6.27E-04		1.72	1.89E-02		1.02	3.02E-01

GOX1527		Flagellar basal body rod protein FlgC		2.65	3.05E-03		1.83	1.23E-02		1.22	8.89E-02
GOX1542		Putative aluminum resistance protein		0.40	1.50E-04		0.85	7.65E-02		1.00	4.87E-01
GOX1543		Hypothetical protein GOX1543		0.43	1.11E-03		0.82	7.69E-03		0.91	2.35E-01
GOX1549		Methyl-accepting chemotaxis protein		2.06	6.42E-04		1.93	3.00E-02		1.14	3.60E-04
GOX1551		Chemotaxis protein CheY		2.16	7.08E-05		1.95	1.61E-03		1.06	1.23E-01
GOX1563		Hypothetical protein GOX1563		0.21	4.36E-03		0.71	5.34E-02		0.71	3.94E-02
GOX1567		DedA family protein		0.48	7.86E-04		0.86	3.32E-03		0.74	3.46E-02
GOX1569		Tricorn protease homolog		0.40	3.22E-04		1.07	1.96E-01		0.99	3.98E-01
GOX1572		Amino acid ABC transporter ATP-binding protein		0.43	3.87E-04		0.85	2.53E-02		0.89	9.83E-03
GOX1576		Transposase (class II)		2.70	2.28E-03		1.17	2.21E-02		0.94	2.90E-01
GOX1577		ATP-dependent Clp protease ATP-binding subunit ClpB		2.82	1.08E-05		1.30	6.63E-02		0.91	1.74E-01
GOX1578		Hypothetical protein GOX1578		2.92	1.46E-03		1.27	5.28E-02		1.09	2.75E-01
GOX1579		Hypothetical protein associated with nus operon		0.39	1.49E-03		0.71	5.96E-03		0.82	6.64E-02
GOX1617		Hypothetical protein GOX1617		2.32	3.64E-04		1.16	2.61E-01		0.94	9.93E-02
GOX1636		5-Aminolevulinate synthase		4.60	1.55E-03		1.18	3.71E-01		0.79	2.83E-01
GOX1642		Carboxypeptidase-related protein		0.20	6.54E-06		0.96	2.86E-01		1.16	2.53E-01
GOX1654		Hypothetical protein GOX1654		2.39	4.40E-04		1.23	5.37E-02		1.00	4.90E-01
GOX1662		Hypothetical protein GOX1662		0.39	6.65E-03		0.95	3.11E-01		0.61	1.97E-02
GOX1664		Recombination factor protein RarA		2.22	2.16E-03		1.07	2.28E-01		0.95	3.02E-01
GOX1671		O-Succinylhomoserine sulfhydrylase		0.29	4.11E-03		0.96	3.73E-01		1.38	1.01E-01
GOX1675		NADH dehydrogenase type II		0.37	1.12E-05		0.95	1.97E-01		1.24	2.21E-02
GOX1688		Peptidoglycan-associated lipoprotein		3.06	1.22E-06		1.42	2.77E-02		0.87	1.49E-01
GOX1697		Hypothetical protein GOX1697		2.44	5.89E-03		1.52	1.16E-02		1.07	2.94E-01
GOX1698		Aminopeptidase		2.00	8.92E-03		1.54	4.66E-02		1.01	4.79E-01
GOX1699		Hypothetical protein GOX1699		0.27	3.57E-04		0.66	7.75E-03		0.74	3.41E-02
GOX1703		Transketolase		0.47	8.92E-03		1.05	3.29E-01		1.01	4.80E-01

GOX1704		Bifunctional transaldolase/phosoglucose isomerase		0.44	1.63E-02		1.02	4.61E-01		1.18	3.11E-01
GOX1705		6-Phosphogluconate dehydrogenase-like protein		0.44	2.28E-02		0.88	4.13E-03		1.16	3.48E-01
GOX1722		Arginine tRNA		2.74	8.23E-04						
GOX1736		Hypothetical protein GOX1736		0.47	3.20E-03		0.86	3.08E-02		0.75	8.73E-02
GOX1742		Hypothetical protein GOX1742		2.37	9.42E-03		1.10	1.64E-01		0.78	6.99E-02
GOX1745		Hypothetical protein GOX1745		2.13	2.59E-03		0.94	3.75E-01		0.82	8.23E-02
GOX1752		Deoxyguanosinetriphosphate triphosphohydrolase		2.27	1.03E-04		1.22	9.70E-03		1.02	3.95E-01
GOX1768		Alkylated DNA repair protein AlkB		2.22	3.84E-03		1.08	1.31E-01		1.15	2.04E-01
GOX1773		Putative LacX protein		3.29	1.92E-03		1.17	9.52E-02		1.03	3.53E-01
GOX1774		Putative ATP-sensitive potassium channel protein		4.03	1.78E-04		1.51	1.62E-02		1.07	1.32E-01
GOX1779		Putative LysM domain protein		6.93	3.03E-05		1.23	8.35E-02		1.49	1.15E-02
GOX1780		30S ribosomal protein S4		0.27	4.71E-04		0.65	3.17E-02		1.03	4.39E-01
GOX1781		Bacterial Peptide Chain Release Factor 3 (RF-3)		0.18	8.97E-04		0.76	7.37E-02		0.92	7.71E-02
GOX1796		TonB-dependent outer membrane receptor		0.45	4.86E-03		0.83	8.36E-06		0.77	7.75E-03
GOX1815		Phosphatidate cytidylyltransferase		0.45	1.11E-02		0.88	1.04E-01		0.85	4.04E-02
GOX1828		GTPase EngB		0.44	8.15E-05		0.78	1.51E-02		0.91	2.00E-01
GOX1829		Acetylglutamate kinase		0.49	2.11E-03		0.80	8.46E-03		0.96	3.67E-01
GOX1832		Succinyl-diaminopimelate desuccinylase		0.43	1.32E-03		0.86	2.19E-01		0.81	3.81E-02
GOX1858		Hypothetical protein GOX1858		2.02	6.72E-04		1.19	8.44E-02		1.36	1.10E-01
GOX1863		Hypothetical protein GOX1863		3.42	2.94E-04		1.40	1.50E-02		0.97	3.78E-01
GOX1864		Protoheme IX farnesyltransferase		2.97	1.63E-03		1.27	4.75E-02		0.90	9.32E-02
GOX1873		DNA mismatch repair protein		0.41	6.59E-04		0.71	2.55E-02		0.74	1.99E-02
GOX1875		Hypothetical protein GOX1875		2.05	1.21E-03		1.15	2.13E-01		0.76	5.60E-03
GOX1883		Porphobilinogen deaminase		2.13	1.06E-03		1.10	2.57E-01		1.36	9.69E-02

GOX1895		Hypothetical protein GOX1895		4.12	1.45E-03		1.47	7.51E-03		0.73	2.05E-02
GOX1896		Coproporphyrinogen III oxidase		6.43	1.73E-03		1.81	2.24E-02		0.88	3.20E-01
GOX1898		Hypothetical protein GOX1898		2.08	1.19E-03		1.14	1.18E-01		1.25	8.28E-02
GOX1900		Putative carboxymethylenebutenolidase		2.09	1.63E-02		1.57	7.00E-03		1.38	1.72E-01
GOX1917		ATP-dependent DNA helicase		2.12	1.52E-02		1.22	4.13E-02		1.12	2.34E-01
GOX1923		Hypothetical protein GOX1923		2.06	1.58E-03		1.10	1.86E-01		0.99	3.75E-01
GOX1928		Hypothetical protein GOX1928		2.94	7.39E-10		1.28	7.52E-03		0.93	3.15E-01
GOX1942		Hypothetical protein GOX1942		2.25	8.45E-04		1.15	1.40E-01		1.05	2.09E-01
GOX1953		5-Methylcytosine-specific restriction enzyme		7.10	3.92E-04		1.86	7.76E-03		0.96	3.34E-01
GOX1957		Putative thiol:disulfide interchange protein II		0.40	2.21E-05		0.84	4.63E-02		0.62	8.18E-03
GOX1971		Galactose-proton symporter		0.26	9.13E-04		0.93	7.32E-02		1.07	2.80E-01
GOX1972		Putative transport protein		0.27	9.18E-04		0.98	2.24E-01		1.21	1.30E-01
GOX1988		Pyridoxamine 5'-phosphate oxidase		5.54	6.45E-04		1.31	1.06E-02		0.74	1.70E-02
GOX1995		Hypothetical protein GOX1995		2.52	1.60E-03		1.19	3.48E-02		1.01	4.48E-01
GOX2010		1-Acyl-sn-glycerol-3-phosphate acyltransferase		0.40	4.54E-02						
GOX2015		NAD(P)-dependent glucose 1-dehydrogenase		0.44	3.10E-03		0.88	1.69E-01		1.40	1.61E-02
GOX2028		Hypothetical protein GOX2028		0.17	1.27E-04		1.07	3.05E-01		1.33	1.47E-01
GOX2030		Chaperone protein DnaK		0.16	4.49E-03		0.87	2.07E-01		0.85	9.52E-02
GOX2039		Acyl-carrier-protein S-malonyltransferase		0.41	2.38E-03		0.84	2.93E-02		0.96	4.18E-01
GOX2041		Acyl carrier protein		0.47	8.08E-04		0.78	1.47E-01		1.05	2.75E-01
GOX2051		Hypothetical protein GOX2051		2.52	2.42E-03		1.21	1.98E-02		1.02	3.21E-01
GOX2052		Hypothetical protein GOX2052		2.83	6.38E-03		1.33	3.41E-02		1.10	3.07E-01
GOX2053		Hypothetical protein GOX2053		2.34	3.39E-02		1.43	1.37E-01		0.97	3.97E-01
GOX2063		Hypothetical protein GOX2063		2.38	1.79E-04		1.19	1.80E-01		0.85	5.66E-02
GOX2066		Glutaminase		8.58	1.26E-03		1.40	5.58E-02		0.91	6.50E-02
GOX2069		Transcriptional regulator. DeoR family		2.94	1.38E-03		1.38	2.03E-02		1.06	2.78E-01
GOX2073		Formyltetrahydrofolate deformylase		0.39	3.07E-03		0.83	9.52E-02		0.97	1.10E-01

GOX2074		5-Methyltetrahydrofolate-S-homocysteine methyltransferase		0.41	7.53E-07		0.78	2.22E-02		0.97	3.63E-01
GOX2134		Peptidyl-dipeptidase DCP		0.40	5.01E-05		0.97	1.89E-01		1.00	4.57E-01
GOX2135		Hypothetical protein GOX2135		0.47	1.37E-05		0.93	2.07E-01		0.92	1.48E-01
GOX2136		Aminopeptidase		0.47	9.68E-04		1.03	1.52E-01		0.99	4.46E-01
GOX2142		Hypothetical protein GOX2142		0.45	3.90E-05		1.23	7.31E-02		1.44	3.83E-02
GOX2143		ABC transporter ATP-binding protein		0.38	1.16E-03		0.98	3.84E-01		1.01	4.49E-01
GOX2151		Hypothetical protein GOX2151		0.42	2.11E-03		0.94	1.67E-01		1.15	2.24E-01
GOX2152		Hypothetical protein GOX2152		2.58	6.82E-04		1.50	7.19E-03		1.41	3.48E-02
GOX2153		Hypothetical protein GOX2153		2.63	1.96E-03		1.50	1.15E-02		1.47	4.35E-02
GOX2163		Cold shock protein		3.04	8.24E-05		1.19	1.15E-01		1.18	4.64E-03
GOX2165		Transposase (class II)		2.11	9.00E-03		1.21	3.34E-02		1.03	4.32E-01
GOX2167		F_1F_o ATP synthase subunit beta		2.81	4.36E-03		1.20	4.89E-02		0.99	1.09E-02
GOX2168		F_1F_o ATP synthase subunit epsilon		3.14	3.49E-03		1.31	1.68E-02		1.53	9.42E-02
GOX2169		F_1F_o ATP synthase subunit q		2.79	4.94E-03		1.19	4.05E-02		1.57	1.02E-01
GOX2170		F_1F_o ATO synthase subunit r		3.13	1.39E-02		1.23	1.30E-02			
GOX2171		F_1F_o ATP synthase subunit a		3.30	7.59E-03		1.25	2.15E-02		1.30	5.93E-03
GOX2172		F_1F_o ATP synthase subunit c		2.99	7.50E-04		1.22	4.50E-02		0.87	1.79E-01
GOX2173		F_1F_o ATP synthase subunit b		2.64	6.25E-03		1.19	3.81E-02		0.99	4.53E-01
GOX2174		F_1F_o ATP synthase subunit alpha		2.38	8.40E-03		1.26	1.84E-02		1.16	1.39E-01
GOX2187		Gluconate 5-dehydrogenase		0.44	5.90E-04		0.92	2.82E-01		1.47	4.10E-02
GOX2205		Hypothetical protein GOX2205		2.02	8.34E-03		0.78	7.15E-02		1.12	3.17E-01
GOX2207		Methylenetetrahydrofolate reductase		2.20	1.19E-02		0.95	2.93E-01		1.48	7.70E-02
GOX2209		Truncated transposase (class I)		2.05	2.18E-02		1.17	2.04E-01		1.05	3.47E-01
GOX2225		Thiamine biosynthesis protein ThiC		2.10	1.21E-04		1.01	4.93E-01		0.98	3.06E-01
GOX2246		Hypothetical protein GOX2246		3.52	8.30E-05		1.29	1.66E-02		1.30	8.55E-02
GOX2252		Hypothetical protein GOX2252		2.60	1.28E-04		1.07	2.05E-01		1.12	1.59E-01

GOX2253		Putative oxidoreductase		2.46	6.82E-05		1.16	8.07E-02		1.42	2.82E-03
GOX2258		Putative phytoene synthase		0.45	3.67E-04		0.84	2.35E-02		0.88	8.16E-02
GOX2260		Squalene-hopene cyclase		0.42	4.83E-04		0.76	8.06E-02		0.75	1.65E-01
GOX2272		Membrane-bound dipeptidase		2.51	1.98E-04		1.32	1.23E-01		1.04	1.98E-01
GOX2274		CDP-diacylglycerol-glycerol-3-phosphate 3-phosphatidyltransferase		2.83	5.93E-05		1.11	8.97E-02		1.01	4.71E-01
GOX2278		Hypothetical protein GOX2278		2.53	5.58E-05		1.23	1.19E-01		0.82	1.66E-01
GOX2299		Adenylosuccinate lyase		0.49	2.73E-03		0.92	2.01E-01		1.16	1.92E-02
GOX2308		Delta-aminolevulinic acid dehydratase		3.08	2.77E-07		1.63	3.80E-02		1.31	3.17E-03
GOX2311		Hypothetical protein GOX2311		2.03	1.39E-03		1.36	1.01E-02		0.81	2.04E-02
GOX2326		Hypothetical protein GOX2326		3.03	2.69E-04		1.11	1.75E-01		1.06	3.13E-01
GOX2366		Hypothetical protein GOX2366		2.04	1.48E-02		1.01	4.89E-01		1.12	1.99E-01
GOX2376		Putative aldehyde dehydrogenase		0.44	3.31E-03		1.03	4.06E-01		1.76	2.10E-02
GOX2397		Small heat shock protein		2.32	4.25E-04		1.21	8.97E-04		1.02	4.39E-01
GOX2401		Protein translocase subunit SecF		0.48	2.41E-04		0.84	1.28E-02		0.99	4.48E-01
GOX2402		Preprotein translocase subunit SecD		0.39	2.54E-03		0.92	2.71E-01		0.76	7.52E-02
GOX2406		RNA polymerase sigma factor E (sigma-24)		2.53	3.37E-03		1.34	2.94E-02		1.03	4.11E-01
GOX2409		ABC transporter, cytochrome *bd* biogenesis CydD		2.26	4.23E-06		1.41	8.39E-03		1.62	9.02E-03
GOX2410		ABC transporter, cytochrome *bd* biogenesis CydC		2.48	3.04E-03		1.32	7.01E-02		1.34	7.25E-02
GOX2413		Hypothetical protein GOX2413		3.24	3.29E-04		1.34	4.91E-02		1.15	1.59E-01
GOX2455		Putative phage-related protein		2.55	3.56E-03		1.11	2.07E-01		1.11	1.64E-01
GOX2457		Phage DNA Packaging Protein		2.75	6.38E-04		1.07	2.54E-01		0.90	3.07E-01
GOX2461		Hypothetical protein GOX2461		2.19	7.04E-03		1.08	9.86E-18			
GOX2470		Hypothetical protein GOX2470		2.54	4.78E-03		1.25	5.89E-02		0.96	3.82E-01
GOX2471		Transcriptional regulator, XRE family		2.32	9.96E-03		1.10	2.10E-01		1.18	1.56E-01
GOX2486		Cyteine tRNA		2.54	1.21E-03						
GOX2487		Outer membrane protein TolC		3.80	7.60E-04		1.47	2.79E-02		1.05	3.08E-01

GOX2488		Hypothetical protein GOX2488		2.35	1.60E-04		1.05	3.38E-01		1.10	1.75E-01
GOX2491		Dihydroxy-acid dehydratase		0.35	1.81E-04		0.83	2.15E-02		0.74	7.89E-03
GOX2500		Formamidopyrimidine-DNA glycosylase		2.13	1.09E-03		1.04	3.40E-01		0.87	1.50E-01
GOX2520		Hypothetical protein GOX2520		4.15	1.04E-03		1.42	1.32E-01		1.32	3.65E-02
GOX2546		Replication protein A		0.42	3.86E-03		0.99	4.14E-01		1.06	3.15E-01
GOX2560		RND-type multidrug efflux pump, membrane permease		0.49	2.93E-03		1.05	3.17E-01		0.94	3.28E-01
GOX2561		RND-type multidrug efflux pump, outer membrane protein		0.50	1.16E-03		0.99	7.71E-02		1.02	4.22E-01
GOX2578		Putative isochorismatase		0.46	1.87E-03		1.02	3.68E-01		0.99	4.39E-01
GOX2580		Hypothetical protein GOX2580		0.42	3.27E-04		1.07	2.63E-01		0.94	2.12E-03
GOX2603		Replicator initiator RepC		0.42	6.97E-04		0.98	2.82E-01		0.79	5.91E-02
GOX2616		DotI		0.35	4.13E-03		1.04	2.94E-01		1.06	1.21E-01
GOX2646		DNA integration/recombination/invertion protein		3.15	2.08E-03		1.23	7.12E-02		1.25	4.08E-02
GOX2647		Hydroxyacylglutathione hydrolase		2.15	1.51E-05		1.25	2.98E-02		1.01	4.70E-01
GOX2659		Transposase		2.38	9.18E-04		1.21	1.13E-01		1.18	1.10E-01
GOX2675		Transposase		2.47	3.08E-04		1.08	2.64E-01		0.98	3.52E-01
GOX2684		NAD(P)H-dependent 2-cyclohexen-1-one reductase		3.17	6.71E-05		1.58	9.60E-03		1.36	1.26E-02
GOX2685		Transposase		2.77	2.06E-03		1.15	1.25E-01		1.05	1.60E-01
GOX2699		Hypothetical protein GOX2699		2.17	1.72E-05		1.19	5.60E-03		1.15	1.68E-01
GOX2719		Transposase		10.98	5.65E-05		1.37	2.99E-02		0.86	2.39E-01
GOX2720		Hypothetical protein GOX2720		12.34	2.03E-04		1.40	1.21E-01		0.93	3.63E-01
GOX2733		Hypothetical protein GOX2733		2.00	7.37E-03		1.15	2.58E-01		0.91	1.78E-01
GOX2734		Hypothetical protein GOX2734		2.07	1.12E-02		1.14	2.31E-01		0.92	2.68E-01

3.4. Terminal oxidases in *G. oxydans* 621H

Own contribution to this manuscript about 40%. I constructed the cytochrome oxidase deletion mutants and carried out all experimental work except for the RAMOS cultivations and the measurements of oxygen consumption. I wrote a draft of the manuscript. I am first author of the manuscript together with Bettina Luchterhand.

To be submitted to the Journal of Bacteriology

Impact factor: 3.825

Characterization of cytochrome *bd*- and cytochrome bo_3-terminal oxidase deletion mutants of *G. oxydans* reveals bo_3 oxidase as the rate-limiting factor of the respiratory chain

ABSTRACT

The obligatory aerobic acetic acid bacterium *G. oxydans* oxidizes a variety of substrates in the periplasm by membrane-bound dehydrogenases, which transfer the reducing equivalents to ubiquinone. Two quinol oxidases, cytochrome bo_3 and cytochrome *bd*, then catalyze transfer of the electrons to molecular oxygen with concomitant formation of water. In this study, mutants lacking either of these terminal oxidases were characterized with respect to growth, H^+/O ratios and cytochrome content. Deletion of the *cydAB* genes for cytochrome *bd* oxidase had no obvious influence on these parameters. Using a respiration activity monitoring system and adjusting different levels of oxygen availability, a low affinity of cytochrome *bd* oxidase to oxygen was demonstrated. These results were supported by measurement of oxygen consumption in a respirometer. Deletion of the *cyoBACD* genes for cytochrome bo_3 oxidase resulted in a severe growth defect on agar plates and in shake flasks. The H^+/O ratio of the Δ*cyo* mutant with mannitol as substrate was 0.49 ± 0.06 and thus 61% lower than that of the reference strain (1.26 ± 0.06), indicating that cytochrome bo_3 oxidase is the main component for proton extrusion via the respiratory chain. In support of this, plasmid-based overproduction of cytochrome bo_3 oxidase resulted in an improved growth yield.

INTRODUCTION

Gluconobacter oxydans is a Gram-negative, obligate aerobic, rod-shaped α-proteobacterium belonging to the family of acetic acid bacteria (22). Due to its many membrane-bound dehydrogenases that incompletely oxidize sugars and sugar alcohols stereo- and regioselectively in the periplasm, *G. oxydans* is used since long in industrial biotechnology (16). Important applications are in the production of vitamin C or of 6-amino-L-sorbose, an intermediate in the synthesis of the antidiabetic drug miglitol (42).

G. oxydans possesses 32 membrane-bound dehydrogenases, 11 with known and 21 with unknown substrate specificity (Fig. 1) (17). Electrons are transferred from the various dehydrogenases via pyrroloquinoline quinone (PQQ), PQQ plus cytochrome *c*, or FAD to ubiquinone. Electron transfer from ubiquinol to oxygen is catalyzed by two terminal oxidases, cytochrome *bd* and cytochrome bo_3 (2) (Fig. 1). Interestingly, the genome sequence of *G. oxydans* 621H revealed the presence of the *qcrABC* genes for a cytochrome bc_1 complex and of a *cycA* gene for a soluble cytochrome *c*, whereas genes for a cytochrome *c* oxidase were absent (39). Furthermore, genome sequencing revealed that *G. oxydans* possesses only a non-proton-pumping single subunit NADH dehydrogenase encoded by the *ndh* gene. Whereas genes for a succinate-quinone oxidoreductase were lacking, the gene *mqo* for a malate:quinone oxidoreductase was identified.

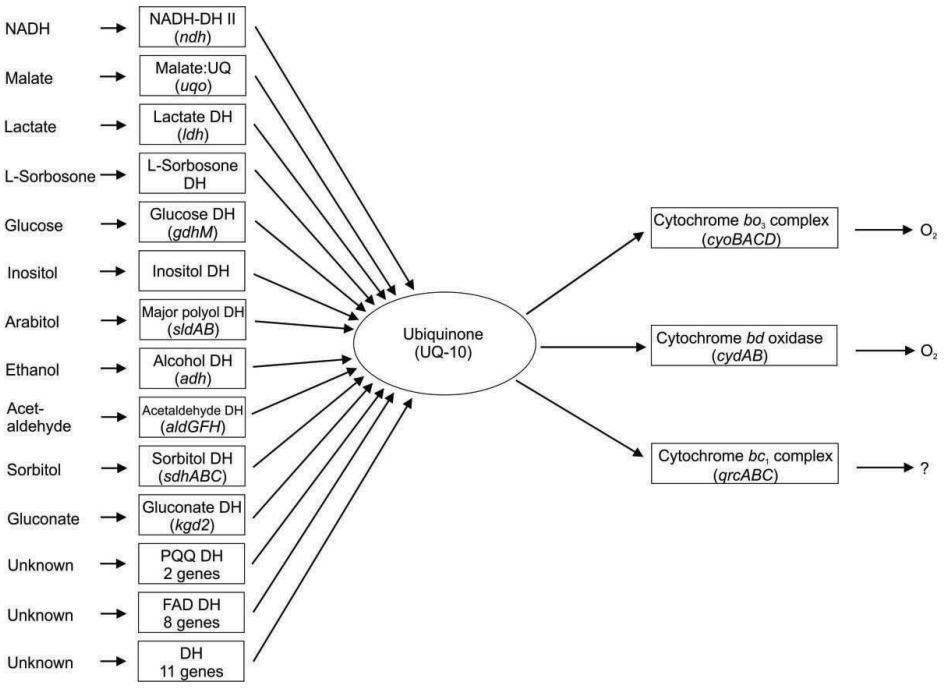

FIG 1 Overview of the components of the respiratory chain of *G. oxydans*. DH, dehydrogenase.

The cytochrome bo_3 quinol oxidase of *Gluconobacter suboxydans* IFO 12528 (now *G. oxydans*) has been purified and characterized (29). It belongs to the superfamily of heme-copper oxygen reductases and contains heme *b*, heme *o* and a copper ion as prosthetic

groups. The reaction catalyzed by cytochrome bo_3 quinol oxidase contributes to the generation of proton-motive force in two ways. On the one hand, ubiquinol is oxidized at the periplasmic side of the membrane, with the protons released to the periplasm and the electrons transferred to the binuclear heme o_3-Cu center. As the protons for water formation stem from the cytoplasm, an electrochemical proton gradient is established. On the other hand, heme-copper oxygen reductases can use the free energy associated with electron transfer from ubiquinol to dioxygen to pump protons across the membrane, further contributing to the establishment of proton-motive force (41). In *Escherichia coli* the bo_3 oxidase is synthesized under conditions of high aeration.

Cytochrome *bd* oxidase of *G. oxydans* was characterized as a cyanide-insensitive oxidase (2). Biochemical and spectroscopic studies of overexpression strains revealed the presence of heme b_{558}, b_{595} and *d* (33). Cytochrome *bd* oxidases are unable to pump protons, but can generate proton-motive force by oxidizing ubiquinol at the periplasmic side of the membrane and taking up protons for water formation from the cytoplasm (6, 31). In *E. coli* maximal synthesis of cytochrome *bd* occurs under microaerobic conditions (19).

The use of *G. oxydans* in biotechnological processes is limited due to its poor cell yield that results in a cost-intensive formation of biomass. *G. oxydans* IFO3293 cells cultivated with glucose as the carbon source in a bioreactor reach a cell yield 0.09 $g_{cdw}/g_{glucose}$ (25, 43). In comparison to these values *E. coli* reaches a value of 0.49 $g_{cdw}/g_{glucose}$ and *Bacillus subtilis* of 0.32 $g_{cdw}/g_{glucose}$ (15, 51).

It has been shown that the cell yield directly correlates with the number of protons moved across the membrane upon an oxygen pulse (H^+/O ratio) in many bacteria (27, 32). Whereas *Acetobacter pasteurianus* reaches a maximal cell yield of 13.1 g mol ethanol^{-1} and a H^+/O ratio of 1.9 ± 0.1, *Paracoccus pantotropha* reaches a cell yield of 25.2 g mol ethanol^{-1} and a H^+/O ratio of 4.9 ± 0.3 (27).

To gain further insights into energy generation of *G. oxydans* that can help in the rational design of new producer strains, in-frame deletion mutants of the terminal oxidases were constructed and characterized with respect to growth, respiration activity and H^+/O ratio. The results indicate that the cytochrome bo_3 oxidase is the main terminal oxidase in *G. oxydans* having an essential function in ATP synthesis via proton extrusion whereas the cytochrome *bd* oxidase is of minor importance under the tested conditions.

MATERIALS AND METHODS

Materials. Chemicals were obtained from Sigma-Aldrich (Taufkirchen, Germany), Qiagen (Hilden, Germany), Merck (Darmstadt, Germany) and Roche Diagnostics (Mannheim, Germany).

Bacterial strains, plasmids and media. The bacterial strains and plasmids used in this study are listed in Table 1. *Escherichia coli* strains were cultivated in lysogeny broth (LB) medium (4, 5) or on LB agar plates at 37°C. When required, kanamycin was added to a final concentration of 50 µg ml^{-1}. *G. oxydans* ATCC 621H Δ*upp* (ATCC 621H is identical to DSM 2343) (38) (Peters et al. 2012) strains were cultivated on mannitol medium containing 220 mM (4% w/v) mannitol, 4 g l^{-1} yeast extract, 2.5 g l^{-1} $MgSO_4$ x 7 H_2O, 1 g l^{-1} $(NH_4)_2SO_4$ and 1 g l^{-1} KH_2PO_4. The initial pH value of the medium was 6.0. *G. oxydans* possesses a natural resistance against cefoxitin. As a precaution to prevent bacterial contaminations, 50 µg ml^{-1} cefoxitin was added to the pre-culture media. When required, kanamycin was added (50 µg ml^{-1}).

Cloning and DNA techniques. For DNA manipulation standard methods were used as described by Sambrook and Russel (45). For PCR reactions, genomic DNA isolated from *G. oxydans* 621H Δ*upp* was used as template. Competent cells of *E. coli* were prepared with $CaCl_2$ and transformed as described by Hanahan (20). DNA sequencing was performed by Agowa (Berlin, Germany) and Eurofins MWG Operon (Ebersberg, Germany). Oligonucleotides were synthesized by Biolegio (Nijmegen, Netherlands) and are listed in Table 1.

TABLE 1 Bacterial strains, plasmids and oligonucleotides used in this work

Strain. plasmid or oligonucleotide	Characteristics or strains and plasmids or primer sequence (5'→ 3' sequence)[a]	Source or added restriction site
Strain		
E. coli DH5αF'	*endA*1, *hsdR*17 (rk^-, mk^+), *supE*44, *thi*-1, *recA*1, *gyrA*96, *relA*1, Δ(*lacIZYA-argF*), U169, *deoR*, F'(Φ80*dlacZ* Δ(*lacZ*)M15)	(20)
E. coli S17-1	Δ*recA*, *endA*1, *hsdR*17, *supE*44, *thi*-1, tra^+	(50)
G. oxydans Δ*upp*	*G. oxydans* 621H derivative with a deletion of GOX0327 coding for uracil phosphoribosyltransferase, reference strains in this study	A. Ehrenreich (TU Munich)

G. oyxdans Δ*upp* Δ*cydAB*	*G. oxydans* Δ*upp* derivative with a deletion of the genes *cydA* (GOX0278) and *cydB* (GOX0279) coding for cytochrome *bd* oxidase	This work
G. oxydans Δ*upp* Δ*cyoBACD*	*G. oxydans* Δ*upp* derivative with a deletion of the genes *cyoBACD* (GOX1911-1914) coding for cytochrome bo_3 oxidase	This work
Plasmid		
pAJ63a	Kan^R; pK18mobGII derivative; *lacZ*, *mob*, *oriV*, contains GOX0327 for uracil phosphoribosyltransferase including its promoter region	(38)
pAJ-*cydAB*	Kan^R; pAJ63a derivative used for marker-free deletion of the *cydAB* genes; contains an overlap extension PCR product covering the 20-bp upstream region of *edd* and the 36 bp downstream region of *eda*	This work
pAJ-*cyoBACD*	Kan^R; pAJ63a derivative used for marker-free deletion of the *cyoBACD* genes; contains an overlap extension PCR product covering 20 bp upstream region and the 67 bp downstream region of *gnd*	This work
pBBR1p384	Kan^R, pBBR1MCS-2 derivative containing the promoter region of *gox0384* for target gene expression	U. Deppenmeier (University Bonn); (24)
pBBR1p384-*cyoBACD*	Kan^R, pBBR1p384 derivative expressing *cyoBACD*	This work
pBBR1p384-*cydAB*	Kan^R, pBBR1p384 derivative expressing *cydAB*	This work
pBBR1p384-*cydABCD*	Kan^R, pBBR1p384 derivative expressing *cydABCD*	This work
Oligonucleotides		
cydAB_forw_FIA	TCTCCGGACAACCGGATCAC	
cydAB_rev_FIA	GTAGTGATGTCCGGCCATGTCGATTGCCTTCTG GGTAGATGGCGAAACGC	
cydAB_forw_FIB	AAGGCAATCGACATGGCCGGACATCACTACCAC TGAGAACAGGGAGGCCG	
cydAB_rev_FIB	CTGTTCGACAGTCTGCATCGC	
cydAB_mut_forw	ATCGCTCTCACAGCATCG	
cydAB_mut_rev	GGGCATGTGTCGTATGTC	
cydAB_screen_forw	TGAACACGCTGGAATACC	
cydAB_screen_rev	CATCGTGTCGTGCAGTTC	
cyoBACD_forw_FIA	GGGTTCGCTCAGATAACAAG	
cyoBACD_rev_FIA	GGACATCATGTTGATCATCCGTTCCGGCTTGCAG TAGTCGCCGGGAAACG	
cyoBACD_forw_FIB	AAGCCGGAACGGATGATCAACATGATGTCCCGC TAAGGTTTCTTTCGAAA	
cyoBACD_rev_FIB	ACGGATTGCGTGGAAGTC	
cyoBACD_mut_forw	GTCTATGATGCGCTGACG	
cyoBACD_mut_rev	CGATCGGAGACGTCAATG	
cyoBACD_forw	CTGGCGAAGAACAAGAAG	
cyoBACD_rev	GGTGCTGGTGTTCATGTG	

cydAB_compl_forw_XhoI	AGTTCGCTCGAGCTACCCAGAAGGCAATCGAC	XhoI
cydAB_compl_rev_KpnI	TGACTTGGTACCCAGCCCAGATCGCCACGAAC	KpnI
cydCD_compl_forw_EcoRI	GGCACGGAATTCGTCGGGCTTTTGCGACCTAT	EcoRI
cydCD_compl_rev_XhoI	GCGTAGCTCGAGCAGGATAGAGAGGTGTGAAG	XhoI
cyoBACD_compl_forw_XhoI	TGCGATCTCGAGACTACTGCAAGCCGGAACGG	XhoI
cyoBACD_compl_rev_KpnI	GTACTGGGTACCAAGGGCTGGCAGGATTTCTC	KpnI

[a]Underlined sequences indicate the regions used for overlap-extension PCR or restriction enzyme sites.

Construction of in-frame deletion mutants. Construction of *G. oxydans* Δ*upp* in-frame deletion mutants of the genes *cydAB* and *cyoBACD* was performed using a recently described method in which fluorouracil is used to select for the second homologous recombination event leading to chromosomal excision of the plasmid vector (38). For the deletion of *cyoBACD*, plasmid pAJ-*cyoBACD* was constructed as follows. 500 bp of the upstream region of *cyoA* and 500 bp of the downstream region of *cyoD* were amplified using the oligonucleotide pairs cyoBACD_forw_FlA/ cyoBACD_rev_FlA and cyoBACD_forw_FlB/ cyoBACD_rev_FlB and Phusion DNA polymerase (Fisher Scientific, Schwerte, Germany). The two PCR products were fused by overlap extension PCR with Platinum® Pfx DNA polymerase (Invitrogen, Darmstadt, Germany) using the oligonucleotides cyoBACD_forw_FlA/cyoBACD_rev_FlB. The resulting 1 kb PCR product was cloned into the SmaI restricted plasmid pAJ63a that is non-replicative in *G. oxydans*. After conjugative transfer of pAJ-*cyoBACD* from *E. coli* S17-1 to *G. oxydans* Δ*upp*, colonies were screened by PCR for chromosomal integration of pAJ-*cyoBACD* via a single homologous crossover event using the oligonucleotides cyoBACD_mut_forw and cyoBACD_mut_rev. Positive clones were inoculated overnight in 20 ml mannitol medium containing cefoxitin and kanamycin and used as a preculture for the fluorouracil enforced vector excision as described before (43). Fluorouracil-resistant colonies were screened by PCR for the chromosomal deletion of *cyoBACD* using the oligonucleotide pair cyoBACD_mut_forw/cyoBACD_mut_rev and cyoBACD_forw/cyoBACD_rev. The up- and downstream regions of the deleted genes were sequenced and the corresponding strain was named *G. oxydans* Δ*upp* Δ*cyoBACD*. Deletion of the *cydAB* genes was performed analogously with the help of plasmid pAJ-*cydAB*, which contains the upstream region of *cydA* fused to the downstream region of *cydB*. The desired strain obtained after allelic exchange was called *G. oxydans* Δ*upp* Δ*cydAB*.

Complementation studies. For complementation of the deletion mutants, the broad-host-range plasmid pBBR1p384 was used to construct three expression plasmids. The *cyoBACD* region (GOX1911-1914) including 20 bp upstream of the predicted start codon of *cyoB* was amplified using Phusion DNA polymerase (Fisher Scientific, Schwerte, Germany) with the oligonucleotides cyoBACD_compl_forw_XhoI/ cyoBACD_compl_rev_KpnI. The *cydAB* region (GOX0278-0279) including 20 bp upstream of the predicted start codon of *cydA* was amplified using Phusion DNA polymerase (Fisher Scientific, Schwerte, Germany) with the oligonucleotides cydAB_compl_forw_XhoI and cydAB_compl_rev_KpnI. The PCR products were digested with XhoI and KpnI and cloned into pBBR1p384 restricted with the same enzyme, resulting in plasmids pBBR1p384-*cyoBACD* and pBBR1p384-*cydAB.* The *cydCD* region (GOX2409-2410) including 31 bp upstream of the predicted start codon was amplified using Phusion DNA polymerase (Fisher Scientific, Schwerte, Germany) with the oligonucleotides cydCD_compl_forw_EcoRI and cydCD_compl_rev_XhoI. The PCR product was digisted with EcoRI and XhoI and cloned into pBBR1p384-*cydAB* restricted with the same enzymes, resulting in plasmid pBBR1p384-*cydABCD.* Using *E. coli* S17-1 as host, these plasmids and as a control the pBBR1p384 vector were transferred into the desired G. *oxydans* strains by conjugation.

For growth experiments with the plasmid-carrying strains, 20 ml of mannitol medium in a 100 ml baffled shake flask (3 baffles 1 x 2.5 cm each) was inoculated with cells from agar plates and incubated for 24 h at 30°C and 140 rpm. A second preculture (80 ml of mannitol medium in a 500 ml baffled shake flask, (3 baffles 1.5 x 5 cm each) was inoculated with 1% (v/v) of the first preculture and incubated for 16 h at 30°C and 140 rpm. This preculture was then used for inoculation of the main culture (100 ml mannitol medium in a 500 ml baffled shake flask (3 baffles 1.5 x 5 cm each) to an OD_{600} of 0.3. At selected time points samples for the measurement of the optical density and for HPLC analysis were taken. All cultivations were carried out in a Minitron incubation shaker (Infors HT, Basel, Switzerland).

Characterization of respiration activity and growth. Cultivations of *G. oxydans* 621H Δ*upp* and deletion mutants were performed using a self-made respiration activity monitoring system which enables the online measurement of oxygen transfer rate (OTR), carbon dioxide transfer rate (CTR) and respiration quotient (RQ) in eight parallel flasks (3). Commercial versions are available from Kuhner (Birsfelden, Switzerland) or Hitech Zang (Herzogenrath, Germany). This device was intensively used already in other investigations to study and characterize microbial systems (36, 48, 49). Offline sampling was conducted with the help of parallel 250 ml unbaffled shake flasks running simultaneously at identical conditions (30°C, 50 mm shake diameter) as the RAMOS cultivations in a ISF-4-W Kuhner

shaker (Birsfelden, Switzerland). Each sample flask was only used for one sampling in order to avoid a change of the flask filling volume. As a preculture, mannitol medium was inoculated with *G. oxydans* cells from a glycerol stock and grown overnight at 30°C. The main culture was inoculated with the preculture to an OD_{600} of 0.1. Non-limiting oxygen supply was achieved by using 10 ml mannitol medium and a shaking frequency of 350 rpm. For oxygen limiting conditions, different volumes (20 – 60 ml) of mannitol medium were used and a shaking frequency of 200 rpm. Samples of the cultures grown in parallel to the RAMOS cultures were taken at selected time points and analyzed regarding pH, optical density, and sugar concentrations.

H^+/O measurements. For determination of H^+/O ratios, 50 ml of mannitol medium (*G. oxydans*) or LB medium (*E. coli*) were inoculated to an OD_{600} of 0.3. Cells were grown to an OD_{600} of 1.5 at 30°C (*G. oxydans*) or 37°C (*E. coli*) at 140 rpm in baffled 500 ml shake flasks (3 baffles, 1.5 x 5 cm each) in a Minitron incubation shaker (Infors HT, Basel, Switzerland). Cells were harvested by centrifugation at 10,414 x *g* for 3 min at 4°C and washed twice with 25 ml 200 mM KCl each. Cells were resuspended in 1 ml 200 mM KCl and centrifuged for 5 min at 16,100 x *g* and 4°C. The supernatant was discarded and the cells were resuspended in 200 µl of 200 mM KCl. 50 µL of the cell suspension was added to 2.5 ml of an anaerobic buffer, containing 1 mM MES pH 6.0, 200 mM KCl, 50 mM KSCN, 10 mM mannitol and 24 µg ml^{-1} valinomycin, leading to a final OD_{600} of about 7 (8), which was present in a closed reaction vessel. The vessel was thermostatted at 30°C and kept anaerobic by a flow of argon. The medium in the vessel was continuously mixed with a magnetic stirrer. The pH of the medium was recorded using a micro pH electrode (Mettler Toledo, Gießen, Germany) in combination with a Seven Easy pH meter (Mettler Toledo, Gießen, Germany) and the software LabX direct pH (Mettler Toledo, Gießen, Germany). After the pH remained constant, defined volumes (12.5 µl – 50 µl) of oxygen-saturated 150 mM KCl solution were added. The solubility of O_2 in 150 mM KCl at 30°C was 223 µM which equates to 0.223 nmoles O_2/µl and therefore 0.445 ng atoms O/µl, giving a final value of 11 ng atoms O in 25 ul air-saturated 150 mM KCl**.** Calibration of the pH electrode was performed using 2.5 µl, 5 µl and 10 µl of an anaerobic 5 mM HCl solution (5 µl 5 mM HCl = 25 ng-ions H^+). The maximal acidification observed after addition of oxygen-saturated KCl was used for calculation of the H^+/O ratio without correction for the proton influx into the cells that occurred during the acidification (26). The determined H^+/O ratios therefore represented minimal values. Doubling of the concentrations of valinomycin or thiocyanate did not significantly affect the measured H^+/O values, indicating that proton translocation was not limited by insufficient charge equalization.

Respirometry. A respirometer with an electrochemical oxygen electrode was used to characterize the oxygen affinity of the reference strain and the deletion mutants. 2 ml of an overnight culture were centrifuged (5 min, 10,000 x *g*, room temperature) and the supernatant was removed. The cell pellet was resuspended in fresh complex medium to obtain a cell suspension with an OD_{600} of 15. To calibrate the respirometer, 4.9 ml of mannitol medium were filled in the measuring chamber, which was constantly mixed by a magnetic stirrer. Air saturation of the medium was achieved via surface aeration until a constant value was reached. As soon as air saturation was obtained, 100 µl of the concentrated cell suspension were transferred to the measuring chamber which was afterwards quickly closed. Bubbles inside the measuring chamber had to be avoided since they would act as oxygen source during the measurement. The voltage corresponding to the dissolved oxygen tension (DOT) was recorded continuously by a computer.

The oxygen solubility of the complex medium (0.0011 mol/L/bar) was calculated as described recently (44, 46, 47).

Determination of substrate and product concentrations by HPLC analysis. 1 ml culture was centrifuged for 5 min at 10,000 x *g* and the supernatant was filtered through a 0.2 µm PVDF filter (Carl Roth, Karlsruhe, Germany) prior to HPLC analysis. Mannitol and fructose were quantified using a Carbohydrate Pb^{2+} column 300x8 including a pre-column (CS-Chromatographie Service, Langerwehe, Germany) at 80°C in the experiments accompanying RAMOS cultivations. H_2O was used as eluent at a flow rate of 0.6 ml min^{-1}. Retention times for fructose and mannitol were 20 and 30 min, respectively. 5-Ketofructose as well as fructose and mannitol (complementation experiments) were quantified with a Rezex RCM-Monosaccharide 300×7.8 mm column (Phenomenex, Aschaffenburg, Germany) at 60°C using H_2O as the eluent at a flow rate of 0.6 ml min^{-1}. The indicated metabolites were detected by a refractive index detector. Retention times for 5-ketofructose, fructose and mannitol were 13.47, 15.23 and 19.95 min, respectively. Calibration curves were made using a series of standards ranging from 0–10 g l^{-1} mannitol, 0-15 g l^{-1} fructose and from 0–5 g l^{-1} for 5-ketofructose.

RESULTS

Construction of *G. oxydans* mutants lacking terminal oxidases. In order to investigate the role of the two terminal oxidases in *G. oxydans*, deletion mutants lacking either the *cydAB* genes for cytochrome *bd* oxidase or the *cyoBACD* genes for cytochrome bo_3 oxidase

were constructed. To obtain the *bd* mutant, 12 fluorouracil-resistant colonies obtained after the second homologous recombination event were analyzed by PCR and three of them were found to have the *cydAB* deletion. The strains were named *G. oxydans* Δ*upp* Δ*cydAB*1-3. The subsequent experiments were performed with the clone no. 1. To identify a strain lacking cytochrome bo_3 oxidase, more than 500 fluorouracil-resistant colonies had to be analyzed after the second homologous recombination event and only one of these was found to carry the *cyoBACD* deletion. The strain was named *G. oxydans* Δ*upp* Δ*cyoBACD*. The 100-fold difference in the appearance of *cydAB* and *cyoBACD* mutants already indicates that cytochrome bo_3 oxidase is of major importance for *G. oxydans*, whereas cytochrome *bd* oxidase is dispensable under the chosen growth conditions.

Growth and respiration activity of terminal oxidase mutants. Growth experiments on agar plates containing mannitol medium revealed a severe growth defect of strain *G. oxydans* Δ*upp* Δ*cyoBACD*, as the colonies grew much slower and reached a much smaller size than those of the reference strain. In contrast, strain *G. oxydans* Δ*upp* Δ*cydAB* behaved like the reference strain (Fig. 2).

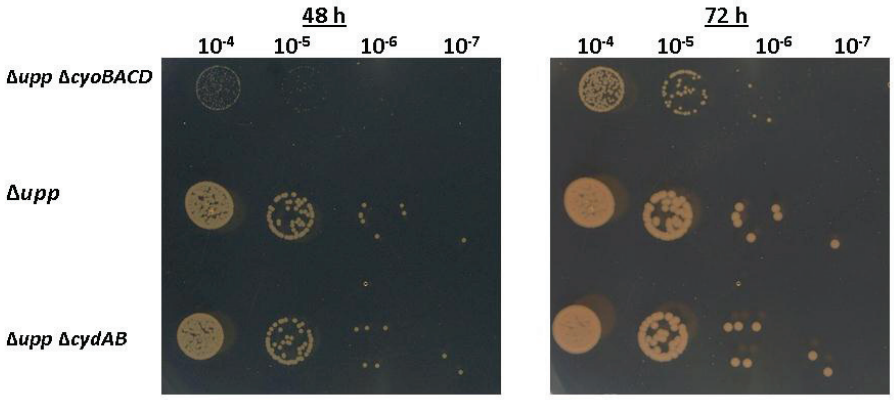

FIG 2 Growth of the indicated *G. oxydans* strains on agar plates containing mannitol medium with 1.5% agar. The plates were incubated for 48 h or 72 h at 30°C. A preculture was grown in 20 ml mannitol medium for 24 h. After the OD_{600} of all precultures was adjusted to an OD_{600} of 1, the suspension was diluted 10^{-4} to 10^{-7} in mannitol medium. 10 µl of each dilution was dropped on the agar plates. Three biological replicates of the experiment were performed with comparable results. One representative experiment is shown here.

Growth and respiration activity of the terminal oxidase mutants was analyzed in more detail using RAMOS and shake flask cultivations, both under oxygen-excess and oxygen-limited conditions (Figs. 3 and 4 and Table 2). The results obtained confirmed the findings obtained on agar plates. The final OD_{600} values were reduced in strain *G. oxydans* Δ*upp* Δ*cyoBACD*, whereas no growth difference could be detected between the strain lacking cytochrome *bd* oxidase and the reference strain, neither under oxygen excess nor under oxygen-limited conditions.

Under oxygen excess, *G. oxydans* Δ*upp and G. oxydans* Δ*upp* Δ*cydAB* reached their maximal oxygen transfer rates (OTR) of about 37 mmol l^{-1} h^{-1} after 7 h. The time-points of maximal OTR correlated with the time-point, when more than 60% of mannitol had been consumed, which is predominantly oxidized in the periplasm to fructose (43). *G. oxydans* Δ*upp* Δ*cyoBACD* reached a maximal OTR of 24 mmol $l^{-1}h^{-1}$ after 9 h, due to the by 27% reduced growth rate. The specific maximal oxygen consumption rate of the *cyo* mutant was reduced by 13% compared to the reference strain, that of the *cyd* mutant by 2%. The specific maximal CO_2 production rate of the *cyo* mutant was increased by 34% compared to the reference strain, whereas that of the *cyd* mutant was decreased by 8%. After complete consumption of mannitol, the OTR of all three strains decreased to 2 to 5 mmol l^{-1} h^{-1}, as only a small fraction of fructose was oxidized to ketofructose. During the cultivations the pH dropped from 6 to 4.5, presumably due to acetate formation (43).

TABLE 2 Growth-related parameters and respiration activities obtained during cultivation of the indicated *G. oxydans* strains under non-limiting oxygen supply and under oxygen limitation. Dry cell weight per liter was obtained using following empirical correlation: $DCW = 0.1675 \ln(OD_{600}) + 0.4684$ ($R^2 = 0.9593$).

G. oxydans strain	μ_{max} [h^{-1}]	OD_{600}	OTR_{max} [mM h^{-1}]	Spec. max. O_2 cons. rate [µmol min^{-1} $mg_{protein}^{-1}$]	Total O_2 cons. [mM]	CTR_{max} [m**M** h^{-1}]	Spec. max. CO_2 prod. rate [µmol min^{-1} $mg_{protein}^{-1}$]	Total CO_2 form. [mM]
Non-limiting oxygen supply								
Δ*upp*	0.40	3.49	37	2.08[1] (100%)	194[2]	12	0.62[1] (100%)	100[2]
Δ*upp* Δ*cydAB*	0.41	3.58	36	2.05 (99%)	183	11	0.57 (92%)	91
Δ*upp* Δ*cyoBACD*	0.30	2.12	24	1.56 (75%)	154	8	0.52 (84%)	66

Oxygen limitation								
Δ*upp*	0.38	2.81	13	0.93[1] (100%)	162[2]	6	0.38[1]	66[2]
Δ*upp* Δ*cydAB*	0.37	2.81	13	0.93 (100%)	171	5.5	0.35	65
Δ*upp* Δ*cyoBACD*	0.23	1.59	12	0.76 (82%)	142	3.5	0.22	44

[1]Calculated using the OD values at the time of maximal OTR and CTR, respectively.

[2]These values refer to an initial mannitol concentration of 40 g l^{-1} (220 mM) and were obtained by integrating the OTR and CTR curves in Fig. 3 and 4 over time.

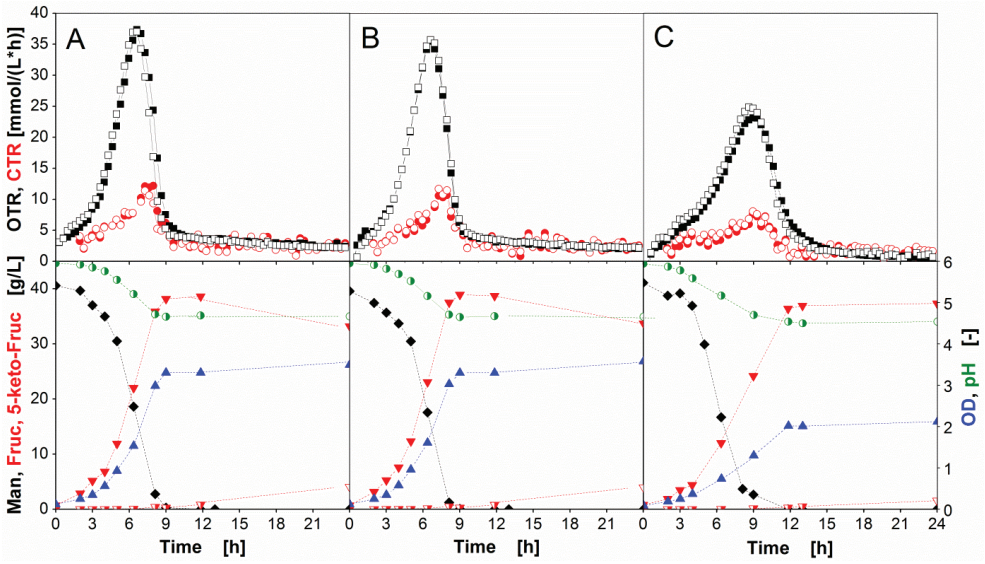

FIG 3 Growth of *G. oxydans* Δ*upp* (A), *G. oxydans* Δ*upp* Δ*cydAB* (B) and *G. oxydans* Δ*upp* Δ*cyoBACD* (C) in mannitol medium at 30°C under oxygen excess. The 250 ml flasks contained 10 ml medium and were shaken at 350 rpm with a shaking diameter of 50 mm. In the upper panels, the oxygen transfer rates (OTR)(■,□) and the carbon dioxide transfer rates (CTR)(●,○) of two independent cultures are shown. In the lower panels, the OD_{600} (▲), the pH of the medium (◑), and the concentrations of mannitol (Man) (◆), fructose (Fruc) (▼), and 5-keto-fructose (5-keto-Fruc) (▽) are shown. RAMOS experiments were conducted as duplicates and show an excellent reproducibility.

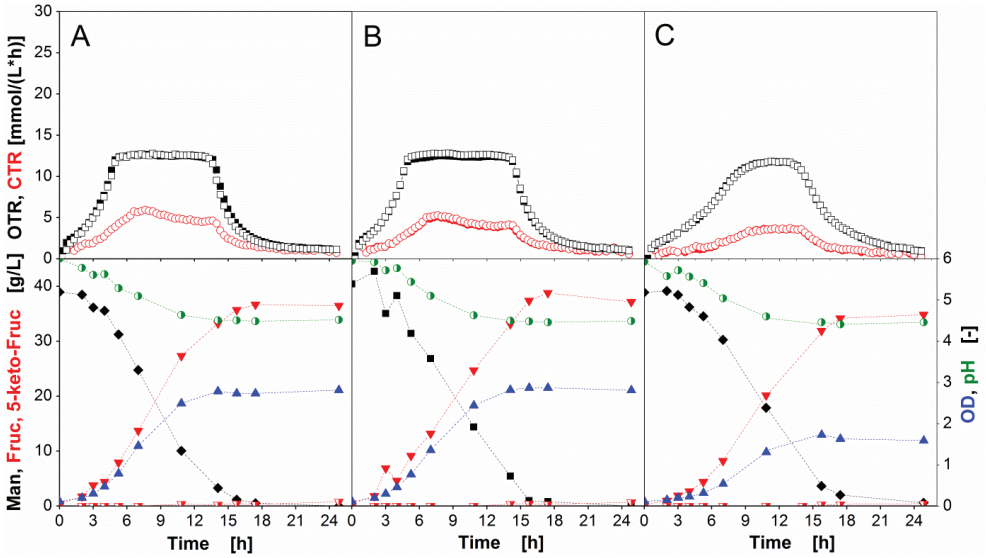

FIG 4 Growth of *G. oxydans* Δ*upp* (A), *G. oxydans* Δ*upp* Δ*cydAB* (B) and *G. oxydans* Δ*upp* Δ*cyoBACD* (C) in mannitol medium at 30°C under oxygen limitation. The 250-ml flasks contained 40 ml medium and were shaken at 200 rpm with a shaking diameter of 50 mm. In the upper panels, the oxygen transfer rates (OTR) (■,□) and the carbon dioxide transfer rates (CTR) (●,○) of two independent cultures are shown. In the lower panels, the OD_{600} (▲), the pH of the medium (◑), and the concentrations of mannitol (Man) (◆), fructose (Fruc) (▼), and 5-keto-fructose (5-keto-Fruc) (⧩) are shown. RAMOS experiments were conducted as duplicates and show an excellent reproducibility.

The results of the oxygen-limited cultivations of strains *G. oxydans* Δ*upp,* Δ*upp* Δ*cydAB* and Δ*upp* Δ*cyoBACD* are shown in Fig. 4 and Table 2. In comparison to cultivation under oxygen excess, OTR, CTR, oxygen consumption, OD_{600} and growth rate were reduced significantly, whereas the overall results were similar. As expected, the OTR remained constant during the time of oxygen limitation, visible as a horizontal plateau in the OTR graph. In the case of the reference strain and the *cydAB* mutant, the kinetics of OTR showed that both strains abruptly ran into oxygen limitation, whereas in the case of the *cyo* mutant OTR was diminished long before the cells reached the maximal OTR value. To further investigate this phenomenon, RAMOS experiments were conducted with varying medium volumes (20 – 60 ml) to achieve different degrees of oxygen limitation (Fig. 5). In all cases, the OTR kinetics of the reference strain and the *cyo* mutant were comparable to that observed in Fig. 4. Thus, the reference strain and the *cydAB* mutant are capable of high respiration rates also when oxygen becomes limiting, whereas the *cyo* mutant lacks this

ability. This indicates that cytochrome bo_3 oxidase has a high oxygen affinity, whereas cytochrome *bd* oxidase has a low oxygen affinity. Similar results as shown here for mannitol-grown cells were also observed for glucose-grown cells (data not shown), confirming that they are not dependent on the carbon source.

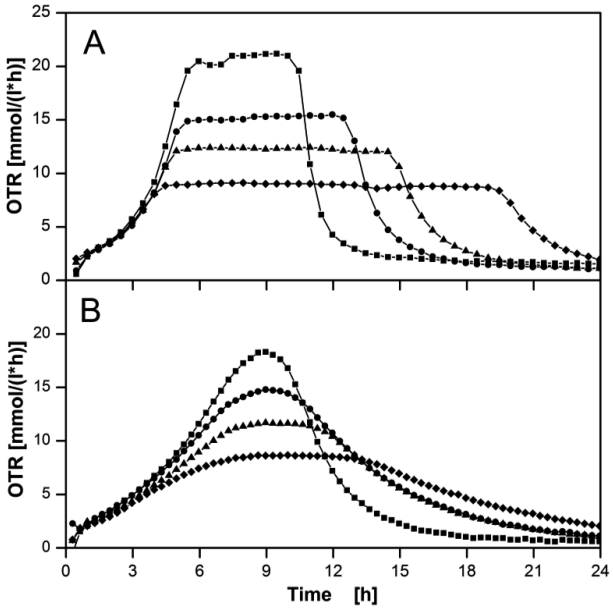

FIG 5 Comparison of OTRs of strains *G. oxydans* Δ*upp* (A) and *G. oxydans* Δ*upp* Δ*cyoBACD* (B) in mannitol medium at 30°C at oxygen-limited conditions. The 250-ml unbaffled flasks contained 20 ml (■), 30 ml (●), 40 ml (▲) or 60 ml (◆) medium and were shaken at 200 rpm with a shaking diameter of 50 mm. The maximal OTR values obtained for the reference strain were 21.0, 15.0, 12.5, and 9.0 mmol l^{-1} h^{-1}, those for the *cyo* mutant were 18.5, 14.5, 11.5, 8.5 mmol l^{-1} h^{-1}.

Respirometry. To further analyze the respiration activities of the reference strain and the terminal oxidase mutants, oxygen consumption was measured in a respirometer (Fig. 6). Oxygen consumption of the strain lacking cytochrome bo_3 oxidase occurred significantly slower than that of the reference strain and the *bd* oxidase deletion mutant. Comparison of the slope of DOT curves, which is equivalent to the oxygen transfer rates, demonstrated a 30% lower value for the bo_3-deleted strain (2.3 ± 0.06 mM h^{-1} Δ*upp* Δ*cyoBACD,* 3.55 ± 0.11

mM h^{-1} Δ*upp* Δ*cydAB* and 3.26 ± 0.03 mM h^{-1} Δ*upp*). Additionally, the relation of $OTR_{\Delta upp\ \Delta bo3}$ to $OTR_{\Delta upp}$ is in good agreement with the corresponding ratio of specific growth rates μ_{max}. At low oxygen concentrations (~10% DOT at the least) reference strain and *bd* deletion mutant showed a reduced consumption of oxygen. The effect was most prominent for strain *G. oxydans* Δ*upp* Δ*cyoBACD* (~25% DOT), supporting the hypothesis of a low oxygen affine terminal cytochrome *bd* oxidase.

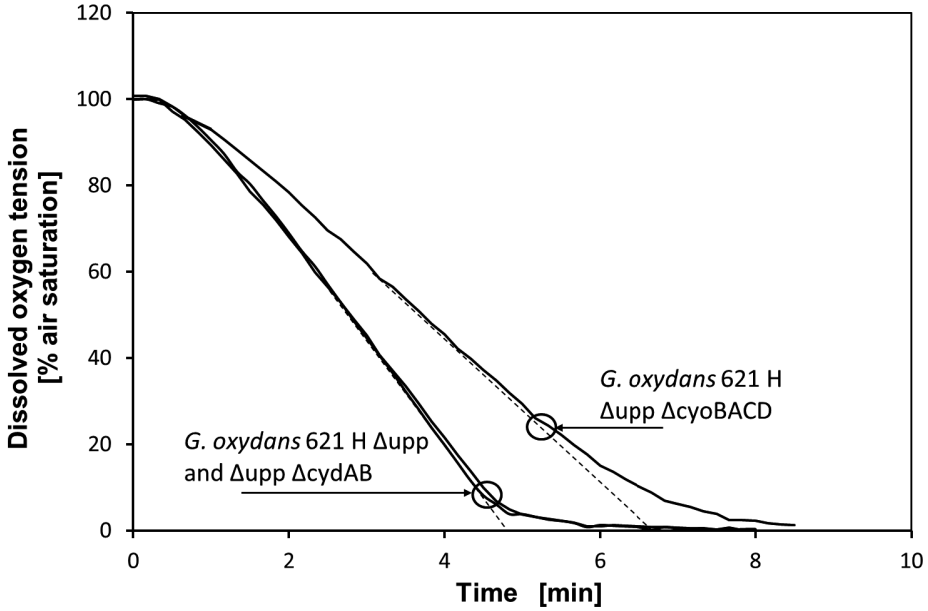

FIG 6 Oxygen consumption of *G. oxydans* Δ*upp* (solid line), *G. oxydans* Δ*upp* Δ*cyoBACD* (dotted line) and *G. oxydans* Δ*upp* Δ*cydAB* (dash dot) in a respirometer with an electrochemical oxygen electrode. Experimental conditions: Complex medium with 40 g l^{-1} mannitol, room temperature. The initial OD_{600} was in all 3 cases adjusted to 0.3. The experiments were conducted in triplicate; one exemplary curve for each strain is shown.

H^+/O ratio measurements. The low biomass yield of *G. oxydans* could result from a low H^+/O ratio, causing inefficient energy conservation during substrate oxidation. The mutants constructed in this work allowed determining the H^+/O ratios in the presence of only one terminal oxidase. These experiments were performed with mannitol as energy source, which is oxidized in the periplasm by the major polyol dehydrogenase SldAB to fructose with concomitant reduction of ubiquinone. The average H^+/O ratio of the reference strain *G.*

oxydans Δ*upp* containing both terminal oxidases determined from 10 independent experiments was 1.26 ± 0.06 (Table 4). Control experiments under identical conditions (30°C, pH 6) using *E. coli* DH5αF' showed an average H^+/O ratio of 3.04 ± 0.11, demonstrating that the low values measured for *G. oxydans* were not an artifact of the experimental setup used for measurement of proton translocation. Strain *G. oxydans* Δ*upp* Δ*cydAB* lacking cytochrome *bd* oxidase showed a comparable H^+/O ratio to the reference strain (H^+/O = 1.31 ± 0.16), which was in agreement of the unimpaired growth of mutant under the tested conditions. The Δ*upp* Δ*cyoBACD* strain, on the other hand, showed a 56% reduction of the H^+/O ratio (0.56 ± 0.11) compared to the reference strain, indicating cytochrome bo_3 oxidase is predominantly responsible for respiratory proton translocation in *G. oxydans*. The low H^+/O ratio of the *cyo* mutant is a likely explanation for the poor growth of the strain on agar medium and in shake flask experiments.

TABLE 3 H^+/O ratio of three *G. oxydans* 621H strains and *E. coli* as a reference with mannitol as carbon source

Strain	H^+/O ratio Volume of air-saturated 150 mM KCl for oxygen pulse		
	12.5 µl	25 µl	50 µl
G. oxydans 621H Δ*upp*	1.19 ± 0.11 (10)[1]	1.34 ± 0.10 (10)	1.24 ± 0.10 (10)
G. oxydans 621H Δ*upp* Δ*cydAB*	n.d.[3]	1.31 ± 0.16 (8)	n.d.
G. oxydans 621H Δ*upp* Δ*cyoBACD*	n.d	0.56 ± 0.11 (8)	n.d.
E. coli DH5αF'[2]	2.89 ± 0.23 (10)	3.16 ± 0.21 (10)	3.05 ± 0.17 (10)

[1]The numbers in brackets indicate the number of independent experiments.
[2]*E. coli* was used as a control strain for the experimental setup.
[3]n.d., not determined.

Complementation of terminal oxidases. For complementation studies, the genes *cyoBACD, cydAB* and *cydABCD* with their native ribosomal binding sites were cloned into the expression vector pBBR1p384, resulting in plasmids pBBRp384-*cyoBACD,* pBBRp384-*cydAB* and pBBRp384-*cydABCD.* After transfer of the plasmids in the desired *G. oxydans* strains, growth of the recombinants in mannitol medium was tested. Plasmid-based expression of either *cydAB* or *cydABCD* in the reference strain Δ*upp* and in the mutant Δ*upp* Δ*cydAB* had no influence on the growth properties (data not shown). In contrast, plasmid-based expression of the *cyoBACD* genes led to improved growth (Fig. 7). In the reference strain Δ*upp* carrying pBBRp384-*cyoBACD* the growth rate was increased by 8% compared to

the strain carrying pBBRp384 (from 0.39 ± 0.01 h^{-1} to 0.42 ± 0.00 h^{-1}) and the final OD_{600} by 20% (from 4.05 ± 0.13 to 4.88 ± 0.09). In the mutant strain Δ*upp* Δ*cyoBACD* carrying pBBRp384-*cyoBACD,* the growth rate was increased by 60% compared to the strain carrying pBBRp384 (from 0.27 ± 0.03 h^{-1} to 0.43 ± 0.00 h^{-1}) and the final OD_{600} by 69% (from 2.92 ± 0.05 to 4.93 ± 0.05). The time-delay of mannitol oxidation and fructose formation in strain *G. oxydans* Δ*upp* pBBRp384-*cyoBACD* compared to strain Δ*upp* Δ*cyoBACD* pBBRp384-*cyoBACD* may be due to the higher initial mannitol concentration of the former culture.

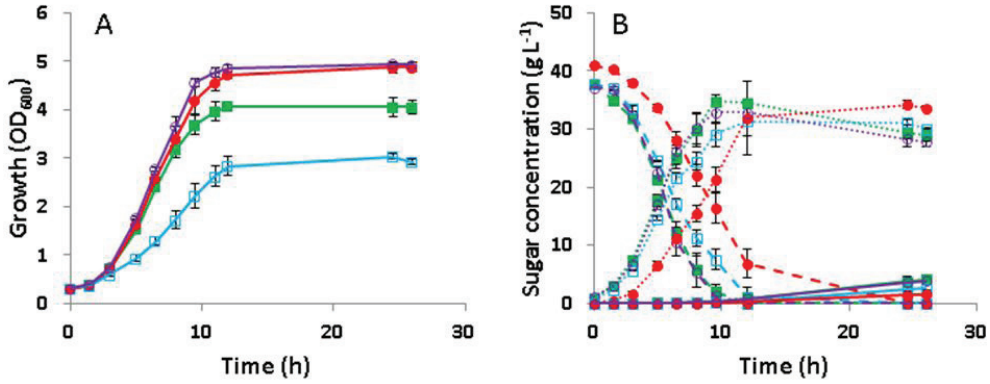

FIG 7 Growth (A), substrate consumption and product formation (B) of the *G. oxydans* strains Δ*upp* pBBRp384 (■), Δ*upp* pBBRp384-*cyoBACD* (●), Δ*upp* Δ*cyoBACD* pBBRp384 (□) and Δ*upp* Δ*cyoBACD* pBBRp384-*cyoBACD* (○). The strains were cultivated in shake flasks with mannitol medium at 30°C and 140 rpm. Mannitol, dashed line; fructose, dotted line; 5-ketofructose, continuous line. Mean values and standard deviations of three independent cultures are shown.

DISCUSSION

In this study the roles of the two terminal oxidases of *G. oxydans* 621H, cytochrome *bd* oxidase and cytochrome bo_3 oxidase, were investigated. Deletion of the corresponding genes revealed that neither of the two terminal oxidases is essential for growth of *G. oxydans* in a mannitol-yeast extract medium, but that the cytochrome bo_3-type oxidase is of major importance for energy generation and biomass formation.

Shake flask and RAMOS cultivations demonstrated that the absence of cytochrome *bd* oxidase had no influence on growth and respiration activity, neither under oxygen excess nor

under oxygen limitation. The reference strain and the *bd* oxidase deletion mutant consumed almost equal quantities of oxygen (oxygen excess: 194 and 182 mM; oxygen limitation: 162 and 171 mM) (Table 2). Since 110 mM of O_2 is needed for complete conversion of 220 mM mannitol to fructose, the values of oxygen consumption indicate a total oxidation of mannitol, as was supported by HPLC analysis. Nevertheless, quantities of consumed oxygen exceeded 110 mM by far (Table 2) indicating a further oxidation of fructose to 5-ketofructose and carbon dioxide. On the contrary, the strain lacking cytochrome bo_3 oxidase showed lowered oxygen consumption values (oxygen excess 154 mM; oxygen limitation 142 mM), being in agreement with a reduced biomass formation and an inhibited uptake of fructose or oxidation of fructose to 5-ketofructose. Furthermore, CO_2 formation was reduced in the strain lacking cytochrome bo_3 oxidase compared to the reference strain (oxygen excess 66 to 100 mM; oxygen limitation 44 to 66 mM). CO_2 is primarily produced in the pentose phosphate pathway (34). Another intracellular pathway that would lead to a release of CO_2 is the conversion of pyruvate to acetaldehyde (25, 38). HPLC analysis revealed that uptake of sugar was reduced significantly in the strain lacking cytochrome bo_3 oxidase (deletion mutant 4 mM, reference strain 13 mM) during the course of cultivation at oxygen excess which possibly explains the reduced biomass and CO_2 formation. In addition, it has been shown that *G. oxydans* can grow on complex medium even if neither of the two intracellular pathways for sugar metabolism is active. The strain needs to take up e.g. amino acids from the yeast extract present in the culture medium (43). This as well resulted in a reduced biomass and CO_2 formation, due to a reduced uptake of mannitol and/or fructose.

When the RAMOS cultivations were performed under conditions leading to oxygen limitation during growth, the strain lacking cytochrome bo_3 oxidase did not show a clear horizontal plateau that was observed for the reference strain and the *bd* oxidase mutant (Fig. 5). Instead, the OTR slowly approached the maximal value possible under the chosen conditions. This result indicated a low oxygen affinity of cytochrome *bd*, the only remaining terminal oxidase in the bo_3 mutant.

This assumption was supported by measurements performed in the respirometer (Fig. 6). While the concentration of dissolved oxygen tension (DOT) declined similarly in the experiments with the reference strain and the strain lacking cytochrome *bd* oxidase until a value of 10% DOT was reached, the amount of DOT for the cytochrome bo_3 deletion strain declined less. An additional proof for the low oxygen affinity of *bd* oxidase is the divergence of linear decline at higher DOT (25 to 30%) of strain Δ*upp* Δ*cyoBACD*. At low oxygen concentrations (10 to 20% saturation) all investigated strains slowed down their oxygen consumption. This is in agreement with results obtained by Matsushita et al., who have indications for a low oxygen affine cytochrome *bd* oxidase, too (personal communication). *E.*

coli possesses a high-affinity cytochrome *bd* oxidase, having a K_m value of 4.5 nM for oxygen (13). In contrast, the CioAB of *C. jejuni* and of *A. vinelandii* have similar Km values for oxygen of 0.8 µM (21) and 4.5 - 5.7 µM (14), respectively. These values indicate, that the CioAB have a lower oxygen affinity compared to *E. coli* cytochrome *bd* oxidase, as the K_m value is in the range of *E. coli* cytochrome bo_3 oxidase (0.1 µM – 1.1 µM). DNA sequences of the genes *cydAB* of *G. oxydans* are more closely related to *cioA* and *cioB* from *Pseudomonas aeruginosa* and *Zymomonas mobilis* than to *cydA* and *cydB* from *E. coli* (33). Thus, *G. oxydans* cytochrome *bd* oxidase might as well belong to low oxygen-affinity CioAB oxidases.

Next to growth and respiration activity, absence of cytochrome *bd* oxidase did not affect respiration-dependent proton extrusion of *G. oxydans*, whereas absence of cytochrome bo_3 oxidase caused a significant reduction in the H^+/O ratio. Reduced minus oxidized spectra of purified membranes showed an increase in cytochrome *d* content in the strain lacking *cyoBACD*, indicating an overexpression of the genes encoding cytochrome *bd* oxidase (data not shown). Accordingly, in DNA microarray experiments of the *cyoBACD* deletion mutant versus the reference strain 3.6-5.4-fold increased mRNA ratios of the *cydAB* genes (GOX0278-GOX0279) were observed (data not shown). However, since growth and H^+/O ratio were impaired in the *cyoBACD* deletion mutant, the *bd* oxidase obviously could not compensate the absence of the bo_3 oxidase. This agrees with results obtained by Matsushita et al. where lowering of the external pH led to a decrease in H^+/O from 1.7-2.3 (pH 6) to 1.2-1.5 (pH 4), depending on the substrate used, presumably due to an increased expression of *bd* oxidase (28). Due to the low H^+/O ratio, *G. oxydans* Δ*upp* Δ*cyoBACD* is limited in the efficiency of oxidative phosphorylation via the H^+-dependent F_1F_o-ATP synthase. However, *G. oxydans* possesses a second F_1F_o-ATP synthase (39), that might use Na^+ instead of H^+ for ATP synthesis (18). As DNA microarray analysis of strains lacking cytochrome bo_3 oxidase versus the reference strain showed an upregulation of some genes encoding the Na^+-dependent F_1F_o-ATPase (GOX2167-2175; data not shown), there might exist an alternative pathway to restore energy generation, provided that an up to now unknown primary sodium pump is present in *G. oxydans*.

The measured H^+/O ratios of 1.26 ± 0.06 for *G. oxydans* were low compared to H^+/O ratios in a range of 3.4-4.0 reported for *E. coli* agreeing well with our values using a non-optimized system for *E. coli* (10, 26). In contrast to *G. oxydans*, *E. coli* possesses two NADH-ubiquinone reductases, NDH-I, a multi-subunit proton-pumping complex enzyme (9), and the single-subunit NDH-II, which lacks an energy coupling site (12). Since the electrogenic NDH-I is preferentially synthesized during anaerobic growth in the presence of alternate electron acceptors, during aerobic growth the nonelectrogenic NDH-II is the dominant NADH:Q

oxidoreductase (52). The genome of *G. oxydans* only encodes the gene for NDH-II (39) and, therefore, NADH oxidation does not add to the H^+/O ratio in both organisms under aerobic conditions. In *E. coli* the cytochrome bo_3 oxidase acts as an active proton pump, whereas the cytochrome *bd* oxidases, cytochrome *bd*-I and cytochrome *bd*-II, do not (7, 40, 41). However, the latter enzymes usually generate proton motive force as protons used for the generation of water are taken from the cytoplasmic space (7, 31) and proton derived from quinol oxidation are delivered to the periplasmic space. Hence, the reaction is coupled to charge separation across the membrane. The H^+/O ratio of cytochrome bo_3 oxidase is taken as 4, whereas the H^+/O ratio of cytochrome *bd* oxidases is 2. Based on the composition of the respiratory chain of *G. oxydans,* H^+/O ratios in the range of 2 – 4 would be expected. However, as our results, as well as those presented by Matsushita et al. are lower than the values reported for *E. coli* there must be a difference between the respiratory chains of both organisms concerning energy generation (28). One assumption is that the cytochrome *bd* oxidase of *Gluconobacter* species does not take part in the formation of charge separation, but is functioning as a bypass oxidase leading to low H^+/O ratios (30). However, under our cultivation conditions the respective phenotype of the Δ*cydAB* mutant was not observable.

There are a number of speculative hypotheses to explain the low H^+/O ratios determined for *G. oxydans*: (i) It may be assumed that the protons for the reduction of oxygen to water do not stem from the cytoplasm but from the periplasm thus impeding charge separation across the membrane. Such an assumption is largely ruled out by results of X-ray crystallographic structures of haem-copper reductases (1, 37) and determination of the proton-motive force of the cytochrome *bd*-II oxidase of *E. coli* that generated a H^+/e^- ratio of 0.94 ± 0.18 (7). (ii) Membranes have a passive leak for protons so that there is a non-energy conserving back-flow of protons into the cells (11); it may be assumed that the membrane of *G. oxydans* has a strongly pronounced leakiness. (iii) A reverse electron transfer from reduced cytochrome *c* via the cytochrome bc_1 complex to the ubiquinone pool would result in a reduction of the membrane potential (53). (iv) The cytochrome bo_3 oxidase of *Vitreoscilla* sp. has been shown to function as a primary Na^+ pump (23, 35); assuming the same for the cytochrome bo_3 of *G. oxydans* this would lead to the observed low H^+/O ratios.

Surprisingly, plasmid-based complementation of the strain *G. oxydans* Δ*upp* Δ*cyoBACD* resulted not only in a reversal to wild-type-like growth, but even to an increased growth rate and an increased final OD_{600}. This is in agreement with results obtained for *E. coli*. Overexpression of cytochrome bo_3 oxidase in an *E. coli* strain lacking both terminal oxidases resulted in an increased cell yield (32). The same result was obtained in the *G. oxydans* reference strain overexpressing cytochrome bo_3 oxidase.

In this work the role of the two terminal oxidases in *G. oxydans* was analyzed and revealed a major importance of cytochrome bo_3 oxidase under the tested conditions, whereas the role of the cytochrome *bd* oxidase still remains unclear. In contrast to the *E. coli* cytochrome *bd* oxidase that has a high affinity for oxygen, the cytochrome *bd* oxidase of *G. oxydans* obviously has a low affinity. The fact that deletion of the *cydAB* genes did not result in a growth phenotype leads to the conclusion that under the chosen conditions the entire electron flux to oxygen was directed via the cytochrome bo_3 oxidase. Surprisingly, overproduction of cytochrome bo_3 led to an increased biomass formation. This means that in the reference strain cytochrome bo_3 oxidase is the rate-limiting factor of the respiratory chain. Obviously, the activity of the major polyol dehydrogenase SldAB is high enough to deliver sufficient electrons via the UQ-pool to an elevated concentration of cytochrome bo_3 allowing an increased proton-pumping capacity of the cells. This gain of energy explains the increased growth yield and final OD_{600} of a strain overexpressing the genes encoding for cytochrome bo_3 oxidase. Thus, the respiratory chain components appear to be a promising starting point for further optimization of *G. oxydans* as an industrial organism.

ACKNOWLEDGEMENTS

We are most grateful to Armin Ehrenreich and Wolfgang Liebl (Technical University of Munich, Germany) for providing the strains and protocols used for generating the *G. oxydans* deletion mutants and Uwe Deppenmeier (University of Bonn, Germany) for providing plasmid pBBR1p384. We thank Jayne Louise Wilson (The University of Sheffield, UK) for advising us on the method of H^+/O measurement. We also thank DSM Nutritional Products (Kaiseraugst, Switzerland) for financial support and Dietmar Laudert, Günter Pappenberger and Hans-Peter Hohmann (DSM Nutritional Products) for their scientific input and their continued disposition for discussion. This work was funded by the German Ministry of Education and Research (BMBF) within the GenoMik-Transfer program (grant 0315632D and B).

REFERENCES

1. **Abramson J, Riistama S, Larsson G, Jasaitis A, Svensson-Ek M, Laakkonen L, Puustinen A, Iwata S, Wikström M.** 2000. The structure of the ubiquinol oxidase from *Escherichia coli* and its ubiquinone binding site. Nat. Struct. Biol. **7:**910-917.
2. **Ameyama M, Matsushita K, Shinagawa E, Adachi O.** 1987. Sugar-oxidizing respiratory chain of *Gluconobacter suboxydans*. Evidence for a branched respiratory

chain and characterization of respiratory chain-linked cytochromes. Agric. Biol. Chem. **51:**2943-2950.

3. **Anderlei T, Zang W, Papaspyrou M, Büchs J.** 2004. Online respiration activity measurement (OTR, CTR, RQ) in shake flasks. Biochem. Eng. J. **17:**187-194.
4. **Bertani G.** 2004. Lysogeny at mid-twentieth century: P1, P2, and other experimental systems. J. Bacteriol. **186:**595-600.
5. **Bertani G.** 1951. Studies on lysogenesis. I. The mode of phage liberation by lysogenic *Escherichia coli*. J. Bacteriol. **62:**293-300.
6. **Borisov VB, Gennis RB, Hemp J, Verkhovsky MI.** 2011. The cytochrome *bd* respiratory oxygen reductases. Biochim. Biophys. Acta **1807:**1398-1413.
7. **Borisov VB, Murali R, Verkhovskaya ML, Bloch DA, Han H, Gennis RB, Verkhovsky MI.** 2011. Aerobic respiratory chain of *Escherichia coli* is not allowed to work in fully uncoupled mode. Proc. Nat. Acad. Sci. USA **108:**17320-17324.
8. **Bott M, Thauer RK.** 1989. Proton translocation coupled to the oxidation of carbon monoxide to CO_2 and H_2 in *Methanosarcina barkeri*. Eur. J. Biochem. **179:**469-472.
9. **Brandt U, Kerscher S, Drose S, Zwicker K, Zickermann V.** 2003. Proton pumping by NADH:ubiquinone oxidoreductase. A redox driven conformational change mechanism? FEBS Lett. **545:**9-17.
10. **Brice JM, Law JF, Meyer DJ, Jones CW.** 1974. Energy conservation in *Escherichia coli* and *Klebsiella pneumoniae*. Biochem. Soc. Transact. **2:**523-526.
11. **Brown GC.** 1992. The leaks and slips of bioenergetic membranes. FASEB journal : official publication of the Federation of American Societies for Experimental Biology **6:**2961-2965.
12. **Calhoun MW, Oden KL, Gennis RB, de Mattos MJ, Neijssel OM.** 1993. Energetic efficiency of *Escherichia coli*: effects of mutations in components of the aerobic respiratory chain. J. Bacteriol. **175:**3020-3025.
13. **D'mello R, Hill S, Poole RK.** 1996. The cytochrome *bd* quinol oxidase in *Escherichia coli* has an extremely high oxygen affinity and two oxygen-binding haems: implications for regulation of activity *in vivo* by oxygen inhibition. Microbiology **142 (Pt 4):**755-763.
14. **D'mello R, Hill S, Poole RK.** 1994. Determination of the oxygen affinities of terminal oxidases in *Azotobacter vinelandii* using the deoxygenation of oxyleghaemoglobin and oxymyoglobin: cytochrome *bd* is a low-affinity oxidase. Microbiology **140:**395-402.
15. **Dauner M, Sonderegger M, Hochuli M, Szyperski T, Wüthrich K, Hohmann HP, Sauer U, Bailey JE.** 2002. Intracellular carbon fluxes in riboflavin-producing *Bacillus*

subtilis during growth on two-carbon substrate mixtures. Appl. Environ. Microbiol. **68:**1760-1771.

16. **De Ley J, Gillis M, Swings J.** 1984. The genus *Gluconobacter*. Krieg NR, Holt JG (eds) Bergey's Manual of Systematic Bacteriology **vol 1:**pp 267–278.
17. **Deppenmeier U, Hoffmeister M, Prust C.** 2002. Biochemistry and biotechnological applications of *Gluconobacter* strains. Appl. Microbiol. Biotechnol. **60:**233-242.
18. **Dibrova DV, Galperin M, Mulkidjanian A.** 2010. Characterization of the N-ATPase, a distinct, laterally transferred Na^+-translocating form of the bacterial F-type membrane ATPase. Bioinformatics **26:**1473–1476.
19. **Fu HA, Iuchi S, Lin EC.** 1991. The requirement of ArcA and Fnr for peak expression of the *cyd* operon in *Escherichia coli* under microaerobic conditions. Mol. Gen. Genet. **226:**209-213.
20. **Hanahan D, Jessee J, Bloom FR.** 1991. Plasmid transformation of *Escherichia coli* and other bacteria. Meth. Enzymol. **204:**63-113.
21. **Jackson RJ, Elvers KT, Lee LJ, Gidley MD, Wainwright LM, Lightfoot J, Park SF, Poole RK.** 2007. Oxygen reactivity of both respiratory oxidases in *Campylobacter jejuni*: the *cydAB* genes encode a cyanide-resistant, low-affinity oxidase that is not of the cytochrome *bd* type. J. Bacteriol. **189:**1604-1615.
22. **Kersters K, Lisdiyanti P, Komagata K, Swings J.** 2006. The family *Acetobacteriaceae*: The genera *Acetobacter*, *Acidomonas*, *Asaia*, *Gluconacetobacter*, *Gluconobacter* and *Kozakia*. In: Dworkin M, Falkow S, Rosenberg E, Schleifer K-H, Stackebrandt E (eds.) The Prokaryotes. Vol. 5, 3rd edition. Springer-Verlag GmbH, Heidelberg p. 163-200.
23. **Kim SK, Stark BC, Webster DA.** 2005. Evidence that Na^+-pumping occurs through the D-channel in *Vitreoscilla* cytochrome *bo*. Biochem. Biophys. Res. Commun. **332:**332-338.
24. **Kovach ME, Elzer PH, Hill DS, Robertson GT, Farris MA, Roop RM, 2nd, Peterson KM.** 1995. Four new derivatives of the broad-host-range cloning vector pBBR1MCS, carrying different antibiotic-resistance cassettes. Gene **166:**175-176.
25. **Krajewski V, Simić P, Mouncey NJ, Bringer S, Sahm H, Bott M.** 2010. Metabolic engineering of *Gluconobacter oxydans* for improved growth rate and growth yield on glucose by elimination of gluconate formation. Appl. Environ. Microbiol. **76:**4369-4376.
26. **Lawford HG, Haddock BA.** 1973. Respiration-driven proton translocation in *Escherichia coli*. Biochem. J. **136** 217-220.

27. **Luttik M, Van Spanning R, Schipper D, Van Dijken JP, Pronk JT.** 1997. The low biomass yields of the acetic acid bacterium *Acetobacter pasteurianus* are due to a low stoichiometry of respiration-coupled proton translocation. Appl. Environ. Microbiol. **63:**3345-3351.

28. **Matsushita K, Nagatani Y, Shinagawa E, Adachi O, Ameyama M.** 1989. Effect of extracellular pH on the respiratory chain and energetics of *Gluconobacter suboxydans*. Agr. Biol. Chem. **53:**2895-2902.

29. **Matsushita K, Shinagawa E, Adachi O, Ameyama M.** 1987. Purification, characterization and reconstitution of cytochrome *o*-type oxidase from *Gluconobacter suboxydans*. Biochim. Biophys. Acta **894:**304-312.

30. **Matsushita K, Toyama H, Adachi O.** 2004. Respiratory chains in acetic acid bacteria: Membrane-bound periplasmic sugar and alcohol respirations. Zannoni, D. (ed): Respiration in Archaea and Bacteria. (Advances in Photosynthesis and Respiration) **Springer, Dordrecht, The Netherlands. Vol. 16:**pp. 81-99.

31. **Miller MJ, Gennis RB.** 1985. The cytochrome *d* complex is a coupling site in the aerobic respiratory chain of *Escherichia coli*. J. Biol. Chem. **260:**14003-14008.

32. **Minohara S, Sakamoto J, Sone N.** 2002. Improved H^+/O ratio and cell yield of *Escherichia coli* with genetically altered terminal quinol oxidases. J. Biosc. Bioeng. **93:**464-469.

33. **Mogi T, Ano Y, Nakatsuka T, Toyama H, Muroi A, Miyoshi H, Migita CT, Ui H, Shiomi K, Omura S, Kita K, Matsushita K.** 2009. Biochemical and spectroscopic properties of cyanide-insensitive quinol oxidase from *Gluconobacter oxydans*. J. Biochem. **146:**263-271.

34. **Olijve W, Kok JJ.** 1979. Analysis of growth of *Gluconobacter oxydans* in glucose containing media. Arch. Microbiol. **121:**283-290.

35. **Park C, Moon JY, Cokic P, Webster DA.** 1996. Na^+-translocating cytochrome *bo* terminal oxidase from *Vitreoscilla*: some parameters of its Na^+ pumping and orientation in synthetic vesicles. Biochemistry **35:**11895-11900.

36. **Peña C, Galindo E, Büchs J.** 2011. The viscosifying power, degree of acetylation and molecular mass of the alginate produced by *Azotobacter vinelandii* in shake flasks are determined by the oxygen transfer rate. Proc. Biochem. **46:**290-297.

37. **Pereira MM, Sousa FL, Verissimo AF, Teixeira M.** 2008. Looking for the minimum common denominator in haem-copper oxygen reductases: towards a unified catalytic mechanism. Biochim. Biophys. Acta. **1777:**929-934.

38. **Peters B, Junker A, Brauer K, Mühlthaler B, Kostner D, Mientus M, Liebl W, Ehrenreich A.** 2012. Deletion of pyruvate decarboxylase by a new method for

efficient markerless gene deletions in *Gluconobacter oxydans*. Appl. Microbiol. Biotechnol.:Epub ahead of print, DOI 10.1007/s00253-00012-04354-z.

39. **Prust C, Hoffmeister M, Liesegang H, Wiezer A, Fricke WF, Ehrenreich A, Gottschalk G, Deppenmeier U.** 2005. Complete genome sequence of the acetic acid bacterium *Gluconobacter oxydans*. Nat. Biotechnol. **23:**195-200.
40. **Puustinen A, Finel M, Haltia T, Gennis RB, Wikström M.** 1991. Properties of the two terminal oxidases of *Escherichia coli*. Biochemistry **30:**3936-3942.
41. **Puustinen A, Finel M, Virkki M, Wikström M.** 1989. Cytochrome *o* (*bo*) is a proton pump in *Paracoccus denitrificans* and *Escherichia coli*. FEBS Lett. **249:**163-167.
42. **Raspor PP, Goranovič D.** 2008. Biotechnological applications of acetic acid bacteria. Crit. Rev. Biotechnol. **28:**101-124.
43. **Richhardt J, Bringer S, Bott M.** 2012. Mutational analysis of the pentose phosphate and Entner-Doudoroff pathways in *Gluconobacter oxydans* reveals improved growth of a Δ*edd* Δ*eda* mutant on mannitol. Appl. Environ. Microbiol. **78:**6975-6986.
44. **Rischbieter E, Schumpe A.** 1996. Gas solubilities in aqueous solutions of organic substances. J. Chem. Eng. Data **41:**809-812.
45. **Sambrook J, Russell DW.** 2001. Molecular cloning: a laboratory manual, 3rd ed. Cold Spring Harbor Laboratory Press, Cold Spring Harbor, N.Y.
46. **Schumpe A, Deckwer W-D.** 1979. Estimation of O_2 and CO_2 solubilities in fermentation media. Biotechnol Bioeng **21:**1075- 1078.
47. **Schumpe A, Quicker G, Deckwer W-D.** 1982. Gas solubilities in microbial culture media. Adv. Biochem. Eng. Biotechnol. Reaction Engineering, Fiechter, A., ed., Springer-Verlag, Berlin, Heidelberg, New York **24:**2-38.
48. **Seletzky JM, Noak U, Fricke J, Welk E, Eberhard W, Knocke C, Büchs J.** 2007. Scale-up from shake flasks to fermenters in batch and continuous mode with *Corynebacterium glutamicum* on lactic acid based on oxygen transfer and pH. Biotechnol. Bioeng. **98:**800-811.
49. **Silberbach M, Maier B, Zimmermann M, Büchs J.** 2003. Glucose oxidation by *Gluconobacter oxydans*: characterization in shaking-flasks, scale-up and optimization of the pH profile. Appl. Microbiol. Biotechnol. **62:**92-98.
50. **Simon R, Priefer U, Pühler A.** 1983. A broad host range mobilization system for *in vivo* genetic-engineering-transposon mutagenesis in Gram-negative bacteria. Bio-Technol **1:**784-791.
51. **Soini J, Ukkonen K, Neubauer P.** 2008. High cell density media for *Escherichia coli* are generally designed for aerobic cultivations - consequences for large-scale bioprocesses and shake flask cultures. Microb. Cell Fact. **7:**26.

52. **Tran QH, Bongaerts J, Vlad D, Unden G.** 1997. Requirement for the proton-pumping NADH dehydrogenase I of *Escherichia coli* in respiration of NADH to fumarate and its bioenergetic implications. Eur. J. Biochem. **244:**155-160.

53. **van der Oost J, Schepper M, Stouthamer AH, Westerhoff HV, van Spanning RJ, de Gier JW.** 1995. Reversed electron transfer through the bc_1 complex enables a cytochrome *c* oxidase mutant (delta aa_3/cbb_3) of *Paracoccus denitrificans* to grow on methylamine. FEBS Lett. **371:**267-270.

4. Discussion

4.1. Carbon metabolism of *G. oxydans*

The carbon metabolism of *G. oxydans* is characterized by its many membrane-bound dehydrogenases that incompletely oxidize sugars and sugar alcohols in the periplasm. Cytoplasmic sugar metabolism proceeds with only a small portion of the carbon source present in the medium. In this study, the roles of the two pathways for intracellular sugar metabolism, the EDP and the PPP, were investigated. To this end, two deletion mutants were constructed, lacking either the gene encoding 6-phosphogluconate dehydrogenase (*gnd*) leading to a non-functional PPP or lacking the genes 6-phosphogluconate dehydratase and KDPG aldolase (*edd* and *eda*), resulting in a non-functional EDP. Interestingly, enzyme activity measurements of 6-phosphogluconate dehydrogenase and glucose 6-phosphate dehydrogenase (encoded by *zwf*) showed that five of the eight obtained Δ*gnd* mutants lacked glucose 6-phosphate dehydrogenase activity. Sequence analysis revealed that this was due to the insertion of additional base pairs in the *zwf* gene leading to shortened proteins. The three strains *G. oxydans* Δ*upp* Δ*edd-eda*, *G. oxydans* Δ*upp* Δ*gnd* and *G. oxydans* Δ*upp* Δ*gnd zwf** were characterized with the three carbon sources mannitol, glucose and glycerol. In contrast to mannitol and glucose, growth with glycerol was found to be non-reproducible and therefore was not analyzed further (unpublished data). One reason for the non-reproducibility might be that the oxidation product of glycerol, dihydroxyacetone (DHA), is toxic and leads to growth inhibition (Claret et al. 1992; Ohrem and Voss 1995; Hekmat et al. 2003).

4.1.1 The role of the EDP and the PPP in sugar metabolism

As outlined in the introduction (part 2.2.3), the two pathways for intracellular sugar metabolism differ in energetic efficiency and formation of reduction equivalents (Kruger and von Schaewen 2003).

Sole use of the EDP:

1 mol glucose 6-phosphate ➔ 2 mol acetate/acetyl-CoA + 2 mol CO_2 + 4 mol NAD(P)H + 2 mol ATP

Sole use of the PPP:

1 mol glucose 6-phosphate ➔ 1 mol acetate/acetyl-CoA + 4 mol CO_2 + 8 mol NAD(P)H + 2 mol ATP

The partially cyclic PPP yields twice as much NAD(P)H and CO_2 than the EDP whereas the amount of acetate is reduced by 50%. The NAD(P)H can theoretically be converted to NADH by the PntA1A2B transhydrogenase and then be reoxidized via NADH dehydrogenase and the terminal oxidases (Jackson et al. 2002; Rauch et al. 2010). Generation of a proton motive force across the membrane drives ATP formation via the F_1F_o ATP synthase. In the following paragraph, the results obtained for growth with mannitol and glucose as the carbon sources of PPP- and EDP-deficient strains in comparison to the reference strain will be discussed with regard to the above mentioned equations.

The two PPP-deficient strains *G. oxydans* Δ*upp* Δ*gnd* and *G. oxydans* Δ*upp* Δ*gnd zwf** revealed severly inhibited growth and complete absence of the second growth phase in comparison to the reference strain *G. oxydans* Δ*upp*. The absence of the second growth phase of the two deletion mutants directly correlated with a reduced sugar consumption in phase II, whereas in growth phase I both strains consumed mannitol/ glucose completely. A similar phenotype was obtained by plasmid-based overexpression of *edd* and *eda* when cultivated with mannitol. One reason for the inhibited growth and sugar consumption in the second growth phase of the PPP-deficient strains might be due to an insufficient energy supply, as only half as much NAD(P)H is formed via the EDP, and/or an insufficient rate of fructose/gluconate catabolism via the EDP. Another reason for the reduced growth rate and final OD_{600} of the strains Δ*upp* Δ*gnd* and Δ*upp* Δ*gnd zwf** in comparison to the reference strain might be due to an accumulation of the toxic compounds 6-phosphogluconate or KDPG in the cells. Addition of gluconate to an *E. coli* strain lacking KDPG aldolase or overexpressing 6-phosphogluconate dehydratase resulted in a rapid accumulation of KDPG within the cell accompanied by an immediate and significant decrease in growth (Fuhrman et al. 1998). A similar phenotype was observed for *Pseudomonas cepacia* mutants deficient in either 6-phosphogluconate dehydratase or KDPG aldolase. The *P. cepacia* mutants failed to utilize glucose, gluconate or fructose as carbon source presumably due to an accumulation of KDPG, 6-phosphogluconate or both (Allenza and Lessie 1982). Absence of the PPP by deletion of the gene encoding 6-phosphogluconate dehydrogenase leads to a severly inhibited growth and the formation of suppressor mutants in *G. oxydans* with an inactive glucose 6-phosphate dehydrogenase (Δ*gnd* Δ*zwf**). Deletion of the gene encoding 6-phosphogluconate dehydrogenase (*gndA*) in *Bacillus subtilis* and thereby blocking the PPP leads to a similar phenotype, even though the EMP and not the PPP is the predominant pathway for sugar metabolism (Zamboni et al. 2004). The maximum specific growth rate of this strain was significantly lower compared to the reference strain, as it is the case in *G. oxydans*. Furthermore, the *B. subtilis* Δ*gndA* mutants exhibited an unusually long log-phase when first cultivated on minimal medium with glucose that could be observed after each subcultivation. Thus, it is supposed that an adaption or an unstable suppressor is

necessary to permit growth without an oxidative PPP and thereby redirecting the flux completely via the EMP. In *B. subtilis* a siginificantly reduced growth rate in comparison to the reference strain could also be observed by deletion of the gene encoding glucose 6-phosphate dehydrogenase (*zwf*), indicating that the PPP might play a role in NAD(P)H formation in this organism as well (Palmisano et al. 1989). In contrast to the results described for *B. subtilis* deletion of the gene encoding glucose 6-phosphate dehydrogenase in *E. coli* exhibited no clear physiological phenotype, as growth rate, biomass yield and glucose uptake rate were in the same range as described for the reference strain (Fischer and Sauer 2003). This indicates that neither the PPP nor the EDP is essential for growth with glucose as carbon source. On the other hand, deletion of the gene encoding phosphoglucose isomerase resulted in a severly reduced growth rate and no flux via the EMP, but in this case the EDP contributed to about 30% in glucose metabolism, and the remining 70% were metablized via the PPP (Fischer and Sauer 2003). This was surprising, as the EDP is the energetically less efficient pathway compared to the reference strain and a complete redirection of the carbon flux via the PPP was expected.

Metabolism of glucose 6-phosphate via the EDP theoretically can lead to eqiumolar amounts of acetate and CO_2, whereas via the partially cyclic PPP the theoretically maximal ratio of acetate/CO_2 is only 0.25. As CO_2 might be released in other reactions as well, a discrepancy of these theoretical from measured values has to be considered. The PPP-deficient strains show an increased acetate/CO_2 ratio compared to the reference strain. *G. oxydans* Δ*upp* Δ*gnd* and *G. oxydans* Δ*upp* Δ*gnd zwf** show a ratio of 0.68 and 0.65 respectively when cultivated with glucose as the carbon source and of 0.55 and 0.23 respectively when cultivated on mannitol, whereas the reference strain shows a ratio of 0.22 (glucose) and 0.12 (mannitol). Apparently, in strain *G. oxydans* Δ*upp* Δ*gnd zwf** the ratio is not increased as much as in strain *G. oxydans* Δ*upp* Δ*gnd* when cultivated on mannitol. The strain lacking glucose 6-phosphate dehydrogenase activity was unable to metabolize mannitol or fructose intracellularly and thus the acetate/CO_2 ratio does not stem from the metabolism of fructose/glucose 6-phosphate via the EDP. Presumably, the strain took up precursors for biosynthesis of cell constituents from the yeast extract present in the medium when cultivated on mannitol. As has been reported before, *G. oxydans* is unable to grow on minimal medium lacking all amino acids, even though sequence analysis revealed that *G. oxydans* owns the gene composition to synthesize all amino acids by itself (Stokes and Larsen 1945; Rao and Stokes 1953; Prust et al. 2005). On the other hand, both PPP-deficient strains were able to metabolize glucose by the EDP via soluble glucose dehydrogenase and gluconate kinase. As nearly no differences in glucose metabolism were detectable between strain Δ*upp* Δ*gnd* and Δ*upp* Δ*gnd zwf**, it is most likely that sugar metabolism via the soluble glucose dehydrogenase (*gdhS*) was the preferred route in both

deletion mutanst. ^{13}C-MFA analysis of *G. oxydans* cells grown on glucose revealed that in phase I only 9% of the glucose taken up by the cells was converted via glucokinase to glucose 6-phosphate, whereas the residual 91% were oxidized to gluconate by the soluble glucose dehydrogenase (Hanke et al., in preparation). Interestingly, deletion of *gdhS* resulted only in a minor growth inhibition in the second growth phase and the strain was slightly inhibited in 5-KGA formation in the first growth phase (Kiefler 2012). Thus, as neither deletion of *gdhS* nor inactivation of *zwf* leads to significant growth disturbances, *G. oxydans* seems to be able to use both pathways. Due to the membrane oxidation of glucose to gluconate, both strains also have the possibility to take up gluconate, thereby circumventing both, *gdhS* and *zwf.*

Whereas both PPP-deficient strains showed a similar significantly inhibited growth behavior with mannitol and glucose as the carbon sources, a different growth behavior was observable in the EDP-deficient strains. With mannitol as carbon source growth could be improved by deletion of the genes encoding the EDP (*edd* and *eda*) or by overexpression of *gnd*. The deletion mutant reached a 24% increased final OD_{600} coming along with a 40% elevated fructose uptake. Furthermore, the growth yield was enhanced in the first growth phase (growth on mannitol) by 43%. One reason might be the enhanced formation of NAD(P)H via the PPP and therefore the improved possibility of ATP generation. Interestingly, deletion of *edd* and *eda* seems not to be an advantage when *G. oxydans* is cultivated with glucose as the carbon source. The deletion mutant did not show an increasd final OD_{600} nor an altered growth rate compared to the reference strain and no improved uptake of sugar was detectable. One reason might be might be that the EDP was active to a lowered extent with glucose instead of mannitol as carbon source. Thus, deletion of *edd* and *eda* would have a minor influence on growth. ^{13}C-flux analysis with *G. oxydans* and glucose as the carbon source showed that in phase I 32% of the formed 6-phosphogluconate are metabolized via the EDP and in phase II only 7%, showing that in *G. oxydans* the PPP is the main pathway for glucose/gluconate metabolism (Hanke et al., in preparation). Unfortunately, nothing is known about carbon flux distribution during mannitol metabolism. To consolidate the assumption that the EDP plays a more prominent role for mannitol catabolism at least in the first growth phase, flux analysis with mannitol as carbon source should be performed. Another reason for the different growth behaviors of the EDP deletion mutant on glucose and mannitol might be the different utilization of mannitol and glucose via the membrane oxidation. Both carbon sources are rapidly, and independently of the intracellular pathway composition, oxidized in the periplasm to fructose or gluconate, respectively. Afterwards, part of the fructose is taken up by the cells and a small part is further oxidized to 5-ketofructose (2.2.1). In contrast, the majority of gluconate, is oxidized in the periplasm to 2-ketogluconate by the membrane-bound gluconate-2-dehydrogenase (2.2.2). During this reaction, electrons

are directly transferred to the ubiquinone pool and can be used for the formation of a proton gradient via the respiratory chain. As the rate of gluconate oxidation is much higher than the rate of fructose oxidation in the periplasm, growth on glucose seems to be largely independent from the generation of intracellular reduction equivalents and thus, an increased use of the PPP might not lead to a growth advantage in comparison to the reference strain. In contrast to results obtained for *G. oxydans* EDP-deficient strains, mutants of *Pseudomonas aeruginosa* deficient in the EDP were not able to grow on glucose or mannitol as the carbon sources, even though genes encoding the PPP exist, indicating a major role of the EDP in these organisms (Blevins et al. 1975). It has been shown that gluconate metabolism is completely achieved via the EDP in several *Pseudomonas* species (Stern et al. 1960). The same has been shown for *E. coli*, in which gluconate is catabolized via an inducible Entner-Doudoroff pathway (Eisenberg and Dobrogosz 1967). This seems not to be the case in *G. oxydans* as participation of the EDP in the second growth phase (growth on gluconate) is even diminished (Hanke et al., in preparation).

One most interesting fact is the acetate formation in the EDP-deficient strains compared to the reference strain. Due to the disrupted TCA cycle, acetate is formed as a product in *G. oxydans*. ^{13}C-MFA has shown, that flux into the TCA cycle is nearly absent (Hanke at al, in preparation; Ostermann S., personal communication). With mannitol as the carbon source, the deletion mutant and the reference strain produce nearly the same amounts of acetate (Δ*upp* 32 ± 1 mM, Δ*upp* Δ*edd-eda* 28 ± 1 mM). On the contrary, with glucose as the carbon source, the amount of acetate formed is reduced by ~50% in the EDP deficient strain (Δ*upp* 61 ± 1 mM, Δ*upp* Δ*edd-eda* 31 ± 5 mM). With both substrates, acetate formation is time-delayed in the Δ*edd-eda* compared to the reference strain. The results obtained for glucose as the carbon source fit the assumption, that via the EDP twice as much acetate is formed from glucose 6-phosphate than via the PPP. Thus, the sole use of the PPP should lead to a decreased formation of acetate. The fact that this is not the case with mannitol as the carbon source might be explained by the increased uptake of fructose by the EDP deficient strain, whereas the amount of sugar consumed by this strain is the same compared to the reference strain with glucose as the carbon source. As the deletion mutant takes up 40% more fructose in the second growth phase compared to the reference strain, similar amounts of acetate are formed even though the PPP is used as the sole pathway for energy generation.

When cultivated with glucose as the carbon source the Δ*edd-eda* deletion mutant required nearly 50% more hydrochloric acid than the reference strain in the second growth phase to keep the pH constant. In growth phase I, the pH drops due to the formation of gluconic acid by oxidation of glucose and a base has to be titrated to the culture to keep the pH at a constant level. On the contrary, in growth phase II, due to the intracellular degradation of gluconic acid, hydrochloric acid has to be added to the culture to maintain a pH value of 6. In

an approach where the pH control was turned off in the second growth phase, growth of the deletion mutant was severely inhibited in comparison to the reference strain and the final optical density was reduced. This was accompanied by a faster and a stronger increase of the pH from 6 up to 7.5. Both, the deletion mutant and the reference strain, showed an inhibition in gluconate metabolism and formation of 2-KGA and acetate, but the effects were more drastic in the deletion mutant. In nature, acetate might be used for pH regulation of the surrounding medium. In the experiment lacking pH control in the second growth phase, sensibility of *G. oxydans* cells to pH values above 6 became obvious, as growth was inhibited significantly. Possibly, *G. oxydans* maintains its environment at an optimal pH range via acetate formation.

Summing up, the results indicate that neither of the two pathways for intracellular sugar metabolism, the EDP and the PPP, is essential for growth with mannitol or glucose as the carbon sources. Nevertheless, the PPP is the main intracellular route for glucose and mannitol degradation as well as energy generation in *G. oxydans*, whereas the EDP is dispensable or even unfavourable. Interestingly, the prevalence of the PPP as major catabolic pathway is a feature not often observed in bacteria. In a comparative ^{13}C-MFA of glucose metabolism in seven bacterial species (*Agrobacterium tumefaciens*, two pseudomonads, *Sinorhizobium meliloti*, *Rhodobacter sphaeroides*, *Zymomonas mobilis*, and *Paracoccus versutus*) it was shown that glucose was predominantly degraded via the EDP and the PPP had a solely anabolic function (Fuhrer et al. 2005). In the model organisms *E. coli* and *B. subtilis* on the other hand, the EMP was the predominant pathway for glucose metabolism (Fuhrer et al. 2005). Thus, *G. oxydans* belongs to a third group of organisms using the PPP as main route for cytoplasmic sugar metabolism.

4.2. The respiratory chain of *G. oxydans*

The respiratory chain of *G. oxydans* comprises two terminal oxidases, cytochrome *bd* oxidase and cytochrome bo_3 oxidase. To enlighten the impact of both terminal oxidases for growth of *G. oxydans* two deletion mutants were constructed. One lacked the genes encoding cytochrome *bd* oxidase (*cydAB*); the other lacked the genes encoding cytochrome bo_3 oxidase (*cyoBACD*). The genome sequence revealed that *G. oxydans* possesses genes (*qcrABC*) encoding a cytochrome bc_1 complex and soluble cytochrome *c* (*cycA*) but that genes encoding a cytochrome *c* oxidase are absent. Thus, the function of the cytochrome bc_1 complex remains enigmatic. To elucidate the function of the cytochrome bc_1 complex and to find out the consequences of its absence on global gene expression DNA microarray analysis was performed with a Δ*qrcABC* deletion mutant versus the wild type.

4.2.1 The role of the cytochrome bc_1 complex in *G. oxydans*

In order to obtain hints on the function of the cytochrome bc_1 complex in *G. oxydans*, DNA microarray analysis was performed. In a former study it had been shown that growth and sugar metabolism of the Δ*qcrABC* deletion mutant differed from the wild type when cultivated at pH 4 and oxygen excess with mannitol as carbon source (Hanke 2010). Therefore, these conditions were chosen for the comparison of global gene expression. In total, 55 genes showed a differential expression (Δ*qrcABC*/wild type) (full list of genes in paragraph 3.3, supplementary data), of which 75% also showed altered expression during oxygen limitation (Hanke et al. 2012).

The most interesting results were obtained for genes that are involved in energy metabolism and respiration. The mRNA levels of the gene cluster comprising the *pntA1A2B* genes and two genes for alcohol dehydrogenases/aldehyde reductase (GOX0310-0314, ratio 3.1–4.0) and the *cyoBACD* cluster (GOX1911-1914, ratio 2.1–2.3) were increased in the Δ*qrcABC* mutant. Increased expression of the cytochrome bo_3 oxidase genes suggested an insufficient electron transfer to oxygen via the remaining respiratory chain components in the Δ*qrcABC* mutant. This supports the assumption that the cytochrome bc_1 complex is functional and participates in respiration. Unfortunately, the DNA microarray gave no hints on the identity of the electron end acceptor of the cytochrome bc_1 complex. The same situation as in *G. oxyydans* can be found in the two related acetic acid bacteria, *A. pasteurianus* and *A. aceti* (Azuma et al. 2009; Sakurai et al. 2011). Other acetic acid bacteria such as *A. methanolicus* and *Granulibacter bethesdenis* are known to express cytochrome *c* oxidase, but they lack genes encoding a cytochrome bc_1 complex (Chan and Anthony 1991; Matsushita et al. 1992; Greenberg et al. 2007). In *A. methanolicus*, cytochrome *c* oxidase, methanol oxidase and cytochromes c_L and c_H are only expressed when cells are cultivated with methanol as carbon source, but not during growth with other carbon sources like glucose or glycerol. In cells grown with glucose or glycerol, electrons are transferred from the dehydrogenases via the ubiquinone pool to a *bo*-type oxidase. Interestingly, in *A. methanolicus*, unlike *G. oxydans*, the presence of a cytochrome bc_1 complex has not been shown, but it is assumed that the electrons are directly channeled from methanol dehydrogenase to cytochrome *c* oxidase via soluble cytochrome *c* (Matsushita et al. 1992).

4.2.2 The role of the terminal oxidases in *G. oxydans*

In this study, the role of the two terminal oxidases, cytochrome *bd* oxidase and cytochrome bo_3 oxidase was elucidated. Already the construction of the deletion mutants gave an indication concerning the importance of the terminal oxidases. While deletion of the genes encoding cytochrome *bd* oxidase worked easily, identification of a strain lacking

cytochrome bo_3 oxidase was time-consuming. More than 500 colonies had to be screened for the isolation of only one deletion mutant. This indicated that cytochrome bo_3 oxidase is the main terminal oxidase in *G. oxydans,* but neither of the two terminal oxidases is essential for survival.

Absence of cytochrome *bd* oxidase did not affect growth or proton extrusion via the respiratory chain after an oxygen pulse (H^+/O ratio), whereas absence of the genes encoding cytochrome bo_3 oxidase caused a severe growth defect. This was accompanied by a significantly reduced H^+/O ratio in comparison to the reference strain. Plasmid-based overexpression of the genes *cyoBACD* in the *G. oxydans* reference strain led to an increase of the final OD_{600} by 20% in comparison to the reference strain carrying only the vector without the *cyoBACD* genes. In contrast, overexpression of the genes *cydAB* encoding cytochrome *bd* oxidase resulted in an unaltered final cell density in comparison to the reference strain. In *E. coli* overexpression of the genes encoding cytochrome bo_3 oxidase in a *cydAB*-*cyoBACD*-deficient strain led to an increased final cell densitiy as well (Minohara et al. 2002).

Reduced-minus-oxidized difference spectra of the strain lacking cytochrome bo_3 oxidase showed an increased peak size at 626 nm, corresponding to the absorption peak of cytochrome *d*. This agrees with DNA microarray analyses of the Δ*cyoBACD* mutant showing a 3.6-5.4-fold increased expression of the genes *cydA* and *cydB* (GOX0278 and GOX0279) compared to the reference strain (full list of genes in Appendix 6.1). As growth and the H^+/O ratio of Δ*cyoBACD* mutant were significantly reduced, overexpression of *cydAB* could not compensate the lack of cytochrome bo_3 oxidase. Reduced-minus-oxidized spectra of the strain lacking cytochrome *bd* oxidase did not differ from the reference strain, which is in agreement with results published by Mogi et al. (Mogi et al. 2009). Cytochrome *bd* oxidase from *E. coli* and the cyanide-insensitive *bd*-type oxidase from *P. aeruginosa* (CioAB) are induced under low oxygen conditions (Matsushita et al. 1983; Cunningham et al. 1997). DNA microarray analyses of *G. oxydans* also revealed that the genes encoding cytochrome *bd* oxidase were upregulated under oxygen limitation (Hanke et al. 2012). Furthermore, it was shown that expression of the *cydAB* genes is higher at pH 4 than at pH 6, which again agrees with results reported by Matsushita et al. (Matsushita et al. 1989; Hanke et al. 2012). This indicates that the cytochrome *bd* oxidase might have an additional function at low pH values or under oxygen limited conditions, which are likely to occur in natural habitats of *G. oxydans*. Nevertheless, growth of the strain Δ*upp* Δ*cydAB* did not differ from the reference strain at pH 4 and under oxygen-limited growth conditions (unpublished data). However, RAMOS cultivations performed with the strain lacking cytochrome bo_3 oxidase under conditions leading to oxygen limitation during growth showed a different behavior of the OTR time course than obtained for the reference strain and *bd* oxidase mutant indicating a low

oxygen affinity of cytochrome *bd*. This is further corroborated by the similarity of genes *cydAB* of *G. oxydans* to the low oxygen-affine CioAB oxidases CioAB from *P. aeruginosa* and *Z. mobilis* (Mogi et al. 2009). The sole deletion of the genes encoding cytochrome *bd* oxidase did not result in an improved growth, but elevated final cell densities were attainable by overexpression of *cyoBACD*. It may be assumed that the activity of cytochrome *bd* oxidase is negligible under the tested conditions.

The H^+/O ratios obtained in this study for *G. oxydans* are rather low in comparison to those obtained e.g. for *E. coli* even though both possess cytochrome *bd* and cytochrome bo_3 as terminal oxidases. Control experiments with *E. coli* using the same experimental setup showed that this was not due to a technical problem, as the values achieved were in the range of H^+/O ratios reported previously (Lawford and Haddock 1973; Brice et al. 1974). The H^+/O values reported in this study agree with the values obtained by Matsushita et al. for *G. oxydans* wild type cells cultivated at pH 6 and pH 4 and using different carbon sources and endogenous NADH as respiratory substrate, which were in a range of 1.1-1.5 (pH 4) and 1.7-2.3 (pH 6) (Matsushita et al. 1989). Matsushita et al. suggested that the cytochrome *bd* oxidase does not take part in charge separation at all (Matsushita et al. 2004). Instead, it was supposed to work as an non-energy generating bypass, as the proton gradient generated by the rapid periplasmic oxidation of sugar/alcohols would exert a feedback inhibition on the terminal oxidases which in turn would cause a high reduction state of the ubiquinone pool and deprive the membrane dehydrogenases of their electron acceptor. One solution to this problem suggested by these authors is that at least a part of the respiratory chain has a route not coupled to the build up of proton-motive force. Another possibility would be that electron transfer and energy generation in the respiratory chain are uncoupled in some way (Matsushita et al. 2004). A respective growth phenotype of the Δ*cydAB* mutant was not observed under our cultivation conditions.

In *E. coli* the oxidation of UQH_2 to UQ leads to the release of two protons into the periplasmic space, resulting in charge separation across the membrane. As protons for the formation of water from oxygen are taken up from the cytoplasm, a net flux of two protons across the membrane occurs, being in agreement with the H^+/O ratio for cytochrome *bd* oxidase of two (Miller and Gennis 1985; Borisov et al. 2011a). Cytochrome bo_3 oxidase works as an active proton pump, thus a H^+/O ratio of four is assumed (Puustinen et al. 1989; Chepuri et al. 1990). In Fig. 6A, this model of the respiratory chain is presented. The values measured for *G. oxydans* are much lower than the values calculated for *E. coli*. A speculative hypothesis to explain the lower H^+/O ratios in *G. oxydans* compared to *E.coli* is the suggestion that protons used for the generation of water from oxygen are taken up from the periplasmic space as shown in Fig. 6B. Such a hypothesis was made for *E. coli bd*-II oxidase in a study, where the H^+/e^- ratio was calculated to 0.2 ± 0.1, representing a respiratory chain

capable of functioning in a fully uncoupled mode (Bekker et al. 2009). As the results were disproved, this hypothesis was not discussed further. Borisov et al. showed that both cytochrome *bd* oxidases in *E. coli* produce a H^+/e^- ratio of 1 (Borisov et al. 2011b). In this case, the release of protons from the oxidation of UQH_2 into the periplasm is accompanied by an uptake of two protons for the formation of water from oxygen. Thus, a net-flux of zero protons occurs, leading to an expected H^+/O ratio of zero for cytochrome *bd* oxidase. As cytochrome bo_3 oxidase still works as a proton pump, an H^+/O ratio of two is calculated for this model. The H^+/O values measured for the reference strain and the cytochrome *bd* deficient strain are 1.26 and 1.31, respectively. As no correction for the proton influx into the cells that occurred during the acidification has been made, the determined H^+/O ratios represent minimal values. Thus, the measured values might fit to the proposed model. On the contrary, H^+/O values for the cytochrome bo_3 deficient strain are 0.56, whereas zero would be expected. Thus, there must be an additional respiratory component contributing to the generation of proton-motive force. With reference to the genome of *G. oxydans* the cytochrome bc_1 complex may be involved.

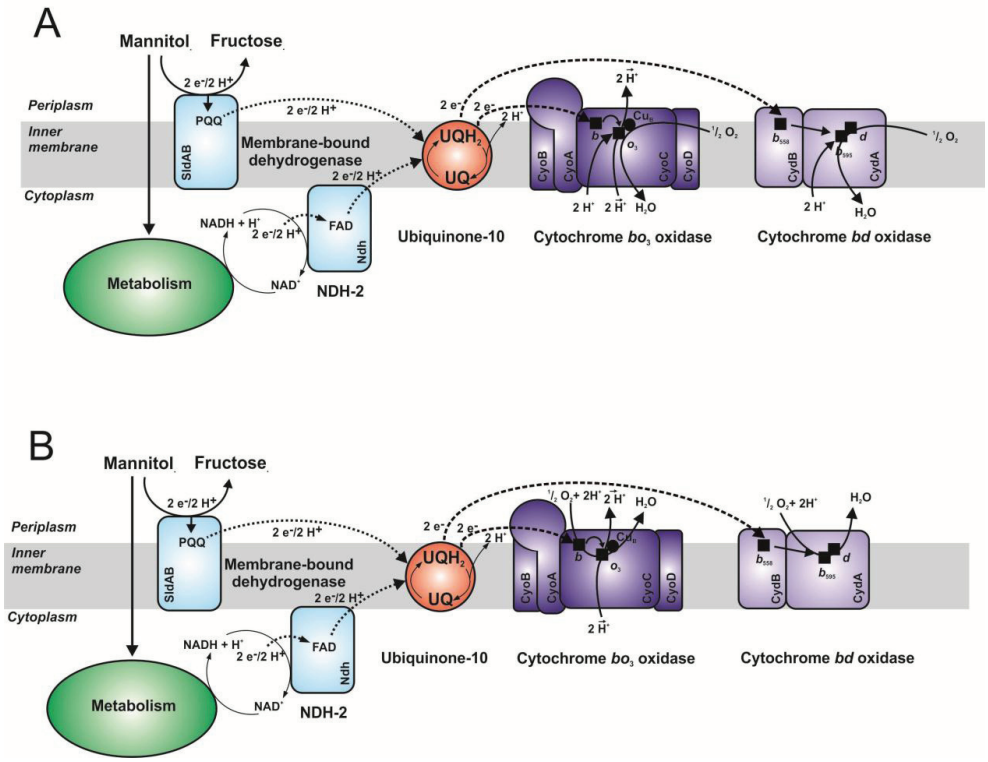

Fig 6: Scheme of the respiratory chain of *G. oxydans* presenting two possible models for delivery of protons and electrons from the cytoplasmic (A) or periplasmic (B) side of the cytoplasmic membrane.

Another difference beween *G. oxydans* and *E. coli* is the oxidation of the substrate. The catalytic center of the membrane-bound major polyol dehydrogenase SldAB is located in the periplasm and delivers 2 H^+ and 2 e^- for the reduction of ubiquinone-10 from outside the cells to the ubiquinone pool, whereas the NADH dehydrogenase delivers 2 H^+ and 2 e^- from the cytoplasm. Nevertheless, in both cases charge separation across the membrane occurs due to the release of protons via the oxidation from UQH_2 to UQ and the origin of the protons should not have an impact on H^+/O ratios. This is in agreement with results obtained by Matsushita et al., in which respiration with endogenous substrates leads to similar H^+/O values as obtained e.g. for glucose (2.3 ± 0.4 and 1.8 ± 0.3, respectively) (Matsushita et al. 1989). For A*cetobacer pasteurianus* that possesses cytochrome *bd* and cytochrome bo_3 oxidase as well as *G. oxydans* as terminal oxidases, H^+/O ratios in a range of 1.9 ± 0.1 for the oxidation of ethanol are reported. Thus, the proposed model of the respiratory chain might be applicable to other acetic acid bacteria as well (Luttik et al. 1997).

Due to the low H^+/O ratio *G. oxydans* Δ*upp* Δ*cyoBACD* is limited in energy generation via F_1F_o-ATP synthase. *G. oxydans* possesses a second F_1F_o-synthase that possibly can use Na^+ instead of H^+ for ATP formation (Prust et al. 2005; Dibrova et al. 2010). As some of the genes encoding this alternative ATP synthase were upregulated in the strain lacking cytochrome bo_3 oxidase, there might exist an alternative pathway to restore energy generation, provided that an up to now unknown primary sodium pump is present in *G. oxydans* (Appendix 6.1, supplementary data).

The fact that deletion of the *cydAB* genes did not result in a growth phenotype leads to the conclusion that under the chosen conditions the entire electron flux to oxygen was directed via the cytochrome bo_3 oxidase. Surprisingly, overproduction of cytochrome bo_3 led to an increased biomass formation. This means that in the reference strain cytochrome bo_3 oxidase is the rate-limiting factor of the respiratory chain. Obviously, the activity of the major polyol dehydrogenase SldAB is high enough to deliver sufficient electrons via the UQ-pool to an elevated concentration of cytochrome bo_3 allowing an increased proton-pumping capacity of the cells. This gain of energy explains the increased growth yield and final OD_{600} of a strain overexpressing the genes encoding for cytochrome bo_3 oxidase.

4.3 Conclusions

In this study the respiratory chain and the central carbon metabolism have been investigated to gain a better understanding of the participation of the two intracellular pathways for sugar metabolism, the EDP and the PPP, and the two terminal oxidases, the cytochrome *bd* and cytochrome bo_3 oxidase. Results concerning the central carbon metabolism have shown that neither of the pathways is essential for growth. However, the PPP is the main pathway for cytoplasmic sugar metabsolism in *G. oxydans*, which is very unusual in bacteria. On the other hand, the EDP is dispensable and absence might even have a positive effect.

Analysis of the respiratory chain revealed that neither cytochrome *bd* nor cytochrome bo_3 oxidase is essential for survival of *G. oxydans*. However, the cytochrome bo_3 oxidase is the main terminal oxidase as it is assumed to work as an active proton pump as described for other bacteria. In this work, a model for the respiratory chain is proposed, in which the formation of water occurs in the periplasm and not in the cytoplasm. This might explain the low H^+/O ratios in *G. oxydans* and other acetic acid bacteria, which in turn might be a reason for the low biomass yields.

The application of *G. oxydans* in biotechnological processes is limited due to the cost-extensive production of biomass. In this work, three alternative pathways for rising biomass formation of *G. oxydans* with mannitol as the carbon source were identified:

(I) deletion of the genes encoding 6-phosphogluconate dehydrogenase (*edd*) and KDPG-aldolase (*eda*)
(II) overexpression of gene encoding glucose 6-phosphate dehydrogenase, *gnd*
(III) overexpressin of genes encoding cytochrome bo_3 oxidase, *cyoBACD*

These findings might be useful for the rational design of new producer strains for industrial processes.

4.4. Outlook

The results obtained in this work show great potential for the optimization of current producer strains of *G. oxydans* in industrial biotechnology. Three possibilities were presented that allow increased biomass formation with mannitol as carbon source. Thereby, the costs for cell mass of *G. oxydans* used in biotechnological processes with resting cells can be reduced.

In future attempts, a combinatorial approach should be performed, e.g. overexpressing cytochrome bo_3 oxidase in a strain lacking the genes for the EDP. This might lead to a further enhancement of growth. The surplus of NAD(P)H generated by the sole use of the PPP is used by NDH-II dehydrogenase to channel electrons into the respiratory chain. Due to the overexpression, electrons will be mainly channeled to the cytochrome bo_3 oxidase. As the cytochrome bo_3 oxidase was shown to actively take part in the formation of a proton gradient across the membrane, this might lead to an increased formation of ATP via F_1F_0-ATP synthase. Furthermore, expression of a type I NADH-dehydrogenase possibly could also improve the formation of a proton gradient across the membrane.

Another important question emerged in this work concerning the energetic differences of mannitol and glucose catabolism. The question why growth was improved due to the deletion of the EDP with mannitol as carbon source but not with glucose might be answered by investigating a Δ*upp* Δ*edd-eda* strain lacking in addition to deletion of *edd* and *eda* the genes encoding the membrane-bound gluconate dehydrogenase. Furthermore, ^{13}C-MFA with mannitol as carbon source might reveal a different use of the two pathways for intracellular sugar metabolism, the EDP and the PPP. Until now, unfortunately, no minimal medium is available for analysis of ^{13}C-MFA, making the evaluation of the results obtaine with cells

grown in complex medium more complicated. As soon as this problem is solved the differential pathway regulation in *G. oxydans* with either glucose or mannitol as the carbon sources could be demonstrated and the use of deletion mutants will consolidate the results.

An additional strategy for growth optimization and improvement of cell yield is the complementation of the TCA cycle in combination with heterologous expression of phosphofructokinase. In a recently published study it has been shown, that due to deletion of pyruvate decarboxylase pyruvate is secreted by *G. oxydans*, as the flux into the interrupted TCA cycle is limited (Kiefler 2012; Peters et al. 2012). This problem might be overcome by expression of a succinate dehydrogenase thereby closing the TCA cycle and possibly leading to better growth.

5. Literature

Ameyama, M., Matsushita, K., Shinagawa, E. and Adachi, O. (1987) Sugar-oxidizing Respiratory Chain of *Gluconobacter suboxydans*. Evidence for a Branched Respiratory Chain and Characterization of Respiratory Chain-Linked Cytochromes. *Agric Biol Chem* 51 2943-2950.

Anraku, Y. (1988) Bacterial electron transport chains. *Annu Rev Biochem* 57, 101-132.

Asai, T. (1935) Taxonomic studies on acetic acid bacteria and allied oxidative bacteria isolated from fruits. A new classification of the oxidative bacteria. *J Agr Chem Soc Jpn* 11, 499-513, 610-620, 674-708.

Azuma, Y., Hosoyama, A., Matsutani, M., Furuya, N., Horikawa, H., Harada, T., Hirakawa, H., Kuhara, S., Matsushita, K., Fujita, N. and Shirai, M. (2009) Whole-genome analyses reveal genetic instability of *Acetobacter pasteurianus*. *Nucleic Acids Res* 37, 5768-5783.

Baart, G.J., Langenhof, M., van de Waterbeemd, B., Hamstra, H.J., Zomer, B., van der Pol, L.A., Beuvery, E.C., Tramper, J. and Martens, D.E. (2010) Expression of phosphofructokinase in *Neisseria meningitidis*. *Microbiology* 156, 530-542.

Battey, A.S., Duffy, S. and Schaffner, D.W. (2002) Modeling yeast spoilage in cold-filled ready-to-drink beverages with *Saccharomyces cerevisiae, Zygosaccharomyces bailii,* and *Candida lipolytica*. *Appl Environ Microbiol* 68, 1901-1906.

Bizouarn, T., Althage, M., Pedersen, A., Tigerstrom, A., Karlsson, J., Johansson, C. and Rydstrom, J. (2002) The organization of the membrane domain and its interaction with the NADP(H)-binding site in proton-translocating transhydrogenase from *E. coli*. *Biochim Biophys Acta* 1555, 122-127.

Borisov, V.B., Gennis, R.B., Hemp, J. and Verkhovsky, M.I. (2011) The cytochrome *bd* respiratory oxygen reductases. *Biochim Biophys Acta* 1807, 1398-1413.

Brandt, U., Kerscher, S., Drose, S., Zwicker, K. and Zickermann, V. (2003) Proton pumping by NADH:ubiquinone oxidoreductase. A redox driven conformational change mechanism? *FEBS Lett* 545, 9-17.

Bremus, C., Herrmann, U., Bringer-Meyer, S. and Sahm, H. (2006) The use of microorganisms in L-ascorbic acid production. *J Biotechnol* 124, 196-205.

Calhoun, M.W., Oden, K.L., Gennis, R.B., de Mattos, M.J. and Neijssel, O.M. (1993) Energetic efficiency of *Escherichia coli*: effects of mutations in components of the aerobic respiratory chain. *J Bacteriol* 175, 3020-3025.

Chepuri, V., Lemieux, L., Au, D.C. and Gennis, R.B. (1990) The sequence of the *cyo* operon indicates substantial structural similarities between the cytochrome o ubiquinol oxidase of *Escherichia coli* and the aa_3-type family of cytochrome *c* oxidases. *J Biol Chem* 265, 11185-11192.

Chinnawirotpisan, P., Matsushita, K., Toyama, H., Adachi, O., Limtong, S. and Theeragool, G. (2003) Purification and characterization of two NAD-dependent alcohol dehydrogenases (ADHs) induced in the quinoprotein ADH-deficient mutant of *Acetobacter pasteurianus* SKU1108. *Biosci Biotechnol Biochem* 67, 958-965.

Claret, C., Bories, A. and Soucaille, P. (1992) Glycerol inhibition of growth and dihydroxyacetone production by *Gluconobacter oxydans*. *Curr Microbiol* 25, 149-155.

Cotton, N.P., White, S.A., Peake, S.J., McSweeney, S. and Jackson, J.B. (2001) The crystal structure of an asymmetric complex of the two nucleotide binding components of proton-translocating transhydrogenase. *Structure* 9, 165-176.

D'Mello, R., Hill, S. and Poole, R.K. (1996) The cytochrome bd quinol oxidase in *Escherichia coli* has an extremely high oxygen affinity and two oxygen-binding haems: implications for regulation of activity in vivo by oxygen inhibition. *Microbiology* 142 (Pt 4), 755-763.

Daniel, R.M. (1970) The electron transport system of *Acetobacter suboxydans* with particular reference to cytochrome. *Biochim Biophys Acta* 216, 328-341.

Dauner, M., Sonderegger, M., Hochuli, M., Szyperski, T., Wuthrich, K., Hohmann, H.P., Sauer, U. and Bailey, J.E. (2002) Intracellular carbon fluxes in riboflavin-producing *Bacillus subtilis* during growth on two-carbon substrate mixtures. *Appl Environ Microbiol* 68, 1760-1771.

De Ley, J., Gillis, M. and Swings, J. (1984) The genus *Gluconobacter*. *Krieg NR, Holt JG (eds) Bergey's manual of systematic bacteriology* vol 1, pp 267–278.

Deppenmeier, U. and Ehrenreich, A. (2009) Physiology of acetic acid bacteria in light of the genome sequence of *Gluconobacter oxydans*. *J Mol Microbiol Biotechnol* 16, 69-80.

Deppenmeier, U., Hoffmeister, M. and Prust, C. (2002) Biochemistry and biotechnological applications of *Gluconobacter* strains. *Appl Microbiol Biotechnol* 60, 233-242.

Euzeby, J. (2005) Validation of publication of new names and new combinations previously effectively published outside the IJSEM. *Int J Syst Evol Microbiol* 55, 983-985.

Georgiou, C.D., Dueweke, T.J. and Gennis, R.B. (1988) Beta-galactosidase gene fusions as probes for the cytoplasmic regions of subunits I and II of the membrane-bound cytochrome d terminal oxidase from *Escherichia coli*. *J Biol Chem* 263, 13130-13137.

Gossele, F., Van den Mooter, M., Verdonck, L., Swings, J. and De Ley, J. (1981) The nitrogen requirements of *Gluconobacter, Acetobacter* and *Frateuria*. *Antonie Van Leeuwenhoek* 47, 289-296.

Greenfield, S. and Claus, G.W. (1972) Nonfunctional tricarboxylic acid cycle and the mechanism of glutamate biosynthesis in *Acetobacter suboxydans*. *J Bacteriol* 112, 1295-1301.

Gupta, A., Singh, V.K., Qazi, G.N. and Kumar, A. (2001) *Gluconobacter oxydans*: its biotechnological applications. *J Mol Microbiol Biotechnol* 3, 445-456.

Hancock, R.D. (2009) Recent patents on vitamin C: opportunities for crop improvement and single-step biological manufacture. *Recent Pat Food Nutr Agric* 1, 39-49.

Hanke, T. (2010) Studies on central carbon metabolism and respiration of *Gluconobacter oxydans* 621H. *Dissertation; Forschungszentrum Jülich GmbH*.

Hanke, T., Richhardt, J., Polen, T., Sahm, H., Bringer, S. and Bott, M. (2012) Influence of oxygen limitation, absence of the cytochrome bc_1 complex and low pH on global gene expression in *Gluconobacter oxydans* 621H using DNA microarray technology. *J Biotechnol* doi:10.1016/j.jbiotec.2011.12.020.

Hauge, J.G., King, T.E. and Cheldelin, V.H. (1955) Oxidation of dihydroxyacetone via the pentose cycle in *Acetobacter suboxydans*. *J Biol Chem* 214, 11-26.

Heefner, D.L. and Claus, G.W. (1976) Change in quantity of lipids and cell size during intracytoplasmic membrane formation in *Gluconobacter oxydans*. *J Bacteriol* 125, 1163-1171.

Jackson, J.B., White, S.A., Quirk, P.G. and Venning, J.D. (2002) The alternating site, binding change mechanism for proton translocation by transhydrogenase. *Biochemistry* 41, 4173-4185.

Kallnik, V., Meyer, M., Deppenmeier, U. and Schweiger, P. (2010) Construction of expression vectors for protein production in *Gluconobacter oxydans*. *J Biotechnol* 150, 460-465.

Katzen, F., Becker, A., Ielmini, M.V., Oddo, C.G. and Ielpi, L. (1999) New mobilizable vectors suitable for gene replacement in gram-negative bacteria and their use in mapping of the 3' end of the *Xanthomonas campestris* pv. campestris *gum* operon. *Appl Environ Microbiol* 65, 278-282.

Kersters, K. and De Ley, J. (1968a) An easy screening assay for the enzymes of the Entner-Doudoroff pathway. *Antonie Van Leeuwenhoek* 34, 388-392.

Kersters, K. and De Ley, J. (1968b) The occurrence of the Entner-Doudoroff pathway in bacteria. *Antonie Van Leeuwenhoek* 34, 393-408.

Kersters, K., Lisdiyanti, P., Komagata, K. and Swings, J. (2006) The family *Acetobacteriaceae*: The genera *Acetobacter*, *Acidomonas*, *Asaia*, *Gluconacetobacter*, *Gluconobacter*, and *Kozakia*. *In: Dworkin M, Falkow S, Rosenberg E, Schleifer K-H, Stackebrandt E (eds),The Prokaryotes Vol 5, 3rd edition Springer-Verlag GmbH, Heidelberg* p. 163-200.

Kita, K., Kasahara, M. and Anraku, Y. (1982) Formation of a membrane potential by reconstructed liposomes made with cytochrome b562-o complex, a terminal oxidase of *Escherichia coli* K12. *J Biol Chem* 257, 7933-7935.

Krajewski, V., Simic, P., Mouncey, N.J., Bringer, S., Sahm, H. and Bott, M. (2010) Metabolic engineering of *Gluconobacter oxydans* for improved growth rate and growth yield on glucose by elimination of gluconate formation. *Appl Environ Microbiol* 76, 4369-4376.

Kruger, N.J. and von Schaewen, A. (2003) The oxidative pentose phosphate pathway: structure and organisation. *Curr Opin Plant Biol* 6, 236-246.

Lauraeus, M., Haltia, T., Saraste, M. and Wikstrom, M. (1991) *Bacillus subtilis* expresses two kinds of haem-A-containing terminal oxidases. *Eur J Biochem* 197, 699-705.

Lawford, H.G. and Haddock, B.A. (1973) Respiration-driven proton translocation in *Escherichia coli*. *Biochem J* 136, 217-220.

Leisinger, T. (1965) [Studies on the systematics and metabolism of acetic acid bacteria]. *Zentralbl Bakteriol Parasitenkd Infektionskr Hyg* 119, 329-376.

Ludwig, B. (1992) Terminal oxidases in *Paracoccus denitrificans*. *Biochim Biophys Acta* 1101, 195-197.

Matsushita, K., Nagatani, Y., Shinagawa, E., Adachi, O. and Ameyama, M. (1989) Effect of extracellular pH on the respiratory chain and energetics of *Gluconobacter suboxydans*. *Agr Biol Chem* 53, 2895-2902.

Matsushita, K., Shinagawa, E., Adachi, O. and Ameyama, M. (1987) Purification, characterization and reconstitution of cytochrome *o*-type oxidase from *Gluconobacter suboxydans*. *Biochim Biophys Acta* 894, 304-312.

Matsushita, K., Toyama, H. and Adachi, O. (2004) Respiratory Chains and Bioenergetics of Acetic Acid Bacteria. *Advances in microbial physiology* 36, 247-301.

Meyer, M., Schweiger, P. and Deppenmeier, U. (2012) Effects of membrane-bound glucose dehydrogenase overproduction on the respiratory chain of *Gluconobacter oxydans*. *Appl Microbiol Biotechnol*.

Miller, M.J. and Gennis, R.B. (1985) The cytochrome *d* complex is a coupling site in the aerobic respiratory chain of *Escherichia coli*. *J Biol Chem* 260, 14003-14008.

Minohara, S., Sakamoto, J. and Sone, N. (2002) Improved H+/O ratio and cell yield of *Escherichia coli* with genetically altered terminal quinol oxidases. *J Biosci Bioeng* 93, 464-469.

Mogi, T., Ano, Y., Nakatsuka, T., Toyama, H., Muroi, A., Miyoshi, H., Migita, C.T., Ui, H., Shiomi, K., Omura, S., Kita, K. and Matsushita, K. (2009) Biochemical and spectroscopic properties of cyanide-insensitive quinol oxidase from *Gluconobacter oxydans*. *J Biochem* 146, 263-271.

Olijve, W. and Kok, J.J. (1979a) Analysis of growth of *Gluconobacter oxydans* in glucose containing media. *Arch Microbiol* 121, 283-290.

Olijve, W. and Kok, J.J. (1979b) An analysis of the growth of *Gluconobacter oxydans* in chemostat cultures. *Arch Microbiol* 121, 291-297.

Parmentier, S., Beauprez, J., Arnaut, F., Soetaert, W. and Vandamme, E.J. (2005) *Gluconobacter oxydans* NAD-dependent, D-fructose reducing, polyol dehydrogenases activity: screening, medium optimisation and application for enzymatic polyol production. *Biotechnol Lett* 27, 305-311.

Pedersen, A., Karlsson, G.B. and Rydstrom, J. (2008) Proton-translocating transhydrogenase: an update of unsolved and controversial issues. *J Bioenerg Biomembr* 40, 463-473.

Peters, B., Junker, A., Brauer, K., Muhlthaler, B., Kostner, D., Mientus, M., Liebl, W. and Ehrenreich, A. (2012) Deletion of pyruvate decarboxylase by a new method for efficient markerless gene deletions in *Gluconobacter oxydans*. *Appl Microbiol Biotechnol*.

Prust, C. (2004) Entschlüsselung des Genoms von *Gluconobacter oxydans* 621H – einem Bakterium von industriellem Interesse. *Dissertation, Universität Göttingen*.

Prust, C., Hoffmeister, M., Liesegang, H., Wiezer, A., Fricke, W.F., Ehrenreich, A., Gottschalk, G. and Deppenmeier, U. (2005) Complete genome sequence of the acetic acid bacterium *Gluconobacter oxydans*. *Nat Biotechnol* 23, 195-200.

Puustinen, A., Finel, M., Haltia, T., Gennis, R.B. and Wikstrom, M. (1991) Properties of the two terminal oxidases of *Escherichia coli*. *Biochemistry* 30, 3936-3942.

Puustinen, A., Finel, M., Virkki, M. and Wikstrom, M. (1989) Cytochrome o (bo) is a proton pump in *Paracoccus denitrificans* and *Escherichia coli*. *FEBS Lett* 249, 163-167.

Raspor, P.P. and Goranovič, D. (2008) Biotechnological applications of acetic acid bacteria. *Crit Rev Biotechnol* 28, 101-124.

Rauch, B., Pahlke, J., Schweiger, P. and Deppenmeier, U. (2010) Characterization of enzymes involved in the central metabolism of *Gluconobacter oxydans*. *Appl Microbiol Biotechnol* 88, 711-718.

Schedel, M. (2000) Regioselective oxidation of aminosorbitol with Gluconobacter oxydans, a key reaction in the industrial synthesis of 1-deoxynojirimycin. *Kelly DR (ed) Biotechnology; Wiley-VCH, Weinheim* vol 8b, pp 296–308.

Schultz, B.E. and Chan, S.I. (1998) Thermodynamics of electron transfer in *Escherichia coli* cytochrome *bo*3. *Proc Natl Acad Sci U S A* 95, 11643-11648.

Schweiger, P., Volland, S. and Deppenmeier, U. (2007) Overproduction and characterization of two distinct aldehyde-oxidizing enzymes from *Gluconobacter oxydans* 621H. *J Mol Microbiol Biotechnol* 13, 147-155.

Schweikert, S. (2011) Transcriptional responses and transcriptional regulators of *Gluconobacter oxydans* 621H. *Dissertation; Forschungszentrum Jülich GmbH*.

Siedler, S., Bringer, S., Blank, L.M. and Bott, M. (2011) Engineering yield and rate of reductive biotransformation in *Escherichia coli* by partial cyclization of the pentose phosphate pathway and PTS-independent glucose transport. *Appl Microbiol Biotechnol* DOI 10.1007/s00253-011-3626-3.

Soini, J., Ukkonen, K. and Neubauer, P. (2008) High cell density media for *Escherichia coli* are generally designed for aerobic cultivations - consequences for large-scale bioprocesses and shake flask cultures. *Microb Cell Fact* 7, 26.

Svitel, J., Tkac, J., Vostiar, I., Navratil, M., Stefuca, V., Bucko, M. and Gemeiner, P. (2006) *Gluconobacter* in biosensors: applications of whole cells and enzymes isolated from *Gluconobacter* and *Acetobacter* to biosensor construction. *Biotechnol Lett* 28, 2003-2010.

Tonouchi, N., Sugiyama, M. and Yokozeki, K. (2003) Coenzyme specificity of enzymes in the oxidative pentose phosphate pathway of *Gluconobacter oxydans*. *Biosci Biotechnol Biochem* 67, 2648-2651.

Tran, Q.H. and Unden, G. (1998) Changes in the proton potential and the cellular energetics of *Escherichia coli* during growth by aerobic and anaerobic respiration or by fermentation. *Eur J Biochem* 251, 538-543.

Yamada, Y., Hosono, R., Lisdyanti, P., Widyastuti, Y., Saono, S., Uchimura, T. and Komagata, K. (1999) Identification of acetic acid bacteria isolated from Indonesian sources, especially of isolates classified in the genus *Gluconobacter*. *J Gen Appl Microbiol* 45, 23-28.

Yamada, Y. and Yukphan, P. (2008) Genera and species in acetic acid bacteria. *Int J Food Microbiol* 125, 15-24.

6. Appendix

6.1. Supplementary data: DNA-microarray analysis of strain *G. oxydans* Δ*bo*$_3$ versus the reference strain

Cells were cultivated in a baffled shake shake flasks with mannitol as the carbon source and harvested at OD_{600} = 1.5. RNA extraction, cDNA labeling and DNA microarray analysis was performed as described by Hanke et al. 2012. Genes showing a mRNA ratio ≥ 2 and ≤ 0.5 and a p-value ≤ 0.05 are presented (Δ*upp* Δ*bo*$_3$/ Δ*upp*). The ratios are mean values of three independent experiments (n=3). An overall view of up- and downregulated genes as well as a sorting in functional categories is presented.

***G. oxydans* Δ*upp* Δ*bo3* versus *G. oxydans* Δ*upp* (reference); mRNA ratio of 102 genes ≥2.0**

Gene	Annotation	Gene name	mRNA ratio	n	*p*-Value
GOX0057	Protein with GGDEF and EAL domain		2.11	3	1.36E-02
GOX0069	Hypothetical membrane-spanning protein		2.13	3	1.03E-02
GOX0135	Transcriptional regulator, Ros/MucR family		2.30	3	1.99E-04
GOX0278	Cytochrome *bd* ubiquinol oxidase subunit I	*cydA*	5.43	3	9.28E-03
GOX0279	Cytochrome *bd* ubiquinol oxidase subunit II	*cydB*	3.61	3	2.01E-02
GOX0290	Putative oxidoreductase		2.43	3	4.35E-02
GOX0291	Putative ferredoxin subunit of ring-hydroxylating dioxygenase	*hca*	3.69	3	9.29E-03
GOX0311	NAD(P) transhydrogenase subunit α2	*pntA2*	2.46	3	6.48E-03
GOX0312	NAD(P) transhydrogenase subunit b	*pntB*	2.19	3	1.36E-03
GOX0313	Alcohol:NAD^+ oxidoreductase		2.22	3	1.20E-02
GOX0433	Hypothetical protein GOX0433		4.81	3	1.16E-02
GOX0442	Hypothetical protein GOX0442		2.67	3	3.50E-02
GOX0475	Hypothetical protein GOX0475		2.36	3	2.13E-02
GOX0498	Hypothetical protein GOX0498		2.38	3	1.52E-02
GOX0502	Putative oxidoreductase		2.05	3	3.69E-02
GOX0503	Hypothetical protein GOX0503		2.23	3	4.46E-02
GOX0519	Hypothetical outer membrane protein		2.35	3	2.05E-02
GOX0532	ExbB protein	*exbB*	3.40	3	2.46E-02
GOX0545	Putative outer membrane receptor for iron transport		2.72	3	9.08E-04
GOX0566	Ubiquinol-cytochrome *c* oxidoreductase. cytochrome *b*	*qrcB*	2.03	3	5.60E-03
GOX0570	Hypothetical protein GOX0570		3.51	3	2.57E-02

GOX0576	Hypothetical protein GOX0576		2.31	3	1.36E-02
GOX0635	Hypothetical protein GOX0635		2.53	3	2.06E-02
GOX0646	Putative oxidoreductase		2.37	3	2.12E-02
GOX0647	Putative exporter protein, ArAE family	*fusB*	2.96	3	2.43E-02
GOX0673	Ferrous iron transport protein A (FeoA)	*feoA*	4.40	3	2.14E-04
GOX0674	Ferrous iron transport protein B (FeoB)	*feoB*	2.51	3	1.03E-02
GOX0679	Conserved protein of the SAM superfamily		3.71	3	1.90E-02
GOX0707	DNA starvation/stationary phase protection protein Dps	*dps*	3.46	3	1.33E-02
GOX0726	Hypothetical protein GOX0726		5.83	3	3.85E-02
GOX0756	Alcohol dehydrogenase 15 kDa subunit		2.14	3	5.42E-02
GOX0814	PTS system IIA component	*ptsIIA*	2.13	3	2.38E-03
GOX0815	Hypothetical protein GOX0815		2.39	3	1.75E-02
GOX0875	AtsE protein		2.19	3	9.83E-03
GOX0881	Arylesterase		2.31	3	3.51E-03
GOX0890	Hypothetical protein GOX0890		2.39	3	2.47E-02
GOX0915	Hypothetical protein GOX0915		2.28	3	1.34E-04
GOX1050	dTDP-4-dehydrorhamnose reductase		2.24	3	9.65E-04
GOX1051	dTDP-4-dehydrorhamnose 3.5-epimerase		2.62	3	4.93E-03
GOX1052	Glucose-1-phosphate thymidylyltransferase, C-terminus		2.64	3	2.93E-03
GOX1053	dTDP-glucose 4,6-dehydratase		2.32	3	4.02E-03
GOX1068	Alcohol dehydrogenase large subunit		2.19	3	5.43E-03
GOX1107	O-antigen biosynthesis protein RfbC		3.19	3	2.05E-03
GOX1132	Hypothetical protein GOX1132		2.42	3	3.95E-04
GOX1246	TonB-dependent receptor protein		3.56	3	6.79E-03
GOX1276	Secreted protein of amidohydrolase family		2.01	3	2.53E-02
GOX1302	Paraquat-inducible protein A		2.43	3	1.10E-02
GOX1303	Paraquat-inducible protein B		2.18	3	2.57E-02
GOX1332	Alkyl hydroperoxide reductase subunit C		2.20	3	9.98E-03
GOX1357	Putative electron transport protein		2.63	3	1.81E-02
GOX1385	Hypothetical protein GOX1385		2.01	3	1.11E-02
GOX1457	Hypothetical protein GOX1457		2.11	3	3.65E-02
GOX1458	Putative oxidoreductase		2.47	3	1.90E-02
GOX1462	Putative oxidoreductase		3.88	3	3.47E-02
GOX1463	ATP-dependent Clp protease, ATP-binding subunit ClpV	*clpV*	2.41	3	4.16E-02
GOX1615	Putative oxidoreductase		4.34	3	2.11E-04
GOX1636	5-Aminolevulinate synthase		2.75	3	3.85E-02
GOX1697	Hypothetical protein GOX1697		2.17	3	1.12E-02
GOX1698	Aminopeptidase		2.33	3	4.39E-03
GOX1712	Aldehyde dehydrogenase		2.90	3	4.34E-02
GOX1748	Bacterioferritin	*bfr*	4.90	3	2.82E-02
GOX1774	Putative ATP-sensitive potassium channel protein		3.17	3	6.71E-03

GOX1800	Superoxide dismutase		2.00	3	1.92E-02
GOX1801	Putative oxidoreductase		2.38	3	3.63E-02
GOX1840	Hypothetical protein GOX1840		5.16	3	4.51E-02
GOX1841	Hypothetical protein GOX1841		14.16	3	7.46E-04
GOX1877	Glutathione peroxidase		2.06	3	1.57E-02
GOX1895	Hypothetical protein GOX1895		2.00	3	1.04E-06
GOX1896	Coproporphyrinogen III oxidase		2.73	3	5.19E-02
GOX1899	Putative oxidoreductase		2.02	3	1.18E-02
GOX1900	Putative carboxymethylenebutenolidase		2.54	3	6.95E-03
GOX1951	Hypothetical protein GOX1951		3.28	3	6.87E-03
GOX1953	5-Methylcytosine-specific restriction enzyme		4.05	3	2.70E-02
GOX1992	Osmotically inducible protein C, peroxyredoxin	*osmC*	4.90	3	1.37E-02
GOX2019	Putative esterase		2.11	3	1.17E-02
GOX2066	Glutaminase	*gls*	2.62	3	3.06E-02
GOX2069	Transcriptional regulator, DeoR family		2.52	3	7.54E-03
GOX2083	Hypothetical protein GOX2083		2.40	3	1.72E-02
GOX2096	Major polyol dehydrogenase large subunit	*sldA*	2.53	3	1.36E-02
GOX2097	Major polyol dehydrogenase small subunit	*sldB*	2.70	3	7.42E-05
GOX2108	NADH-dependent iron-containing alcohol dehydrogenase		2.15	3	6.69E-03
GOX2152	Hypothetical protein GOX2152		3.12	3	1.77E-03
GOX2153	Hypothetical protein GOX2153		2.97	3	9.32E-04
GOX2168	F_1F_o-ATP synthase subunit e	*atpC*	2.11	3	8.67E-03
GOX2170	F_1F_o-ATP synthase subunit r	*atpR**	2.36	3	2.71E-02
GOX2171	F_1F_o-ATP synthase subunit a	*atpB*	2.52	3	2.06E-02
GOX2172	F_1F_o-ATP synthase subunit c	*atpE*	2.25	3	5.27E-02
GOX2174	F_1F_o-ATP synthase subunit α	*atpA*	2.45	3	2.59E-02
GOX2199	Probable myosin-crossreactive antigen		4.46	3	6.39E-04
GOX2200	Probable myosin-crossreactive antigen		2.82	3	5.17E-02
GOX2246	Hypothetical protein GOX2246		2.89	3	2.71E-02
GOX2253	Putative oxidoreductase		2.60	3	4.68E-03
GOX2308	Delta-aminolevulinic acid dehydratase		2.66	3	5.22E-03
GOX2407	Putative RNA polymerase sigma-E factor (sigma-24) protein 2		2.32	3	5.02E-02
GOX2410	ABC transporter, cytochrome *bd* biogenesis CydC	*cydC*	2.02	3	3.04E-02
GOX2413	Hypothetical protein GOX2413		2.20	3	1.69E-02
GOX2470	Hypothetical protein GOX2470		2.24	3	1.80E-03
GOX2494	Hypothetical protein GOX2494		2.33	3	2.39E-02
GOX2683	Hypothetical protein GOX2683		2.71	3	3.22E-02
GOX2684	NAD(P)H-dependent 2-cyclohexen-1-one reductase		2.10	3	6.24E-03
GOX2698	Hypothetical protein GOX2698		2.30	3	1.23E-03
GOX2699	Hypothetical protein GOX2699		2.89	3	1.78E-04

***G. oxydans* Δ*upp* Δ*bo3* versus *G. oxydans* Δ*upp* (reference); mRNA ratio of 208 genes ≤0.5**

Gene	Annotation	Gene name	mRNA ratio	n	*p*-Value
GOX0035	Hypothetical protein GOX0035		0.39	3	4.60E-03
GOX0036	Enoyl[acyl-carrier-protein] reductase (FabL. NADPH)	*fabL*	0.48	3	2.41E-02
GOX0053	Hypothetical protein GOX0053		0.24	3	2.10E-02
GOX0066	Competence protein ComM		0.35	3	2.27E-02
GOX0074	Elongation factor Ts	*tsf*	0.40	3	3.11E-03
GOX0075	30S Ribosomal protein S2		0.34	3	4.92E-03
GOX0088	Trigger factor		0.44	3	3.84E-04
GOX0103	Carboxypeptidase-related protein		0.49	3	8.83E-03
GOX0116	Fatty acid/phospholipid synthesis protein		0.48	3	9.45E-03
GOX0126	Flagellar motor protein MotA	*motA*	0.41	3	3.37E-02
GOX0127	Chemotaxis MotB protein		0.13	3	3.39E-02
GOX0140	50S Ribosomal protein L27		0.38	3	1.16E-03
GOX0160	UDP-N-acetylenolpyruvoylglucosamine reductase		0.46	3	1.95E-02
GOX0193	Isopropylmalate isomerase, large subunit		0.30	3	4.74E-03
GOX0194	50S Ribosomal protein L19	*rplS*	0.38	3	6.37E-03
GOX0195	tRNA (Guanine-N(1)-)-methyltransferase		0.40	3	3.25E-03
GOX0196	30S Ribosomal protein S16	*rpsP*	0.35	3	6.27E-03
GOX0197	Signal recognition particle protein	*ffh*	0.38	3	7.30E-03
GOX0246	Hypothetical protein GOX0246		0.15	3	1.79E-02
GOX0247	Hypothetical protein GOX0247		0.47	3	3.35E-02
GOX0248	Hypothetical protein GOX0248		0.44	3	8.34E-03
GOX0254	Putative Fe-S-cluster redox enzyme		0.38	3	6.64E-03
GOX0272	Hypothetical protein GOX0272		0.36	3	2.50E-02
GOX0305	30S Ribosomal protein S18		0.42	3	1.28E-02
GOX0306	SSU Ribosomal protein S6P		0.36	3	5.90E-04
GOX0348	HlyD family secretion protein		0.48	3	4.34E-02
GOX0359	Adenylate kinase		0.36	3	7.95E-03
GOX0360	Preprotein translocase subunit SecY	*secY*	0.37	3	2.13E-03
GOX0361	LSU Ribosomal protein L15P		0.33	3	3.13E-03
GOX0362	LSU Ribosomal protein L30P		0.29	3	7.76E-03
GOX0363	30S Ribosomal protein S5		0.29	3	3.66E-05
GOX0364	50S Ribosomal protein L18		0.23	3	8.89E-03
GOX0365	50S Ribosomal protein L6		0.31	3	1.63E-03
GOX0366	30S Ribosomal protein S8		0.31	3	6.46E-03
GOX0367	30S Ribosomal protein S14		0.37	3	9.81E-04
GOX0368	50S Ribosomal protein L5		0.24	3	1.00E-02
GOX0369	LSU Ribosomal protein L24P		0.22	3	3.05E-03
GOX0370	LSU Ribosomal protein L14P		0.22	3	6.73E-03
GOX0371	SSU Ribosomal protein S17P		0.31	3	9.17E-03
GOX0372	LSU Ribosomal protein L29P		0.32	3	3.24E-03

GOX0373	50S Ribosomal protein L16		0.26	3	6.00E-03
GOX0374	30S Ribosomal protein S3		0.39	3	5.13E-04
GOX0375	50S Ribosomal protein L22		0.37	3	4.80E-04
GOX0376	SSU Ribosomal protein S19P		0.34	3	2.97E-17
GOX0377	50S Ribosomal protein L2		0.40	3	3.77E-03
GOX0378	LSU Ribosomal protein L23P		0.40	3	6.36E-03
GOX0379	50S Ribosomal protein L4		0.42	3	2.00E-04
GOX0380	50S Ribosomal protein L3		0.40	3	9.82E-03
GOX0381	30S Ribosomal protein S10		0.34	3	2.79E-02
GOX0382	Elongation factor Tu	*tuf*	0.45	3	1.31E-02
GOX0383	30S Ribosomal protein S7		0.37	3	1.12E-03
GOX0384	30S Ribosomal protein S12		0.37	3	5.08E-03
GOX0385	RNA polymerase. subunit b’	*rpoC*	0.46	3	2.14E-02
GOX0387	50S Ribosomal protein L7/L12		0.31	3	7.17E-04
GOX0388	LSU Ribosomal protein L10P		0.33	3	5.98E-03
GOX0389	50S Ribosomal protein L1		0.29	3	1.46E-02
GOX0390	50S Ribosomal protein L11		0.37	3	3.38E-04
GOX0403	Hypothetical protein GOX0403		0.49	3	5.66E-03
GOX0405	TonB-dependent outer membrane receptor		0.11	3	5.77E-03
GOX0415	Putative transport protein		0.49	3	2.44E-02
GOX0420	Flagellar biosynthesis protein A		0.18	3	2.25E-03
GOX0421	Flagellar motor switch protein		0.05	3	5.14E-03
GOX0422	Hypothetical protein GOX0422		0.06	3	7.08E-05
GOX0423	Flagellar motor switch protein G		0.07	3	2.79E-03
GOX0424	Flagellar MS-ring protein		0.05	3	5.29E-03
GOX0425	Basal-body rod modification protein FlgD	*flgD*	0.14	3	2.36E-02
GOX0426	Hypothetical protein GOX0426		0.10	3	2.44E-02
GOX0451	30S Ribosomal protein S9		0.34	3	3.38E-03
GOX0452	50S Ribosomal protein L13		0.38	3	2.59E-02
GOX0515	Hypothetical protein GOX0515		0.42	3	6.22E-03
GOX0560	Diguanylate cyclase		0.39	3	3.61E-02
GOX0596	30S Ribosomal protein S1		0.34	3	1.32E-02
GOX0619	Hypothetical protein GOX0619		0.34	3	2.95E-02
GOX0620	Chemotactic signal-response protein CheL	*cheL*	0.24	3	1.81E-02
GOX0621	Flagellar basal body P-ring protein		0.30	3	4.35E-02
GOX0693	Hypothetical protein GOX0693		0.24	3	3.66E-02
GOX0694	Hypothetical protein GOX0694		0.15	3	2.47E-02
GOX0695	Hypothetical protein GOX0695		0.11	3	2.38E-02
GOX0696	Flagellar motor switch protein FliM		0.12	3	1.95E-02
GOX0697	Flagellar FliL protein	*fliL*	0.15	3	2.16E-02
GOX0699	L-asparagine permease		0.37	3	2.72E-02
GOX0758	Porin		0.21	3	8.51E-03
GOX0766	Methyl-accepting chemotaxis protein		0.28	3	1.19E-02

GOX0772	Transcriptional regulator		0.47	3	1.70E-02
GOX0778	Two component sensor histidine kinase		0.42	3	1.49E-03
GOX0787	Flagellin B		0.06	3	3.66E-03
GOX0788	Flagellin assembly protein	*mviN*	0.13	3	1.79E-02
GOX0809	L-asparaginase II		0.38	3	2.97E-03
GOX0825	Hypothetical protein GOX0825		0.24	3	3.51E-02
GOX0835	Adenine phosphoribosyltransferase		0.49	3	1.79E-02
GOX0873	Levansucrase		0.48	3	1.27E-02
GOX0907	TonB-dependent outer membrane receptor		0.45	3	8.63E-03
GOX0909	Thiol:disulfide interchange protein DsbD		0.48	3	8.45E-03
GOX0926	Sulfate adenylyltransferase subunit 1 / adenylylsulfate kinase		0.36	3	7.12E-03
GOX0927	Sulfate adenylyltransferase subunit 2		0.35	3	1.85E-03
GOX0928	Phosphoadenosine phosphosulfate reductase		0.28	3	4.45E-03
GOX0945	TonB-dependent outer membrane receptor		0.08	3	9.76E-03
GOX0952	Flagellar basal body P-ring biosynthesis protein FlgA	*flgA*	0.29	3	4.96E-02
GOX0953	Flagellar basal body rod protein FlgG	*flgG*	0.09	3	1.40E-02
GOX0954	Flagellar basal-body rod protein FlgF	*flgF*	0.11	3	2.11E-02
GOX0960	Protein with GGDEF and EAL domain		0.41	3	2.82E-02
GOX1003	Septum formation associated protein (Maf-like protein)		0.48	3	1.46E-03
GOX1017	TonB-dependent outer membrane receptor		0.17	3	4.55E-02
GOX1025	Flagellar hook-associated protein FlgL	*flgL*	0.10	3	1.50E-02
GOX1026	Flagellar hook-associated protein 1 FlgK	*flgK*	0.09	3	2.95E-02
GOX1027	Flagellar hook protein FlgE	*flgE*	0.07	3	1.23E-02
GOX1091	Spermidine synthase		0.50	3	4.35E-02
GOX1114	Vitamin B12-dependent ribonucleotide reductase		0.31	3	1.22E-03
GOX1141	LSU Ribosomal protein L25P		0.35	3	5.81E-03
GOX1142	Peptidyl-tRNA hydrolase		0.42	3	1.33E-02
GOX1197	Hypothetical protein GOX1197		0.43	3	2.59E-02
GOX1198	Sulfite reductase (Ferredoxin)		0.34	3	1.31E-02
GOX1199	Putative oxidoreductase		0.46	3	9.24E-03
GOX1208	Hypothetical protein GOX1208		0.48	3	1.12E-02
GOX1209	Hypothetical protein GOX1209		0.14	3	5.36E-03
GOX1210	Hypothetical protein GOX1210		0.24	3	8.67E-03
GOX1211	Phage DNA Packaging Protein		0.22	3	1.10E-02
GOX1212	Phage portal protein		0.21	3	9.21E-03
GOX1213	Phage minor structual protein GP20		0.24	3	1.52E-02
GOX1214	Hypothetical protein GOX1214		0.21	3	9.48E-03
GOX1215	Hypothetical protein GOX1215		0.21	3	6.90E-03
GOX1216	Hypothetical protein GOX1216		0.20	3	9.86E-03
GOX1217	Hypothetical protein GOX1217		0.22	3	1.19E-02
GOX1218	Phage tail sheath protein		0.20	3	1.20E-02

GOX1219	Hypothetical protein GOX1219		0.20	3	1.57E-02
GOX1220	Hypothetical protein GOX1220		0.22	3	1.29E-02
GOX1221	Phage-recombinase-like protein		0.20	3	1.67E-02
GOX1222	Hypothetical protein GOX1222		0.24	3	1.82E-02
GOX1223	Hypothetical protein GOX1223		0.25	3	2.02E-02
GOX1224	Phage-related baseplate assembly protein		0.28	3	1.30E-02
GOX1225	Putative phage tail protein		0.20	3	1.35E-02
GOX1226	Hypothetical protein GOX1226		0.24	3	6.60E-03
GOX1227	Hypothetical protein GOX1227		0.25	3	1.50E-02
GOX1228	Hypothetical protein GOX1228		0.24	3	1.90E-02
GOX1229	Hypothetical protein GOX1229		0.26	3	2.30E-02
GOX1231	Gluconate 2-dehydrogenase subunit α	*gndB*	0.50	3	3.23E-03
GOX1237	Acetylornithine aminotransferase		0.47	3	5.34E-02
GOX1264	DNA processing chain A		0.48	3	7.95E-03
GOX1273	Hypothetical protein GOX1273		0.49	3	3.11E-02
GOX1286	Hypothetical protein GOX1286		0.23	3	1.14E-03
GOX1287	Biopolymer transport ExbB protein		0.32	3	7.75E-03
GOX1288	Biopolymer transport ExbD protein		0.36	3	1.75E-02
GOX1289	Biopolymer transport ExbD protein		0.42	3	1.11E-02
GOX1291	Flagellar basal body L-ring protein		0.19	3	2.77E-02
GOX1310	F_1F_o-ATP synthase subunit d	*atpH*	0.46	3	2.27E-03
GOX1317	Ile tRNA		0.31	3	8.31E-03
GOX1416	Porin B precursur		0.46	3	3.12E-02
GOX1436	Adenosine deaminase	*tadA*	0.49	3	1.43E-02
GOX1455	ATP-dependent RNA helicase		0.42	3	1.98E-02
GOX1523	Flagellar biosynthetic protein FlhB	*flhB*	0.29	3	4.47E-03
GOX1524	Flagellar biosynthetic protein FliR	*fliR*	0.39	3	1.89E-02
GOX1525	Flagellar biosynthetic protein FliQ	*fliQ*	0.06	3	1.98E-02
GOX1526	Flagellar hook-basal body protein FleE	*fleE*	0.06	3	2.66E-02
GOX1527	Flagellar basal body rod protein FlgC	*flgC*	0.06	3	1.68E-02
GOX1528	Flagellar basal-body rod protein FlgB	*flgB*	0.05	3	2.21E-02
GOX1530	Hypothetical protein GOX1530		0.24	3	2.27E-02
GOX1531	Flagellar biosynthesis protein FliP	*fliP*	0.46	3	4.98E-03
GOX1543	Hypothetical protein GOX1543		0.42	3	7.74E-03
GOX1549	Methyl-accepting chemotaxis protein		0.27	3	1.43E-02
GOX1550	Chemotaxis protein CheX	*cheX*	0.27	3	2.08E-02
GOX1551	Chemotaxis protein CheY	*cheY*	0.21	3	9.23E-03
GOX1552	Chemotaxis protein CheA	*cheA*	0.20	3	1.40E-02
GOX1553	Chemotaxis protein CheW		0.31	3	6.48E-03
GOX1554	Chemotaxis protein CheR		0.22	3	6.77E-03
GOX1579	Hypothetical protein associated with nus operon		0.46	3	1.87E-03
GOX1582	Translation initiation factor IF-2		0.48	3	3.45E-03
GOX1585	SSU Ribosomal protein S15P		0.49	3	3.06E-02
GOX1586	Polynucleotide		0.46	3	4.24E-03

	phosphorylase/polyadenylase				
GOX1587	Putative 2-nitropropane dioxygenase		0.36	3	1.32E-02
GOX1613	Protein with GGDEF and EAL domain		0.13	3	2.65E-02
GOX1632	Hypothetical protein GOX1632		0.15	3	6.36E-03
GOX1642	Carboxypeptidase-related protein		0.49	3	1.81E-02
GOX1661	Bacterioferritin comigratory protein		0.47	3	2.09E-02
GOX1674	Hypothetical protein GOX1674		0.47	3	1.43E-02
GOX1693	Cell cycle transcriptional regulator CtrA	*ctrA*	0.11	3	9.35E-03
GOX1694	Flagellum-specific ATP synthase		0.26	3	1.63E-02
GOX1695	Hypothetical protein GOX1695		0.42	3	8.87E-03
GOX1699	Hypothetical protein GOX1699		0.24	3	7.45E-04
GOX1737	Rod shape-determining protein MreB		0.39	3	4.63E-03
GOX1780	30S Ribosomal protein S4	*rpsD*	0.34	3	7.62E-03
GOX1781	Bacterial Peptide Chain Release Factor 3 (RF-3)		0.39	3	1.36E-02
GOX1804	Hypothetical protein GOX1804		0.36	3	1.38E-03
GOX1805	Hypothetical protein GOX1805		0.36	3	5.66E-03
GOX1830	Hypothetical protein GOX1830		0.30	3	1.73E-02
GOX1836	N-formylmethionylaminoacyl-tRNA deformylase		0.48	3	8.43E-03
GOX1857	Uncharacterized PQQ-containing dehydrogenase 1		0.06	3	2.35E-03
GOX1866	PmbA protein		0.47	3	2.57E-02
GOX1870	Hypothetical protein GOX1870		0.34	3	3.69E-02
GOX1873	DNA mismatch repair protein		0.44	3	2.25E-02
GOX1903	TonB-dependent receptor protein		0.09	3	7.96E-03
GOX1911	Cytochrome bo_3 ubiquinol oxidase subunit II	*cyoB*	0.00	3	1.07E-03
GOX1912	Cytochrome bo_3 ubiquinol oxidase subunit I	*cyoA*	0.00	3	8.68E-04
GOX1913	Cytochrome bo_3 ubiquinol oxidase subunit III	*cyoC*	0.00	3	5.80E-04
GOX1914	Cytochrome bo_3 ubiquinol oxidase subunit IV	*cyoD*	0.01	3	3.21E-04
GOX1966	Hypothetical protein GOX1966		0.39	3	2.35E-03
GOX2017	Hypothetical protein GOX2017		0.33	3	1.81E-03
GOX2028	Hypothetical protein GOX2028		0.24	3	5.41E-03
GOX2030	Chaperone protein DnaK	*dnaK*	0.48	3	2.44E-03
GOX2074	5-Methyltetrahydrofolate-S-homocysteine methyltransferase		0.49	3	3.09E-02
GOX2130	Hypothetical protein GOX2130		0.38	3	2.79E-02
GOX2132	Hypothetical protein GOX2132		0.28	3	1.16E-02
GOX2133	Hypothetical protein GOX2133		0.24	3	2.84E-03
GOX2205	Hypothetical protein GOX2205		0.18	3	1.32E-03
GOX2206	5-methyltetrahydropteroyltriglutamate-homocysteine methyltransferase		0.17	3	3.44E-03
GOX2207	Methylenetetrahydrofolate reductase		0.29	3	6.54E-03
GOX2249	Aspartyl-tRNA synthetase		0.49	3	3.55E-02
GOX2373	Protein of Rieske non-heme iron		0.14	3	1.98E-02

	oxygenase family. putative ring-hydroxylating dioxygenase				
GOX2386	Hypothetical protein GOX2386		0.28	3	2.37E-02

Category: Respiration and Energy Metabolism

Gene	Annotation	Gene name	mRNA ratio	n	*p*-Value
GOX0254	Putative Fe-S-cluster redox enzyme		0.38	3	6.64E-03
GOX1231	Gluconate 2-dehydrogenase subunit α	*gndB*	0.50	3	3.23E-03
GOX1310	F_1F_o-ATP synthase subunit d	*atpH*	0.46	3	2.27E-03
GOX1587	Putative 2-nitropropane dioxygenase		0.36	3	1.32E-02
GOX1911	Cytochrome bo_3 ubiquinol oxidase subunit II	*cyoB*	0.00	3	1.07E-03
GOX1912	Cytochrome bo_3 ubiquinol oxidase subunit I	*cyoA*	0.00	3	8.68E-04
GOX1913	Cytochrome bo_3 ubiquinol oxidase subunit III	*cyoC*	0.00	3	5.80E-04
GOX1914	Cytochrome bo_3 ubiquinol oxidase subunit IV	*cyoD*	0.01	3	3.21E-04
GOX0278	Cytochrome *bd* ubiquinol oxidase subunit I	*cydA*	5.43	3	9.28E-03
GOX0279	Cytochrome *bd* ubiquinol oxidase subunit II	*cydB*	3.61	3	2.01E-02
GOX0311	NAD(P) transhydrogenase subunit α2	*pntA2*	2.46	3	6.48E-03
GOX0312	NAD(P) transhydrogenase subunit b	*pntB*	2.19	3	1.36E-03
GOX0313	Alcohol:NAD^+ oxidoreductase		2.22	3	1.20E-02
GOX0566	Ubiquinol-cytochrome *c* oxidoreductase. cytochrome *b*	*qrcB*	2.03	3	5.60E-03
GOX2069	Transcriptional regulator. DeoR family		2.52	3	7.54E-03
GOX2096	Major polyol dehydrogenase large subunit	*sldA*	2.53	3	1.36E-02
GOX2097	Major polyol dehydrogenase small subunit	*sldB*	2.70	3	7.42E-05
GOX2168	F_1F_o-ATP synthase subunit e	*atpC*	2.11	3	8.67E-03
GOX2170	F_1F_o-ATP synthase subunit r	*atpR**	2.36	3	2.71E-02
GOX2171	F_1F_o-ATP synthase subunit a	*atpB*	2.52	3	2.06E-02
GOX2172	F_1F_o-ATP synthase subunit c	*atpE*	2.25	3	5.27E-02
GOX2174	F_1F_o-ATP synthase subunit α	*atpA*	2.45	3	2.59E-02
GOX2410	ABC transporter, cytochrome *bd* biogenesis CydC	*cydC*	2.02	3	3.04E-02

Category: Metabolism

Gene	Annotation	Gene name	mRNA ratio	n	*p*-Value
GOX0036	Enoyl[acyl-carrier-protein] reductase (FabL. NADPH)	*fabL*	0.48	3	2.41E-02
GOX0103	Carboxypeptidase-related protein		0.49	3	8.83E-03
GOX0116	Fatty acid/phospholipid synthesis protein		0.48	3	9.45E-03
GOX0160	UDP-N-acetylenolpyruvoylglucosamine reductase		0.46	3	1.95E-02
GOX0193	Isopropylmalate isomerase, large subunit		0.30	3	4.74E-03
GOX0359	Adenylate kinase		0.36	3	7.95E-03
GOX0560	Diguanylate cyclase		0.39	3	3.61E-02

GOX0873	Levansucrase		0.48	3	1.27E-02
GOX0909	Thiol:disulfide interchange protein DsbD		0.48	3	8.45E-03
GOX0926	Sulfate adenylyltransferase subunit 1 / adenylylsulfate kinase		0.36	3	7.12E-03
GOX0927	Sulfate adenylyltransferase subunit 2		0.35	3	1.85E-03
GOX0928	Phosphoadenosine phosphosulfate reductase		0.28	3	4.45E-03
GOX1091	Spermidine synthase		0.50	3	4.35E-02
GOX1114	Vitamin B12-dependent ribonucleotide reductase		0.31	3	1.22E-03
GOX1198	Sulfite reductase (Ferredoxin)		0.34	3	1.31E-02
GOX1211	Phage DNA Packaging Protein		0.22	3	1.10E-02
GOX1212	Phage portal protein		0.21	3	9.21E-03
GOX1213	Phage minor structual protein GP20		0.24	3	1.52E-02
GOX1218	Phage tail sheath protein		0.20	3	1.20E-02
GOX1221	Phage-recombinase-like protein		0.20	3	1.67E-02
GOX1224	Phage-related baseplate assembly protein		0.28	3	1.30E-02
GOX1237	Acetylornithine aminotransferase		0.47	3	5.34E-02
GOX1436	Adenosine deaminase	*tadA*	0.49	3	1.43E-02
GOX1642	Carboxypeptidase-related protein		0.49	3	1.81E-02
GOX1661	Bacterioferritin comigratory protein		0.47	3	2.09E-02
GOX1866	PmbA protein		0.47	3	2.57E-02
GOX2074	5-Methyltetrahydrofolate-S-homocysteine methyltransferase		0.49	3	3.09E-02
GOX2206	5-methyltetrahydropteroyltriglutamate-homocysteine methyltransferase		0.17	3	3.44E-03
GOX2207	Methylenetetrahydrofolate reductase		0.29	3	6.54E-03
GOX2373	Protein of Rieske non-heme iron oxygenase family, putative ring-hydroxylating dioxygenase		0.14	3	1.98E-02
GOX0756	Alcohol dehydrogenase 15 kDa subunit		2.14	3	5.42E-02
GOX0875	AtsE protein		2.19	3	9.83E-03
GOX0881	Arylesterase		2.31	3	3.51E-03
GOX1050	dTDP-4-dehydrorhamnose reductase		2.24	3	9.65E-04
GOX1051	dTDP-4-dehydrorhamnose 3,.5-epimerase		2.62	3	4.93E-03
GOX1052	Glucose-1-phosphate thymidylyltransferase, C-terminus		2.64	3	2.93E-03
GOX1053	dTDP-glucose 4,6-dehydratase		2.32	3	4.02E-03
GOX1068	Alcohol dehydrogenase large subunit		2.19	3	5.43E-03
GOX1107	O-antigen biosynthesis protein RfbC		3.19	3	2.05E-03
GOX1276	Secreted protein of amidohydrolase family		2.01	3	2.53E-02
GOX1636	5-Aminolevulinate synthase		2.75	3	3.85E-02
GOX1698	Aminopeptidase		2.33	3	4.39E-03
GOX1712	Aldehyde dehydrogenase		2.90	3	4.34E-02
GOX1748	Bacterioferritin	*bfr*	4.90	3	2.82E-02
GOX1877	Glutathione peroxidase		2.06	3	1.57E-02
GOX1896	Coproporphyrinogen III oxidase		2.73	3	5.19E-02

GOX1953	5-Methylcytosine-specific restriction enzyme		4.05	3	2.70E-02
GOX2066	Glutaminase	*gls*	2.62	3	3.06E-02
GOX2108	NADH-dependent iron-containing alcohol dehydrogenase		2.15	3	6.69E-03
GOX2308	Delta-aminolevulinic acid dehydratase		2.66	3	5.22E-03
GOX2684	NAD(P)H-dependent 2-cyclohexen-1-one reductase		2.10	3	6.24E-03

Category: Regulation and Signal transduction

Gene	Annotation	Gene name	mRNA ratio	n	*p*-Value
GOX0066	Competence protein ComM		0.35	3	2.27E-02
GOX0197	Signal recognition particle protein	*ffh*	0.38	3	7.30E-03
GOX0772	Transcriptional regulator		0.47	3	1.70E-02
GOX0778	Two component sensor histidine kinase		0.42	3	1.49E-03
GOX0960	Protein with GGDEF and EAL domain		0.41	3	2.82E-02
GOX1613	Protein with GGDEF and EAL domain		0.13	3	2.65E-02
GOX1693	Cell cycle transcriptional regulator CtrA	*ctrA*	0.11	3	9.35E-03
GOX0057	Protein with GGDEF and EAL domain		2.11	3	1.36E-02
GOX0135	Transcriptional regulator, Ros/MucR family		2.30	3	1.99E-04
GOX2407	Putative RNA polymerase sigma-E factor (sigma-24) protein 2		2.32	3	5.02E-02

Category: Transport

Gene	Annotation	Gene name	mRNA ratio	n	*p*-Value
GOX0348	HlyD family secretion protein		0.48	3	4.34E-02
GOX0360	Preprotein translocase subunit SecY	*secY*	0.37	3	2.13E-03
GOX0405	TonB-dependent outer membrane receptor		0.11	3	5.77E-03
GOX0699	L-asparagine permease		0.37	3	2.72E-02
GOX0758	Porin		0.21	3	8.51E-03
GOX0907	TonB-dependent outer membrane receptor		0.45	3	8.63E-03
GOX0945	TonB-dependent outer membrane receptor		0.08	3	9.76E-03
GOX1017	TonB-dependent outer membrane receptor		0.17	3	4.55E-02
GOX1287	Biopolymer transport ExbB protein		0.32	3	7.75E-03
GOX1288	Biopolymer transport ExbD protein		0.36	3	1.75E-02
GOX1289	Biopolymer transport ExbD protein		0.42	3	1.11E-02
GOX1416	Porin B precursur		0.46	3	3.12E-02
GOX1903	TonB-dependent receptor protein		0.09	3	7.96E-03
GOX0532	ExbB protein	*exbB*	3.40	3	2.46E-02
GOX0673	Ferrous iron transport protein A (FeoA)	*feoA*	4.40	3	2.14E-04
GOX0674	Ferrous iron transport protein B (FeoB)	*feoB*	2.51	3	1.03E-02
GOX0814	PTS system IIA component	*ptsIIA*	2.13	3	2.38E-03
GOX1246	TonB-dependent receptor protein		3.56	3	6.79E-03

Category: Motility

Gene	Annotation	Gene name	mRNA ratio	n	*p*-Value
GOX0126	Flagellar motor protein MotA	*motA*	0.41	3	3.37E-02
GOX0127	Chemotaxis MotB protein		0.13	3	3.39E-02
GOX0420	Flagellar biosynthesis protein A		0.18	3	2.25E-03
GOX0421	Flagellar motor switch protein		0.05	3	5.14E-03
GOX0423	Flagellar motor switch protein G		0.07	3	2.79E-03
GOX0424	Flagellar MS-ring protein		0.05	3	5.29E-03
GOX0425	Basal-body rod modification protein FlgD	*flgD*	0.14	3	2.36E-02
GOX0620	Chemotactic signal-response protein CheL	*cheL*	0.24	3	1.81E-02
GOX0621	Flagellar basal body P-ring protein		0.30	3	4.35E-02
GOX0696	Flagellar motor switch protein FliM		0.12	3	1.95E-02
GOX0697	Flagellar FliL protein	*fliL*	0.15	3	2.16E-02
GOX0766	Methyl-accepting chemotaxis protein		0.28	3	1.19E-02
GOX0787	Flagellin B		0.06	3	3.66E-03
GOX0788	Flagellin assembly protein	*mviN*	0.13	3	1.79E-02
GOX0952	Flagellar basal body P-ring biosynthesis protein FlgA	*flgA*	0.29	3	4.96E-02
GOX0953	Flagellar basal body rod protein FlgG	*flgG*	0.09	3	1.40E-02
GOX0954	Flagellar basal-body rod protein FlgF	*flgF*	0.11	3	2.11E-02
GOX1025	Flagellar hook-associated protein FlgL	*flgL*	0.10	3	1.50E-02
GOX1026	Flagellar hook-associated protein 1 FlgK	*flgK*	0.09	3	2.95E-02
GOX1027	Flagellar hook protein FlgE	*flgE*	0.07	3	1.23E-02
GOX1291	Flagellar basal body L-ring protein		0.19	3	2.77E-02
GOX1523	Flagellar biosynthetic protein FlhB	*flhB*	0.29	3	4.47E-03
GOX1524	Flagellar biosynthetic protein FliR	*fliR*	0.39	3	1.89E-02
GOX1525	Flagellar biosynthetic protein FliQ	*fliQ*	0.06	3	1.98E-02
GOX1526	Flagellar hook-basal body protein FleE	*fleE*	0.06	3	2.66E-02
GOX1527	Flagellar basal body rod protein FlgC	*flgC*	0.06	3	1.68E-02
GOX1528	Flagellar basal-body rod protein FlgB	*flgB*	0.05	3	2.21E-02
GOX1531	Flagellar biosynthesis protein FliP	*fliP*	0.46	3	4.98E-03
GOX1549	Methyl-accepting chemotaxis protein		0.27	3	1.43E-02
GOX1550	Chemotaxis protein CheX	*cheX*	0.27	3	2.08E-02
GOX1551	Chemotaxis protein CheY	*cheY*	0.21	3	9.23E-03
GOX1552	Chemotaxis protein CheA	*cheA*	0.20	3	1.40E-02
GOX1553	Chemotaxis protein CheW		0.31	3	6.48E-03
GOX1554	Chemotaxis protein CheR		0.22	3	6.77E-03
GOX1694	Flagellum-specific ATP synthase		0.26	3	1.63E-02
GOX1737	Rod shape-determining protein MreB		0.39	3	4.63E-03

Category: Stress

Gene	Annotation	Gene name	mRNA ratio	n	*p*-Value
GOX2030	Chaperone protein DnaK	*dnaK*	0.48	3	2.44E-03
GOX0707	DNA starvation/stationary phase protection protein Dps	*dps*	3.46	3	1.33E-02
GOX1302	Paraquat-inducible protein A		2.43	3	1.10E-02

GOX1303	Paraquat-inducible protein B		2.18	3	2.57E-02
GOX1332	Alkyl hydroperoxide reductase subunit C		2.20	3	9.98E-03
GOX1463	ATP-dependent Clp protease. ATP-binding subunit ClpV	*clpV*	2.41	3	4.16E-02
GOX1800	Superoxide dismutase		2.00	3	1.92E-02
GOX1992	Osmotically inducible protein C, peroxyredoxin	*osmC*	4.90	3	1.37E-02

Category: Transcription and Translational machinery

Gene	Annotation	Gene name	mRNA ratio	n	*p*-Value
GOX0074	Elongation factor Ts	*tsf*	0.40	3	3.11E-03
GOX0075	30S Ribosomal protein S2		0.34	3	4.92E-03
GOX0088	Trigger factor		0.44	3	3.84E-04
GOX0140	50S Ribosomal protein L27		0.38	3	1.16E-03
GOX0194	50S Ribosomal protein L19	*rplS*	0.38	3	6.37E-03
GOX0195	tRNA (Guanine-N(1)-)-methyltransferase		0.40	3	3.25E-03
GOX0196	30S Ribosomal protein S16	*rpsP*	0.35	3	6.27E-03
GOX0305	30S Ribosomal protein S18		0.42	3	1.28E-02
GOX0306	SSU Ribosomal protein S6P		0.36	3	5.90E-04
GOX0361	LSU Ribosomal protein L15P		0.33	3	3.13E-03
GOX0362	LSU Ribosomal protein L30P		0.29	3	7.76E-03
GOX0363	30S Ribosomal protein S5		0.29	3	3.66E-05
GOX0364	50S Ribosomal protein L18		0.23	3	8.89E-03
GOX0365	50S Ribosomal protein L6		0.31	3	1.63E-03
GOX0366	30S Ribosomal protein S8		0.31	3	6.46E-03
GOX0367	30S Ribosomal protein S14		0.37	3	9.81E-04
GOX0368	50S Ribosomal protein L5		0.24	3	1.00E-02
GOX0369	LSU Ribosomal protein L24P		0.22	3	3.05E-03
GOX0370	LSU Ribosomal protein L14P		0.22	3	6.73E-03
GOX0371	SSU Ribosomal protein S17P		0.31	3	9.17E-03
GOX0372	LSU Ribosomal protein L29P		0.32	3	3.24E-03
GOX0373	50S Ribosomal protein L16		0.26	3	6.00E-03
GOX0374	30S Ribosomal protein S3		0.39	3	5.13E-04
GOX0375	50S Ribosomal protein L22		0.37	3	4.80E-04
GOX0376	SSU Ribosomal protein S19P		0.34	3	2.97E-17
GOX0377	50S Ribosomal protein L2		0.40	3	3.77E-03
GOX0378	LSU Ribosomal protein L23P		0.40	3	6.36E-03
GOX0379	50S Ribosomal protein L4		0.42	3	2.00E-04
GOX0380	50S Ribosomal protein L3		0.40	3	9.82E-03
GOX0381	30S Ribosomal protein S10		0.34	3	2.79E-02
GOX0382	Elongation factor Tu	*tuf*	0.45	3	1.31E-02
GOX0383	30S Ribosomal protein S7		0.37	3	1.12E-03
GOX0384	30S Ribosomal protein S12		0.37	3	5.08E-03

GOX0385	RNA polymerase, subunit b'	*rpoC*	0.46	3	2.14E-02
GOX0387	50S Ribosomal protein L7/L12		0.31	3	7.17E-04
GOX0388	LSU Ribosomal protein L10P		0.33	3	5.98E-03
GOX0389	50S Ribosomal protein L1		0.29	3	1.46E-02
GOX0390	50S Ribosomal protein L11		0.37	3	3.38E-04
GOX0451	30S Ribosomal protein S9		0.34	3	3.38E-03
GOX0452	50S Ribosomal protein L13		0.38	3	2.59E-02
GOX0596	30S Ribosomal protein S1		0.34	3	1.32E-02
GOX0809	L-asparaginase II		0.38	3	2.97E-03
GOX0835	Adenine phosphoribosyltransferase		0.49	3	1.79E-02
GOX1003	Septum formation associated protein (Maf-like protein)		0.48	3	1.46E-03
GOX1141	LSU Ribosomal protein L25P		0.35	3	5.81E-03
GOX1142	Peptidyl-tRNA hydrolase		0.42	3	1.33E-02
GOX1264	DNA processing chain A		0.48	3	7.95E-03
GOX1317	Ile tRNA		0.31	3	8.31E-03
GOX1455	ATP-dependent RNA helicase		0.42	3	1.98E-02
GOX1582	Translation initiation factor IF-2		0.48	3	3.45E-03
GOX1585	SSU Ribosomal protein S15P		0.49	3	3.06E-02
GOX1586	Polynucleotide phosphorylase/polyadenylase		0.46	3	4.24E-03
GOX1780	30S Ribosomal protein S4	*rpsD*	0.34	3	7.62E-03
GOX1781	Bacterial Peptide Chain Release Factor 3 (RF-3)		0.39	3	1.36E-02
GOX1836	N-formylmethionylaminoacyl-tRNA deformylase		0.48	3	8.43E-03
GOX1873	DNA mismatch repair protein		0.44	3	2.25E-02
GOX2249	Aspartyl-tRNA synthetase		0.49	3	3.55E-02

Category: Predicted functions

Gene	**Annotation**	**Gene name**	**mRNA ratio**	**n**	***p*-Value**
GOX0415	Putative transport protein		0.49	3	2.44E-02
GOX1199	Putative oxidoreductase		0.46	3	9.24E-03
GOX1225	Putative phage tail protein		0.20	3	1.35E-02
GOX1857	Uncharacterized PQQ-containing dehydrogenase 1		0.06	3	2.35E-03
GOX0290	Putative oxidoreductase		2.43	3	4.35E-02
GOX0291	Putative ferredoxin subunit of ring-hydroxylating dioxygenase	*hca*	3.69	3	9.29E-03
GOX0502	Putative oxidoreductase		2.05	3	3.69E-02
GOX0545	Putative outer membrane receptor for iron transport		2.72	3	9.08E-04
GOX0646	Putative oxidoreductase		2.37	3	2.12E-02
GOX0647	Putative exporter protein, ArAE family	*fusB*	2.96	3	2.43E-02
GOX0679	Conserved protein of the SAM superfamily		3.71	3	1.90E-02
GOX1357	Putative electron transport protein		2.63	3	1.81E-02
GOX1458	Putative oxidoreductase		2.47	3	1.90E-02

GOX1462	Putative oxidoreductase		3.88	3	3.47E-02
GOX1615	Putative oxidoreductase		4.34	3	2.11E-04
GOX1774	Putative ATP-sensitive potassium channel protein		3.17	3	6.71E-03
GOX1801	Putative oxidoreductase		2.38	3	3.63E-02
GOX1899	Putative oxidoreductase		2.02	3	1.18E-02
GOX1900	Putative carboxymethylenebutenolidase		2.54	3	6.95E-03
GOX2019	Putative esterase		2.11	3	1.17E-02
GOX2199	Probable myosin-crossreactive antigen		4.46	3	6.39E-04
GOX2200	Probable myosin-crossreactive antigen		2.82	3	5.17E-02
GOX2253	Putative oxidoreductase		2.60	3	4.68E-03

Category: Hypothetical proteins

Gene	**Annotation**	**Gene name**	**mRNA ratio**	**n**	***p*-Value**
GOX0035	Hypothetical protein GOX0035		0.39	3	4.60E-03
GOX0053	Hypothetical protein GOX0053		0.24	3	2.10E-02
GOX0246	Hypothetical protein GOX0246		0.15	3	1.79E-02
GOX0247	Hypothetical protein GOX0247		0.47	3	3.35E-02
GOX0248	Hypothetical protein GOX0248		0.44	3	8.34E-03
GOX0272	Hypothetical protein GOX0272		0.36	3	2.50E-02
GOX0403	Hypothetical protein GOX0403		0.49	3	5.66E-03
GOX0422	Hypothetical protein GOX0422		0.06	3	7.08E-05
GOX0426	Hypothetical protein GOX0426		0.10	3	2.44E-02
GOX0515	Hypothetical protein GOX0515		0.42	3	6.22E-03
GOX0619	Hypothetical protein GOX0619		0.34	3	2.95E-02
GOX0693	Hypothetical protein GOX0693		0.24	3	3.66E-02
GOX0694	Hypothetical protein GOX0694		0.15	3	2.47E-02
GOX0695	Hypothetical protein GOX0695		0.11	3	2.38E-02
GOX0825	Hypothetical protein GOX0825		0.24	3	3.51E-02
GOX1197	Hypothetical protein GOX1197		0.43	3	2.59E-02
GOX1208	Hypothetical protein GOX1208		0.48	3	1.12E-02
GOX1209	Hypothetical protein GOX1209		0.14	3	5.36E-03
GOX1210	Hypothetical protein GOX1210		0.24	3	8.67E-03
GOX1214	Hypothetical protein GOX1214		0.21	3	9.48E-03
GOX1215	Hypothetical protein GOX1215		0.21	3	6.90E-03
GOX1216	Hypothetical protein GOX1216		0.20	3	9.86E-03
GOX1217	Hypothetical protein GOX1217		0.22	3	1.19E-02
GOX1219	Hypothetical protein GOX1219		0.20	3	1.57E-02
GOX1220	Hypothetical protein GOX1220		0.22	3	1.29E-02
GOX1222	Hypothetical protein GOX1222		0.24	3	1.82E-02
GOX1223	Hypothetical protein GOX1223		0.25	3	2.02E-02
GOX1226	Hypothetical protein GOX1226		0.24	3	6.60E-03
GOX1227	Hypothetical protein GOX1227		0.25	3	1.50E-02

GOX1228	Hypothetical protein GOX1228		0.24	3	1.90E-02
GOX1229	Hypothetical protein GOX1229		0.26	3	2.30E-02
GOX1273	Hypothetical protein GOX1273		0.49	3	3.11E-02
GOX1286	Hypothetical protein GOX1286		0.23	3	1.14E-03
GOX1530	Hypothetical protein GOX1530		0.24	3	2.27E-02
GOX1543	Hypothetical protein GOX1543		0.42	3	7.74E-03
GOX1579	Hypothetical protein associated with nus operon		0.46	3	1.87E-03
GOX1632	Hypothetical protein GOX1632		0.15	3	6.36E-03
GOX1674	Hypothetical protein GOX1674		0.47	3	1.43E-02
GOX1695	Hypothetical protein GOX1695		0.42	3	8.87E-03
GOX1699	Hypothetical protein GOX1699		0.24	3	7.45E-04
GOX1804	Hypothetical protein GOX1804		0.36	3	1.38E-03
GOX1805	Hypothetical protein GOX1805		0.36	3	5.66E-03
GOX1830	Hypothetical protein GOX1830		0.30	3	1.73E-02
GOX1870	Hypothetical protein GOX1870		0.34	3	3.69E-02
GOX1966	Hypothetical protein GOX1966		0.39	3	2.35E-03
GOX2017	Hypothetical protein GOX2017		0.33	3	1.81E-03
GOX2028	Hypothetical protein GOX2028		0.24	3	5.41E-03
GOX2130	Hypothetical protein GOX2130		0.38	3	2.79E-02
GOX2132	Hypothetical protein GOX2132		0.28	3	1.16E-02
GOX2133	Hypothetical protein GOX2133		0.24	3	2.84E-03
GOX2205	Hypothetical protein GOX2205		0.18	3	1.32E-03
GOX2386	Hypothetical protein GOX2386		0.28	3	2.37E-02
GOX0069	Hypothetical membrane-spanning protein		2.13	3	1.03E-02
GOX0433	Hypothetical protein GOX0433		4.81	3	1.16E-02
GOX0442	Hypothetical protein GOX0442		2.67	3	3.50E-02
GOX0475	Hypothetical protein GOX0475		2.36	3	2.13E-02
GOX0498	Hypothetical protein GOX0498		2.38	3	1.52E-02
GOX0503	Hypothetical protein GOX0503		2.23	3	4.46E-02
GOX0519	Hypothetical outer membrane protein		2.35	3	2.05E-02
GOX0570	Hypothetical protein GOX0570		3.51	3	2.57E-02
GOX0576	Hypothetical protein GOX0576		2.31	3	1.36E-02
GOX0635	Hypothetical protein GOX0635		2.53	3	2.06E-02
GOX0726	Hypothetical protein GOX0726		5.83	3	3.85E-02
GOX0815	Hypothetical protein GOX0815		2.39	3	1.75E-02
GOX0890	Hypothetical protein GOX0890		2.39	3	2.47E-02
GOX0915	Hypothetical protein GOX0915		2.28	3	1.34E-04
GOX1132	Hypothetical protein GOX1132		2.42	3	3.95E-04
GOX1385	Hypothetical protein GOX1385		2.01	3	1.11E-02
GOX1457	Hypothetical protein GOX1457		2.11	3	3.65E-02
GOX1697	Hypothetical protein GOX1697		2.17	3	1.12E-02
GOX1840	Hypothetical protein GOX1840		5.16	3	4.51E-02
GOX1841	Hypothetical protein GOX1841		14.16	3	7.46E-04

GOX1895	Hypothetical protein GOX1895		2.00	3	1.04E-06
GOX1951	Hypothetical protein GOX1951		3.28	3	6.87E-03
GOX2083	Hypothetical protein GOX2083		2.40	3	1.72E-02
GOX2152	Hypothetical protein GOX2152		3.12	3	1.77E-03
GOX2153	Hypothetical protein GOX2153		2.97	3	9.32E-04
GOX2246	Hypothetical protein GOX2246		2.89	3	2.71E-02
GOX2413	Hypothetical protein GOX2413		2.20	3	1.69E-02
GOX2470	Hypothetical protein GOX2470		2.24	3	1.80E-03
GOX2494	Hypothetical protein GOX2494		2.33	3	2.39E-02
GOX2683	Hypothetical protein GOX2683		2.71	3	3.22E-02
GOX2698	Hypothetical protein GOX2698		2.30	3	1.23E-03
GOX2699	Hypothetical protein GOX2699		2.89	3	1.78E-04

Danksagung

Ein ganz besonderer Dank gilt Prof. Michael Bott für die Überlassung des interessanten und spannenden Themas, die gute Betreuung und das stete Interesse am Fortgang meiner Arbeit.

Des Weiteren möchte ich mich bei Herrn Prof. Joachim Ernst für die Übernahme des Zweigutachtens bedanken.

Bei meiner Gruppenleiterin Dr. Stphanie Bringer möchte ich mich ganz besonders bedanken. Durch ihre Ratschläge, Geduld und stete Motivation hat Sie zum Erfolg dieser Arbeit beigetragen!

Zudem möchte ich mich bei unserem Industripartner „DSM Nutritional products“ für die finanzielle Unterstützung und die angenheme Atmosphäre während unserer Meetings bedanken. Ein besonderer Dank für die konstruktiven Ideen und Ratschläge geht dabei an Hans-Peter Hohmann, Dietmar Laudert und Günter Pappenberger.

Ein großer Dank geht auch an die (ehemaligen) Mitglieder meiner Arbeitsgruppe: Helga, Steffi, Ines, Solvej und Tanja. Ohne euch wäre die Zeit im Labor und Büro nur halb so schön gewesen.

Ein weiterer Dank geht an alle Mitarbeiter des IBG-1, die durch eine angenehme Arbeitsatmospähre stets dazu beigetrgagen haben, dass man gerne zur Arbeit gekommen ist. Allen Mitfahrern der MFG Aachen-Jülich danke ich für die schöne Zeit im Auto, die netten Gespräche und die vielen leckeren Kuchen ;)

Ein weiterer Dank geht an meine Freundinnen aus Schulzeiten, bei denen man sich immer mal eine Auszeit vom Laboralltag nehmen konnte. Außerdem danke ich meinen Freunden aus der Münster-Zeit. Unsere vielen gemeinsamen Ausflüge und Skiurlaube waren immer eine willkommene Abwechslung ☺

Zum Schluss möchte ich noch meinen Eltern, meiner Schwester und Familie sowie meinen Großeltern für die Unterstützung und das stete Interesse am Fortgang meiner Arbeit danken! Nach ein Paar Tagen Urlaub in der Heimat sahen die Schwierigkeiten mit *Gluconobacter* oft gar nicht mehr so schlimm aus!

Band / Volume 49
**Signaltransduktion in *Corynebacterium glutamicum*:
Studien zur Rolle von Proteinen mit einer FHA-Domäne**
S. Krawczyk (2012), 125 pp.
ISBN: 978-3-89336-771-9

Band / Volume 50
Analysis of functional domains of Par-4
U.K. Tiruttani Subhramanyam (2012), 85 pp.
ISBN: 978-3-89336-766-5

Band / Volume 51
**Transcriptional responses and transcriptional regulators
of *Gluconobacter oxydans* 621H**
S. K. Schweikert (2012), XVI, 140 pp.
ISBN: 978-3-89336-780-1

Band / Volume 52
**Characterization of the human mu opioid receptor:
Structural and functional studies of a G protein-coupled receptor**
Y. Ma (2012), 129 pp.
ISBN: 978-3-89336-767-2

Band / Volume 53
**Optimierung der Hydroxynitril-Lyase aus Arabidopsis thaliana
für die enantio-selektive Synthese von (R)-Cyanhydrinen**
Entwicklung und Etablierung geeigneter Reaktionsparameter und molekulare Stabilisierung durch rationales Enzymdesign
D. Okrob (2012), XV, 135 pp.
ISBN: 978-3-89336-782-5

Band / Volume 54
**Eine kritische Evaluierung FRET-basierter Biosensoren
als Werkzeuge für die quantitative Metabolitanalytik**
R. Moussa (2012), 113 pp.
ISBN: 978-3-89336-792-4

Band / Volume 55
**Development of Surface-FIDA towards a diagnostic tool
for Alzheimer's disease**
L. Wang-Dietrich (2012), VI, 103 pp.
ISBN: 978-3-89336-801-3

Band / Volume 56
Untersuchungen zur sekretorischen Proteingewinnung industriell relevanter Enzyme mit *Corynebacterium glutamicum*
S. Scheele (2012), vii, 127 pp.
ISBN: 978-3-89336-815-0

Band / Volume 57
Novel insights into the energy metabolism of *Corynebacterium glutamicum* by comprehensive analysis of mutants defective in respiration or oxidative phosphorylation
A. Koch-Körfges (2012), III, 137 pp.
ISBN: 978-3-89336-826-6

Band / Volume 58
Prozessnahe Hochdurchsatzoptimierung der heterologen Proteinproduktion in alternativen Wirtsorganismen
P. Rohe (2012), 165 pp.
ISBN: 978-3-89336-834-1

Band / Volume 59
Validation and characterisation of novel cellular ligands of membrane-associated HIV-1 Nef
E.C.Kammula (2012), 151 pp.
ISBN: 978-3-89336-839-6

Band / Volume 60
Untersuchungen zur Membranintegrität während der Tat-abhängigen Proteintranslokation in *Escherichia coli*
S. Fleckenstein (2013), VI, 160 pp.
ISBN: 978-3-89336-841-9

Band / Volume 61
Characterization of Novel Amyloid-β Peptide (Aβ) Binding Ligands
S. Dornieden (2013), vii, 129 pp.
ISBN: 978-3-89336-844-0

Band / Volume 62
Regulatorische Aspekte der Expression und Sekretion heterologer Proteine in *Corynebacterium glutamicum*
A. R. Chattopadhyay (2013), VIII, 195 pp.
ISBN: 978-3-89336-845-7

Band / Volume 63
***Gluconobacter oxydans* strain development: Studies on central carbon metabolism and respiration**
J. Richhardt (2013), III, 181 pp.
ISBN: 978-3-89336-851-8

Gesundheit / Health
Band / Volume 63
ISBN 978-3-89336-851-8

JÜLICH
FORSCHUNGSZENTRUM